

Second National Winter Weather Workshop
Conducted by the National Weather Service

Raleigh, North Carolina

26-30 September 1988

-Postprints-

Edited by:
Laurence G. Lee
NWS Forecast Office
Raleigh, NC

Scientific Services Division
Eastern Region Headquarters
June 1989

PREFACE

The Second National Winter Weather Workshop was held 26-30 September 1988 in Raleigh, North Carolina. The National Weather Service Eastern Region hosted the workshop. Support was provided by National Weather Service Headquarters.

This volume contains unrefereed articles from the participants who were able to provide a written version of their presentation. A complete set of abstracts is available from the chairman of the program committee.

Program Committee

Laurence G. Lee, Chairman, NWS Forecast Office, Raleigh-Durham, NC
Eugene P. Auciello, NWS Forecast Office, Boston, MA
Dr. Steven Businger, Department of Marine, Earth, and Atmospheric Sciences, North Carolina State University, Raleigh, NC
Rodney F. Gonski, NWS Forecast Office, Raleigh-Durham, NC
Robert W. Kelly, NWS Forecast Office, Columbia, SC
Kenneth D. LaPenta, NWS Forecast Office, Albany, NY
Robert A. Marine, NWS Forecast Office, Portland, ME
Thomas A. Niziol, NWS Forecast Office, Buffalo, NY
James R. Poirier, NWS Forecast Office, New York, NY

Local Arrangements Committee

Robert E. Muller, Chairman, Area Manager/Meteorologist in Charge, NWS Forecast Office, Raleigh-Durham, NC
Dr. Gerald Watson, Department of Marine, Earth, and Atmospheric Sciences, North Carolina State University, Raleigh, NC

For information, please contact:

National Weather Service Forecast Office
Raleigh-Durham International Airport
P.O. Box 165
Morrisville, NC 27560

or

National Weather Service Eastern Region
Scientific Services Division - W/ER3
Airport Corporate Center
630 Johnson Avenue
Bohemia, NY 11716

An article entitled "Summary of the Second National Winter Weather Workshop" (L. Lee et al.) is scheduled for publication in the June 1989 issue (Vol 4, No. 2) of Weather and Forecasting.

Those interested in pursuing the subject matter of Dr. Steven Businger's presentation, "A Review of Cyclogenesis in Cold Air", are referred to "Cyclogenesis in Cold Air Masses" (S. Businger and R. Reed) which is scheduled for publication in the June 1989 issue (Vol. 4, No. 2) of Weather and Forecasting.

The topics covered in Dr. Lance Bosart's presentation, "The Physical Basis for East Coast Cyclogenesis: Some Operational Lessons from Case Studies", are discussed in more detail in the following references: "The Synoptic and Subsynoptic Structure of a Long-Lived Severe Convective System" (M. Branick et al.) in the June 1988 issue (Vol. 116, No. 6) of Monthly Weather Review, "A Case Study of Unusually Intense Atmospheric Gravity Waves" (L. Bosart and A. Seimon) in the October 1988 issue (Vol. 116, No. 10) of Monthly Weather Review, and "Subsynoptic-Scale Structure in a Major Synoptic-Scale Cyclone" (C. O'Handley and L. Bosart) in the March 1989 issue (Vol. 117, No. 3) of Monthly Weather Review.

Details of Mr. H. Michael Mogil's presentation, "Training Development at a WSFO - Easy As A,B,C" are contained in several references. Information regarding the preparation of slides can be found in the August 1988 issue of National Weather Digest (Vol. 13, No. 3) and the preparation of video tape is the subject of an article scheduled to be published in the May 1989 National Weather Digest (Vol. 14, No. 2). A thorough treatment of conducting and documenting research in the operational environment is contained in A Guide for Operational Meteorological Research edited by G. Grice and K. Howard (1988) and published jointly by the following NOAA organizations: National Weather Service, National Severe Storms Laboratory, Environmental Research Laboratories, and National Environmental Satellite, Data, and Information Service.

* * * * *

PROGRAM
SECOND NATIONAL WINTER WEATHER WORKSHOP
Raleigh, NC

Monday 26 September

2:00 PM - 8:00 PM REGISTRATION - Velvet Cloak Inn.

Tuesday 27 September

- 8:00 AM **OPENING REMARKS**
Robert E. Muller, Area Manager/MIC,
National Weather Service Forecast Office, Raleigh, NC.
Susan F. Zevin, Director,
National Weather Service Eastern Region, Garden City, NY.
- 8:10 AM **OPENING PRESENTATION**
THE NATIONAL WEATHER SERVICE IN THE YEAR 2000.
Elbert W. Friday, Jr., Assistant Administrator for Weather
Services, National Weather Service, Silver Spring, MD.
- 8:50 AM **SESSION 1: EAST COAST STORMS.**
Chairperson, Laurence G. Lee,
National Weather Service Forecast Office, Raleigh, NC.
- 8:50 AM **SYNOPTIC STUDIES OF MAJOR SNOWSTORMS ALONG THE EAST COAST. ***
Paul J. Kocin,
NASA Goddard Space Flight Center, Greenbelt, MD.
- 9:15 AM **MODEL DIAGNOSTICS OF EAST COAST STORMS. ***
Louis W. Uccellini,
NASA Goddard Space Flight Center, Greenbelt, MD.
- 9:55 AM **WINTER FORECAST PROBLEMS ASSOCIATED WITH LIGHT TO MODERATE SNOW
EVENTS IN THE MID-ATLANTIC STATES. ***
Jeffrey Homan,
General Sciences Corporation/NASA Goddard Space Flight Center,
Greenbelt, MD.
- 10:20 AM **COFFEE BREAK**
- 10:40 AM **SESSION 2: APPLICATION OF SATELLITE IMAGERY TO WINTER
WEATHER FORECAST PROBLEMS.**
Chairperson, Rodney F. Gonski,
National Weather Service Forecast Office, Raleigh, NC.
- 10:40 AM **INSTABILITY BURSTS AND HEAVY PRECIPITATION FROM EXTRATROPICAL
CYCLONE SYSTEMS. ***
Roderick A. Scofield, Satellite Applications Laboratory,
National Environmental Satellite, Data, and
Information Service, Washington, D.C.

* Denotes article in Post-Print Volume

Tuesday 27 September

- 11:05 AM **SATELLITE VIEW OF CONVECTIVE TYPE CLOUDS AND HEAVY SNOW. ***
Samuel K. Beckman, Satellite Field Services Station,
National Severe Storms Forecast Center, Kansas City, MO.
- 11:30 AM **A METHOD TO DETERMINE THE WIDTH OF SNOW BANDS ASSOCIATED
WITH WINTER STORMS BY USING INFRARED SATELLITE DATA. ***
Allan L. Morrison,
National Weather Service Forecast Office, Chicago, IL.
- 11:55 AM **WHICH SATELLITE PRECIPITATION ESTIMATION TECHNIQUE TO USE?
A LOOK AT THE CHRISTMAS EVE 1987 HEAVY RAIN EVENT IN THE
MISSISSIPPI VALLEY.**
Sheldon J. Kusselson, Synoptic Analysis Branch, National
Environmental Satellite, Data, and Information Service,
Washington, D.C.

12:20 PM **LUNCHEON - POOLSIDE - Guest Speaker: Dr. Walter J. Saucier**

1:45 PM **SESSION 3: EXAMINING WINTER STORMS WITH NEW TECHNOLOGY.**
Chairperson, Eugene P. Auciello,
National Weather Service Forecast Office, Boston, MA.

1:45 PM **MESOSCALE WINTER FORECASTING USING DANPE.**
Lawrence Dunn,
National Weather Service Forecast Office, Denver, CO.

2:25 PM **WINTER EAST COAST LIGHTNING DATA AND SURVEY OF LIGHTNING
STRIKES IN STORMS. ***
Carl C. Ewald, Center Weather Service Unit,
Washington ARTCC, Leesburg, VA.

2:50 PM @ **PERSONAL COMPUTERS, UPPER-AIR ANALYSIS, AND QUASI-GEOSTROPHIC
DIAGNOSTICS IN THE NSFO.**
Michael P. Foster, National Weather Service Southern Region,
Scientific Services Division, Fort Worth, TX.

3:15 PM **BREAK**

3:30 PM **LABORATORY I**
**A THREE- TO TWELVE-HOUR HEAVY PRECIPITATION FORECAST INDEX
FOR EXTRATROPICAL CYCLONE SYSTEMS.**
Roderick A. Scofield, Satellite Applications Laboratory,
National Environmental Satellite, Data, and
Information Service, Washington, D.C.

5:30 PM **END OF LABORATORY**

@ Substitute Presentation
QUASI-GEOSTROPHIC DIAGNOSTICS FOR THE CHRISTMAS WEEKEND
STORM OF 1987
Stan Barnes, NOAA/ERL/Weather Research Program, Boulder, CO.

Wednesday 28 September

- 8:00 AM **OPENING PRESENTATION**
EXPLOSIVE CYCLOGENESIS OVER THE NORTH ATLANTIC - RECENT
NMC MODEL SKILL AND HOW TO TELL THE BIG BLASTS FROM THE
LITTLE POPS. *
Frederick Sanders, Marblehead, MA.
- 8:35 AM ADJOURN TO CONCURRENT SESSIONS.
- 8:40 AM **SESSION 4A: PRECIPITATION TYPE FORECASTING.**
Chairperson, James Poirier,
National Weather Service Forecast Office, New York, NY.
- 8:40 AM THE ROLE OF MELTING IN DETERMINING PRECIPITATION TYPE IN
EASTERN NEW YORK DURING THE STORM OF OCTOBER 4TH, 1987. *
Kenneth D. LaPenta,
National Weather Service Forecast Office, Albany, NY.
- 9:05 AM A PROCEDURE FOR FORECASTING PRECIPITATION TYPE USING NGM LOW
LEVEL TEMPERATURES AND LFM MOS FROZEN PRECIPITATION FORECASTS. *
Joseph A. Ronco, Jr.,
National Weather Service Forecast Office, Portland, ME.
- 9:30 AM WSFO RDU'S LOCAL GUIDANCE FOR PREDICTING PRECIPITATION TYPE. *
Kermit K. Keeter,
National Weather Service Forecast Office, Raleigh, NC.
- 8:40 AM **SESSION 4B: MESOSCALE STRUCTURE OF WINTER STORMS.**
Chairperson, Robert A. Marine,
National Weather Service Forecast Office, Portland, ME.
- 8:40 AM MESOSCALE STRUCTURE IN WINTER STORMS. PART 1:
AN ANALYSIS OF THE CHRISTMAS-WEEKEND STORM OF 1987.
Stan Barnes, Brad Colman, and Ken Howard,
NOAA/ERL/Weather Research Program, Boulder, CO.
- 9:05 AM MESOSCALE STRUCTURE IN WINTER STORMS. PART 2:
COMPOSITE STRUCTURE OF COLORADO FRONT-RANGE SNOWSTORMS.
Edward Tollerud, Cooperative Institute for Research in
Environmental Sciences, University of Colorado, Boulder, Co. and
Kenneth Howard, NOAA/ERL/Weather Research Program,
Boulder, CO.
- 9:30 AM MESOSCALE STRUCTURE IN WINTER STORMS. PART 3:
THE DIAGNOSIS AND PROGNOSIS OF MESOSCALE STRUCTURE IN
SYNOPTIC-SCALE CYCLONES.
Brad Colman,
NOAA/ERL/Weather Research Program, Boulder, CO.
- 9:55 AM COFFEE BREAK

Wednesday 28 September

- 10:20 AM SESSION 5A: PRECIPITATION TYPE FORECASTING. (Continued)
 Chairperson, James Poirier,
 National Weather Service Forecast Office, New York, NY.
- 10:20 AM WINTER PRECIPITATION TYPE. *
 Richard P. McNulty,
 National Weather Service Forecast Office, Topeka, KS.
- 10:45 AM THE SPECIFICATION OF PRECIPITATION TYPE IN WINTER STORMS.
 Michael L. Schichtel,
 NWS/National Meteorological Center, Washington, D.C.
- 10:20 AM SESSION 5B: WINTER STORMS ALONG THE EAST SLOPES OF
 THE COLORADO ROCKIES.
 Chairperson, Robert A. Marine,
 National Weather Service Forecast Office, Portland, ME.
- 10:20 AM SYNOPTIC PATTERNS ASSOCIATED WITH HEAVY SNOW ALONG THE
 FRONT RANGE OF COLORADO.
 Jim Wiesmueller,
 National Weather Service Forecast Office, Denver, CO. and
 Kenneth W. Howard, NOAA/ERL/Weather Research Program,
 Boulder, CO.
- 10:45 AM CLIMATOLOGY OF WINTER PRECIPITATION AT DENVER AND
 COLORADO SPRINGS.
 Jennifer Luppens and Kenneth W. Howard,
 NOAA/ERL/Weather Research Program, Boulder, CO.
- 11:10 AM END OF SESSIONS 5A and 5B
- 11:15 AM SESSION 6: WINTER WEATHER FORECASTING FROM DIFFERING
 PERSPECTIVES.
 Chairperson, Steven Businger, Dept. of Marine, Earth, and
 Atmospheric Sciences, North Carolina State University,
 Raleigh, NC.
- 11:15 AM SNOW FORECASTING USING PHYSICAL PARAMETERS AND PATTERN RECOGNITION.*
 Denis Bachand, Quebec Weather Centre,
 Atmospheric Environment Service, Saint-Laurent, Quebec.
- 11:40 AM THE OPERATIONAL DILEMMA OF HUGE NUMERICAL MODEL DIFFERENCES. *
 Frank Brody, NWS/Meteorological Operations Division,
 National Meteorological Center, Washington, D.C.
- 12:05 PM LUNCH BREAK
- 1:20 PM LABORATORY II
 EYEBALLING Q-VECTORS CAN BE EASY AND FUN. *
 Frederick Sanders, Marblehead, MA.
- 3:20 PM BREAK

Wednesday 28 September

- 3:30 PM LABORATORY III
USE OF SATELLITE IMAGERY TO DETERMINE HEAVY SNOW AREAS.
Samuel K. Beckman, Satellite Field Services Station,
National Severe Storms Forecast Center, Kansas City, MO.
- 5:30 PM END OF LABORATORY
- 7:45 PM GROUP DISCUSSION
TOPIC: NMC MODELS AND REGIONAL WINTER WEATHER PREDICTION.
Ralph A. Petersen,
NOAA/NWS/NMC/Development Division, Washington, D.C.

Thursday 29 September

- 8:00 AM OPENING PRESENTATION
A REVIEW OF CYCLOGENESIS IN COLD AIR.
Steven Businger, Dept. of Marine, Earth, and Atmospheric Sciences,
North Carolina State University, Raleigh, NC.
- 8:35 AM ADJOURN TO CONCURRENT SESSIONS
- 8:40 AM SESSION 7A: WINTER FORECAST PROBLEMS IN THE SOUTH.
Chairperson, Rodney F. Gonski,
National Weather Service Forecast Office, Raleigh, NC.
- 8:40 AM MAJOR ARCTIC OUTBREAKS AFFECTING LOUISIANA. *
Edward B. Mortimer, National Weather Service Forecast Office,
Albuquerque, NM. and
G. Alan Johnson and Henry W.N. Lau,
National Weather Service Forecast Office, Slidell, LA.
- 9:05 AM THE WINTER STORM OF JANUARY 6 AND 7, 1988. *
Frank Makosky and John G. Hoffner,
National Weather Service Forecast Office, Birmingham, AL.
- 9:30 AM WINTER STORM EVENT OF JANUARY 15, 1988, OVER COASTAL
SOUTH CAROLINA. *
Robert W. Kelly and Mary J. Parker,
National Weather Service Forecast Office, Columbia, SC.
- 8:40 AM SESSION 7B: WINTER FORECAST PROBLEMS ALONG THE EAST COAST.
Chairperson, Kenneth D. LaPenta,
National Weather Service Forecast Office, Albany, NY.
- 8:40 AM A METHOD FOR PREDICTING METEOROLOGICAL BOMBS IN THE WESTERN NORTH
ATLANTIC OCEAN. *
Eugene P. Auciello,
National Weather Service Forecast Office, Boston, MA.

Thursday 29 September

- 9:05 AM WINTER WEATHER AND THE CENTER WEATHER SERVICE UNIT. *
Wayne Weeks, Center Weather Service Unit,
Boston ARTCC, Nashua, NH.
- 9:30 AM LATE SEASON SNOWFALLS IN THE NORTH CAROLINA MOUNTAINS ASSOCIATED
WITH CUTOFF LOWS. *
Michael E. Sabones and Kermit K. Keeter,
National Weather Service Forecast Office, Raleigh, NC.
- 9:55 AM COFFEE BREAK
- 10:20 AM SESSION 8A: WINTER FORECAST PROBLEMS IN THE SOUTH. (continued)
Chairperson, Rodney F. Gonski,
National Weather Service Forecast Office, Raleigh, NC.
- 10:20 AM GEORGIA WINTER STORM - JANUARY 7, 1988. *
James Noffsinger and John Laing,
National Weather Service Forecast Office, Atlanta, GA.
- 10:45 AM RELATIONSHIP OF SNOW ACCUMULATION TO SOIL TEMPERATURE
IN SOUTH CAROLINA. *
Milton E. Brown,
National Weather Service Forecast Office, Columbia, SC.
- 10:20 AM SESSION 8B: FORECASTING LAKE EFFECT SNOW.
Chairperson, Kenneth D. LaPenta,
National Weather Service Forecast Office, Albany, NY.
- 10:20 AM AN OVERVIEW OF FORECAST SCHEMES USED BY WSFO CLEVELAND TO
FORECAST LAKE EFFECT SNOW. *
Frank Kieltyka,
National Weather Service Forecast Office, Cleveland, OH.
- 10:45 AM SOME SYNOPTIC AND MESOSCALE INTERACTIONS IN A LAKE EFFECT
SNOWSTORM. *
Thomas Nizioł,
National Weather Service Forecast Office, Buffalo, NY.
- 11:10 AM END OF SESSIONS 8A and 8B
- 11:15 AM SESSION 9: SNOW FORECASTING.
Chairperson, Robert W. Kelly,
National Weather Service Forecast Office, Columbia, SC.
- 11:15 AM SNOW FORECASTING...TYING SOME LOOSE ENDS. *
Edward C. Johnston,
National Weather Service Forecast Office, Milwaukee, WI.
- 11:40 AM TRAJECTORY MODEL FORECASTS OF HEAVY SNOW ALONG THE
EASTERN SEABOARD.
Ronald M. Reap, Techniques Development Laboratory,
National Weather Service, Silver Spring, MD.
- 12:05 PM LUNCH BREAK

Thursday 29 September

- 1:20 PM LABORATORY IV
FORECASTING A MAJOR SNOWSTORM.
Frank Brody, NWS/Meteorological Operations Division,
National Meteorological Center, Washington, D.C.
- 3:20 PM BREAK
- 3:30 PM LABORATORY V
NUMERICAL MODEL INITIAL ANALYSIS - ON TARGET OR OFF?
H. Michael Mogil, Satellite Applications Laboratory,
National Environmental Satellite, Data, and Information Service,
Washington, D.C.
- 5:30 PM END OF LABORATORY
- 7:00 PM BARBECUE BUFFET

Friday 30 September

- 8:00 AM OPENING PRESENTATION
THE PHYSICAL BASIS FOR EAST COAST CYCLOGENESIS:
SOME OPERATIONAL LESSONS FROM CASE STUDIES.
Lance F. Bosart, Department of Atmospheric Science,
State University of New York - Albany, Albany, NY.
- 8:35 AM SESSION 10: PROJECTS GALE AND ERICA.
Chairperson, Thomas Niziol,
National Weather Service Forecast Office, Buffalo, NY.
- 8:35 AM THE ERICA FIELD STUDY. *
Ron Hadlock, Battelle Ocean Sciences, Richland, WA. and
Carl W. Kreitzberg, Drexel University, Philadelphia, PA.
- 9:00 AM FORECASTING AND NOWCASTING FOR ERICA. *
Gregory S. Forbes, Department of Meteorology,
Pennsylvania State University, University Park, PA.
- 9:25 AM NMC INVOLVEMENT IN GALE AND ERICA.
Ralph A. Petersen and Geoff DiMego,
NOAA/NWS/NMC/ Development Division, Washington, D.C.
- 9:50 AM COFFEE BREAK

Friday 30 September

- 10:15 AM SESSION 11: NEW FORECAST TECHNIQUES AND PLANNING FOR THE FUTURE.
Chairperson, Laurence G. Lee,
National Weather Service Forecast Office, Raleigh, NC.
- 10:15 AM HIGH RESOLUTION REMOTE SENSING DATA: FUTURE APPLICATIONS TO WINTER WEATHER FORECASTING.
Wayne E. McGovern, Techniques Development Laboratory,
National Weather Service, Silver Spring, MD.
- 10:40 AM NEXRAD IN WINTER WEATHER.
Alan Nierow, Systems Operations Division,
National Weather Service Eastern Region, Garden City, NY.
- 11:05 AM NWS WINTER WEATHER PROGRAM OF THE FUTURE.
Steve Harned, Warnings and Forecast Branch,
National Weather Service Headquarters, Silver Spring, MD.
- 11:30 AM TRAINING DEVELOPMENT AT A WSFO - EASY AS A,B,C.
H. Michael Mogil, Satellite Applications Laboratory,
National Environmental Satellite, Data, and Information Service,
Washington, D.C.
- 11:55 AM END OF WORKSHOP

TABLE OF CONTENTS

	Page
Preface.	i
Workshop Programiii
Table of Contents.	xi
Synoptic Studies of Major East Coast Snowstorms.	1
P.J. Kocin and L.W. Uccellini	
Model Diagnostics of East Coast Storms	15
L.W. Uccellini, K.F. Brill, P.J. Kocin, and J.S Whitaker	
Winter Forecast Problems Associated With Light to Moderate Snow Events in the Mid-Atlantic States on 14 and 22 February 1986 . . .	31
J.S Homan and L.W. Uccellini	
Instability Bursts and Heavy Precipitation from Extratropical Cyclone Systems (ECSs)	45
R.A. Scofield	
Satellite View of Convective Type Clouds and Heavy Snow.	57
S.F. Beckman	
A Method to Determine the Width of a Snow Band Associated with Winter Storms by Using Infrared Satellite Data	65
A.L. Morrison	
Winter East Coast Lightning Data and Survey of Lightning Strikes in Storms.	74
C.C. Ewald	
Skill in Prediction of Explosive Cyclogenesis Over the Western North Atlantic Ocean, 1987-1988: A Forecast Checklist and NMC Dynamical Models	84
F. Sanders and E.P. Auciello	
Patterns of Thickness Anomaly for Explosive Cyclogenesis Over the West-Central North Atlantic Ocean.	89
F. Sanders and C.A. Davis	
The Role of Melting in Determining Precipitation Type in Eastern New York During the Storm of October 4th, 1987	92
K.D. LaPenta	
A Procedure for Forecasting Precipitation Type Using NGM Low Level Temperatures and LFM MOS Frozen Precipitation Forecasts.113
J.A. Ronco, Jr.	
Local Objective Guidance for Predicting Precipitation Type (LOG/PT) in North Carolina...An Alternative to MOS Guidance. . .	.125
K.K. Keeter, J.W. Cline, and R.P. Green	

Winter Precipitation Type.140
R.P. McNulty	
The Operational Dilemma of Huge Numerical Model Differences.150
F.C. Brody	
Snow Forecasting Using Physical Parameters161
D. Bachand, J. Morissette, and V. Turcotte	
Concerning Q-Vectors.172
F. Sanders	
Major Arctic Outbreaks Affecting Louisiana174
E.B. Mortimer, G.A. Johnson, and H.W.N. Lau	
The Winter Storm of January 6 and 7, 1988.190
F. Makosky and J.G. Hoffner	
Winter Storm Event of January 15, 1988, Over Coastal South Carolina200
R.W. Kelly and M.J. Parker	
A Method for Predicting Meteorological Bombs in the Western North Atlantic Ocean209
E.P. Auciello	
Winter Weather and the Center Weather Service Unit218
W.D. Weeks	
Late Season Snowfalls in the North Carolina Mountains Associated With Cutoff Lows.230
M.E. Sabones and K.K. Keeter	
Georgia Winter Storm - January 7, 1988237
J. Noffsinger and J. Laing	
Relationship of Snow Accumulation to Soil Temperature in South Carolina253
M.E. Brown	
Some Synoptic and Mesoscale Interactions in a Lake Effect Snowstorm.260
T.A. Niziol	
An Overview of Forecast Schemes Used by WSFO Cleveland, Ohio to Forecast Lake Effect Snows.270
F. Kieltyka	
Snow Forecasting: Comments on a Few Loose Ends.279
E.C. Johnston	
ERICA Plans for Winter Storms Field Study.287
R. Hadlock	
ERICA - Experiment on Rapidly Intensifying Cyclones Over the Atlantic288
G.S. Forbes	

Synoptic Studies of Major East Coast Snowstorms

Paul J. Kocin and Louis W. Uccellini¹

¹*Laboratory for Atmospheres NASA/Goddard Space Flight Center Greenbelt, MD 20771*

1. Introduction

The combined effects of heavy snow, high winds and cold temperatures associated with major snowstorms along the East Coast of the United States have had a debilitating effect on some of the nation's most populated metropolitan areas. Heavy snowfall associated with storms known as 'Nor'easters' may maroon millions of people at home, work or in transit, disrupt vital services and endanger the lives of those who venture outdoors.

The ability of weather forecasters to recognize and account for the many elements that influence the development and evolution of these storms is crucial for the accurate prediction of heavy snowfall along the East Coast. Before the advent of numerical weather prediction, attempts to forecast such storms yielded mixed results, at best. The increasing use and sophistication of numerical weather prediction models has improved the forecasts, especially with regard to the timing and location of cyclogenesis, precipitation amounts and location of the rain-snow line. However, even a relatively good numerical model forecast may contain small errors that can have a profound impact on the accuracy of weather forecasts that are disseminated to the general population. The inconsistent quality of the forecasts of these storms suggests that certain physical features and dynamical processes, whose influences vary widely from case to case, are better understood or more accurately simulated than others.

In view of an obvious need for an improved understanding of these storm systems, this paper will provide a brief summary of the horizontal and vertical structures and evolution of 20 major storms, derived from conventional weather analysis, during the period 1955 through 1985. These 20 cases were selected because they had the greatest impact on the largest number of people within a domain that spans the coastal region from Virginia to southern Maine, including the metropolitan areas of New York City, Philadelphia, Boston, Baltimore and Washington, D.C. A more complete description and collection of analyses of individual cases can be found in Kocin and Uccellini (1989), from which this article is derived.

2. Descriptions of 20 major snowstorms

In this section, patterns of snowfall, sea-level pressure, surface wind, temperature and other parameters are examined for the 20 cases to identify meteorological patterns that characterize major East Coast snow events, to determine what case-to-case variability might make generalizations difficult to apply, and to describe the dynamical and physical processes associated with these patterns.

The distribution of heavy snowfall for each of the 20 cases is shown in Fig. 1. Snowfall accumulations in excess of 25 cm occurred in bands averaging 200 to 500 km in width, covered distances of 500 km or more and were generally oriented from southwest to northeast. Snowfalls of 50 cm or greater were observed in every storm, with amounts exceeding 75 cm in eight of the cases.

All 20 cases were characterized by the development and propagation of well-defined cyclonic circulations. Miller (1946) examined 200 cyclones of varying intensity over a 10-year period ending in 1939 and categorized East Coast storm development into 2 types, 'A' and 'B'. Type 'A' storms resemble the classical polar front wave cyclone studied by the Norwegian school (Bjerknes, 1919; Bjerknes and Solberg, 1922). The surface low develops along a frontal boundary separating an outbreak of cold continental air from warmer maritime air. Type 'B' storms represent a more complex sea-level cyclonic development that is unique to the East Coast of the United States. The 'B' systems feature the development of a secondary area of low pressure along the East Coast to the southeast of an occluding primary surface low-pressure center located over the Ohio Valley. The secondary low forms along the primary cyclone's warm front, which separates a shallow wedge of cold air between the Appalachian Mountains and the Atlantic Ocean from warmer air over the ocean. While some doubt exists concerning a physical basis for the Miller classifications, his study cites secondary sea-level development as one of the most intriguing aspects of East Coast cyclogenesis. Secondary cyclogenesis is an important concern to East Coast snow forecasters because the onset of cyclogenesis and the cyclone's subsequent path are key factors in the forecast of when and where the heaviest snow will occur.

The paths of the surface low-pressure centers associated with the 20 cases are shown in Fig. 2. Ten of the 20 cases exhibited the 'B' scenario described by Miller. The primary low centers followed diverse paths from the western Gulf of Mexico, the southern Plains states, and the upper Midwest, with a locus of paths oriented from the southern Plains states to the upper Tennessee and Ohio Valleys. As the primary cyclone approached the Appalachians, a secondary center developed over the northeastern Gulf of Mexico, Georgia, the Carolinas, or the offshore water. The primary low dissipated as the secondary low formed.

The distinctive separation of paths that characterizes the cases exhibiting secondary cyclogenesis is not observed the remaining 10 cases (Fig. 2). All but one

of these systems developed in or propagated across the Gulf Coast region, passed south of the Appalachians, and then northeastward along the East Coast. These systems, as well as the secondary cyclones described in the last paragraph, followed similar paths from eastern North Carolina northeastward to the waters offshore of the Middle Atlantic states and southern New England, passing within approximately 100 to 300 km of the coast. Heaviest snowfall was usually found 100 to 300 km to the left of, and roughly parallel to, the paths of the surface low pressure centers. Although a secondary low center was not observed in these 10 cases, 7 of 10 exhibited a center jump as the surface low appeared to suddenly redevelop further northeast along the coast. The center jumps occurred along the same path as that of the primary low, in contrast to the separate tracks that marked secondary cyclogenesis.

In total, 17 of the 20 cases clearly show a redevelopment and/or sudden acceleration of the surface low along the coast. These characteristics are indicative of the influences of the underlying topography. The Appalachians appear to mark a transition between the areas where primary storm systems weaken and where secondary storms develop and intensify farther east. Secondary cyclogenesis and center jumps also seem to be confined the vicinity of the Carolinas coasts, suggesting that the coastline itself plays an important role.

Deepening rates were also examined as a measure of intensity of the cyclones associated with the snowstorms. In Fig. 3, central sea-level pressures are plotted at 3-h intervals for a 60-h period that includes the initiation, development, and decay of each storm. The minimum sea-level pressures attained by the 20-case sample ranges from 960 to 1000 mb. Deepening, defined as a decrease of central pressure at a rate of at least $-1 \text{ mb } (3h)^{-1}$, occurred generally over a 24- to 48-h period, with an average period of 36 hours. The total amount of deepening ranged from 11 to 52 mb, with an average of 33 mb. Most of the cases exhibited a clearly defined and continuous period of intensification, but a few exhibited multiple periods of deepening, separated by significant intervals of little or no change in pressure.

Rapid deepening, defined as a deepening rate exceeding $-3 \text{ mb } (3h)^{-1}$, occurred in every case except one, and for periods of 6 to 27 hours. In the 10 cases marked by secondary redevelopment, rapid deepening of the *primary* low-pressure center was observed in only 4 cases and lasted no longer than 6 hours. All secondary cyclones, except one, underwent a 12- 24-h period of rapid development. The primary low filled within the expanding circulation of the secondary low within 6 to 27 hours following the onset of secondary cyclogenesis. Among the 10 storms that either exhibited a center jump or no redevelopment, rapid deepening occurred in all cases and for periods of 6 to 27 hours. While heavy snowfall was frequently observed during periods of rapid surface intensification, 2 cases yielded widespread snowfall without surface cyclonic deepening. So, while rapid sea-level development is a common characteristic of many of these storms, it is not a prerequisite for

widespread heavy snowfall. It remains, however, a topic that is the focus of much recent scientific research (ie., Sanders and Gyakum, 1980; Sanders, 1986; Rogers and Bosart, 1986; Uccellini et al., 1987; Abbey et al., 1987).

While cyclogenesis is an integral component of the 20 major snowfalls, surface *anticyclones* often provide and maintain cold temperatures for the heavy snow events. To identify consistent patterns in anticyclone location that characterized the sample, high pressure centers were plotted (Fig. 4) for a 36-h period prior to and during cyclogenesis along the East Coast. Anticyclone centers followed paths from central Canada, either (1) eastward across Ontario and Quebec, toward the Maritime provinces or New England, or (2) southward toward the northern and central Plains states. These two scenarios are depicted schematically in Fig. 5. The sea-level configurations shown in Fig. 5 produce a north-northeasterly flow of air along the coast that drives cold air southward toward the developing cyclone. The orientation of the anticyclone relative to the cyclone results in a low-level air-flow that passes primarily over land, or for only a very limited distance over the ocean before reaching the coast. As a result, the cold air mass is not substantially modified by sensible and latent heating from the nearby ocean. Maximum sea-level pressures within these anticyclones exceeded 1030 mb, and on occasion, surpassed 1050 mb.

Cold air damming and coastal frontogenesis are two processes associated with the cold air outbreaks that can be crucial components of the heavy snow events. When a cold surface high passes to the north of the coastal plain, cold air is channeled southward along the eastern slopes of the Appalachians and is maintained by a combination of effects described in Stauffer and Warner, 1988, Forbes et al., 1987, and Bell and Bosart, 1988. Dammed cold air suppresses low-level warm advection over the coastal plain, and maintains the thermal gradients and warm air advection pattern along the coastline or offshore. As a result, when a primary cyclone and its upper-level forcing approach the Appalachians from the west, the low-level warm air advection pattern shifts to the east of the cold air wedge. This process facilitates the formation of a secondary cyclone along the East Coast as the primary system weakens in the Ohio Valley. As cold air remains trapped over land, air over the ocean is modified by sensible and latent heat fluxes within the ocean-influenced planetary boundary layer. The deformation and convergence of these airstreams result in a zone of enhanced low-level baroclinicity termed 'coastal frontogenesis' (Bosart et al., 1972). Coastal frontogenesis provides a site where low-level convergence, baroclinicity, warm air advections and surface vorticity are maximized (Bosart, 1975), important considerations in the evolution of East Coast snowstorms.

3. Descriptions of upper-level features

An examination of the 500 mb surface shows that *three* patterns of geopotential

heights define the upper-level troughs associated with the sea-level cyclones (Fig. 6). These patterns include (1) the transformation of an 'open-wave' trough into a closed circulation or vortex during cyclogenesis (12 cases), (2) the existence of a closed circulation at 500 mb prior to and during cyclogenesis (4 cases), and (3) 500 mb troughs that did not evolve into closed circulations (4 cases). Increases of amplitude and decreases of half-wavelength between the trough and downstream ridge characterized nearly all cases and are indicative of the enhanced vorticity gradients, vorticity advections and upper-level divergence associated with these storms. The development of diffluence downwind of the trough and a change in the orientation of the trough axis to a negative (northwest-southeast) tilt also characterized the majority of cases.

Distinct 500 mb vorticity maxima were plotted for each case (Fig. 7). The maxima followed a variety of paths, but were initially directed from northwest to southeast in 14 of the 20 cases, indicative of deepening or 'digging' troughs in which the amplitude measured between the trough and upstream ridge axes was increasing with time. Following the initial digging of the troughs in the central United States, the paths of the vorticity maxima typically curved to the east or northeast as they approached the Atlantic coast. With few exceptions, the centers of maximum cyclonic vorticity moved off the coast between North Carolina and New Jersey to positions just south of the southern New England coast. The merger of multiple vorticity centers was clearly observed in 9 cases and indicates a 'phasing' of separate short-wave troughs or jet-stream systems. The interaction of these systems enhances the upper-level vorticity advection and associated divergence as the merging of separate vorticity maxima into one cohesive maximum produces a well-organized pattern of vorticity advection above the developing surface cyclone.

Heavy snow seldom occurs when the vorticity maximum curves to the northeast *before* reaching the East Coast. In cases where the vorticity maximum propagates northeastward into the Ohio Valley, the primary surface cyclone usually maintains a well-defined circulation west of the Appalachians, advecting lower-tropospheric warm air over the coastal plain. While secondary cyclogenesis may still occur and cold air damming may persist over the coastal plain, the warm advection aloft often produces precipitation in the form of rain, freezing rain, or ice pellets, rather than heavy snow.

The 500 mb surface was also examined to identify characteristic geopotential height patterns associated with the sea-level anticyclones over the Great Lakes and southeastern Canada. The sea-level high-pressure systems were found upwind of upper-level troughs propagating across eastern Canada in all 20 cases. The troughs crossed eastern Ontario, Quebec and the Maritime provinces to the offshore waters of the Atlantic Ocean before and during the onset of heavy snowfall in the coastal Northeast. In 19 of the 20 cases, the sea-level anticyclone was located beneath a region of confluent geopotential heights. Confluence was found upwind of the 500

mb trough over eastern Canada, which typically contained a distinct geopotential height minimum or closed circulation. The confluence was also associated with the presence of polar jet streaks across the Northeast. The repeated appearance of upper-level confluence and its connection with the sea-level anticyclones suggest that the development and maintenance of a confluence zone over the northeastern United States or southeastern Canada helps to establish and maintain the lower-tropospheric cold temperatures necessary for snowfall along the coast.

An orientation of upper-level jet streaks and their associated vertical ageostrophic circulations, as identified by Uccellini and Kocin (1987), links many of the preceding surface and upper-level features to the development of heavy snowfall (Fig. 8). As an upper-level trough approaches the East Coast, a surface low pressure system develops within the diffluent exit region of a jet streak downwind of the trough axis. A separate upper-level jet streak is embedded in the confluence over New England. A cold surface anticyclone is usually found beneath the entrance region of this jet streak. Indirect and direct transverse ageostrophic circulations are located in the southern and northern jet streaks, respectively. The rising branches of the two jet streaks merge and contribute to a widespread region of ascent, clouds and precipitation between the jet streak exit and entrance regions. The advection of Canadian air southward in the lower branch of the direct circulation over the northeastern United States maintains the lower-tropospheric temperatures needed for snowfall and is enhanced by cold air damming. The northward advection of warm, moist air in the lower branch of the indirect circulation rises above the cold air north of the surface low. A low-level jet streak typically develops in this branch beneath the diffluent exit region of the upper-level jet.

4. Summary

The description of surface and upper-level characteristics of 20 major East Coast snowstorms is a greatly condensed version of a Meteorological Monograph to be published shortly by the American Meteorological Society. Analyses of the surface and upper-level fields of pressure, geopotential height, wind, and temperature, plus other selected elements, provide a framework for understanding some of the dynamical and thermodynamical processes that contribute to heavy snowfall along the East Coast.

A visual summary of the factors that contribute to heavy snowfall along the East Coast is provided in Fig. 9. The following brief descriptions of the relevant processes show how each influences the development of these storms. Although the processes are treated separately to identify their individual contributions, the non-linear interactions of these processes are crucial for the development of heavy snowfall.

Each of the storms was associated with a well-defined upper-level trough and cyclonic vorticity advections. An increase in amplitude and decrease in wavelength,

the appearance of diffluence downwind of an increasing negatively-tilted trough axis, were all characteristic of the 20 cases and pointed to processes that increase upper-level divergence during surface cyclogenesis. Upper-level jet streaks were an important component of these storms and a particular configuration of jet streaks, one approaching the East Coast and the other located over the northeastern United States or southeastern Canada, were seen as instrumental in establishing conditions suitable for heavy snowfall (Uccellini and Kocin, 1987).

Anticyclones that pass across southeastern Canada or surface high-pressure ridges that extend eastward from anticyclones over the American or Canadian plains provide the cold low-level air that enables precipitation to reach the ground in the form of snow. The position of the anticyclone relative to the evolving storm system is a key factor in driving cold air toward the coastal region, with minimal modification due to its primarily over-land trajectory.

Lower-tropospheric thermal advections are also important components of these storms as they affect deepening rates, vertical motions and energy conversions. The increase of the thermal advections during cyclogenesis is attributable, in part, to the effects of topography on the boundary layer temperature structure. The Appalachian Mountains, the coastline and the varying temperature field within the Atlantic Ocean, in association with the Gulf Stream, contribute to the lower-tropospheric thermal modifications. Cold air damming contributes to the southward advection of cold air and the enhancement of thermal gradients along the coast. Coastal frontogenesis focuses low-level convergence, baroclinicity, warm advection and surface vorticity, providing a channel for the developing cyclone. The fluxes of sensible and latent heat warm and moisten the ocean-influenced planetary boundary layer, contributing to the coastal baroclinicity and the moisture flux necessary for heavy precipitation.

The interactions of these effects are accounted for by the 'self-development' concept defined by Sutcliffe and Forsdyke (1950) and described by Palmen and Newton (1969). A companion paper by Uccellini et al. (1989) discusses these interactions and will not be addressed here.

This paper is intended to show that conventional weather analyses present recognizable patterns that precede and accompany the development of heavy snowstorms along the East Coast. These patterns provide a first step in the generation of conceptual models that can be used by forecasters to predict future heavy snow events in a region greatly affected by their occurrence. A limitation of this study is that only 20 cases were examined, which points to the need for additional research that involves detailed case studies, numerical modeling efforts, and the development of a larger group of cases covering a wider variety of storms, both back in time and forward in time as new cases occur. Through a combination of research efforts ranging from climatological reviews to model-based case studies, together with improved observations of these systems, especially over the ocean, our understanding of these

storms will be enriched and our ability to forecast them with acceptable consistency may be realized.

References.

Abbey, R. F., R. Hadlock, and C. Kreitzberg, 1987: *ERICA Overview Document*. Field Research Project, Version 1, Office of Naval Research, OCNR 11287-7, Arlington, VA, 41 pp.

Bell, G. P., and L. F. Bosart, 1988: Appalachian cold-air damming. *Mon. Wea. Rev.*, *116*, 137-161.

Bjerknes, J., 1919: On the structure of moving cyclones. *Geofys. Publikasjoner, Norske Videnskaps-Akad. Oslo 1*, No. 1, 1-8.

Bjerknes, J. and H. Solberg: Life cycle of cyclones and the polar front theory of atmospheric circulation. *Geofys. Publikasjoner, Norske Videnskaps-Akad. Oslo 3*, No. 1, 1-18.

Bosart, L. F., 1975: New England coastal frontogenesis. *Quart. J. Roy. Meteor. Soc.*, *101*, 957-978.

Bosart, L. F., C. J. Vaudo, and J. J. Helsdon, Jr., 1972: Coastal Frontogenesis. *J. Appl. Meteor.*, *11*, 1236-1258.

Forbes, G. S., R. A. Anthes, and D. W. Thompson, 1987: Synoptic and mesoscale aspects of an Appalachian ice storm associated with cold-air damming. *Mon. Wea. Rev.*, *115*, 564-591.

Kocin, P. J. and L. W. Uccellini, 1989: Snowstorms along the northeastern coast of the United States, 1955-1985. *Meteor. Monogr.*, (in press).

Miller, J. E., 1946: Cyclogenesis in the Atlantic coastal region of the United States. *J. Meteor.*, *3*, 31-44.

Palmen, E., and C. W. Newton, 1969: *Atmospheric Circulation Systems*. Academic Press, 603 pp.

Rogers, E., and L. F. Bosart, 1986: An investigation of explosively deepening oceanic cyclones. *Mon. Wea. Rev.*, *112*, 702-718.

Sanders, F., 1986: Explosive cyclogenesis in the west-central North Atlantic Ocean, 1981-1984. Part I: Composite structure and mean behavior. *Mon. Wea. Rev.*, *114*, 1781-1794.

Sanders, F., and J. R. Gyakum, 1980: Synoptic dynamic climatology of the bomb. *Mon. Wea. Rev.*, *108*, 1589-1606.

Stauffer, D. R., and T. T. Warner, 1987: A numerical study of Appalachian cold-air damming and coastal frontogenesis. *Mon. Wea. Rev.*, *115*, 799-821.

Sutcliffe, R. C., and A. G. Forsdyke, 1950: The theory and use of upper air thickness patterns in forecasting. *Quart. J. Roy. Meteor. Soc.*, *76*, 189-217.

Uccellini, L. W., and P. J. Kocin, 1987: An examination of vertical circulations associated with heavy snow events along the East Coast of the United States. *Wea. and Fore.*, *2*, 289-308.

Uccellini, L. W., K. F. Brill, P. J. Kocin, and J. S. Whitaker, 1989: Model Diagnostics of East Coast Storms. *Second Winter Weather Workshop*, Raleigh, N.C.

Uccellini, L. W., D. Keyser, K. F. Brill, and C. H. Wash, 1985: The Presidents' Day cyclone of 18-19 February 1979: Influence of upstream trough amplification and associated tropopause folding on rapid cyclogenesis. *Mon. Wea. Rev.*, *113*, 962-988.

STORM SNOWFALL FOR TWENTY CASES (≥ 25 CM)

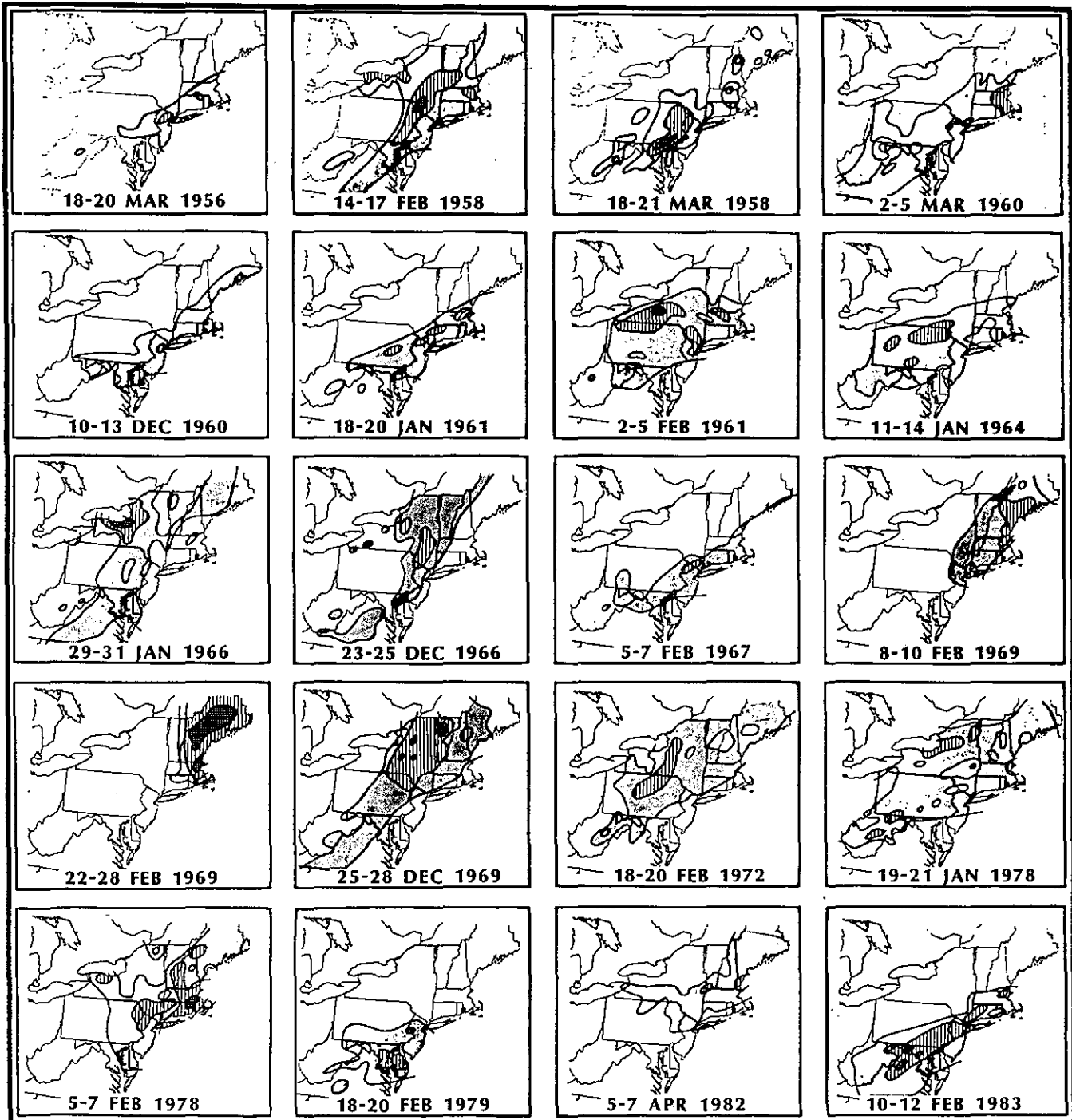


Fig. 1. Storm snowfall in excess of 25 cm for 20 snowstorms between 1955 and 1985 (light shading, 25 to 50 cm; linear shading, 50-75 cm; heavy shading, greater than 75 cm).

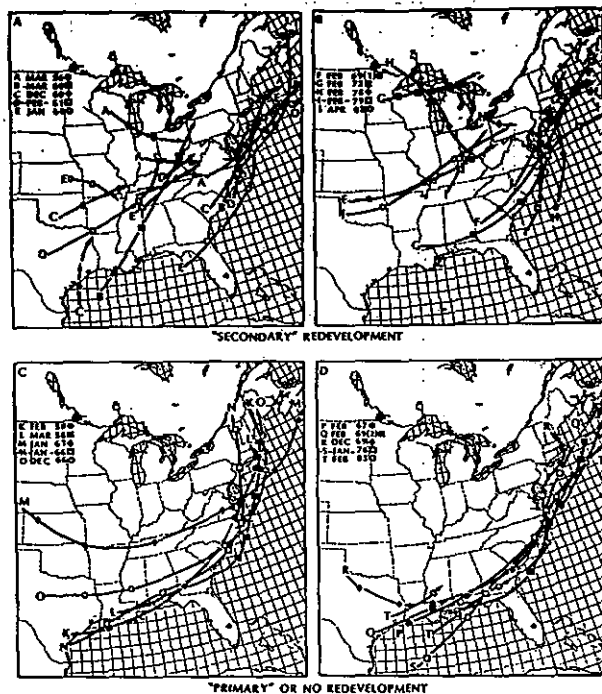


Fig. 2. Paths of low-pressure centers at sea level for 20 cases. Paths are grouped according to (a,b) cases exhibiting "secondary" redevelopment and (c,d) cases exhibiting no redevelopment or only "primary" redevelopment ("center jumps"). Symbols along path represent 12-h positions.

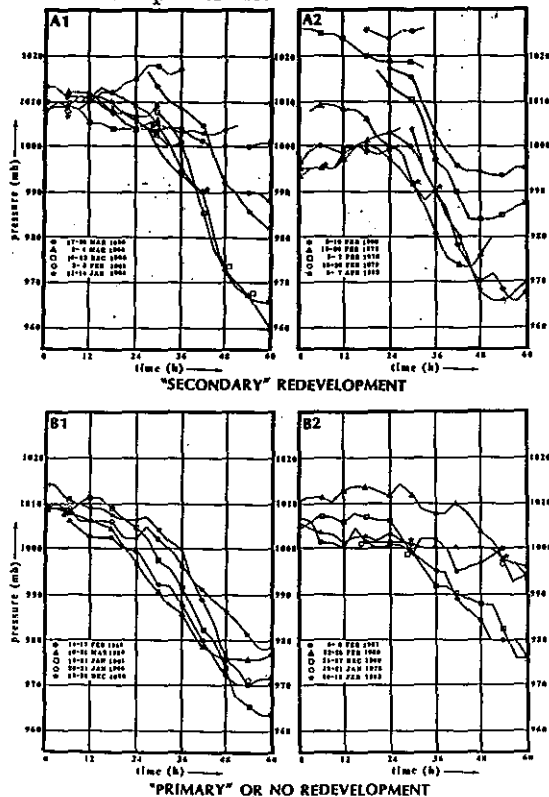


Fig. 3. Time series of central pressures of the sea-level cyclones over the 60-h study period. The 20 cases are grouped as in Fig. 2. In the top two panels, the pressures of the primary low are represented by the thin dotted lines and the secondary low by the solid lines.

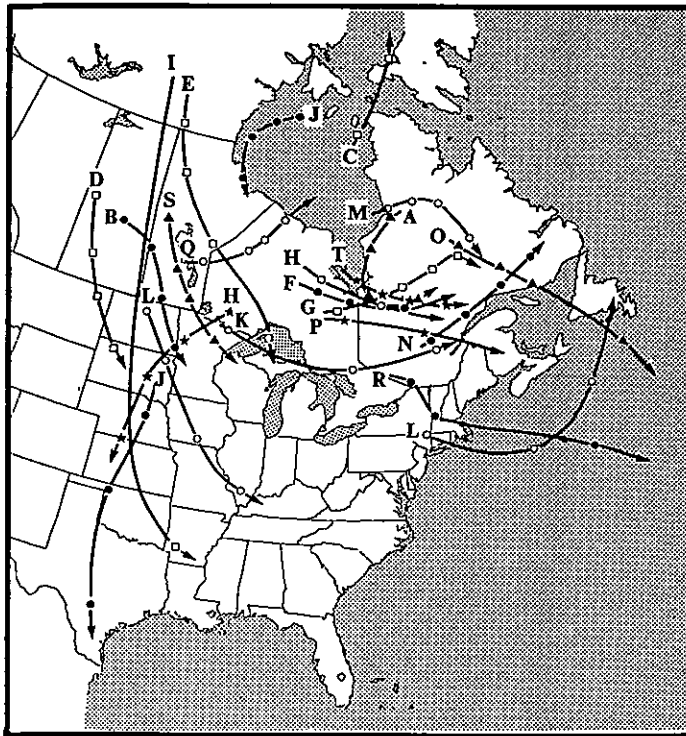


Fig. 4. Paths of anticyclones at sea level.

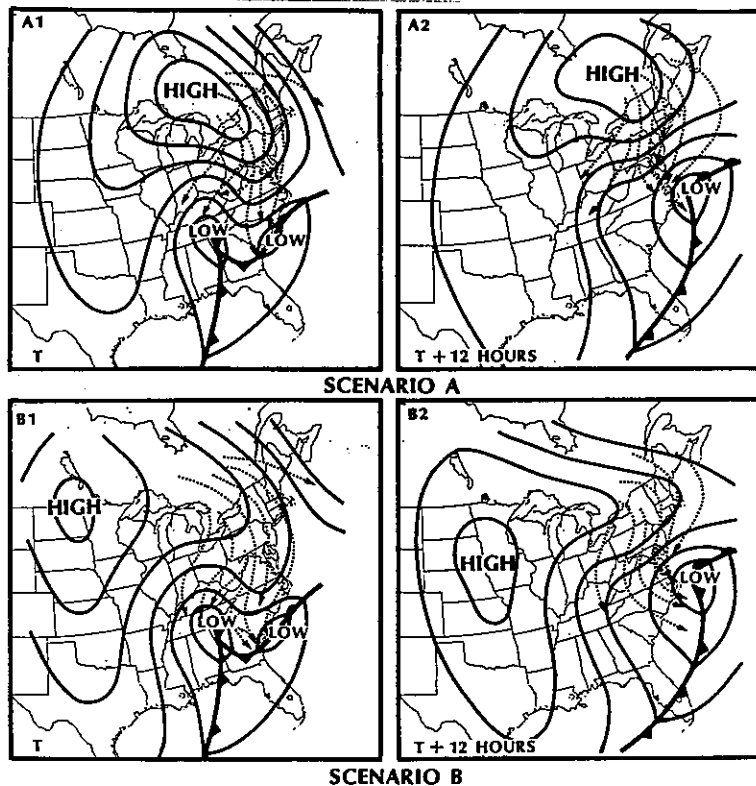


Fig. 5. Schematic of representative streamlines (dotted arrows) and sea-level isobars (solid) for anticyclone-cyclone couplets during major snowstorms along the Northeast coast. Top and bottom panels reflect 12-h sequences. (A1, A2) shows a well-defined anticyclone over Ontario and Quebec and (B1, B2) shows a high-pressure cell over the Plains states ridging eastward to the northeastern United States.

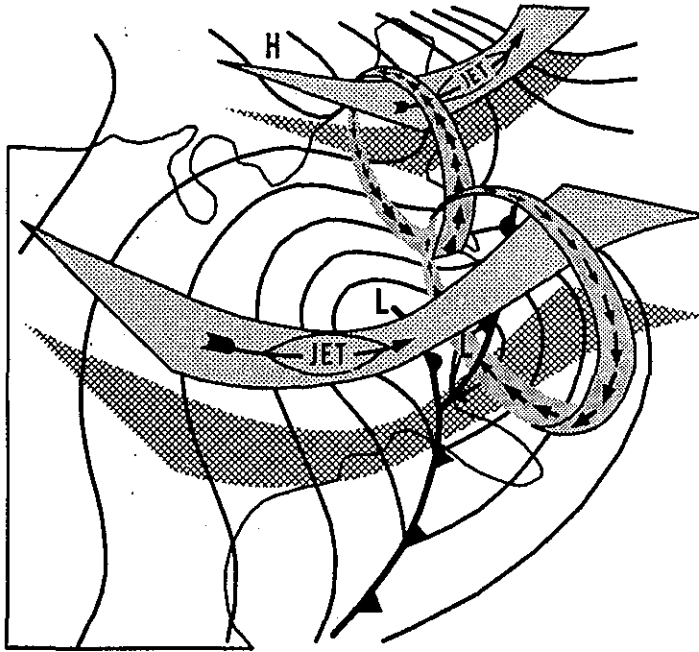


Fig. 8. Schematic of dual jet-related circulation patterns during East Coast snowstorms. Circulations are represented by pinwheels, jet streaks are imbedded within confluent and diffluent regions and solid lines are sea-level isobars.

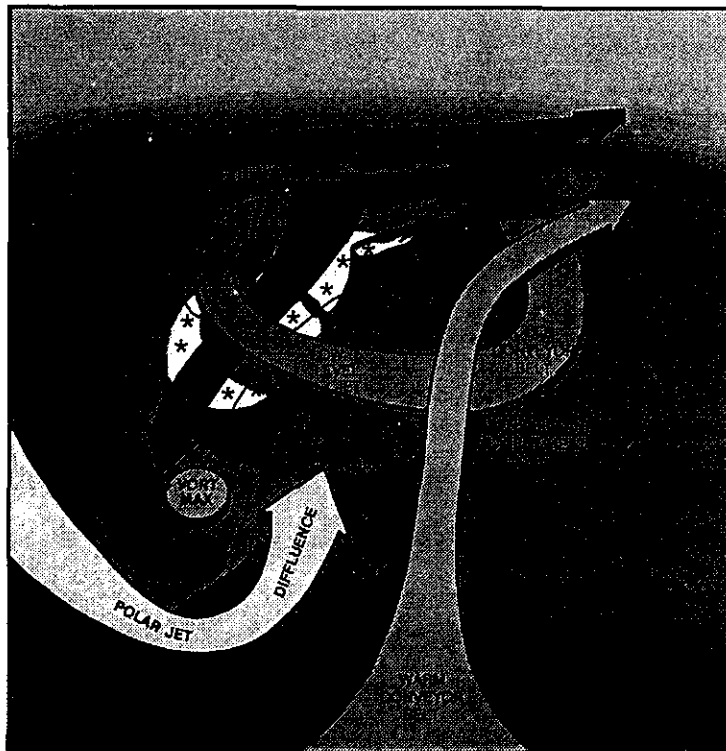


Fig. 9. Schematic of factors that contribute to heavy snowfall along the East Coast of the United States.

MODEL DIAGNOSTICS OF EAST COAST STORMS¹

Louis W. Uccellini, Keith F. Brill², Paul J. Kocin, and Jeffrey S. Whitaker³

Laboratory for Atmospheres
NASA/Goddard Space Flight Center
Greenbelt, MD 20771

1. Introduction

The recent interest in cyclogenesis is generally based on studying cyclones which undergo a period of rapid development. These storms are often marked by severe winds and heavy precipitation and are, in many instances, not predicted well by numerical models.

In their study of "explosive" cyclogenesis in the Northern Hemisphere, Sanders and Gyakum (1980) found that the rapidly-deepening storms occur primarily over the ocean, above or just to the north of the warm ocean currents in the North Atlantic and North Pacific Oceans. Roebber (1984) presents a statistical analysis of the 24-hour deepening rate of a one-year sample of cyclones occurring in the Northern Hemisphere. Roebber's analysis confirms that rapid cyclogenesis occurs primarily near the warm ocean currents. However, he emphasizes that the period of extreme rapid deepening occurs for only a fraction of the time encompassing the cyclogenetic event, a result which is consistent with Kocin and Uccellini's (1988) review of 20 major snowstorms along the East Coast of the United States. The observations that many of these cyclones exhibit a short period of extreme rapid deepening lends support to the terminology of "explosive development" or "rapid development" used by Sanders and Gyakum (1980), among many others, in describing these storms.

2. Observations

It is well known that the presence of upper-level trough/ridge systems and/or jet streak provides an area of divergence in the middle-to-upper troposphere (as estimated by cyclonic vorticity advection) over the developing storm center, as emphasized by Bjerknes (1951), Palmén (1969), Petterssen (1956), Sutcliffe (1950), and many others. As discussed by Bjerknes (1951), "transverse" or cross-stream ageostrophic components in the entrance and exit regions of jet streaks also play a role in the development of surface cyclones and anticyclones. The existence of a trough/ridge system and imbedded jet streak usually precedes the surface cyclogenesis. However, there are examples in which the upper-level curvature in the geopotential height fields is not a dominant feature, and the divergence

¹Workshop report derived from the 1988 NCAR Synoptic Study Symposium; lecture notes written by Yea-Ching Tung provided courtesy of Dr. Frederick Carr.

²General Sciences Corporation, Laurel, MD 20707.

³Department of Meteorology, The Florida State University, Tallahassee, FL 32306.

aloft appears to be related primarily to the presence of a well-defined jet streak (Uccellini, 1984, 1986; Uccellini and Kocin, 1987; Wash *et al.*, 1988).

Uccellini and Kocin (1987) show that a particular configuration of two separate jet streaks can give rise to two interactive, transverse-ageostrophic circulations and contribute to conditions suitable for heavy snowfall along the East Coast: (1) a direct circulation located within the confluent entrance region of a jet streak over the northeastern United States or southeastern Canada; and (2) an indirect circulation in the diffluent exit region of a jet streak associated with a trough in the southeastern United States.

For example, at 1200 UTC 11 February 1983, a strong snowstorm was in progress across Virginia, West Virginia, and Maryland. The 300 mb analysis (Fig. 1) shows that there is an upper-level trough and an upper-level jet streak located near the base of the trough. Confluence geopotential heights over the northeastern United States mark the entrance region of a separate 60 m s^{-1} polar jet streak. The surface low is located beneath the diffluent exit region of the upper-level jet streak over the southeastern United States (Fig. 2). A wedge of high pressure associated with very cold air is located beneath the confluence in the entrance region of the upper-level jet streak located just south of Nova Scotia. The widespread area of heavy snow is located between the two jet streaks.

The interaction of transverse circulations in the exit and entrance regions of the two jet streaks is illustrated by a cross section constructed from Lake Ontario to the North Carolina coast (Fig. 3). A direct transverse circulation is diagnosed in the entrance region of the polar jet streak across the northeastern United States (marked with a "D" in Fig. 3). The ageostrophic wind components at upper levels are directed toward the cyclonic-shear side of the jet, while the low-level return ageostrophic flow is directed toward the anticyclone-shear side of the jet. Subsidence is diagnosed in the coldest air immediately above the surface anticyclone. Ascent is diagnosed in the relatively warmer air where the isentropes are sloped downward toward higher pressure. The ageostrophic components in the lower troposphere appear to contribute to the advection of cold air from New York toward Virginia.

The cross section also displays an indirect transverse circulation (marked with an "I" in Fig. 3) in the exit region of the jet streak over the southeastern United States. In the upper troposphere, the tangential ageostrophic wind components are directed to the anticyclonic shear side of the jet. Ascent and subsidence are located in relatively colder and warmer air, respectively. The lower branch of the indirect circulation acts to transport moisture from the Atlantic Coast toward the region of heavy snow.

The two circulations interact to produce a broad, sloped region of ascent that is conducive to heavy precipitation. The lower branches of the circulations appear to enhance moisture transports and provide for the interaction of very cold and very warm air, creating a favorable environment for the development of heavy snowfall.

In the previous case, direct and indirect circulations were diagnosed in the entrance and exit regions of upper-level jet streaks embedded within confluent and diffluent flow regimes, respectively. As discussed by Shapiro and Kenney (1981) for a jet streak marked by significant cyclonic curvature and by Uccellini *et al.* (1984) for an anticyclonic flow regime preceding the Presidents' Day storm, this simple relationship did not always exist in curved flow regimes.

Although the upper-level trough/ridge system and/or jet streaks contribute to the development of extratropical storms, other characteristics are also common to rapidly developing extratropical storms. These characteristics include:

- (1) An asymmetric distribution of clouds and precipitation surrounding the storm, with the deepest clouds and most extensive area of significant precipitation located poleward of the cyclone center and a clear "tongue" extending toward the center from the western and equatorward sides. The clear tongue represents the area in which stratospheric air marked by high values of potential vorticity descends toward the storm center. As first postulated by Kleinschmidt (Eliassen and Kleinschmidt, 1957) and recently reviewed by Hoskins *et al.* (1985), the stratospheric extrusion represents a "producing mass" for cyclogenesis.
- (2) Low-level baroclinic zones that often serve as the site along which rapid cyclogenesis commences along the east coasts of major continents and near the narrow, warm ocean currents in the North Atlantic and Pacific Oceans, where intense low-level temperature gradients can become established (*e.g.*, Bosart, 1981; Gyakum, 1983a; Reed and Albright, 1986).
- (3) Boundary-layer fluxes of heat and moisture which act to fuel the developing cyclone and to destabilize the lower troposphere in advance of the storm (*e.g.*, Bosart, 1981, Uccellini *et al.*, 1987). This factor also tends to favor rapid cyclogenesis over or near oceans.
- (4) Convective elements are imbedded within the precipitation regime on the poleward side of the cyclone and also along the frontal boundaries associated with these storms. Hypotheses have been presented that the convection plays an active role in contributing to and even initiating rapid cyclogenesis (*e.g.*, Tracton, 1973; Bosart, 1981; Gyakum, 1983b). However, the evidence supporting these hypotheses is still inconclusive.
- (5) In some areas, orographic features play an important role in cyclogenesis. For example, case studies and numerical experiments demonstrate that the Alps exert a significant modifying influence on large-scale flow patterns and jet-streak circulation patterns that contribute to rapid cyclogenesis in the Ligurian Sea just to the west of Italy (*e.g.*, Buzzi and Tibaldi, 1978; Mattocks and Bleck, 1986). It also appears that the Appalachian Mountains play a significant role in influencing the low-level thermal fields (through "damming" of the cold air toward the south) which, along with coastal

frontogenesis, provides a low-level baroclinic zone in the Carolinas, contributing to coastal cyclogenesis (see, *e.g.*, Bosart, 1981; Stauffer and Warner, 1987).

It appears from an increasing number of model-based sensitivity studies and diagnostic analyses of storms along the East Coast of the United States that the rapid development phase of extratropical cyclones is dependent not on the individual contribution of these physical processes, but on a synergistic interaction among them (Uccellini *et al.*, 1987). Furthermore, it appears that the interactions are required for only a short period of time over a relatively small domain to produce these major cyclone events.

3. Numerical Modeling Studies

Since all of the physical processes seem to feed back upon each other, affecting the horizontal and vertical circulation patterns throughout the entire troposphere and lower stratosphere, numerical modeling has become a critical part of the effort to resolve the interaction of various physical processes that contribute to cyclogenesis.

Uccellini *et al.* (1987) used a series of model simulations for the February 1979 Presidents' Day cyclone and showed that a synergistic interaction among jet-streak circulation patterns, boundary layer fluxes, latent heat release and circulation associated with coastal frontogenesis has contributed to (1) rapid development of a low-level jet streak (LLJ), (2) an increase in the low-level mass divergence, and (3) an initial development of a secondary cyclone along the coast.

This model experiment consists of four simulations which are ADB (adiabatic, with surface friction), BLYR NO LHT, LHT NO BLYR, and FULL PHYS. In FULL PHYS simulation, where all physical parameterizations are included, the maximum 850 mb winds and minimum sea-level pressure (SLP) are significantly closer to those observed than in the other simulations (Table 1).

The most accurate simulation of the secondary surface cyclogenesis along the coast is accomplished by FULL PHYS simulation. The maintenance of a distinct pressure ridge east of the Appalachian Mountains, the development of an inverted trough along the southeast coast and associated coastal frontogenesis, and the weakening of the Ohio Valley trough between 06 Z/18 and 18 Z/18 (Figs. 4a-c) agree favorably with analyses provided by Bosart (1981) and Uccellini *et al.* (1984). By 00 Z/19, the coastal system continues to deepen off the South Carolina coast (Fig. 4d), with the 1017 mb central pressure being identical to that of Bosart's (1981) analysis.

A vertical cross section constructed from central Michigan to a position off the Florida coast shows that the transverse circulation is detectable over the Appalachian Mountain region, with a 6 u/s ascending branch located beneath the axis of the subtropical jet (STJ) by 06 Z/18 (Fig. 5a), and greater than $12 \mu\text{b s}^{-1}$ by 12 Z/18 (Fig. 5b). These vertical cross sections also reveal the distinct frontogenesis along the coastline (reflected by the tightening of the gradient of potential temperature immediately along the coasts

in the plane of the cross section). Associated with the coastal frontogenesis is a shallow direct circulation (indicated by a "D" in Fig. 5b), which is marked by a separate ascent maximum in the warmer air to the east of the coastal front and descent in the colder air to the west. The FULL PHYS simulation produces a significant LLJ which develops in the region where the lower branch of the indirect circulation (associated with the STJ) and the upper branch of the direct circulation (associated with coastal frontogenesis and damming) merge near the 850 mb level.

To isolate the processes that contribute to the development of the LLJ a trajectory is shown for a parcel that passes through the low-level wind maximum in FULL PHYS and then compared to a parcel trajectory for ADB (Fig. 6). The trajectory from FULL PHYS confirms that the acceleration of parcels into the developing LLJ is related to (1) the westward movement of the parcel toward the developing coastal trough where the pressure gradient force is changing with time, and (2) the vertical displacement of the parcel through the baroclinic region associated with the coastal front. In effect, the rapid development of the LLJ within three hours represents a three-dimensional adjustment process in which parcels respond not only to horizontal displacement, but also to their vertical displacement within a baroclinic environment.

To determine the effect of the LLJ in the initial decrease of sea-level pressure, the mass flux divergence is computed through $21 Z/18$ for the areas which coincide with both the region of maximum SLP falls (as measured by three-hour tendencies) and the entrance region of the LLJ as simulated in FULL PHYS. The mass divergence profiles (Fig. 7) indicate the increase in the lower-level mass divergence (800 mb-900 mb) coincides with the rapid development of southeasterly winds in the entrance region of the LLJ. A shallow layer of mass convergence below the 900 mb level is consistent with the developing inverted trough along the coast. These persistent regions of mass divergence in the upper and lower troposphere are accompanied by decreasing SLP that marks the initial phase of secondary cyclogenesis along the coast.

Whitaker *et al.* (1988) also used a regional-scale numerical simulation to show that (1) the convergence of air streams originating in the stratosphere (to the west) and the ocean-influenced PBL (to the east) play a significant role in the rapid development phase of the Presidents' Day cyclone; (2) the divergence of the air streams above the 700 mb level contributed to the mass divergence and decrease in SLP; and (3) the development of the vortex involves baroclinic/dynamic and diabatic processes that interact throughout the entire depth of the troposphere.

4. Issues and Summary

While the problem of defining necessary conditions that are applicable to all rapidly developing cyclones remains an unresolved issue, the "self-development" concept defined by Sutcliffe and Forsdyke (1950), and discussed by Palmén and Newton (1969), does provide

a basis for describing the interactions of dynamical and physical processes that contribute to rapid cyclogenesis. The self-development concept has been applied to cyclones along the East Coast of the United States (Kocin and Uccellini, 1988), as depicted schematically in Fig. 8. The approach of an upper-level trough and jet streak moving towards the East Coast and the initial development of a surface cyclone act to focus and enhance the effects of warm-air advection, sensible heat flux, and moisture fluxes in the PBL, and latent heat release above 850 mb north and east of the surface low to warm the lower to middle troposphere near the axis of the upper-level ridge (Fig. 8a). The increased warming associated with these processes affects the divergence aloft in the following manner. The increased warming acts to slow the eastward progression of the upper-level ridge and to increase the ridge amplitude as the trough moves eastward. It amplifies (partly in response to an amplification in the cold air advection pattern to the west of the surface low-pressure center) and attains a negative tilt. The decrease in the wavelength between trough and ridge axes, an increase in the diffluence corresponding to the spread of geopotential height lines downstream of the trough axis, and the increase in the maximum wind speeds of the upper-level jet streaks all combine to enhance the divergence in the middle to upper troposphere above the surface low. The increased upper-level divergence (represented by an enhancement of the cyclonic vorticity advection in Fig. 8b) acts to deepen the cyclone even further.

As the surface low deepens, the lower-tropospheric wind field surrounding the storm increases in strength, especially to the north and east of the low, where the contribution of isallobaric effects and vertical motions to the acceleration of air parcels is large (Whitaker *et al.*, 1988) and frictional effects are minimal. Often, a low-level jet (LLJ) develops to the north and/or east of the storm center, increasing both the moisture transports toward the region of heavy precipitation and the warm-air advection pattern (Fig. 8b). Thus, the development of the LLJ enhances the warm-air advection beneath the ridge, further contributing to the self-development process that continues until the cyclone occludes and the heating is effectively cut off.

Self-development depends on (1) the existence of the upper-level features that concentrate the divergence aloft which is conducive to maximum ascent ahead of the developing surface low, and (2) warming (poleward and east of the surface low) due to diabatic processes and an enhanced thermal advection pattern associated with a low-level baroclinic zone and strong winds. Given the interaction among the various processes, it is not possible to designate one as more important than another in describing rapid cyclogenesis. Furthermore, it is difficult to separate the relative importance of upper and lower tropospheric forcing mechanisms since processes near the top of the troposphere, bottom of the stratosphere, and within the planetary boundary layer interact to influence the trough/ridge system, imbedded jet streaks, and associated vertical circulation patterns that extend throughout the entire troposphere. Thus, future studies on rapid cycloge-

nesis need to focus on describing the nonlinear interactions between the dynamical and physical processes described above. These studies will require enhanced observations combined with well-designed model experiments and improved numerical models to not only increase our understanding of rapid cyclogenesis, but also to enhance our ability to predict the occurrence of these storms with acceptable reliability.

Table 1
Maximum 850 mb winds and minimum SLP from numerical simulations
of the Presidents' Day cyclone

Experiment	Maximum 850 mb Winds		Minimum SLP				
	06Z/18	12Z/18	00Z/18	06Z/18	12Z/18	18Z/18	00Z/19
ADB	5	18	1032	1032	1032	1035	1036
BLYR NO LHT	5	24	1032	1030	1027	1027	1024
LHT NO BLYR	6	21	1032	1030	1032	1036	1036
FULL PHYS	6	31	1032	1028	1024	1022	1017

References

- Bjerknes, J., 1951: Extratropical Cyclones. *Compendium of Meteorology*, T. F. Malone, ed., Amer. Meteor. Soc. 577-598.
- Bosart, L. F., 1981: The Presidents' Day snowstorm of 18-19 February 1979: A subsynoptic-scale event. *Mon. Wea. Rev.*, **109**, 1542-1566.
- Buzzi, A., and S. Tibaldi, 1978: Cyclogenesis in the lee of the Alps: A case study. *Quart. J. Roy. Meteor. Soc.*, **104**, 271-287.
- Eliassen, A., and E. Kleinschmidt, 1957: Dynamic Meteorology. *Handbuch der Physik*, Vol. 48, J. Bartels, ed., Springer-Verlag, 1-154.
- Gyakum, J. R., 1983a: On the evolution of the QE II storm. I. Synoptic aspects. *Mon. Wea. Rev.*, **111**, 1137-1155.
- , 1983b: On the evolution of the QE II storm. II. Dynamic and thermodynamic structure. *Mon. Wea. Rev.*, **111**, 1156-1173.
- Hoskins, B. J., M. E. McIntyre, and A. W. Robertson, 1985: On the use and significance of isentropic potential vorticity maps. *Quart. J. Roy. Meteor. Soc.*, **111**, 877-946.
- Kocin, P. J., and L. W. Uccellini, 1988: *Snowstorms Along the Northeastern Coast of the United States: 1955 to 1985*. Amer. Meteor. Soc. Monograph, Boston, Mass. (accepted).
- Mattocks, C., and R. Bleck, 1986: Jet streak dynamics and geostrophic adjustment processes during the initial stages of lee cyclogenesis. *Mon. Wea. Rev.*, **114**, 2033-2056.
- Palmén, R., and C. W. Newton, 1969: Atmospheric Circulation Systems, Their Structure and Physical Interpretation. In *Geophys. Res.*, Vol. 13, Academic Press, 603 pp.
- Petterssen, S., 1956: *Weather Analysis and Forecasting*, Vol. 1. McGraw-Hill, 428 pp.
- Reed, R. J., and M. D. Albright, 1986: A case study of explosive cyclogenesis in the eastern Pacific. *Mon. Wea. Rev.*, **114**, 2297-2319.

- Roebber, P. J., 1984: Statistical analysis and updated climatology of explosive cyclones. *Mon. Wea. Rev.*, **112**, 1577-1589.
- Sanders, F., and J. R. Gyakum, 1980: Synoptic-dynamic climatology of the "bomb." *Mon. Wea. Rev.*, **108**, 1589-1606.
- Shapiro, M. A., and P. J. Kennedy, 1981: Research aircraft measurements of jet stream geostrophic and ageostrophic winds. *J. Atmos. Sci.*, **38**, 2642-2652.
- Stauffer, D. R., and T. T. Warner, 1987: A numerical study of Appalachian cold-air damming and coastal frontogenesis. *Mon. Wea. Rev.*, **115**, 799-821.
- Sutcliffe, R. C., and A. G. Forsdyke, 1950: The theory and use of upper air thickness patterns in forecasting. *Quart. J. Roy. Meteor. Soc.*, **76**, 189-217.
- Tracton, M. S., 1973: The role of cumulus convection in the development of extratropical cyclones. *Mon. Wea. Rev.*, **101**, 573-592.
- Uccellini, L. W., and P. J. Kocin, 1987: The interaction of jet streak circulations during heavy snow events along the East Coast of the United States. *Weather and Forecasting*, **2**, 289-308.
- , R. A. Petersen, K. F. Brill, P. J. Kocin, and J. J. Tuccillo, 1987: Synergistic interactions between an upper-level jet streak and diabatic processes that influence the development of a low-level jet and a secondary coastal cyclone. *Mon. Wea. Rev.*, **115**, 2227-2261.
- , 1986: The possible influence of upstream upper-level baroclinic processes on the development of the QE II storm. *Mon. Wea. Rev.*, **114**, 1019-1027.
- , 1984: Comments on "Comparative Diagnostic Case Study of East Coast Secondary Cyclogenesis under Weak Versus Strong Synoptic-Scale Forcing." *Mon. Wea. Rev.*, **112**, 2540-2541.
- , P. J. Kocin, R. A. Petersen, C. H. Wash, and K. F. Brill, 1984: The Presidents' Day cyclone of 18-19 February 1979: Synoptic overview and analysis of the subtropical jet streak influencing the pre-cyclogenetic period. *Mon. Wea. Rev.*, **112**, 31-55.
- Wash, C. H., J. E. Peak, W. F. Calland, and W. A. Cook, 1988: Diagnostic study of explosive cyclogenesis during FGGE. *Mon. Wea. Rev.*, **116**, 431-451.
- Whitaker, J. S., L. W. Uccellini, and K. F. Brill, 1988: A model-based diagnostic study of the rapid development phase of the Presidents' Day cyclone. *Mon. Wea. Rev.*, **116** (September issue).

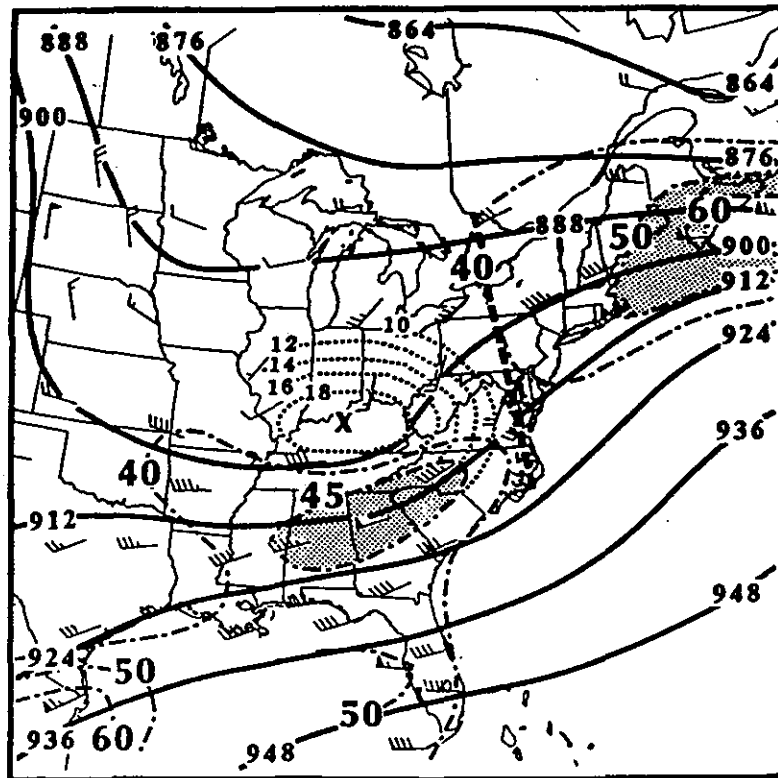


Fig. 1 The 300 mb geopotential height analysis (solid; 888 = 8880 m), isotachs (dot-dashed; 40 = 40 m s⁻¹), and selected isopleths of absolute vorticity (dotted; 18 = 18×10⁻⁵ s⁻¹) with vorticity maximum indicated by "X" at 1200 UTC 11 February 1983. Each flag denotes 25 m s⁻¹, each full barb denotes 5 m s⁻¹, each half-barb denotes 2.5 m s⁻¹, and shading represents wind speed intervals to depict jet streaks. Thick dashed line represents axis of cross section shown in Fig. 3. (From Uccellini and Kocin, 1987.)

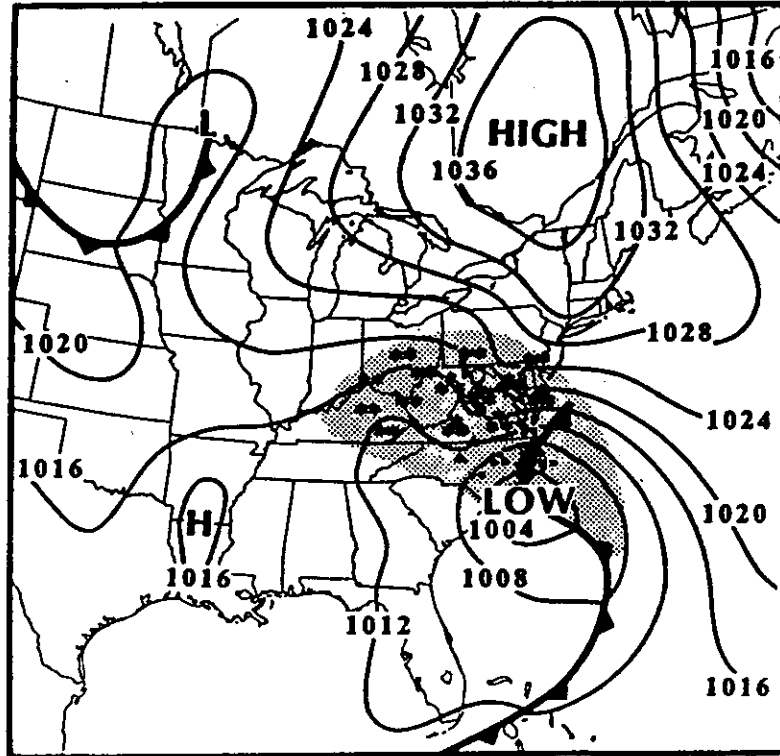


Fig. 2 Surface frontal and isobaric (solid, mb) analysis at 1200 UTC 11 February 1983. Shading represents precipitation. (From Uccellini and Kocin, 1987.)

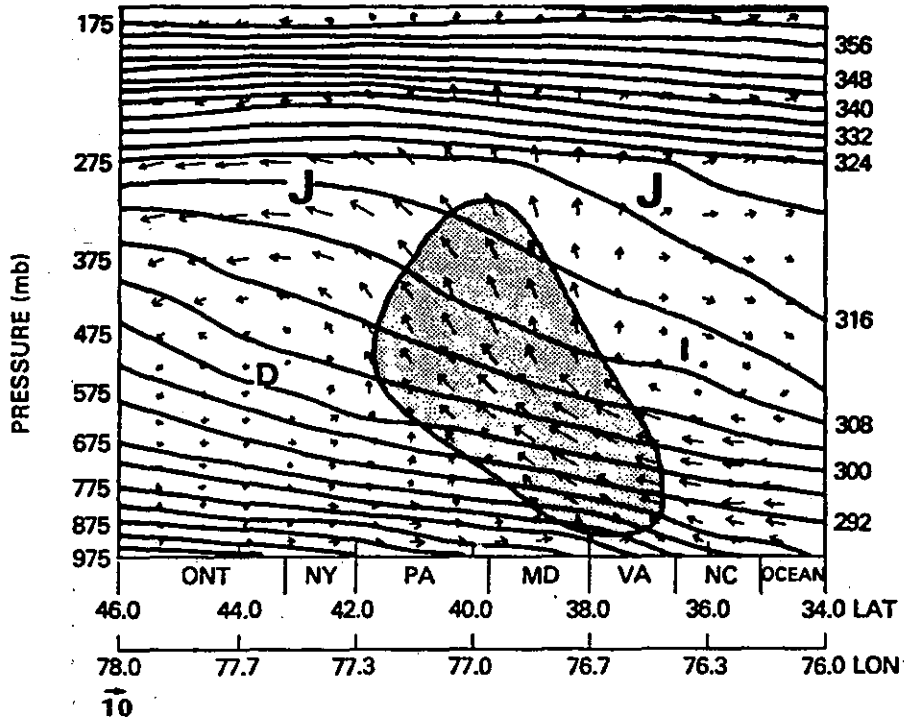


Fig. 3 Vector representation of vertical motions and ageostrophic wind components tangential to the plane of the cross section shown in Fig. 1 at 1200 UTC 11 February 1983, including isentropes (K) at 4K increments. The horizontal vector components are scaled at the bottom of the figure ($m s^{-1}$). Shading represents ascent in excess of $-5 \mu b s^{-1}$, positions of upper-level jet streaks are indicated by J. D and I denote centers of direct and indirect circulations, respectively. (From Uccellini and Kocin, 1987.)

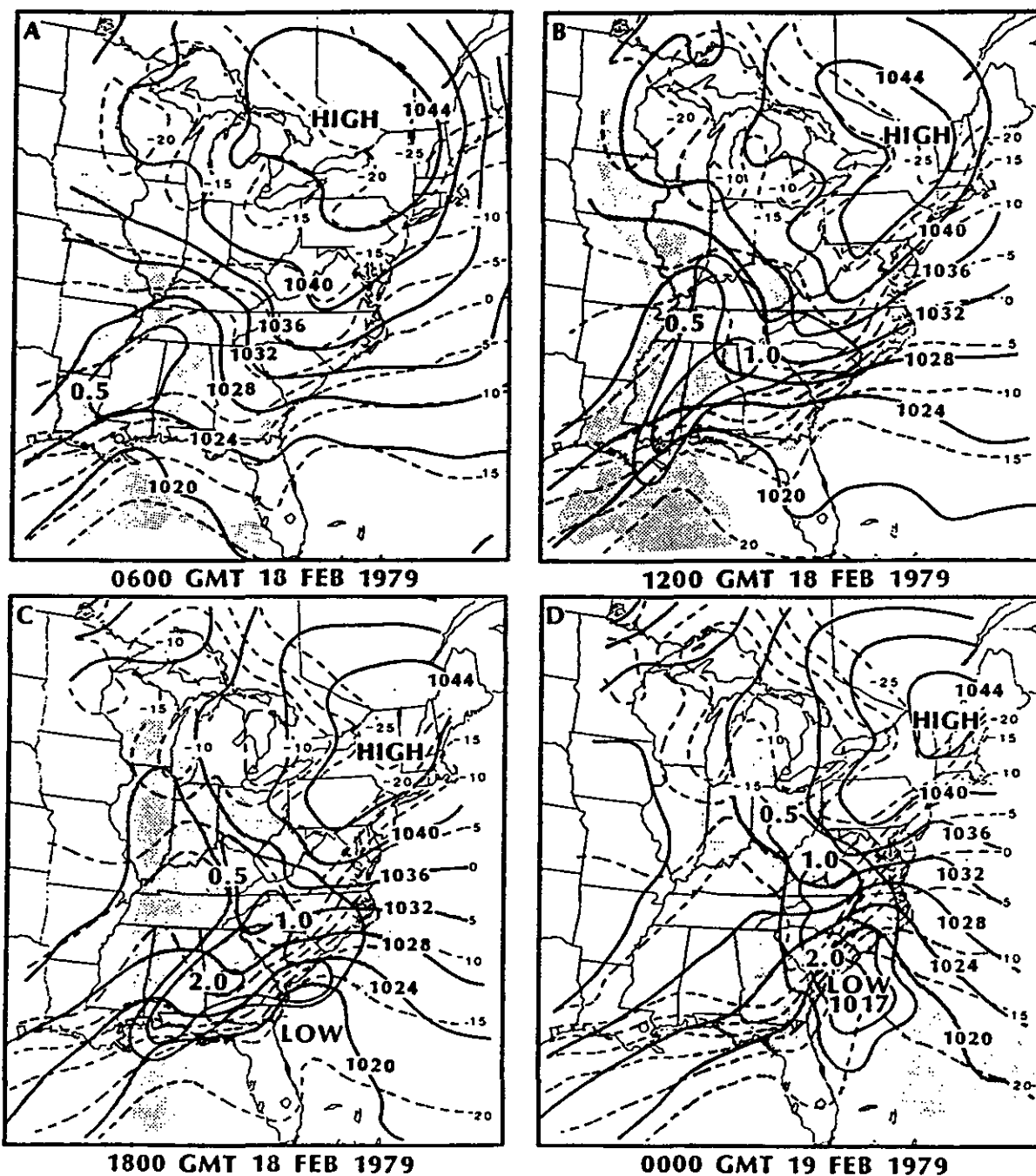


Fig. 4 Sea-level pressure (solid, mb) and isotherm analyses (dashed, °C) for lowest model level (near 1000 mb) for the full physics simulation (FULL PHYS). Alternating intervals of shading indicates six-hourly precipitation amounts greater than 0.02, 0.5, 1.0, and 2.0 cm. Thick dashed line represents inverted sea-level pressure trough. (From Uccellini *et al.*, 1987.)

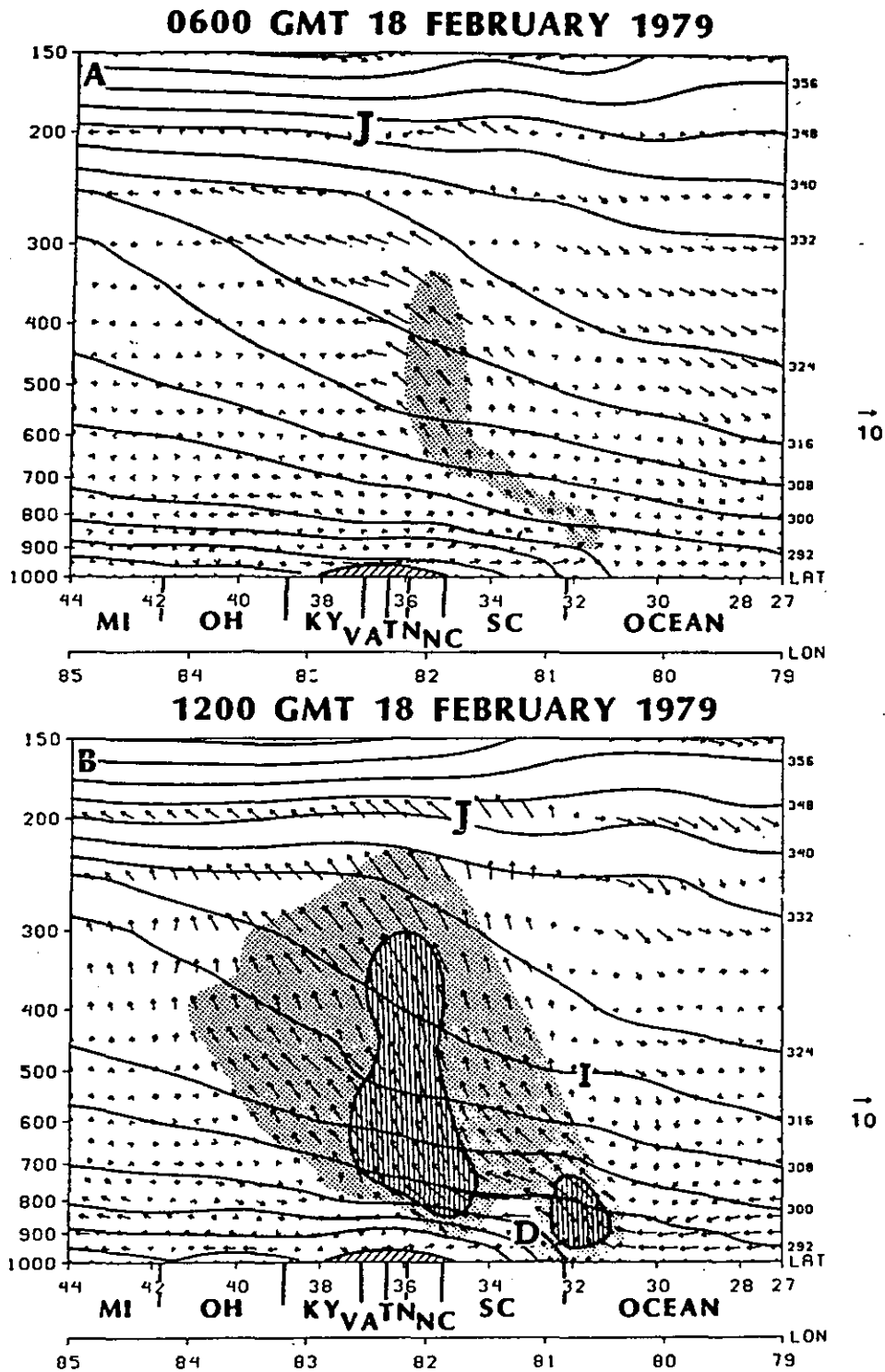


Fig. 5 Vertical cross sections derived from full physics simulation (FULL PHYS). Light and vertical shading indicate regions where ascent is greater than -4 and $-8 \mu\text{b s}^{-1}$, respectively. *D* in (b) refers to the direct circulation associated with coastal frontogenesis. (From Uccellini *et al.*, 1987.)

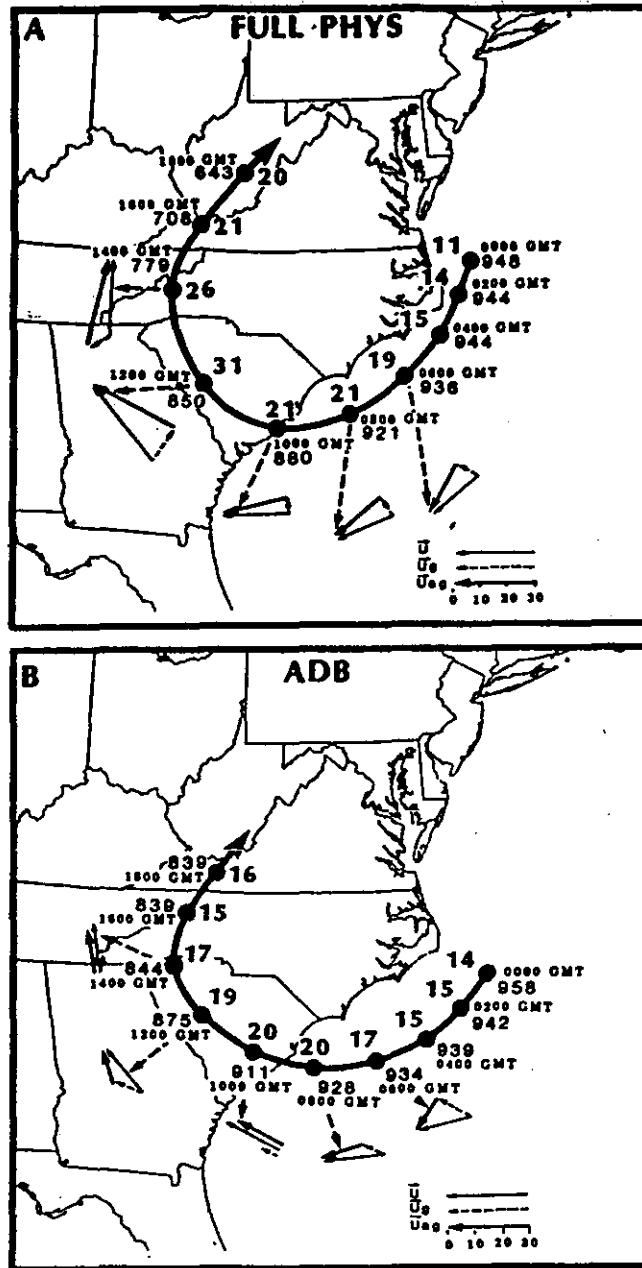


Fig. 6 Low-level trajectory from the (a) full physics simulation (FUL PHYS) and (b) adiabatic simulation (ADB). Two-hourly positions, total wind speed (m s^{-1}), and pressure (mb) indicated. Vector representation for total wind (U), geostrophic wind (U_g), and ageostrophic wind (U_{ag}) presented at two-hour intervals from 0600 through 1400 UTC. Vectors defined and lengths scaled (m s^{-1}) in bottom right corner. (From Uccellini *et al.*, 1987.)

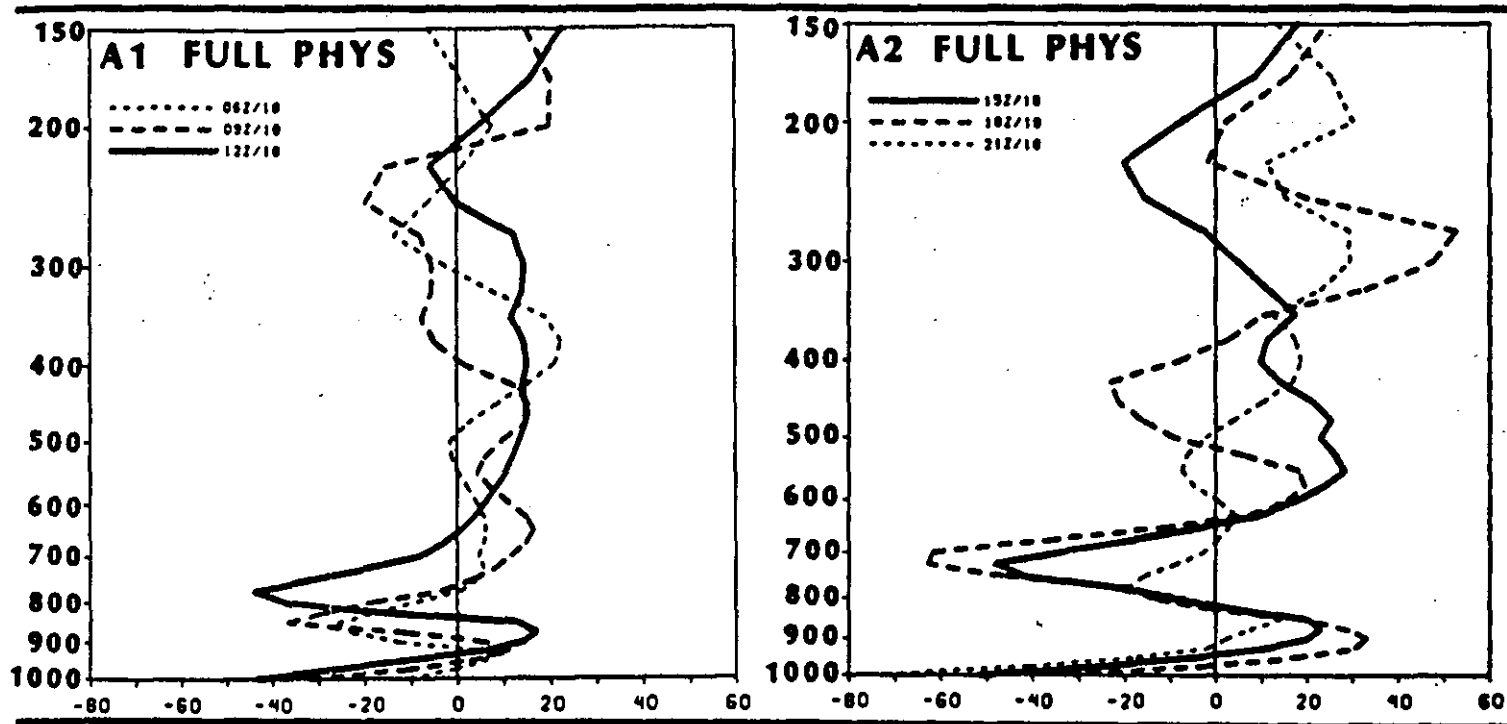


Fig. 7 Vertical profiles of area-averaged mass flux divergence ($10 = 10 \times 10^{-3} \text{ mbs}^{-1}$) computed for 0600 (thin dashed), 0900 (thick dashed), and 1200 UTC (solid) in the left column and 1500 (solid), 1800 (thick dashed), and 2100 UTC (thin dashed) in the right column. Profiles from full physics simulation (FULL PHYS). (From Uccellini *et al.*, 1987.)

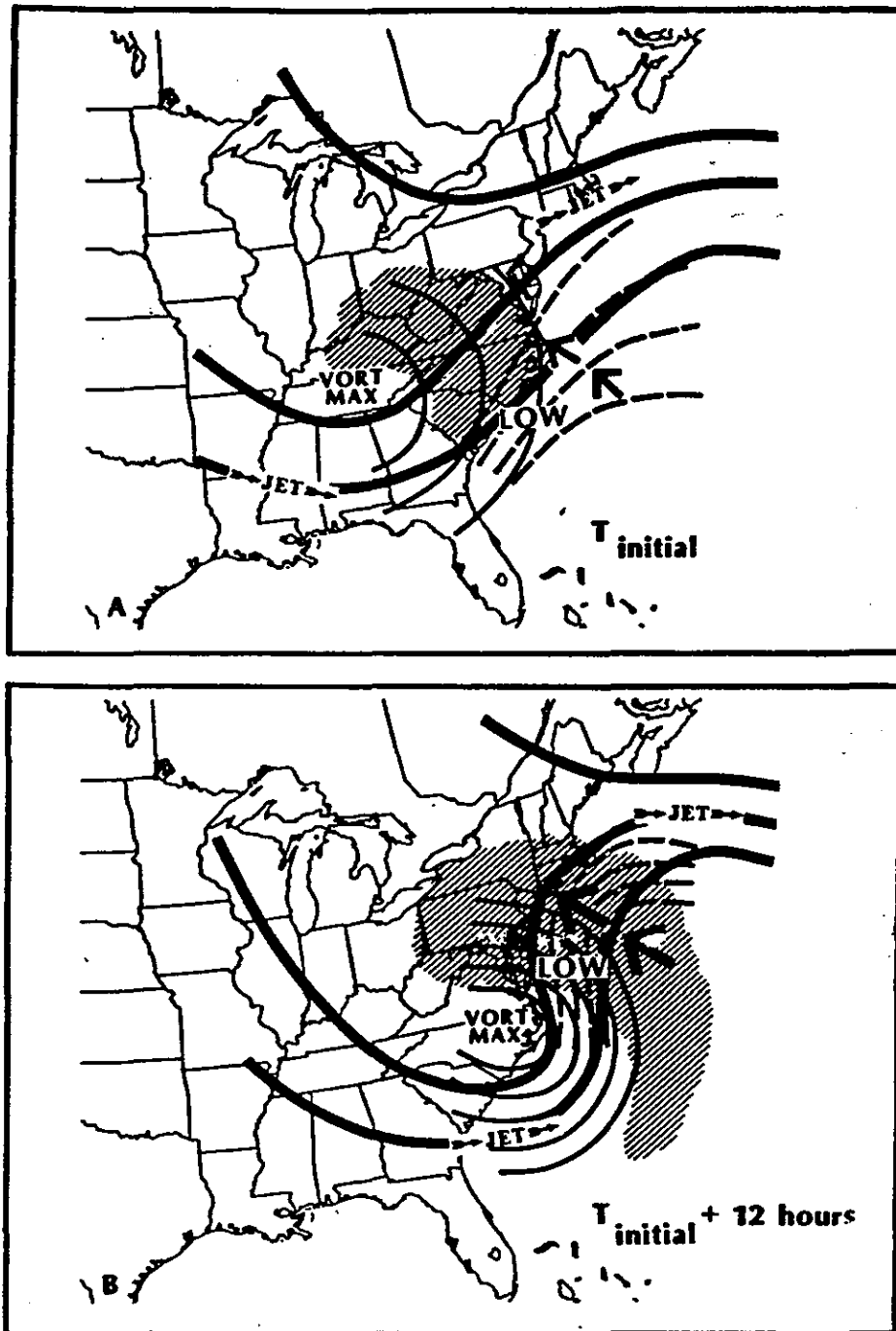


Fig. 8 Schematic of the “self-development” concept that relates how the temperature advections, sensible heat fluxes and moisture fluxes in the PBL, and latent heat release associated with cyclogenesis enhance the amplitude of upper-level waves and decrease the wavelength between trough and ridge axes, which contributes to an increase in upper-level divergence (as inferred by the enhanced cyclonic vorticity advection pattern in (b)) that further enhances cyclogenesis. (From Kocin and Uccellini, 1988.)

Winter Forecast Problems Associated With Light to Moderate Snow Events in the Mid-Atlantic States on 14 and 22 February 1986¹

Jeffrey Homan² and Louis W. Uccellini³

²*General Sciences Corporation, Laurel, MD 20707*

³*NASA/Goddard Space Flight Center, Greenbelt, MD 20771*

1. Introduction

The occurrence of several major snowstorms along the East Coast of the United States during the past decade has generated considerable interest in the published literature. Examples include a review of 18 major snowstorms in the eastern United States by Kocin and Uccellini (1985a,b), analyses of the Presidents' Day snowstorm of 18-19 February 1979 by Bosart (1981), and Uccellini et al. (1984, 1985) and those of the 11-12 February 1983 megapolitan snowstorm by Bosart and Sanders (1986). These storms are an obvious cause for concern to weather forecasters because of their potential impact to metropolitan areas. However, their relatively rare occurrence should not distract forecasters and researchers alike from understanding and predicting the weather associated with weaker systems which occur more frequently. Indeed, as noted by Maddox and Doswell (1982) for severe weather events in the central United States, the forecasting problems associated with the weaker systems can actually be more troublesome than those related with the super storm, since the dynamic and thermodynamic factors that contribute to the weather associated with such systems may be more difficult to analyze, diagnose, and predict.

In this paper, a short review of two case studies of light to moderate snow events which affected the Middle-Atlantic states during 14 and 22 February 1986 are presented. These cases were selected because significantly different snowfall and precipitation patterns were generated by two systems with similar upper-tropospheric and surface features. Furthermore, the numerical forecast guidance and local forecasters displayed minimal skill in forecasting the amount of snow associated with these systems. Synoptic analyses of the 14 February and 22 February 1986 cases are found in section 2. Isentropic analyses are presented in section 3

¹This work is derived from an article which appears in *Weather and Forecasting* by Homan and Uccellini (1987).

that relate the lower-tropospheric thermal, wind, and moisture fields to the different snowfall patterns and rates for each case. The results of these studies are summarized in Section 4.

2. Synoptic Descriptions

a. Case 1: 14 February 1986

The surface weather conditions for the East Coast at 1200 GMT 14 February 1986 were dominated by a cold high-pressure center positioned off the North Carolina coast, accompanied by sub-freezing temperatures as far south as central Georgia (Fig. 1a). A 1008 mb low-pressure center near the Arkansas-Oklahoma border was located along the southern end of a cold front extending southwest from the Great Lakes region. At this time, moderate snow and freezing rain were occurring over Kentucky and Tennessee, where 2.5 to 7.5 cm (1 to 3 in) of snow had already accumulated by 1200 GMT 14 February. By 1800 GMT, the area of low pressure initially in Arkansas consolidated into one center in southern Tennessee and did not deepen (Fig. 1b). Light snow was commencing in the western regions of Maryland and Virginia, but moderate to heavy snow was confined to eastern Kentucky, Tennessee, and southwestern Virginia. During the next 6 hrs the low pressure system weakened slightly while moving slowly eastward and by 0600 GMT 15 February was located over southeastern North Carolina. Most of the Middle-Atlantic area was experiencing light snow, southerly winds, and temperatures below freezing, but the heaviest snow continued to fall south and southwest of Washington, DC, north of a warm front located across the North Carolina-South Carolina border.

At upper levels, the 300- and 500-mb analyses at 1200 GMT 14 February showed a trough extending southward from Iowa to eastern Texas (Figs. 2a and 2b). Cyclonic horizontal wind shear near the base of the trough axis contributed to a vorticity maximum of $16 \times 10^{-5} s^{-1}$ over Oklahoma at the 500-mb level (Fig. 2b), with significant positive vorticity advection (PVA) from Arkansas to Kentucky (not shown). At 850 mb, strong warm-air advection was occurring over the Tennessee Valley. By 0000 GMT 15 February, the 500-mb trough and associated $16 \times 10^{-5} s^{-1}$ vorticity maximum moved into the Ohio Valley (Fig. 2e). However, at 850 mb, the widespread warm-air advection initially over the Tennessee Valley and southeastern states was now mainly confined to the Carolinas and southern Virginia, with little or no indication of a thermal ridge over the southeastern United States. Furthermore, the warm-air advection over Washington, DC, was weak to nonexistent at this time.

An analysis of precipitation and snow totals over the Mid-Atlantic States for this case is shown in Fig. 3. Although a moderate snowfall of 3-5 inches was predicted for the Washington, DC area, most snowfall amounts were in the *light*

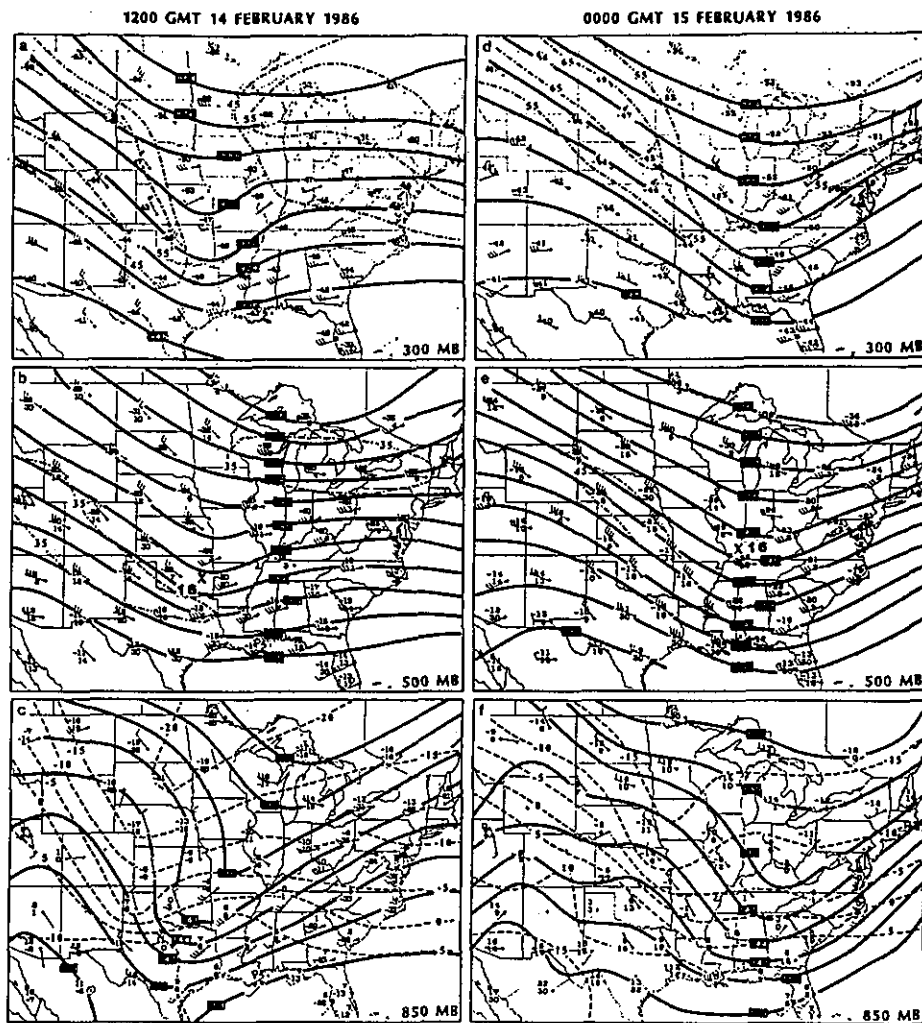


Fig. 2. Upper-level analyses at 300, 500, and 850 mb for 1200 GMT 14 February (a, b, c) and 0000 GMT 15 February (d, e, f).

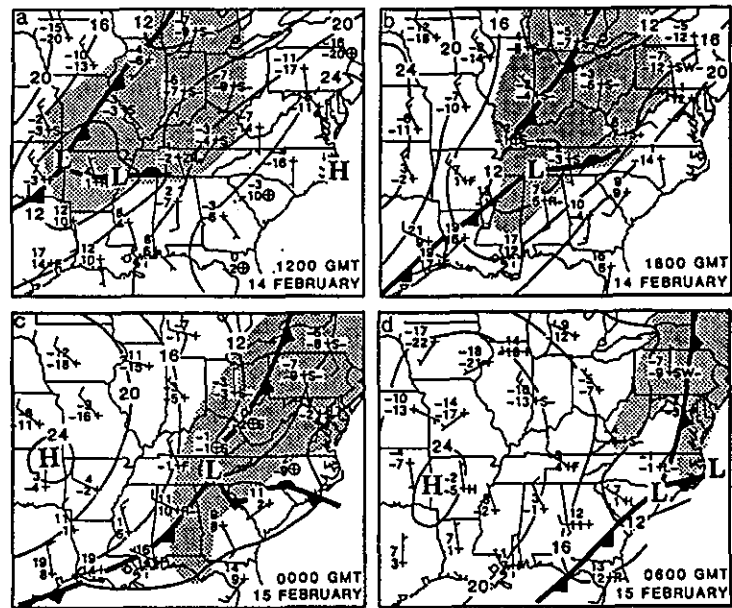


Fig. 1. Three-hourly sea-level pressure (mb) and surface frontal analyses between 1200 GMT 14 February and 0600 GMT 15 February. Shading depicts area of precipitation.

range of 1-3 inches across Maryland and northern Virginia. Precipitation amounts decreased substantially east of the Appalachian Mountains, however, a local maximum of snowfall (3 to 6 in) and precipitation did extend across the southern half of Virginia north of a surface warm front and in an area of significant 850-mb warm-air advection that remained south of Washington, DC. It appears, therefore, that 1) the weakening surface system (which was perhaps related to an unfavorable thermal field east of the mountains), 2) the confinement of the 850-mb warm-air advection pattern to the south of the Washington, DC, region, and 3) the location of the surface warm front in the Carolinas were contributing factors to the precipitation distribution for this case.

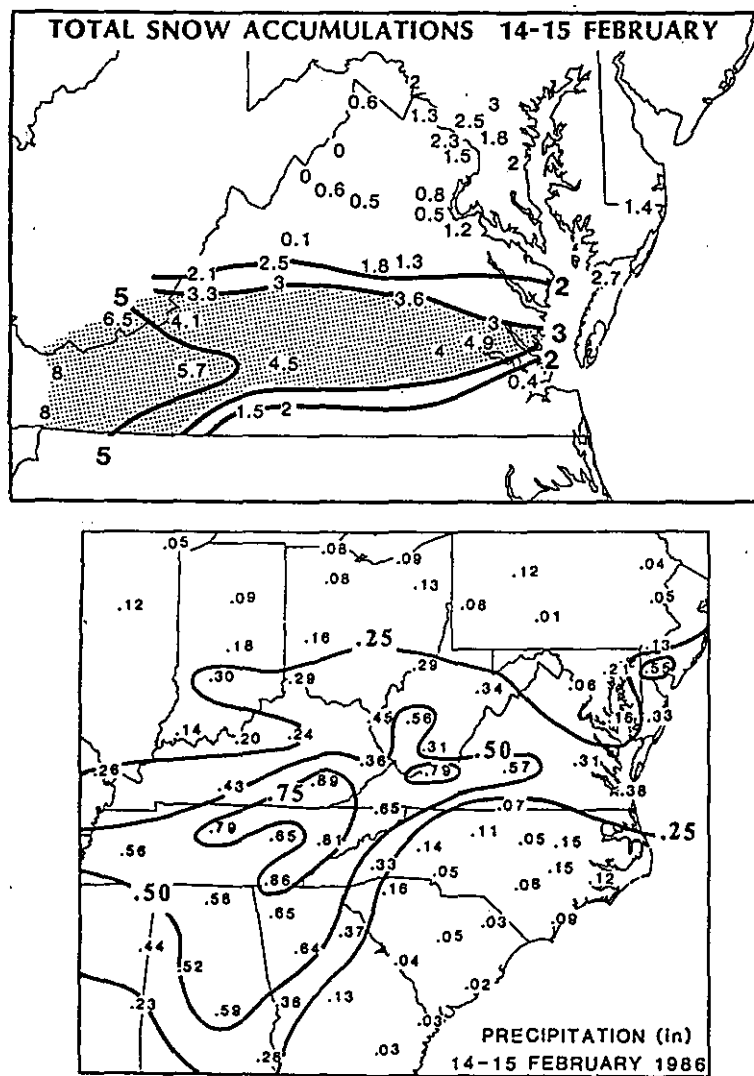


Fig. 3. Snowfall distribution (in) across the Virginia-Maryland area (top) and total precipitation amounts (in) from 1200 GMT 14 February through 1200 GMT 15 February.

b. Case 2: 22 February 1986

During the afternoon and early evening of 22 February, the Washington, DC, area was *surprised* by a moderate snowfall event. At 1200 GMT 22 February, a weak surface low (with a central pressure of 1012 mb) was located in northern Georgia and a surface high-pressure ridge penetrated southward along the East Coast of the United States (Fig. 4a). By 1800 GMT, the surface low moved eastward to South Carolina (Fig. 4b), with an inverted trough extending north toward Ohio and an expanding area of precipitation located from eastern Tennessee to western Virginia. In the following 6 hrs, the surface low moved to the southern South Carolina coast, with an inverted trough extending northward to a low over northeastern Ohio. An area of moderate to heavy precipitation rapidly expanded just east of the trough axis and now covered most of Virginia and Maryland (Fig. 4c). Moderate snow and sleet were observed over the immediate Washington, DC region as temperatures dropped to near freezing shortly after the onset of precipitation. Over central Virginia the precipitation was primarily rain.

The 300- and 500-mb analyses at 1200 GMT 22 February are similar to the 14-15 February case in that a weak to moderate trough stretched north-south across the middle of the United States and was approaching the East Coast (Figs 5a and 5b). At 500 mb, several separate vorticity maxima can be identified along the trough axis, from Minnesota to Texas (Fig. 5b), contributing to a broader area of positive vorticity advection downstream of the trough axis than in the 14 February case. At 850 mb, two distinct troughs can be isolated at 1200 GMT 22 February (Fig. 5c). One trough was located over Minnesota. The second trough was positioned over Kentucky and was characterized by a distinct closed circulation. An easterly component in the wind field over Ohio and West Virginia provides supporting evidence for the second system located just downwind of the 500-mb vorticity maximum located over northern Missouri. By 0000 GMT 23 February, the 300- and 500-mb trough moved eastward to a position extending southeastward from the upper Midwest to the Ohio Valley and then southwestward to the Gulf Coast by 0000 GMT 23 February (Figs. 5d and 5e). At 850 mb, the two troughs originally over Minnesota and Kentucky appear to have combined into one trough with an axis tilted from the northwest to southeast (negative tilt) across Michigan to Virginia (Fig. 5f). As a result, an easterly component to the wind field can be identified across Maryland and Delaware, a marked contrast to 14 February, where southwesterly winds were prevalent across the entire Middle-Atlantic region. A localized warm-air advection pattern developed over Maryland and northern Virginia as the 850-mb winds shifted to the south-southeast along a pronounced temperature gradient that was increasing in magnitude across Virginia and North Carolina.

Local forecasters for the Washington, DC area predicted that *light* snow would begin during the *evening* hours of 22 February with little, if any, accumulation. Yet,

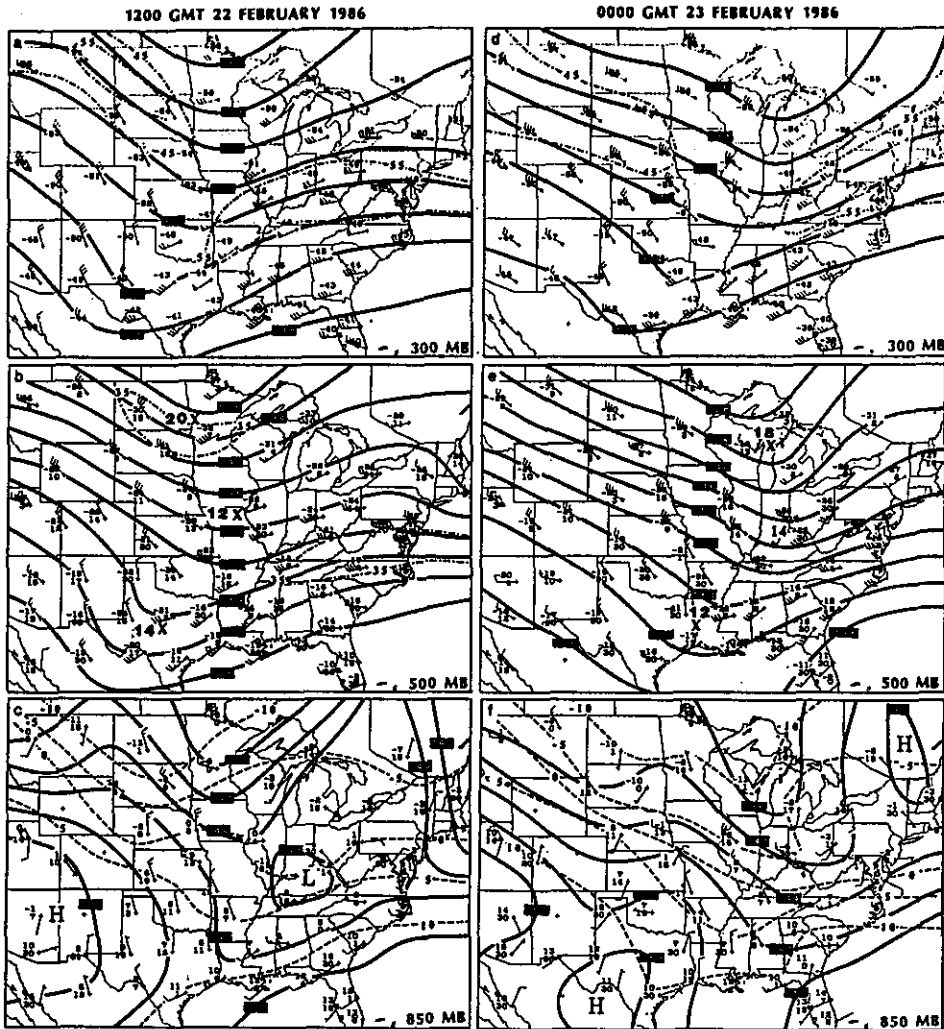


Fig. 5. Upper-level analyses at 300, 500, and 850 mb for 1200 GMT 22 February (a, b, c) and 0000 GMT 23 February (d, e, f).

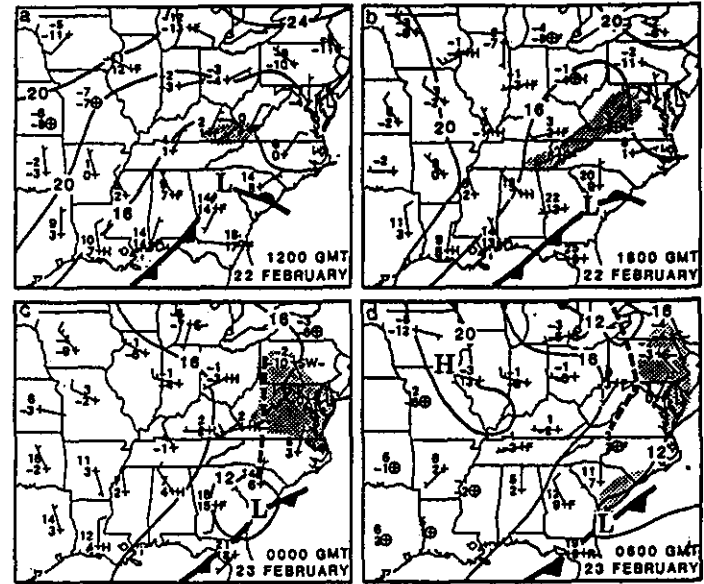


Fig. 4. Three-hourly sea-level pressure (mb) and surface frontal analyses between 1200 GMT 22 February and 0600 GMT 23 February. Shading depicts area of precipitation.

snow began falling by *mid-afternoon* and accumulations ranged from 7.5 to 12.5 cm (3 to 5 in), with the heaviest accumulations in the northern suburbs (Fig. 6). Precipitation amounts greater than $\frac{1}{4}$ in extended into southern Pennsylvania with maximum amounts located over Delaware, Maryland and central Virginia (Fig. 6). Amounts decreased rapidly over southern Virginia.

In the following section, a more detailed examination of the low-level thermal and dynamic processes is presented for each case to highlight the significant differences which might discriminate as to why one case produced light snowfall (and precipitation) in the Washington, DC, area and heavier snowfall (and precipitation) further south, while the second case produced a heavier precipitation area that extended from central Virginia into southern Pennsylvania.

3. An examination of the low-level thermal, wind, and moisture fields for each case

Isentropic analyses are now presented to highlight the different characteristics of the lower-tropospheric thermal fields for each case. These analyses, which include a computation for the vertical motion on isentropic surfaces, are used to diagnose the probable region of maximum ascent that can then be related to the different precipitation distributions for each case.

a. Vertical motion diagnostics in isentropic coordinates

There are several reasons for presenting diagnostics in the isentropic framework in addition to the isobaric coordinate system. As a first approximation, isentropic surfaces can be thought of as material surfaces which can slope through a significant portion of the atmosphere. Thus, one surface can usually be selected to map out the interaction between the lower and middle troposphere in a baroclinic environment. The sloped nature of the isentropic surface also provides for more continuous moisture analyses than either isobaric or Cartesian coordinate surfaces (Uccellini, 1976; Boyle, 1981). Analyses of wind (\vec{V}) and pressure (p) on an isentropic surface can yield a direct, quantitative estimate of the vertical velocity (ω) simply from the expansion of the total derivative ($\frac{dp}{dt}$) where:

$$\omega = \frac{dp}{dt} = \underbrace{\frac{\partial p}{\partial t}}_1 + \underbrace{\vec{V} \cdot \nabla_{\theta} p}_2 + \underbrace{\dot{\theta} \frac{\partial p}{\partial \theta}}_3$$

The local pressure change [term (1)] over a 12-h period can be estimated at specific locations using successive upper-air maps, although the 12-h temporal resolution of the operational data network may severely restrict a proper estimation of this term. The contribution to vertical motion due to the horizontal advection

of pressure [term (2)] is determined from a single map. Air flowing from high pressure on an isentropic surface (relatively warm air) toward lower pressure (relatively colder air) contributes to ascent ($-\omega$) and will be termed "upslope" flow in the remainder of the paper. The contribution to vertical motion derived from term (2) is similar to the contribution related to the temperature advection computed in isobaric or Cartesian coordinates. The diabatic heating term [term (3)] is important in regions of clouds and precipitation. Latent heat release ($\dot{\theta} > 0$) contributes to ascent through individual isentropic surfaces, while evaporative and radiative cooling ($\dot{\theta} < 0$) contribute to descent. The third term is difficult to measure given the uncertainty in computing the magnitude of $\dot{\theta}$. The evaluation of term (3) is further complicated by the fact that the local pressure tendency term will always act against the diabatic term. For example, the release of latent heat ($+\dot{\theta}$) contributes not only to ascent ($-\omega$) through term (3), but also to a local increase in temperature. This local temperature increase forces isentropic surfaces to higher pressure, which contributes to descent ($+\omega$) through term (1). The offsetting nature between the local pressure tendency and diabatic terms has led Saucier (1955) and Uccellini (1976) to note that the pressure advection term provides a good approximation to ω , especially when wind speeds are large and streamlines are at a significant angle to the isobars on an isentropic surface. Thus, the "horizontal" flow along an isentropic surface can be viewed as implicitly including an adiabatic component of the vertical motion which is easy to compute at any given time. In the following sections, isentropic analyses [derived using the Petersen (1986) objective analysis scheme on a 2 X 2 latitude-longitude grid] and vertical motion diagnostics are applied to the 12-h operational database.

b. 14 February 1986

The contribution to vertical motion from terms 1,2 and 3 on the 284-K isentropic surface are shown in Fig. 7 for 1200 GMT 14 and 0000 GMT 15 February 1986. At 1200 GMT, the ascent associated with the advective term is maximized at $6.3 \mu s^{-1}$ over eastern Arkansas (Fig. 7a) and is consistent with the warm-air advection inferred at 850 mb across Tennessee, Kentucky, and Arkansas (Fig. 2c). The contribution to vertical motion related to the local pressure tendencies between 1200 GMT 14 February and 0000 GMT 15 February [term (1) in equation (1)], although much weaker, also contributes to ascent over much of Arkansas and Kentucky (Fig. 7c). Superimposed radar echoes from 1135 GMT reveal the bulk of the precipitation falling in the area of upslope flow, where mixing ratio values exceed 2 g kg^{-1} (not shown).

By 0000 GMT the pressure gradient on the 284-K isentropic surface increases dramatically from Georgia to southern Virginia. The ascent related to term (2) is greater than $6 \mu s^{-1}$ over Georgia and South Carolina (Fig. 7b). In addition,

mixing ratio values on the 284-K surface have increased to greater than 4 g kg^{-1} over this region in response to the increasing moisture advections from the Atlantic Ocean and Gulf of Mexico (not shown). However, this upslope flow weakens considerably over northern Virginia and Maryland to values less than $2 \mu\text{s}^{-1}$, where westerly winds are directed parallel to the isobars. The rising motion in this area is diminished further by the descent related to the local pressure tendency term [term (1)] in equation 1 (Fig 7c). Thus, the evaluation of the vertical motion from the pressure and wind analyses on the 284-K isentropic surface reveals that the region of maximum ascent in the lower to middle troposphere remained to the south of Washington, DC. The precipitation distribution (Fig. 3) is consistent with the vertical motion calculations as the majority of the precipitation is confined to the area south and southwest of Washington, DC.

c. 22 February 1986

For the second case, the 288-K isentropic surface extends from about 975 mb in the southeastern United States to 650 mb over the Great Lakes. At 1200 GMT 22 February, the contribution to the vertical motion related to term (2) shows the existence of two distinct ascent maxima, one over northern Kentucky approaching $1.4 \mu\text{s}^{-1}$ and a much stronger maximum over Wisconsin (Fig. 8a). A small area of precipitation is located within the region of weak upslope flow in eastern Kentucky and western Virginia at 1200 GMT (see Fig. 4a). Although a large pressure gradient exists across the Carolina region, the wind flow is weak and is found to be either parallel to the isobars or directed from low to high pressure, which contributes to descent in that area (Fig. 8a).

By 0000 GMT 23 February, the strongest pressure gradient on the 288-K isentropic surface is now located from northern Georgia to southern Virginia, with south-to-southeasterly flow directed toward lower pressure across most of Virginia, Maryland, and Pennsylvania. This shift in the pressure gradient and the southerly flow regime results in the development of a localized upslope flow pattern in eastern Maryland and Virginia, where values of ascent associated with term (2) are greater than $2 \mu\text{s}^{-1}$ (Fig. 8b). This area of maximum ascent is located 300 km to the northeast of the maximum ascent diagnosed at 0000 GMT 15 February. In addition, the moisture-laden air originally confined to the Southeast has moved northward, coinciding with the expanding radar echoes at 0000 GMT across Maryland and Virginia (not shown). Unlike the 14 February case, the contribution to the vertical motion from the local pressure tendency term adds to the ascent pattern over northern Virginia and Maryland. All these features are consistent with the development of the moderate snow over the Washington, DC, region which occurred prior to 0000 GMT 23 February.

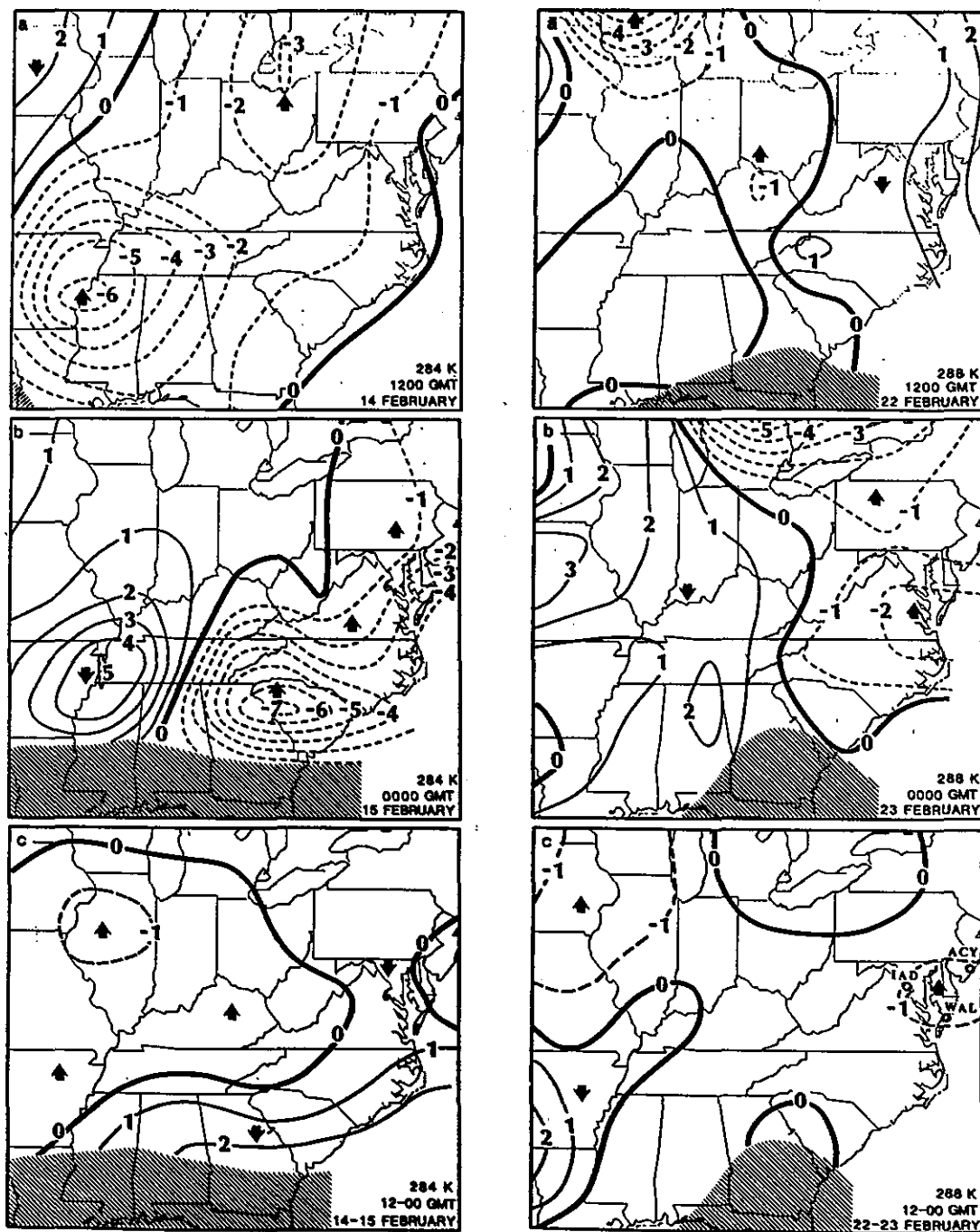


Fig. 7. (left 3 panels) a) Diagnosis of vertical motion field on 284-K isentropic surface related to advection term [term (2)] for 1200 GMT 14 February (dashed lines depict ascent, solid lines depict descent; μs^{-1}). b) Same as (a), but for 0000 GMT 15 February. c) pressure tendency term [term (1)] over 12-h period.

Fig. 8 (right 3 panels) same as Fig. 7 except on 288-K surface for 22-23 February.

d. Discussion

The 14 February and 22 February 1986 cases represent situations in which the evolution of upper-level features and the surface pressure field appear to evolve in a similar manner over a 12-h period. Yet, the lower-tropospheric thermal fields, advection patterns, distribution of ascending motion, and associated precipitation distribution are different. These differences are illustrated in the schematic in Fig. 9. In the 14 February 1986 case, as the PVA/divergence field moved over the Washington, DC, region, the low-level response was marked by an upslope flow regime (850-mb warm-air advection pattern) which was maximized over North Carolina and southern Virginia. Not only were the largest thermal gradients located well to the south of Washington, DC (from Georgia to North Carolina), the deflection of the southerly airstream toward the east (parallel to the isobars) on the 284-K isentropic surface over northern Virginia also limited the upslope flow. The confinement of this upslope flow and low-level convergence to the area south of Washington, DC, effectively cut off the northern extension of the precipitation field by 0000 GMT 15 February. Thus, the maximum ascent and associated precipitation region were confined primarily to the area south of Washington, DC (Fig. 9a).

In the 22 February 1986 case, the upper-level PVA/divergence field moved over the Washington, DC, region as in the previous example. However, in this case, the maximum slope in the isentropic surfaces in the lower troposphere was located farther north [North Carolina and southern Virginia (Fig. 9b)], with the upslope flow extending into Pennsylvania above the colder boundary layer air mass that had been advected south by the north-northeasterly surface winds early on 22 February. The northward displacement of the upslope flow and low-level convergence in this case compared to the 14 February case appears to account for the moderate to heavy precipitation affecting the Washington, DC, area and extending into southern Pennsylvania.

The emphasis in this paper on the evolution of low-level thermal and wind fields and associated advection patterns is similar to the recent studies of convective environments in the middle United States by Maddox and Doswell (1982), and Gaza and Bosart (1985). These diagnostic studies have attempted to focus the attention on low-level forcing for vertical motion related to warm-air advection patterns as a separate entity, especially when the upper-level forcing related to PVA is weak or apparently nonexistent (at least not strong nor extensive enough to be resolved by the operational radiosonde network). Likewise, in the winter storm situations described in this paper, the low-level thermal field appears to be a critical factor in the evolution of the precipitation fields associated with each storm. Nevertheless, the viewpoint depicted in Fig. 9 is based on a concept that the warm-air advection pattern represents a manifestation of the sloped response to upper- and middle-tropospheric divergence in a statically stable, baroclinic environment. Therefore,

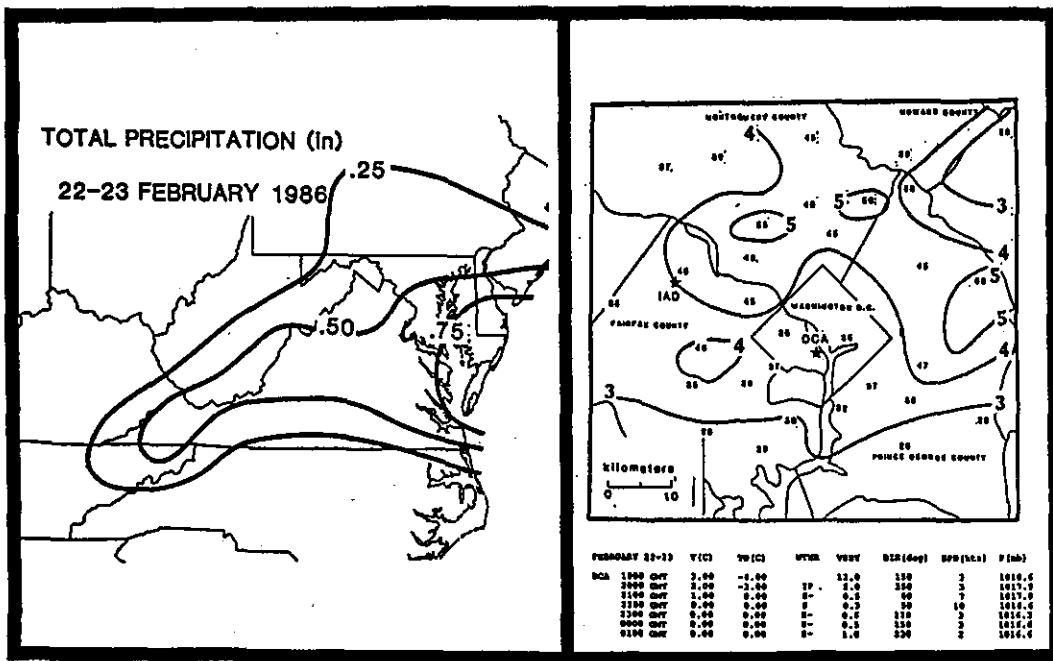


Fig. 6. Total precipitation amounts (in) across the Mid-Atlantic region (left panel) and snowfall distribution (in) across the Washington, DC area for 22-23 February.

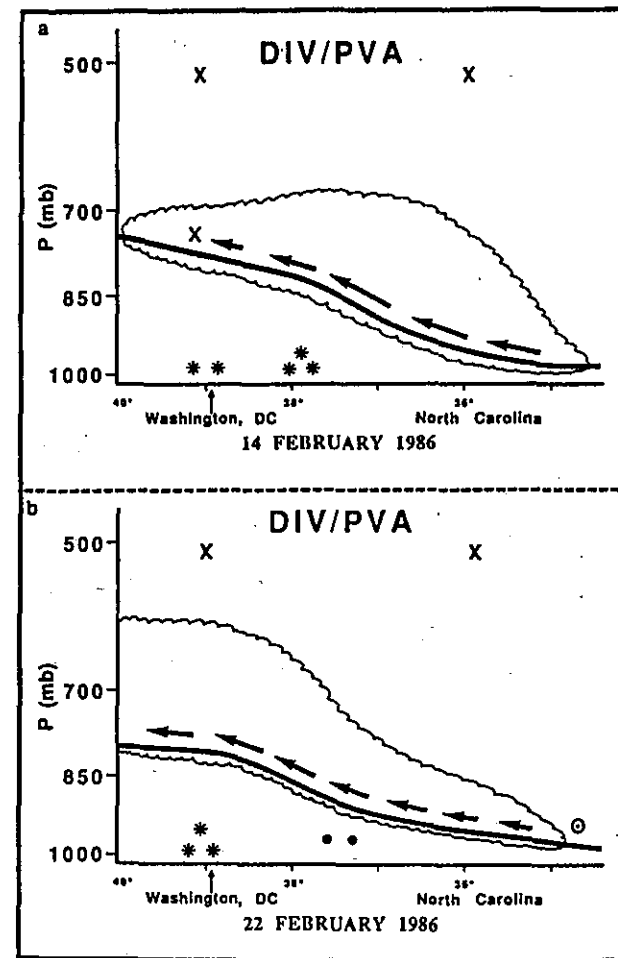


Fig. 9. Schematic cross sections of low-level flow regime for a) 14 February and b) 22 February cases with vertical axis (pressure, mb) and horizontal axis (degrees latitude). Representative isentropic surface indicated by heavy sloped line; upslope flow within plane of cross section illustrated using wind vectors for each case; flow into the page indicated by an X and flow out of the page indicated by \ominus . Clouds represented by scalloped region.

the warm-air advection should not necessarily be viewed as a separate physical process in the forcing of vertical motion.

A unique aspect of these case studies is the use of isentropic analysis routines that provided for straightforward computations of vertical motion fields. These isentropically based vertical motion computations depicted the different ascent patterns that 1) could be directly related to the difference in the low-level thermal distribution and wind fields and 2) could account for the areal distribution of significant precipitation for each case. The application of an isentropic approach for diagnosing the sloped nature of the low-level flow field (and the associated ascent patterns) that characterizes baroclinic regimes provides yet another example of the advantages of isentropic coordinates for diagnosing factors which contribute to significant weather events. These results, combined with the expanding use of isentropic analysis routines in other research institutes, serve as a reminder to Oliver and Oliver's (1951) comments following the cessation of the routine transmission of isentropic charts in the late 1940s:

Experienced forecasters and analysts, however, who had become familiar with the isentropic chart generally felt, and still feel, that a long step backwards was taken when isentropic analysis was abandoned. With the present trends towards the concentration of analysis in large centers, with the increased accuracy of radiosondes, and with the advent of improved communication facilities, the time seems ripe for reinauguration of the isentropic chart. (p. 726).

Given plans for the upgrade of the transmission of data and charts by the National Weather Service (NWS), the time still "seems ripe for the reinauguration" of isentropic-based datasets.

REFERENCES

- Bosart, L. F., 1981: The Presidents' Day snowstorm of 18-19 February 1979: A subsynoptic-scale event. *Mon. Wea. Rev.*, **109**, 1542-1566.
- Bosart and F. Sanders, 1986: Mesoscale structure in the megalopolitan snowstorm of 11-12 February 1983. Part III: A large-amplitude gravity wave. *J. Atmos. Sci.*, **43**, 924-939.
- Boyle, J. S., 1981: Autocorrelations of moisture parameters on isentropic surfaces. *Mon. Wea. Rev.*, **109**, 2401-2404.
- Gaza, R. S., and L. F. Bosart, 1985: The Kansas City severe weather event of 4 June 1979. *Mon. Wea. Rev.*, **113**, 1300-1320.

- Homan, J. H. and L. W. Uccellini, 1987: Winter forecast problems associated with light to moderate snow events in the Mid-Atlantic States on 14 and 22 February 1986. *Wea. and For.* **1**, 206-228.
- Kocin, P. J. and L. W. Uccellini, 1985a: A survey of major East Coast snowstorms, 1960-1963. Part 1: Summary of surface and upper-level characteristics. *NASA TM 86195*, [NTIS N85-27471], 101 pp. (Also tentatively accepted for publication as a Meteorological Monograph.)
- Kocin, P. J. and L. W. Uccellini, 1985b: A survey of major East Coast snowstorms, 1960-1983. Part 2: Case studies of eighteen storms. *NASA TM 86196*, [NTIS N85-27472], 214 pp. (Also tentatively accepted for publication as a Meteorological Monograph.)
- Maddox, R. A., C. A. Doswell III, 1982: An examination of jet stream configurations, 500 mb vorticity advection and low-level thermal advection pattern during periods of intense convection. *Mon. Wea. Rev.*, **110**, 184-197.
- Oliver, V. J., and M. B. Oliver, 1951: Meteorological analysis in the middle latitudes. *Compendium of Meteorology*, Amer. Meteor. Soc., 715-727.
- Petersen, R. A., 1986: Detailed three-dimensional isentropic analysis using an objective cross-sectional approach. *Mon. Wea. Rev.*, **114**, 719-735.
- Saucier, W. J., 1955: *Principles of meteorological analysis*. The Univ. of Chicago Press, Chapt. 8, 250-261.
- Uccellini, L. W., 1976: Operational diagnostic applications of isentropic analysis. *Nat. Wea. Dig.*, **1**, 4-12.
- Uccellini, L. W., P. J. Kocin, R. A. Petersen, C. H. Wash, and K. F. Brill, 1984: The Presidents' Day cyclone of 18-19 February 1979: Synoptic overview and analysis of the subtropical jet streak influencing the pre-cyclogenetic period. *Mon. Wea. Rev.*, **113**, 31-55.
- Uccellini, L. W., D. Keyser, K. F. Brill, and C. H. Wash, 1985: The Presidents' Day cyclone of 18-19 February 1979: Influence of upstream trough amplification and associated tropopause folding on rapid cyclogenesis. *Mon. Wea. Rev.*, **113**, 962-988.

Instability Bursts and Heavy Precipitation from Extratropical Cyclone Systems (ECSs)

by

Roderick A. Scofield

NOAA/NESDIS/Satellite Applications Laboratory
Washington, DC 20233

I. INTRODUCTION

Today one of the greatest challenges of an operational meteorologist is understanding the evolution and characteristics of precipitation within the Extratropical Cyclone System (ECS). It is known that heavy precipitation in ECSs is convective. Convective bands or areas are a dominant feature of the ECS heavy precipitation areas. Heavy precipitation areas associated with ECSs develop and end suddenly and usually occur over small areas. Instability Bursts are one of the primary mechanisms for producing heavy precipitation. Instability Bursts are defined as a maximum destabilization of the atmosphere. Instability Bursts are best detected by using a combination of satellite imagery with instability analyses derived from surface and upper air data and model data. In the satellite imagery, Instability Bursts are identified as subsynoptic scale wave patterns or convective cloud areas or bands embedded within the ECSs. Often these features grow rapidly and the cloud top temperatures become progressively colder in the infrared (IR) imagery; these features appear to "burst" their way into existence. In the surface and upper air data, Instability Bursts are associated with: (1) the maximum advection of unstable air or (2) an upper level disturbance or jet streak passing over an unstable air mass. Instability Bursts can be expected in areas: (1) of 850 mb positive advection of equivalent potential temperature (θ_e) (see Figures 1a, b); (2) of maximum advection of high K index values (K=10-20 for heavy snow; K=20-30 for heavy rain and K>30 for deep convection) (see Figure 2) and (3) where significant vertical motion occurs over a moist and rather unstable air mass ($K \geq 0$, 850 mb θ_e advection can vary from slightly < 0 to slightly > 0 and/or Conditional Symmetric Instability (CSI)* is present (see Figure 2). An Instability Burst by itself is not sufficient to produce heavy precipitation. For heavy precipitation to occur, there must be present (or forecast): the parameters for an Instability Burst, a slow moving or regenerative ECS (except in rapidly deepening systems) and moisture (1000-500 mb precipitable water > 0.5 inches and 1000-500 mb relative humidity $> 60\%$).

*CSI is discussed more thoroughly in Section IV.

II. AN EXAMPLE OF INSTABILITY BURSTS AND HEAVY PRECIPITATION

On December 14, 15, 16, 1987 heavy snow associated with Instability Bursts and ECSs occurred from Oklahoma northeastward to Michigan. Thunder was reported at many locations. In fact the ECS cloud system (M) that "burst" into existence around December 14, 1301 GMT (see Figure 3) looked like a Mesoscale Convective System (MCS). Figure 3 shows the evolution of the cyclone from three features: a MCS at (M), an upper level system at (U) and a squall line at (S) to a mature comma head (C) and comma tail (T) by December 15, 1200 GMT. The surface low deepened 27 mb in 18 hours. 850 mb θ_e advection fields are shown in Figures 4a, 5a, 6 and 7a. The advection field in Figure 6 (December 15, 0600 GMT) is an interpolated field between Figure 5a (December 15, 0000 GMT) and Figure 7a (December 15, 1200 GMT). Twelve hour heavy snowfall analyses (4 or more inches) are illustrated in Figure 4b, 5b and 7b. It is interesting that the maximum advection of θ_e at 850 mb is a very conservative feature that can be tracked from northern Arkansas to southern Michigan. Also, the θ_e advection analysis is oriented in a similar pattern as the heavy snow analyses. Heavy snow fell 1-3° latitude north of the θ_e maximum. Heavy rain occurred along and just north of the axis of maximum θ_e advection. The December 15, 0600 GMT was produced because the θ_e advection field between December 15, 0000 GMT and 1200 moved quite rapidly. During this same time the surface low moved and deepened rapidly.

III. RELATIONSHIP OF INSTABILITY BURSTS TO ECS EVOLUTION AND CYCLOGENESIS

The connection of Instability Bursts to the evolution (Scofield and Spayd, 1984) and deepening of ECSs is not obvious. Instability Bursts appear to be present in most cyclogenetic events but of course other favorable atmospheric conditions must also be present. Other favorable atmospheric conditions are summarized in a check list developed by Auciello (1988) for predicting meteorological bombs in the western North Atlantic Ocean. In this check list, the intensity, speed and coastal crossing of the 500 mb vorticity maxima and the existence of a jet streak of 120 knots or greater at 250 or 300 mb just south of the 500 mb vorticity maximum are of primary importance.

A conceptual model of East Coast Cyclogenesis is shown in Figure 8. Rapid deepening occurs where "everything comes together" and the satellite imagery shows an evolution from the formation of a dry slot on the rear edge of a cloud band to the development of a distinct hooked shaped cloud pattern.

IV. SUMMARY AND CONCLUSIONS

Instability Bursts are one of the primary mechanisms for producing heavy precipitation. Instability Bursts are best detected by using a combination of satellite imagery with instability analyses derived from surface and upper air data and

model data. There are situations when the θ_e and K Index advection fields do not detect Instability Bursts. In such situations, Instability Bursts may take the form of CSI. CSI is one cause of the convective bands or areas associated with heavy precipitation in ECSSs. As described by Bennetts and Hoskins (1979) and others, CSI is a result of: inertial instability (a horizontal instability; restoring forces are centrifugal), convective instability (a vertical instability; restoring forces are gravitational) and an atmosphere at or near saturation. An approximate criteria for CSI is an atmosphere that is near saturation and possesses a large horizontal temperature gradient and a small Richardson Number.

Sometimes Instability Bursts are quite subtle in the visible, IR and 6.7 um water vapor imagery. As a result other satellite channels and satellite sounding derived parameters will be investigated for their utility in the detection of Instability Bursts.

ECS evolution, satellite signatures of heavy precipitation, mechanisms (e.g. Instability Bursts), movement and available moisture form the basis of a short range forecasting technique of heavy precipitation from ECSSs. This ECS technique will be similar to the one produced for MCSs (Jiang Shi and Scofield, 1987).

In closing, Instability Bursts are not only responsible for producing heavy ECS precipitation but also appear to occur on all meteorological scales ranging from the high-topped cumulonimbus systems embedded within the Intertropical Convergence Zone (ITCZ) (influences global circulation) down to smallest rapidly expanding flash flood producing MCS. Instability Bursts appear to be a connecting link between MCSs and ECSSs. As a result, it is probably not a coincidence that many of the heavy snow producing ECSSs (as seen in the satellite imagery) look like MCSs.

V. ACKNOWLEDGMENTS

The author thanks Frances Holt of the Satellite Applications Laboratory of NESDIS for her constructive criticism in the preparation of the manuscript, Tina Cashman for typing, John Shadid and Gene Dunlap for the preparation of illustrations and layout.

VI. REFERENCES

- Auciello, E. R., 1988: A method for predicting meteorological bombs in the western North Atlantic Ocean. Paper presented at the 2nd National Weather Service Winter Weather Workshop, Raleigh, NC, September 26-30, 1988, 9 pp.
- Bennetts, D. A. and B. J. Hoskins, 1979: Conditional symmetric instability - A possible explanation for frontal rainbands. Quart. J. R. Met. Soc., 105, 945-962.

Jiang, Shi and R. A. Scofield, 1987: Satellite observed Mesoscale Convective System (MCS) propagation characteristics and a 3-12 hour heavy precipitation forecast index. NOAA Technical Memo NESDIS 20, U.S. Dept. of Commerce, Washington, DC, 43 pp.

Scofield, R. A. and L. E. Spayd, Jr., 1984: A technique that uses satellite, radar, and conventional data for analyzing and short range forecasting of precipitation from extratropical cyclone. NOAA Technical Memo NESDIS 8, U.S. Dept. of Commerce, Washington, DC, 51 pp.

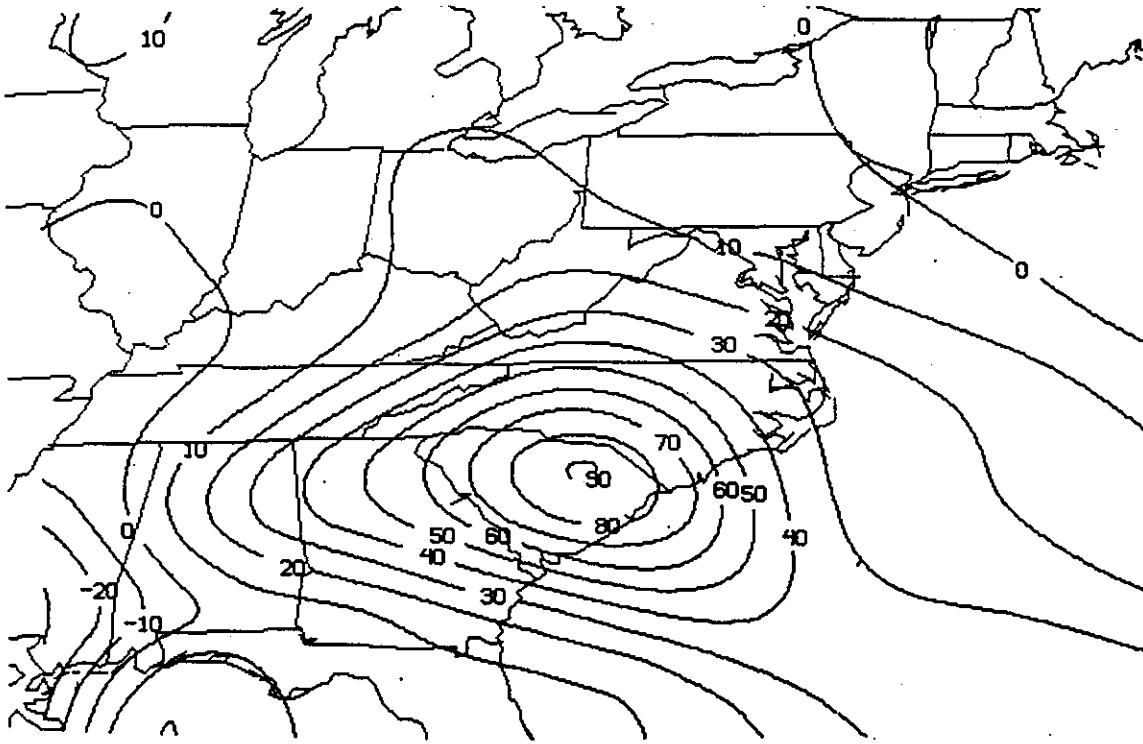


Figure 1a. 850 mb θ_e advection ($^{\circ}/\text{Day}$), January 8, 1988, 0000 GMT; usually the heaviest snow occurs along and north of the axis of maximum θ_e and especially in the tightest gradients of θ_e .

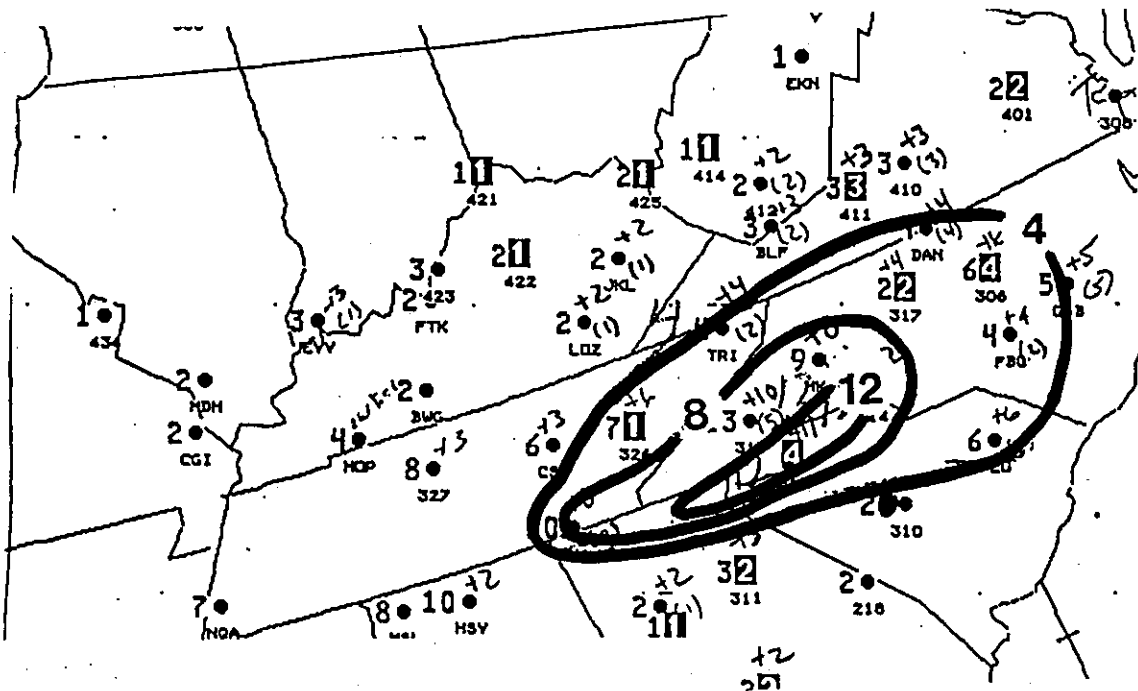


Figure 1b. 12 hour heavy snowfall (inches) ending at January 8, 1988, 0000 GMT.

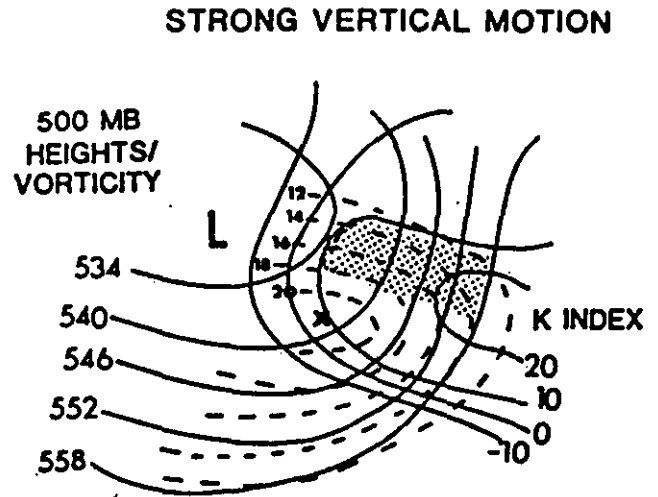
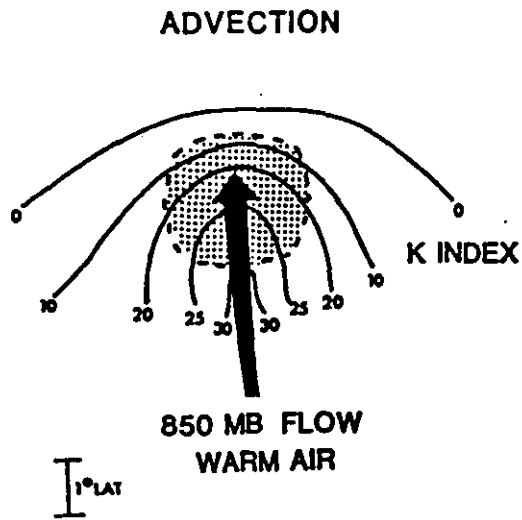


Figure 2. Stability patterns that initiate heavy precipitation in extratropical cyclone systems; stippling represent areas of convective precipitation.

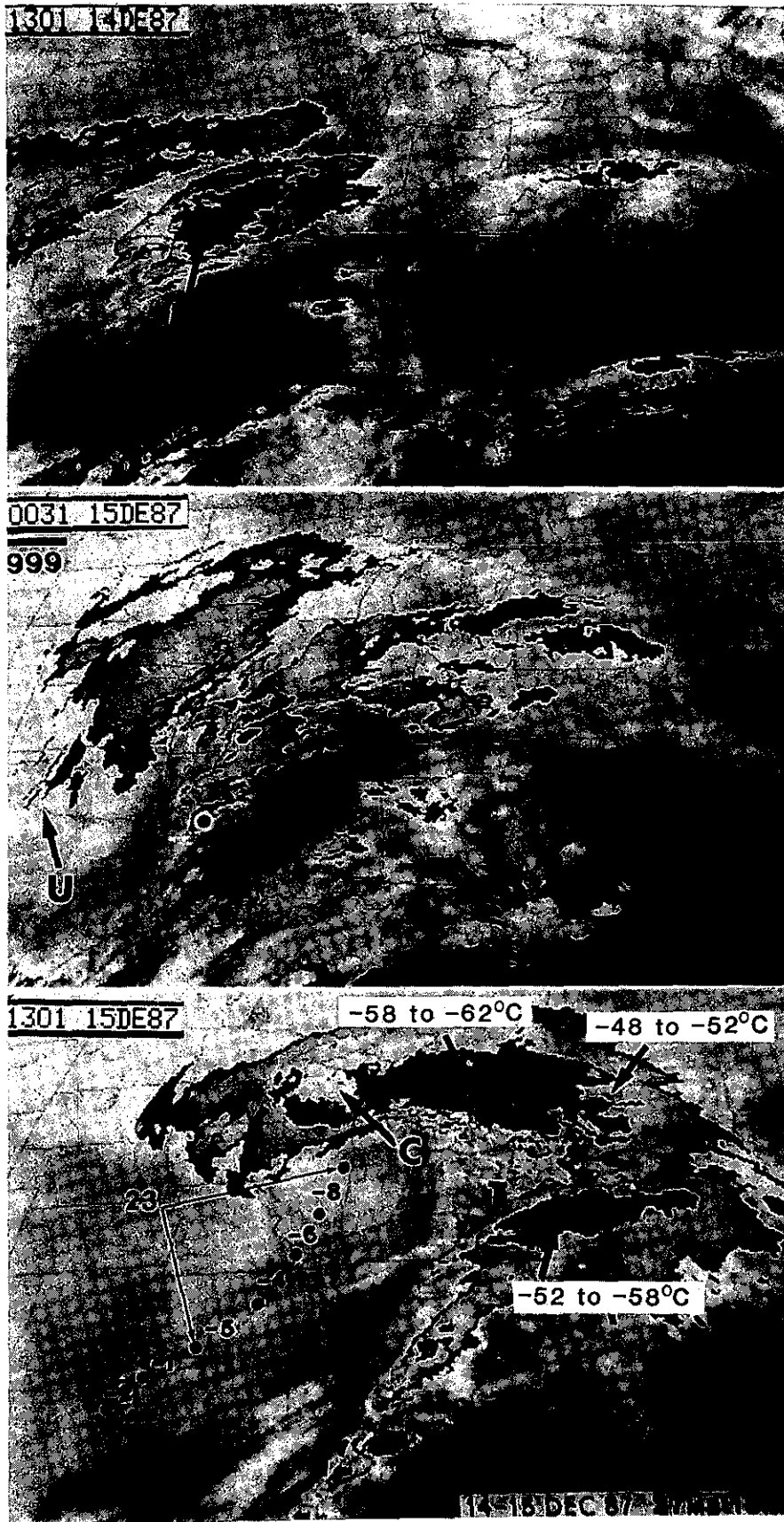


Figure 3. Enhanced IR imagery (CC curve); dots locate position of surface low and the numbers are in units of millibars.

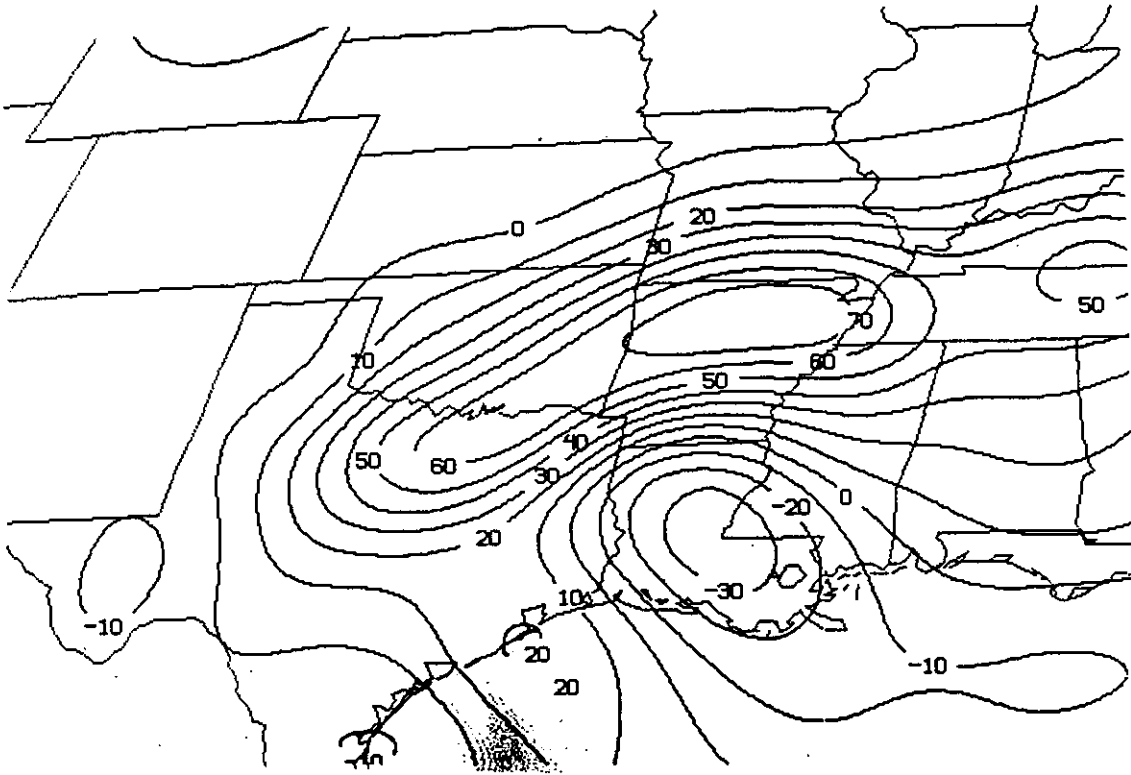


Figure 4a. 850 mb θ_e advection ($^{\circ}$ /Day), December 14, 1987, 1200 GMT.

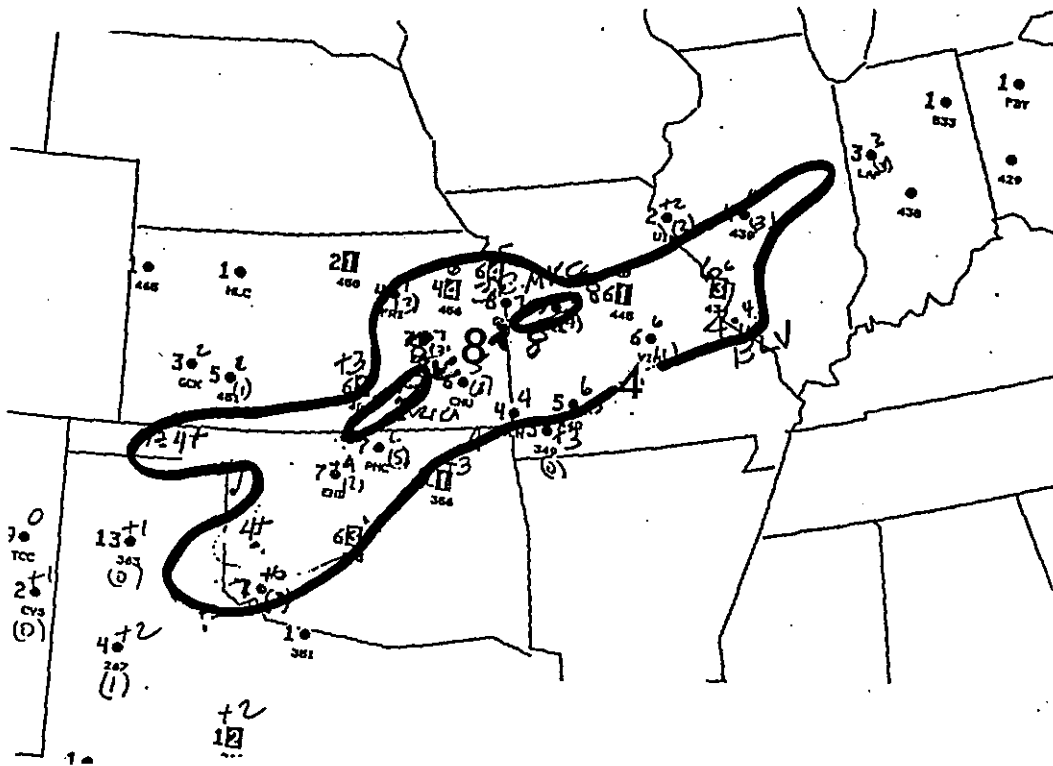


Figure 4b. 12 hour heavy snowfall (inches) ending at December 15, 1987, 0000 GMT.

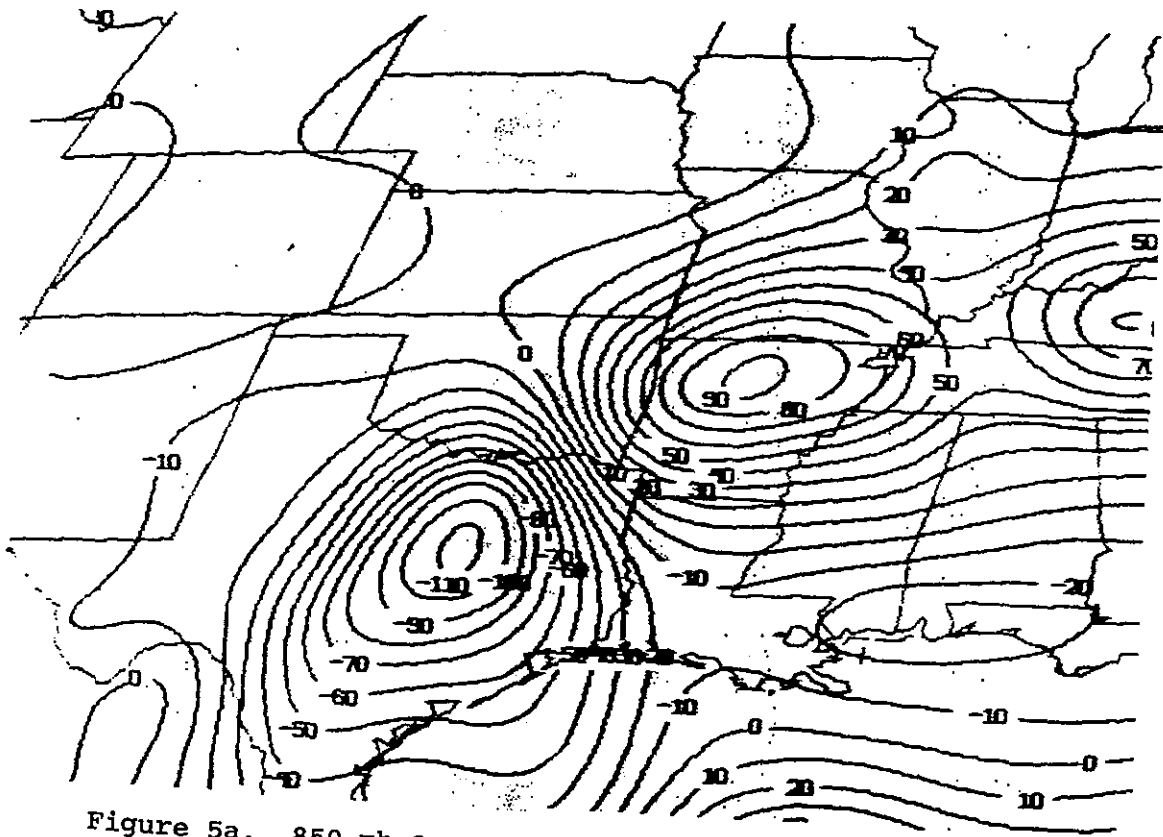


Figure 5a. 850 mb θ_e advection ($^{\circ}/\text{Day}$), December 15, 1987, 0000 GMT.

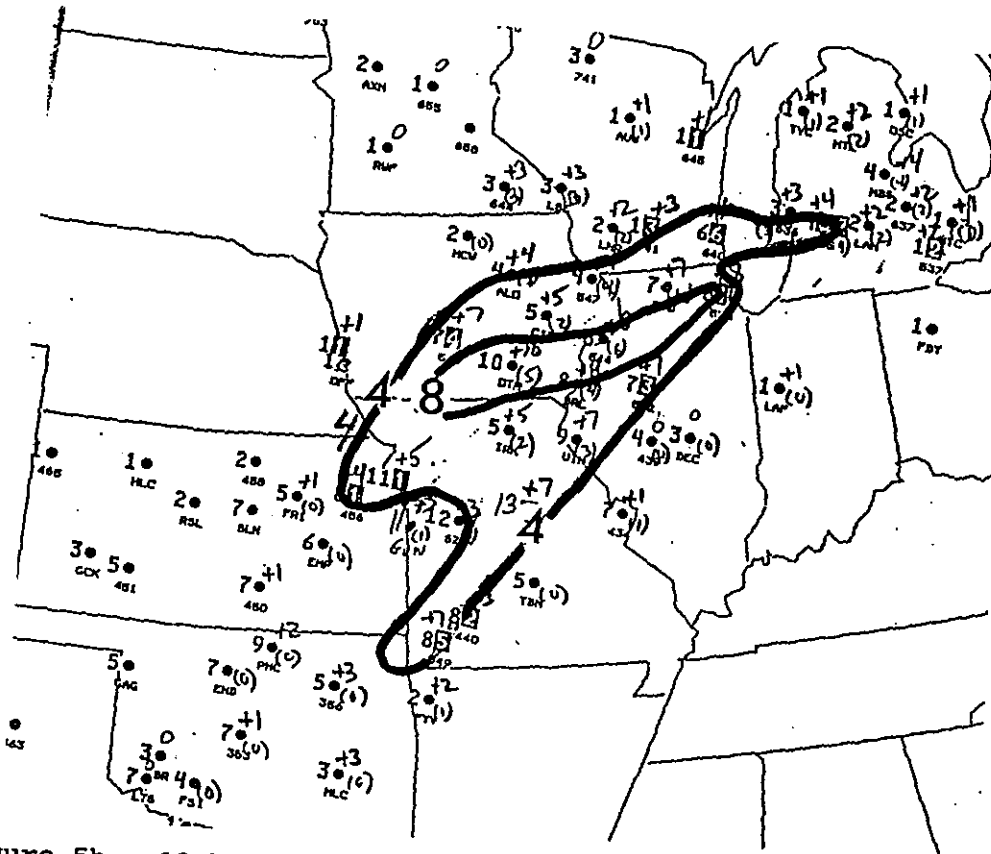


Figure 5b. 12 hour heavy snowfall (inches) ending at December 15, 1987, 1200 GMT.

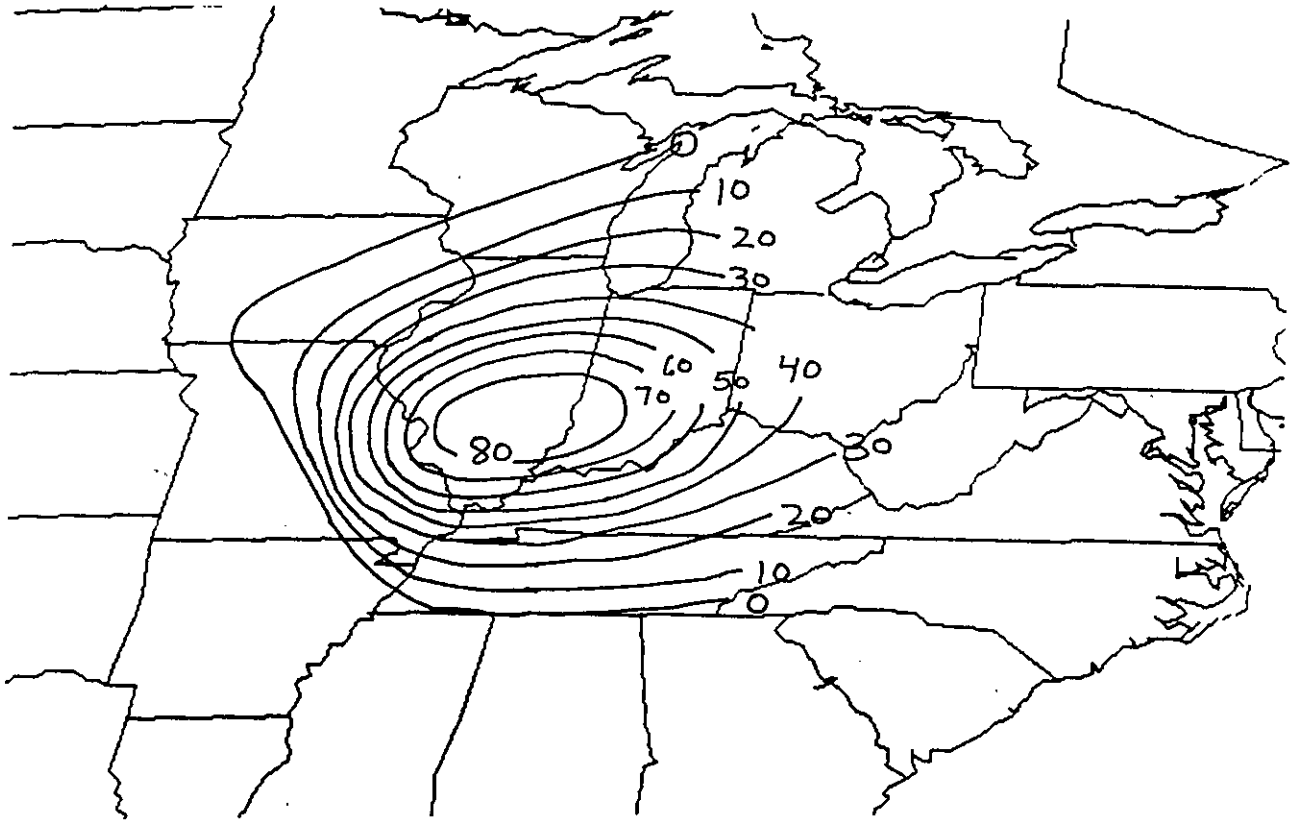


Figure 6. Interpolated 850 mb θ_e advection ($^{\circ}$ /Day),
December 15, 1987, 0600 GMT).

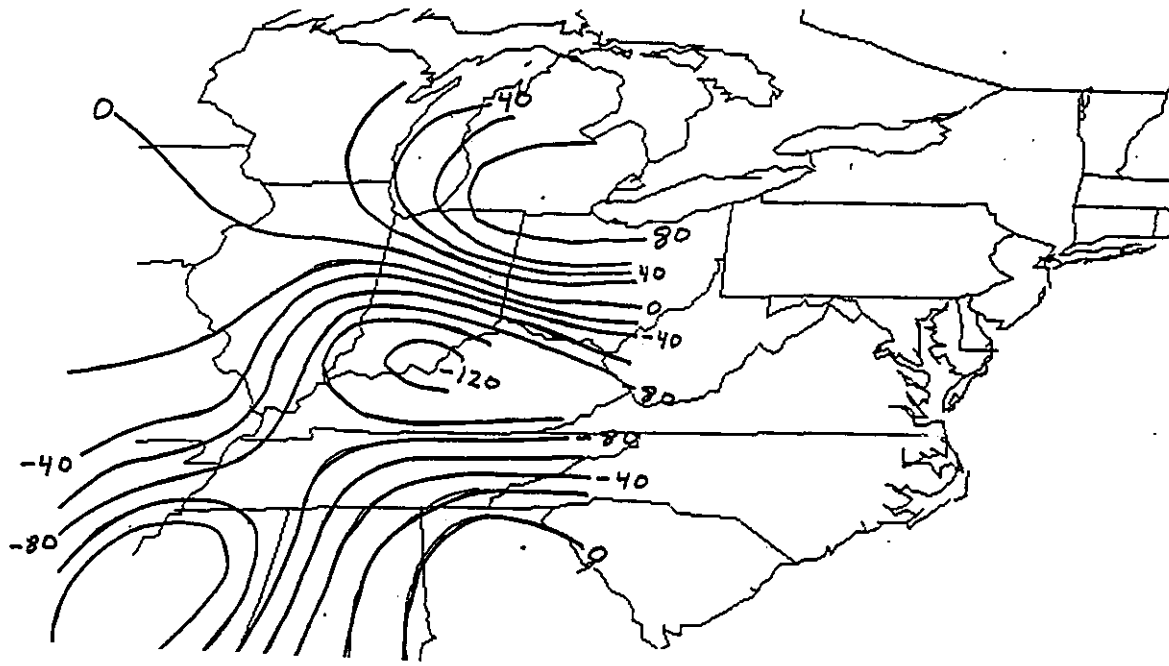


Figure 7a. 850 mb θ_e advection ($^{\circ}$ /Day), December 15, 1987, 1200 GMT.

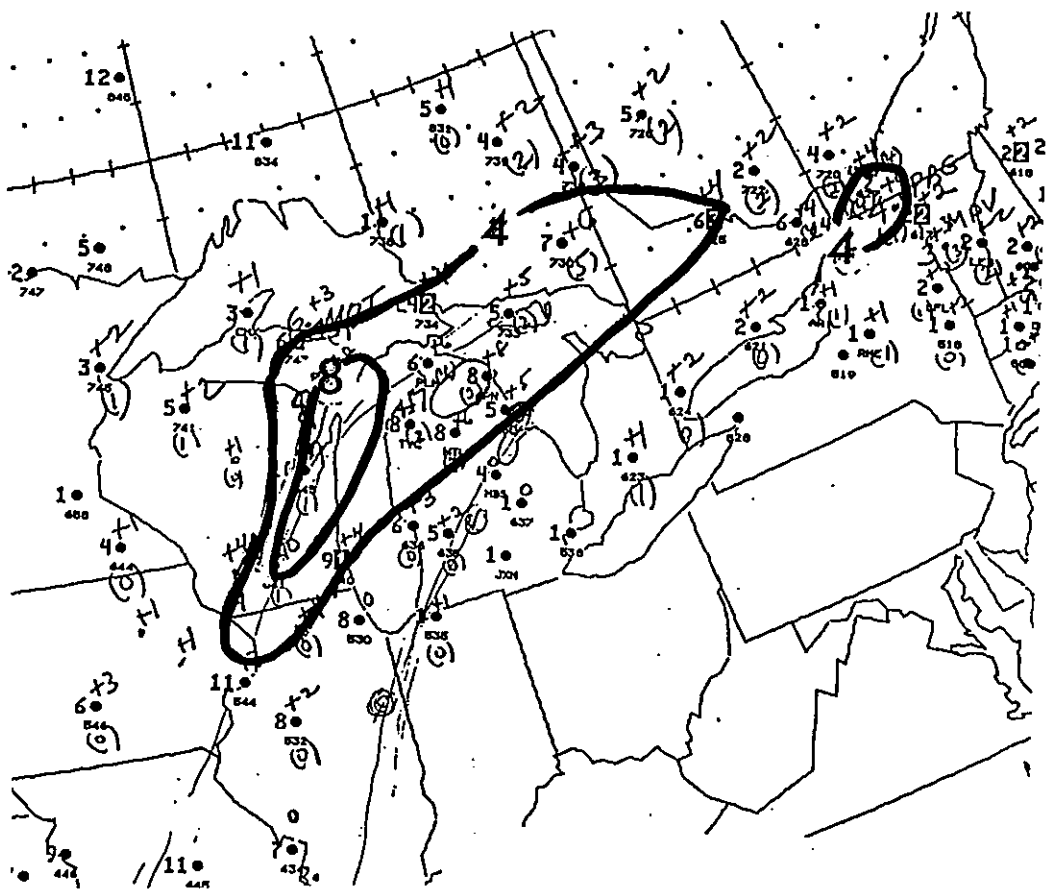
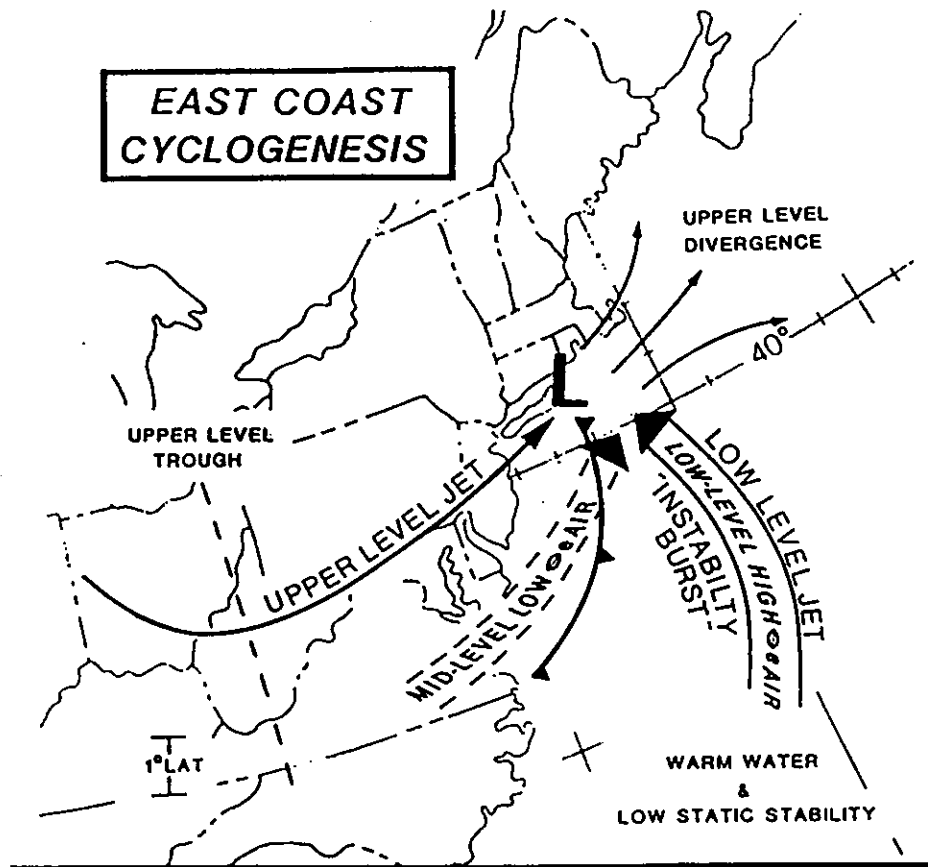


Figure 7b. 12 hour heavy snowfall (inches) ending at December 16, 1987, 0000 GMT.



SATELLITE SIGNATURES OF CYCLOGENESIS

- A COMMA HEAD PATTERN UNDERGOING EVOLUTION (POSSIBLY FROM A LEAF OR SUB-SYNOPTIC SCALE SYSTEM)
- RAPID CLOUD TOP COOLING
- RAPID INCREASE IN CONVECTION (SOMETIMES JUST A PERSISTENCE IN CONVECTION)
- LOW LEVEL POSITIVE VORTICITY, CONVERGENCE AND STABILITY DECREASE FROM SATELLITE WINDS AND SOUNDINGS

Figure 8. A conceptual model of East Coast cyclogenesis and accompanying satellite signatures; θ_e is the equivalent potential temperature.

SATELLITE VIEW OF CONVECTIVE TYPE CLOUDS AND HEAVY SNOW

Samuel K. Beckman
National Severe Storms Forecast Center
Kansas City, MO 64106

This paper documents an explosive cyclogenetic event with thunder and moderate/heavy intensity snowfall from Missouri to Michigan. The animated IR GOES satellite imagery showed convective type clouds forming in the warm/moist and very unstable air mass in the warm sector of the system and moving northward beneath the colder air aloft. The cooling tops of these warm sector clouds suggested vertical growth and was substantiated by the occurrence of ice pellets (IP and IPW) and thunder. As the convective clouds continued northward, the precipitation became mixed with, and eventually changed completely over, to snow. The abrupt increase in snowfall intensity, with rates frequently one to two inches (20-50mm) per hour, associated with convective type clouds are termed "snowbursts".

This paper also examines changes in precipitation type and the causes of two separate thunder areas. One area was in the long fetch of south flow along the warm sector moist tongue. The other was near a Pacific front and leading edge of cold air aloft. The system evolution is also briefly compared to the initial and forecast 12 hour NGM (Nested Grid Model) surface, 500mb height/vorticity and lifted indices.

Since the most dramatic system deepening and the main "snowburst" (thunder/snow) event occurred between 0000 and 1200 UTC on 15 December 1987, this will be the time interval of major study in this paper.

Early in the morning on the 14th, the first session of thunder and snow developed ahead of a minor shortwave trough which accelerated quickly east northeast across east Oklahoma and southwest Missouri into east central Missouri. As often the case, the initial trough helped to pull the low level moisture northward. Snowfall rates were briefly around two (50mm) inches per hour with the initial snowburst but the swift movement kept total accumulations in the two to five (50-125mm) inch range.

The main upper trough moved eastward across the Southern Rockies during the day with a more widespread band of moderate intensity snow spreading east northeast across the panhandle and northwest Texas into central Oklahoma and south Kansas during the afternoon.

By 0000 UTC (Fig. 1a), the upper trough extended from a low (539dm) in extreme west Kansas south across northwest Texas where a 28 unit vorticity center was located. The surface low (1003mb) was over Arkansas (Fig. 2c) and the favorable 534/540dm 1000-500mb snow thickness lines (Fig. 2a) extended from central Oklahoma northeast across north Missouri and southeast Iowa to lower Michigan. The 850mb 0C isotherm curved from east Oklahoma across southwest Missouri into south Indiana. The corresponding GOES IR satellite image (Fig. 3a) showed a band of light grey or second level enhancement (-42C to -52C) cloud top temperatures (A) from east Kansas into Iowa. Surface observations indicated occasional moderate intensity snow was falling in the south part of these colder cloud tops near the 534/540dm 1000-500mb thickness from east central Oklahoma across southeast Kansas into northwest Missouri. Snowfall rates were occasionally one (25mm) inch per hour. The cloud band trailing south across east Oklahoma into north Texas (B) was tracked by satellite the previous 24 hours across the Southern Rockies and Plains and identified with the leading edge of colder air aloft associated with a Pacific front.

Another significant feature in the satellite imagery was a band of thundershowers in the low level moist tongue across central Arkansas and south Missouri (C in Fig. 3a). This convection was supported by notable geostrophic warm advection centers at the 850 and 700mb levels (Fig. 4a) and near the zero lifted index isopleth (Fig. 5a). This convective band, with the coldest IR satellite tops, was associated with occasional moderate intensity rain. The band continued to shift eastward during the night into Illinois and west Kentucky. The importance of this band will be discussed later.

At this time, the more noteworthy convective clouds were the smaller and slightly warmer topped cells over southwest Missouri (D in Fig. 3a). These cells were near the leading edge of colder air aloft (Note the zero line in 700/500mb panels in Fig. 4a) and were producing ice pellets (IP/IPW) or small hail. The convective clouds moved northward across west and central Missouri during the next six hours. Observing stations reported highly variable snowfall intensities and rates which confirmed the convective nature of the precipitation. The possible relationship between convective type clouds and heavy snow has been discussed by Beckman (1986).

A representative sequence of observations for Columbia, Missouri is shown in Table 1. Note the report of thunder with moderate intensity snow in the 0720 UTC special observation followed by an increase to heavy intensity snow and a snowfall rate of 1 inch (25mm) per hour. The snowfall rate increased to 2 inches (50mm) per hour during the ensuing hour while thunder was occurring. There was no additional accumulation after this time.

Table 1. Observations at Columbia, Mo on 15 Dec. 1987.

Time (UTC)	Cig/Vsb(mi)	Wx/Wind Dir-Spd(kt)	Remarks
0351	RS W2X 3/4	S-F 3618G25	PRESFR
0425	SP M11@ 7	S- 0120G27	PRESFR PCPN VRY LGT
0453	RS M11@ 3	S-IP- 0126	PRESFR
0550	RS M10@ 2	S-IP- 3518	90410
0647	RS W1X 1/2	SBS 3625G29	IPE46
0720	SP WOX 1/4	TSBS 2923	TB19 OCNL LTGIC
0748	SA WOX 1/8	TS+BS 3021G26	PRESRR SNOINCR 1/1/11
0850	RS WOX 0	S+BS 2925G36	TE45 SNOINCR 2/3/13
0948	SA WOX 1/4	SBS 3028G39	PKWND 3043/34
1051	SA WOX 1/4	S-BS 3021G32	PRESRR PKWND 3036/15
1131	SP -XM12@ 3/4	S-BS 3026G37	

Satellite images during this time are shown in Figure 3b,c (Columbia, MO is at E). At 0630 UTC, the cloud band tapering south into south Missouri had about passed Columbia. The pressure was falling rapidly (PRESFR) ahead of the band and rising rapidly (PRESRR) behind it (Table 1). The surface winds became more westerly and increased in speed. These changes suggested a surface reflection of a convergence zone (likely Pacific front) aloft near the leading edge of deeper cold air. Surface observations signified that the thunder and heaviest snow occurred in the low topped, unenhanced part of the cyclogenetic system after the cloud band passed. This occurrence of low-topped convective clouds and moderate intensity snow beneath the cold core upper low is very similar to the severe weather events described by Goetsch (1988).

The cloud band continued northeast into western Illinois by 0800 (UTC). Quincy, Il (I in Fig. 3c) reported thunder, moderate intensity snow showers, a wind shift from northeast to west and rising pressure after the cloud band passed, similar to the earlier observation at Columbia. The cloud band was not very well defined over Illinois, but, re-emerged over west Indiana at 1100 UTC (N in Fig. 3e) and continued to develop northeast across north Indiana/south Lake Michigan (P in Fig. 3f).

Another important aspect of this storm was the significance of the long band of precipitation in the warm sector low level moist tongue which originally extended from south Missouri into Arkansas. This band shifted east into Illinois, west Kentucky and Tennessee during the next six hours (Fig. 3b). The importance of the warm sector convection and heavy snow has been debated by Beckman (1988) and Elkins (1988).

At 0630 UTC (Fig. 3b), a north-south band of cold topped convection in satellite imagery (H) was reported by radar and in surface observations as thunder with moderate intensity rain showers. The Chicago (G) and Rockford (F) Illinois areas, on the northern part of this convective line, were reporting moderate intensity snow. These cities were between the 534/540dm 1000-500mb thickness (Fig. 2). Some of the observation sites around Chicago were hearing thunder and observing snowfall rates of 2 inches (50mm) per hour. The higher clouds associated with the deeper convection and thunder turned westward across north Illinois and south Wisconsin during the next several hours (Fig. 3c-f). Snowfall rates of 2 inches (50mm) per hour continued in the Chicago area (G and J) between 0600 and 0900 UTC. Obviously, the deeper convection moving northward in the low level moist tongue was a factor in the large snowfall rates.

Between 1000 and 1200 UTC (Fig. 3d-f), thunder began at Moline (K and M) and quickly changed to IP and heavy intensity snow with rates of 2 inches (50mm) per hour between 1100 and 1200 UTC. Once again, this was on the south side of the colder cloud tops in the frontal cloud band. Thunder was not reported at Dubuque, Iowa (R) nor were there any 2 inch (50mm) per hour snowfall rates. However, a snowfall rate of 1 inch (25mm) per hour did occur for 5 consecutive hours between 1000 and 1500 UTC.

The original band of convective clouds associated with the deeper moisture in the warm sector expanded north and east into Lower Michigan and Wisconsin. Thunder was heard as far north as northern Lower Michigan. During the remainder of the morning, many observation sites over east Wisconsin and northwest Lower Michigan reported moderate and heavy intensity snow with snowfall rates of 1-2 inches (25-50mm) per hour.

The cloud band associated with the cold pool and Pacific front aloft consolidated with the low-level moist tongue cloud band near the Wisconsin/Illinois border. The main effect was to prolong the significant snow across this area during the time of peak cyclogenesis.

The initial 1200 UTC NGM 500 analysis (Fig. 1c) indicated a deeper (by 80dm) and farther east low than the previous 12hr prog (Fig. 1b). The surface low central pressure had dropped 21mb in 12 hours, a definite "bomb"! Corresponding 850/700/500mb geostrophic temperature advection analyses (Fig. 4b) showed dramatic 12 hour changes (Fig. 4a) during this period of rapid cyclogenesis. Also note the position of the zero isoline at 700/500mb which represented the leading edge of cold air aloft and the convective cloud band in satellite imagery (P in Fig. 3f).

The initial NGM Lifted Index (Fig. 5c) verified the rapid destabilization predicted by the 12 hr prog (Fig. 5b) over the Ohio Valley. Note that the known thunder occurred in the zone of +12 to +20 values across north Illinois, southeast Wisconsin and Lower Michigan.

In summary, two separate features were identified in the IR satellite imagery related to convective clouds and moderate/heavy intensity snow. One was identified with a Pacific front near the leading edge of the deep cold air aloft. The moderate intensity snow began with the thunder, became heavy and continued for 1-2 hours after the thunder ended. Snowfall rates increased to 2 inches (50mm) per hour during the "snowburst". The other significant feature was the convection in the fetch of deep moisture in the warm sector. Thunder was reported throughout the moisture band with moderate and heavy intensity rain becoming snow as the moisture flowed northward into the colder environment. Snowfall rates were also around 2 inches (50mm) per hour in the area of convective clouds. Geostrophic warm advection was pronounced through a deep layer (Fig. 4b).

The strong deepening during the time of maximum cyclogenesis was reasonably handled by the 12 hr NGM. Rapid destabilization in the 12 hr NGM lifted indices also verified well.

REFERENCES

Beckman, S.K., 1986: Effects of convective type clouds on heavy snow as viewed by GOES satellite imagery. Preprints Second Conf on Satellite Meteor/Remote Sensing and Appl., Amer. Meteor. Soc., Williamsburg, Va. 212-217. (available on request)

_____, 1988: Reply. Mon. Wea. Rev., 116, (to be published in Dec. issue)

Elkins, H.A., 1988: Comments on "The use of enhanced IR/visible satellite imagery to determine heavy snow areas." Mon Wea. Rev., 116, (to be published in Dec. issue)

Goetsch, E.H., 1988: Forecasting cold core severe weather outbreaks. Preprints Fifteenth Conf. Severe Local Storms, Amer. Meteor. Soc., Baltimore, Md. 468-471.

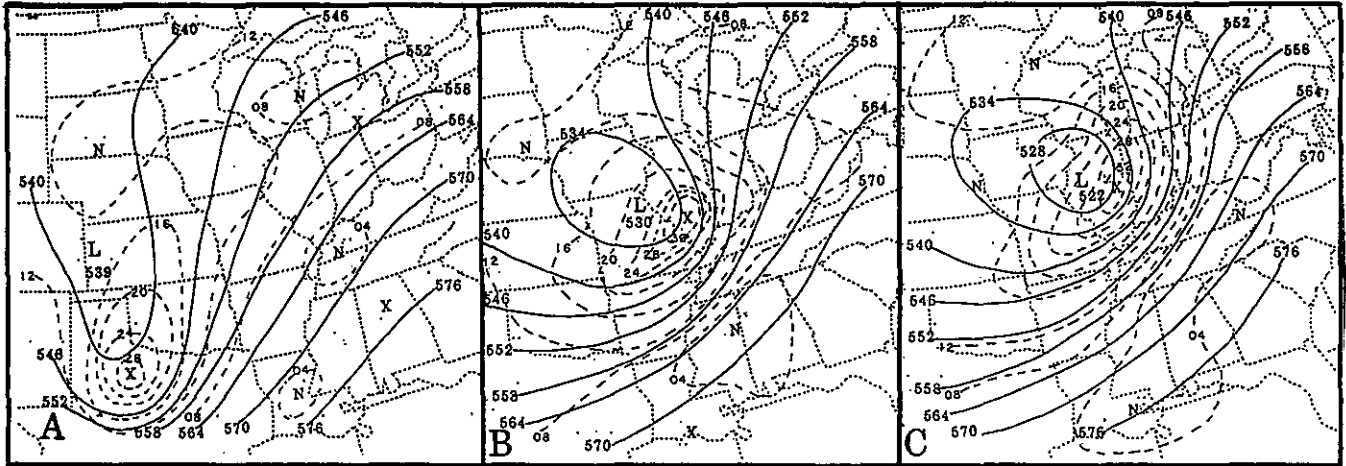


Figure 1. NGM 500mb height/vorticity for 15 Dec 1987. a) Initial analysis. b) 12hr prog valid 1200 UTC. c) Initial analysis for 1200 UTC.

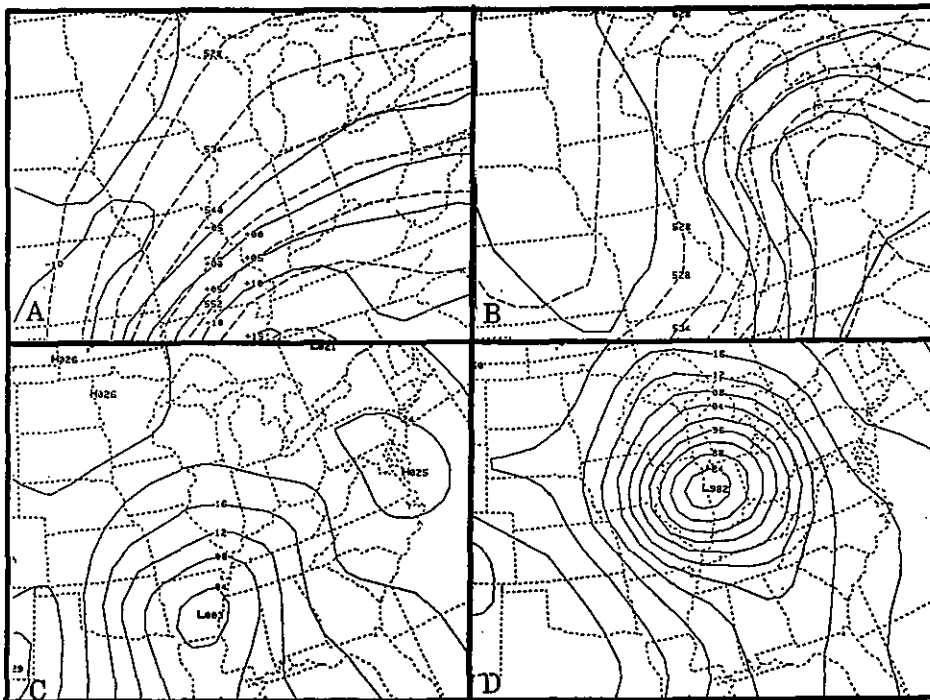


Figure 2. NGM initial analyses for 15 Dec. 1987. a) 850mb temperatures (solid) and 1000-500mb thickness (dash) at 0000 UTC. b) Same for 1200 UTC. c) Surface pressure at 0000 UTC. d) Same for 1200 UTC.

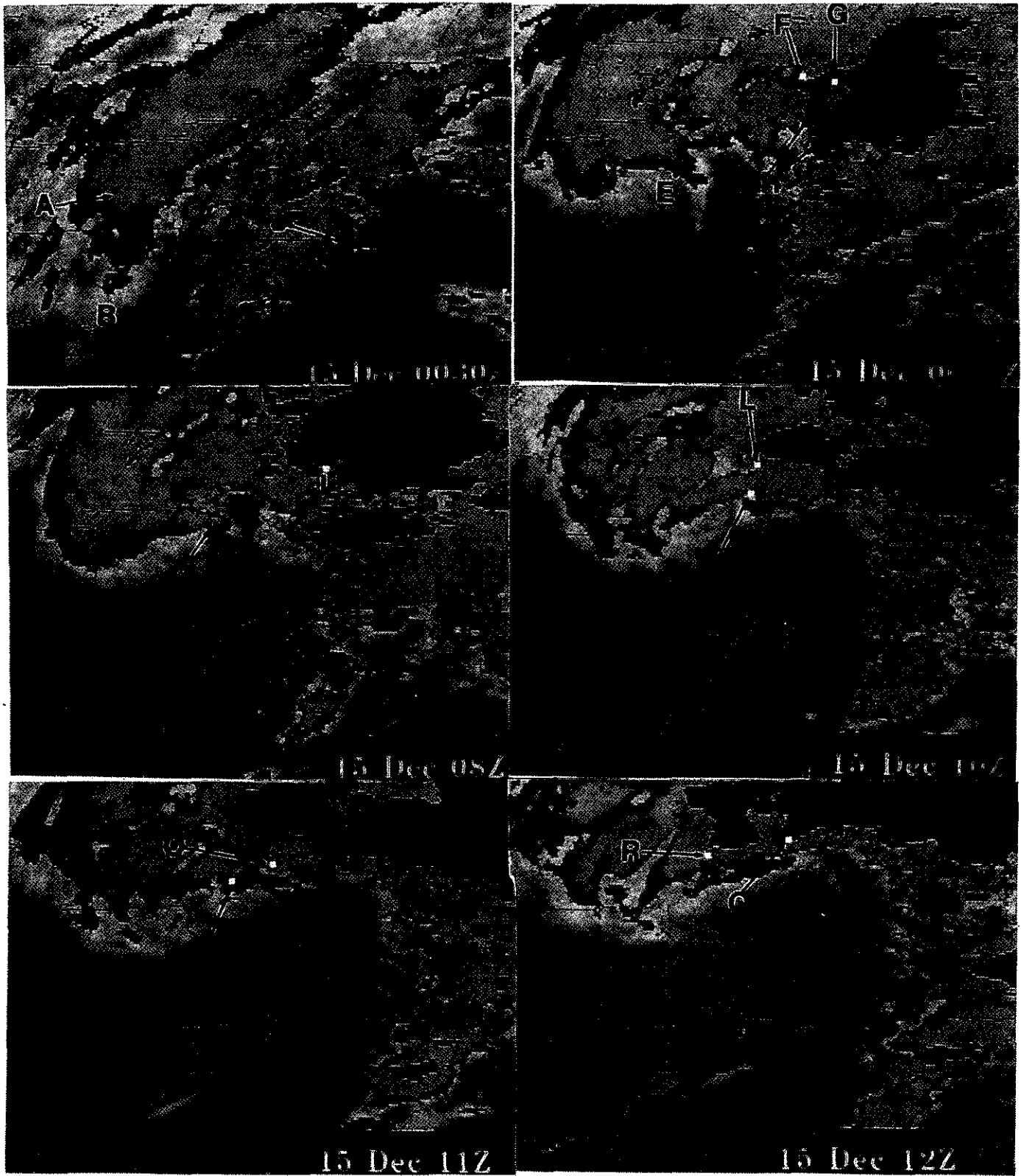


Figure 3. GOES IR satellite imagery with Mb enhancement curve for 15 Dec. 1987. a) 0030 UTC. b) 0630 UTC. c) 0800 UTC. d) 1000 UTC. e) 1100 UTC. f) 1200 UTC.

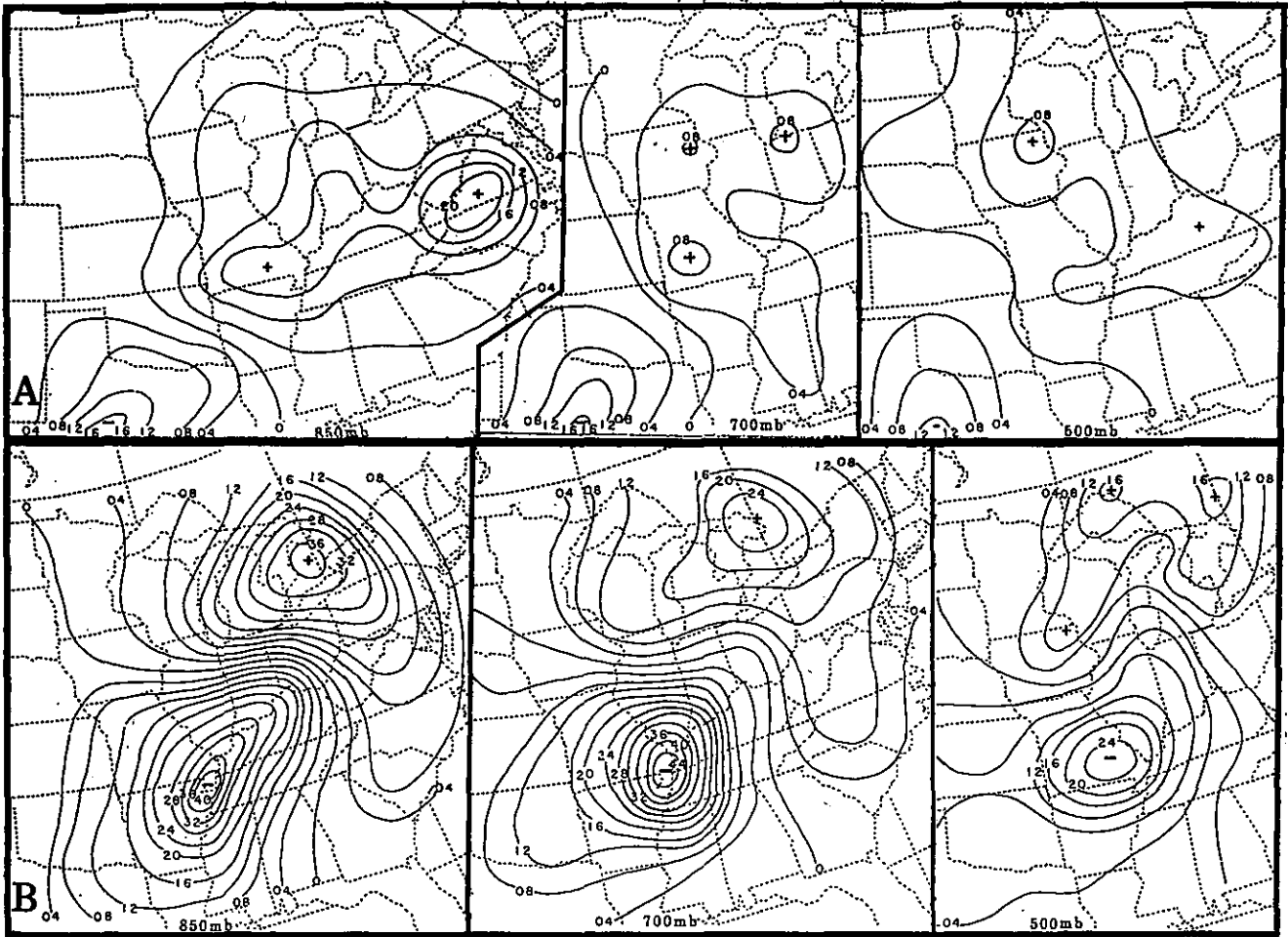


Figure 4. Temperature advection by the geostrophic wind at 850, 700 and 500mb levels for 15 Dec. at a) 0000 UTC. b) 1200 UTC.

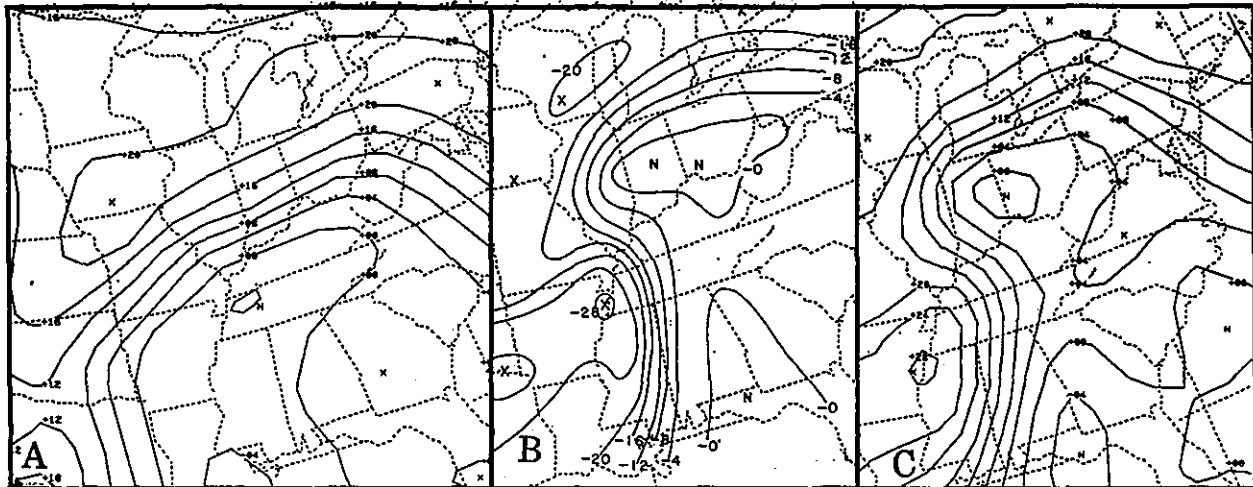


Figure 5. NGM Lifted Indices for 15 Dec. a) Initial at 0000 UTC. b) 12hr prog valid 1200 UTC. c) Initial at 1200 UTC.

...A METHOD TO DETERMINE THE WIDTH OF A SNOW BAND ASSOCIATED WITH WINTER STORMS BY USING INFRARED SATELLITE DATA...

By Allan L. Morrison ¹

INTRODUCTION....

Significant snowfalls in the upper midwest normally fall in relatively narrow bands ranging from 50-200 nm in width. Snow typically falls along the north and west edge of an organized area of precipitation. This area of precipitation is normally associated with an upper level short wave. Prior to the introduction of Satellite data in the field, the method most commonly used to predict the spatial relationship between the snow band and various parameters such as the surface low, 8h mb low etc was a statistically derived technique using previous storms. The basic weakness of using a statistical method is that one must also look at the variability of the data. The greater the variability, the less useful is the average of the data in applying it to a future individual storm. Because of this variable nature of snow bands, using this averaging technique is of limited value. What is needed is an accurate method to pinpoint the exact location of the snowband within each individual storm and extrapolating this snow band into the future.

DISCUSSION

Short waves, especially the stronger ones when clouds are more likely to be in evidence, can be identified using satellite data. The cloud signature most commonly associated with short waves on satellite data is the "comma cloud" that evolves most often when the short waves phases with a baroclinic zone. At this time, surface cyclogenesis often occurs but is not necessary for the comma cloud to take shape. See figure A, which relates the location of snow within the comma cloud and the statistically derived distances from the paths of various weather parameters.

Since comma clouds have several distinct features, it seems reasonable to assume that the precipitation associated with the comma cloud would normally occur in only a portion of it. After examining several snowstorms it was determined that there was a definite relationship between the snow band and the enhanced portion of the comma cloud. In all cases examined snow fell in a band related to the lower half of the comma head. This can be seen by examining the infrared (MB curve) satellite pictures of snowstorm of March 29-30 1987 (see Case I). Note on each satellite picture, the comma head was bisected to the point where it intersected the path of the dry intrusion. The lower half of the comma head was overlayed on a visual satellite picture, following the snowstorm, that depicted the snow band. By repeating this procedure on successive satellite pictures, a composite of overlays onto the visual picture indicated an almost perfect fit between the snow band and the lower half of the comma

1

National Weather Service Forecast Office - Chicago, IL.

head.

More importantly, it was found that you could accurately pinpoint the location of significant snowfall on a real time basis. By employing the technique of overlaying the enhanced portion of the comma cloud (ignoring the discontinuous fragmented portions) on a weather depiction chart the precipitation area is well defined. The precipitation was found to coincide with an area of the comma cloud determined by bisecting the comma cloud from head to tail. See figure B. The precipitation was confined to the lower half of the comma head and the upwind half of the comma tail. The snow was almost exclusively confined to the lower half of the comma head to the left of the dry intrusion path. See Case II (January 9-19 1987) and Case III (January 19-20 1987).

THE METHOD

See figure C. Note that the southern edge of the enhanced portion of the comma cloud determines the southern edge of the snow band and the northwest edge of the bisected comma edge corresponds to the northern edge. The path of the vorticity maximum should be parallel to this snow band and approximately 1 degree of latitude to the right of the southern edge of the snow band. If using this method as a forecast tool...use the path of the vort max...either by extrapolation or the forecasted position of the vort max...to extend the snow band into the future. Another good method is to extrapolate the path of the dry slot. However a note of caution...only use this method if the dry slot is not rotating such as in a shearing out short wave. Otherwise, such as in an occluding type system, the dry slot rotates around the comma cloud. Therefore the path of the vort max is more reliable. In the case of an occluding low, the enhanced portion of the comma head becomes more arced shaped as the dry slot rotates around the circulation center, much like a spiral band. This reduces the amount of enhanced precipitation. After this occurs, the enhanced band is in the form of a narrow arc. See figure D. In this case the snow band may be as wide but snowfall amounts should be reduced. Often the southern portion of the arc disappears so that the snow band narrows, effectively pushing the snow further north from the vort track.

CONCLUSION

This method can be used to determine with pinpoint accuracy where significant snow has fallen up to the present time. This method is unique in that all other observed weather information available to the forecaster are either point sources (weather observation sites), or of limited coverage such as with radar. Obviously one cannot do a good job of forecasting where it will snow if he cannot ascertain where snow has been occurring up to the present time. How can you make adjustments to the computer Models without knowing what is going on "now".

This method can be used to accurately estimate the beginning and

ending times of significant snowfall at any location. Also an estimate of total snowfall at that site can be made using an average snowfall rate of 1 inch per hour which is reasonable with most snowstorms.

As with any method, there are times at which significant snow may fall outside of this calculated snow band. The most likely exception would be the upper portion of the comma tail if the air mass was initially cold enough to produce snow. This is the area just to the right of the dry slot path. If the precipitation in this portion of the comma cloud begins as snow...predicting how much will fall is difficult as it often changes to rain. Fortunately, due to the nature of the comma cloud tail in this area being oriented along a narrow band perpendicular to the approaching dry slot, the duration of precipitation is short. This severely limits potential snowfall. However with the case of convective type precipitation, a quick "shot of heavy snowfall" could result in several inches of snow.

REFERENCES

- Browne, R.f., and R.J. Younkin, 1970: Some relationships between 850 mb lows and heavy snow occurrences over the Central and Eastern United States. Mon., Wea Rev., 98, 399-401.
- Goree, P.A., and R.J. Younkin, 1966: Synoptic climatology of heavy snowfall over the Central and Eastern United States. Mon Wea Rev., 105, 1071-1074.
- Harms, R.W., 1973: Snow forecasting for southeast Wisconsin
- Kadin, C., 1982: The minneapolis snow event -- what did the satellite tell us? Nat. Wea Dig., 7, 13-16
- Scofield, R.A., Spayd, L.E.: A Technique That Uses Satellite, Radar and Conventional Data For Analyzing and Short-Range Forecasting Of Precipitation from Extratropical Cyclones. Weather Service Forecasting Handbook No 6, Cha 3, E1-51.

RELATIONSHIP BETWEEN
SATELLITE + CONVENTIONAL
SYNOPTIC TECHNIQUES

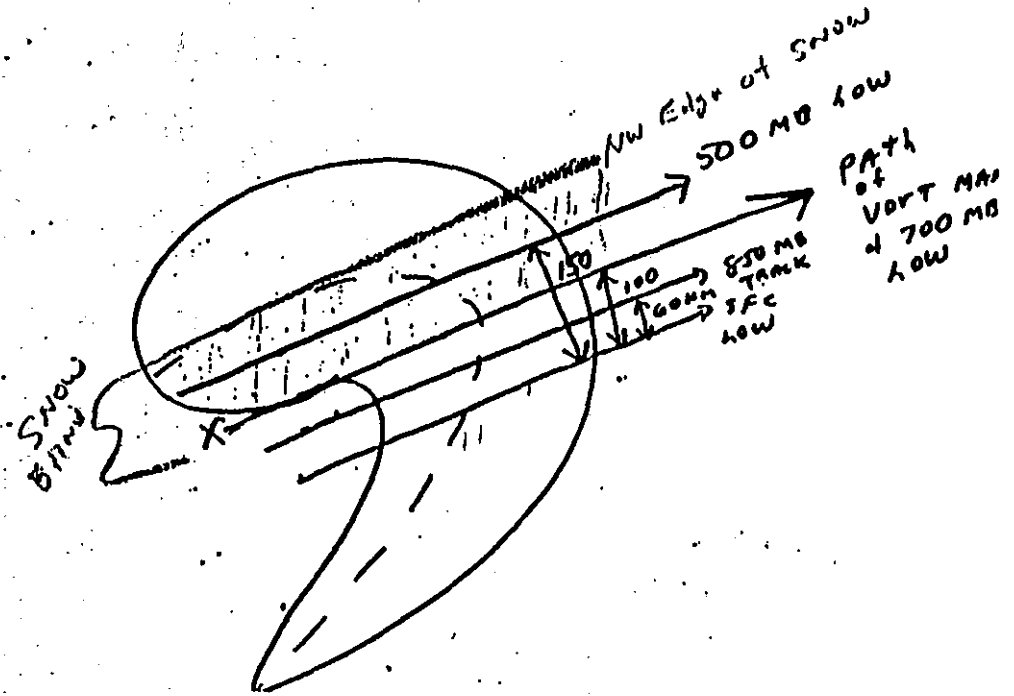


FIGURE A

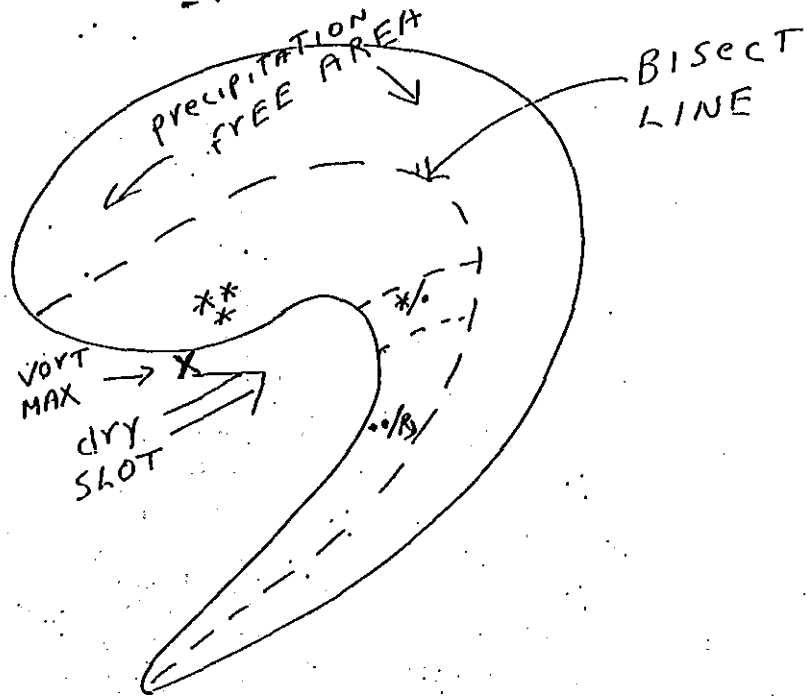


FIGURE B

SHEARING OUT TYPE SHORT WAVE WHERE THE DRY SLOT MOVES STEADILY EASTWARD LAYING OUT A SNOW BAND NEARLY CONSTANT IN WIDTH AND ALONG A STRAIGHT LINE.

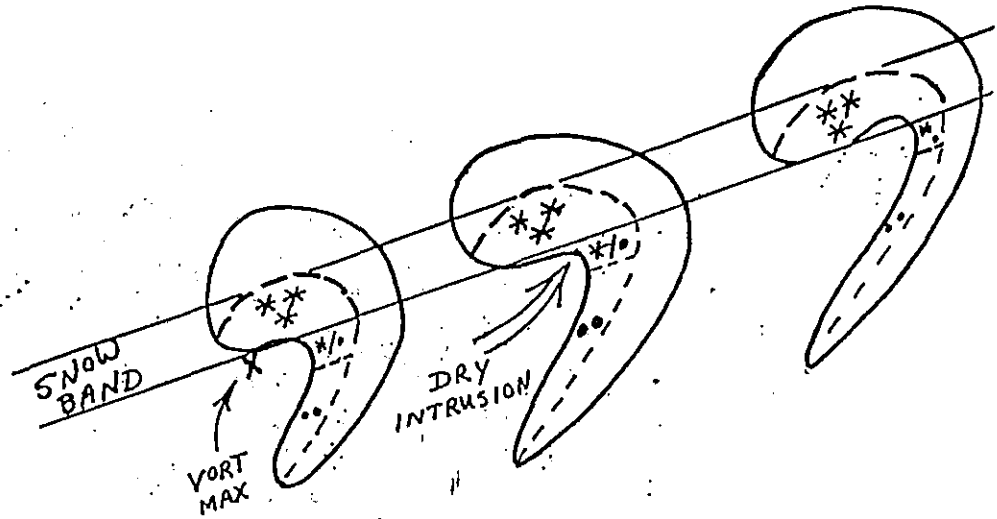


FIGURE C.

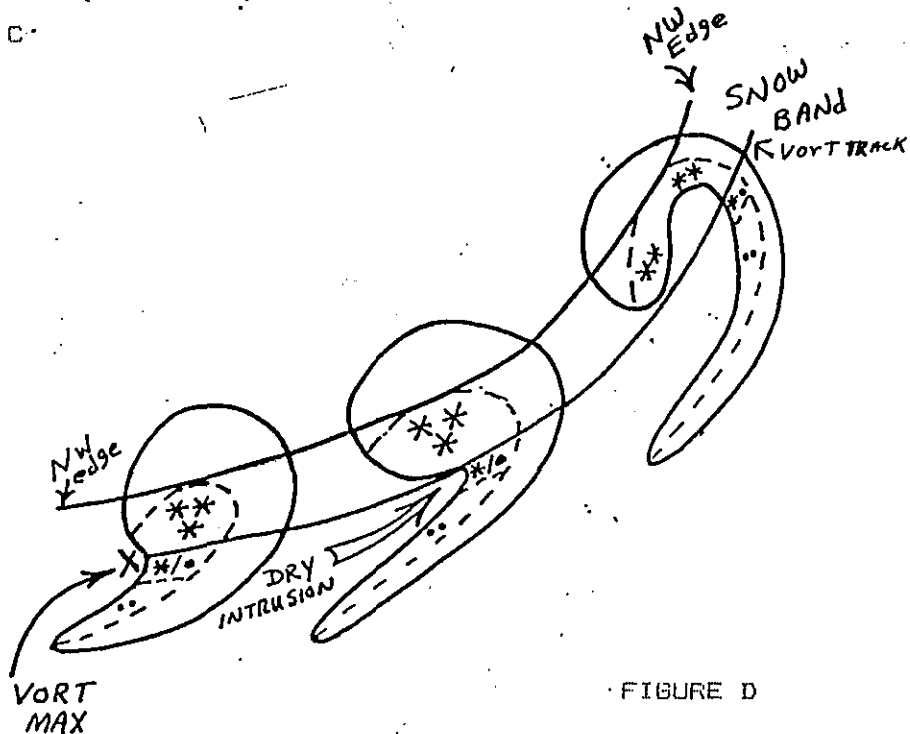
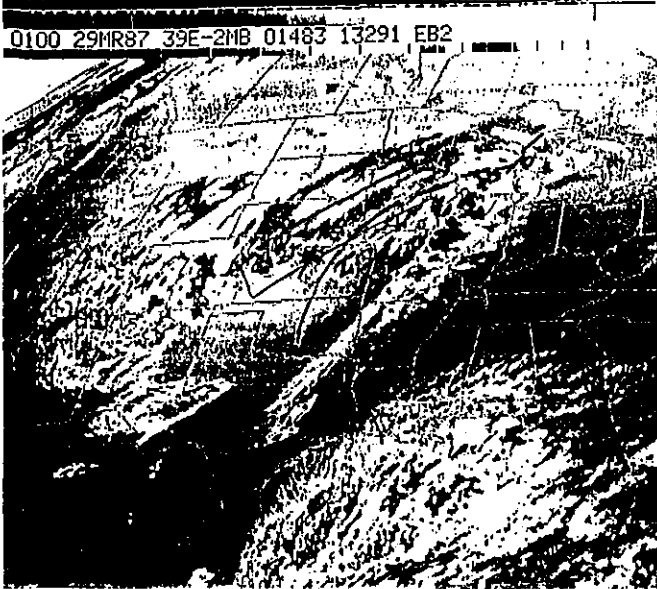


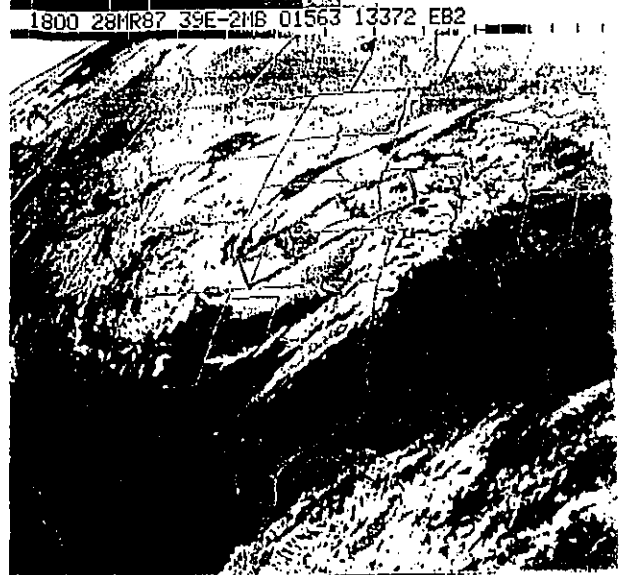
FIGURE D

SHORT WAVE IS SHARPENING UP AND OFTEN CLOSES OFF. THIS IS A TYPICAL OCCLUDING PROCESS AND THE DRY SLOT ROTATES AROUND THE UPPER SYSTEM. THIS RESULTS IN A GRADUAL SHIFT OF THE SNOW BAND TO THE LEFT OF THE VORT MAX PATH. THIS CAUSES THE SNOW BAND TO DECREASE GRADUALLY IN WIDTH.

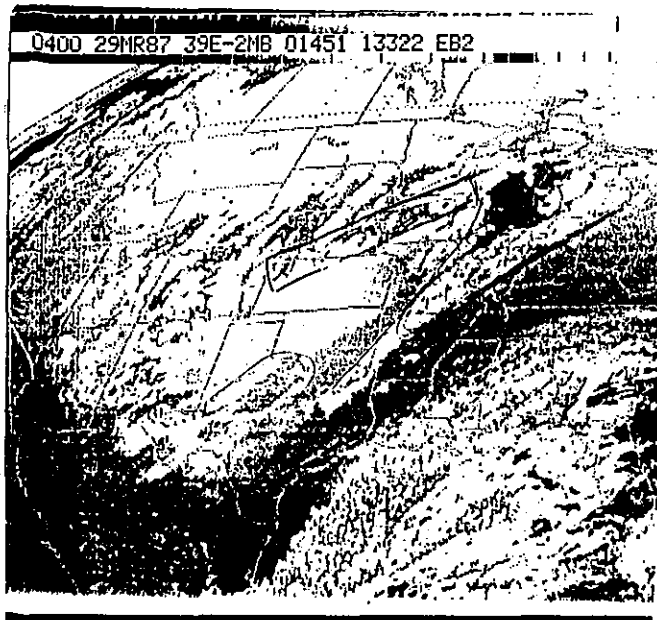
0100Z 29 Mar 87



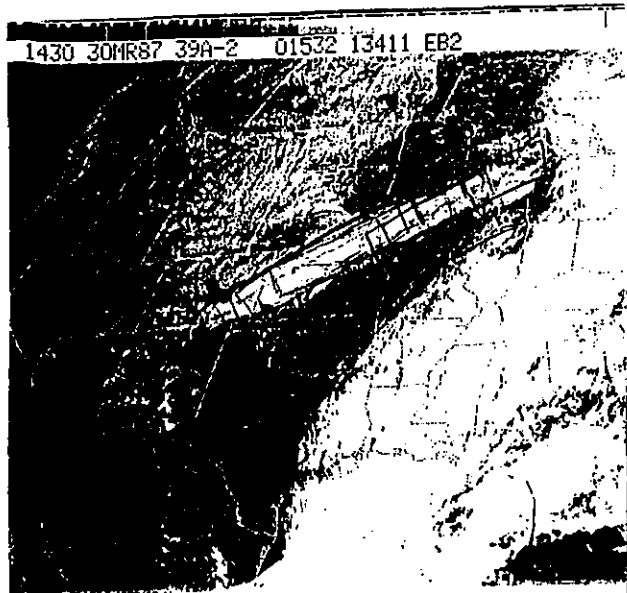
1800Z 28 Mar 87



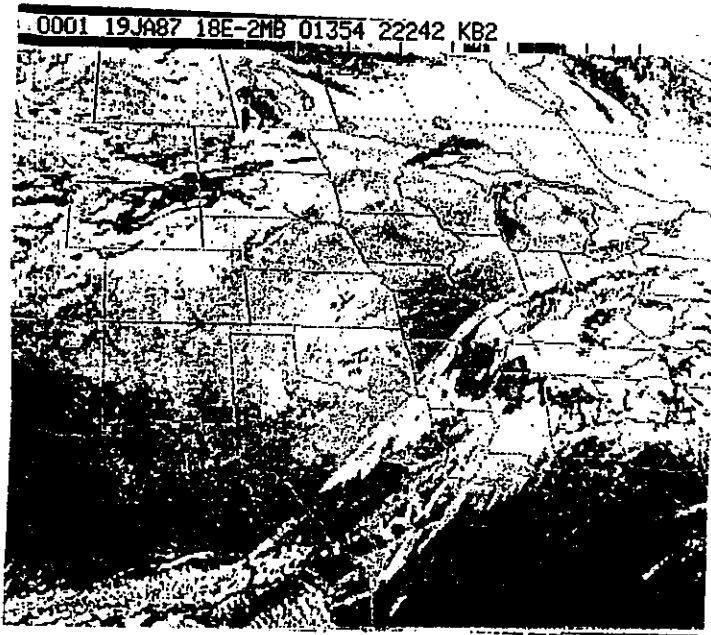
0400Z 29 Mar 87



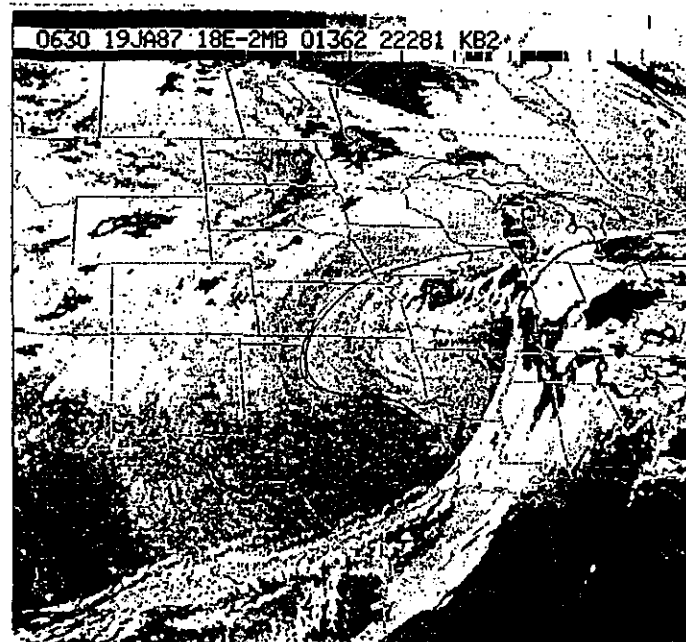
1430Z 30 Mar 87



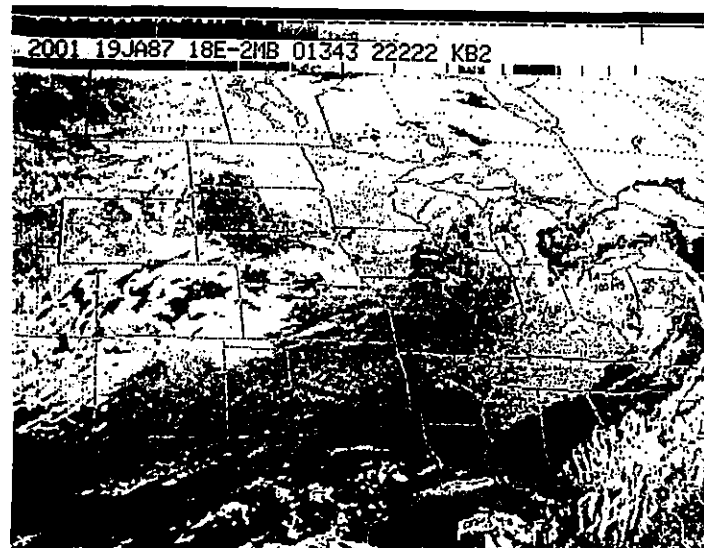
CASE I



0001Z 19 Jan 87

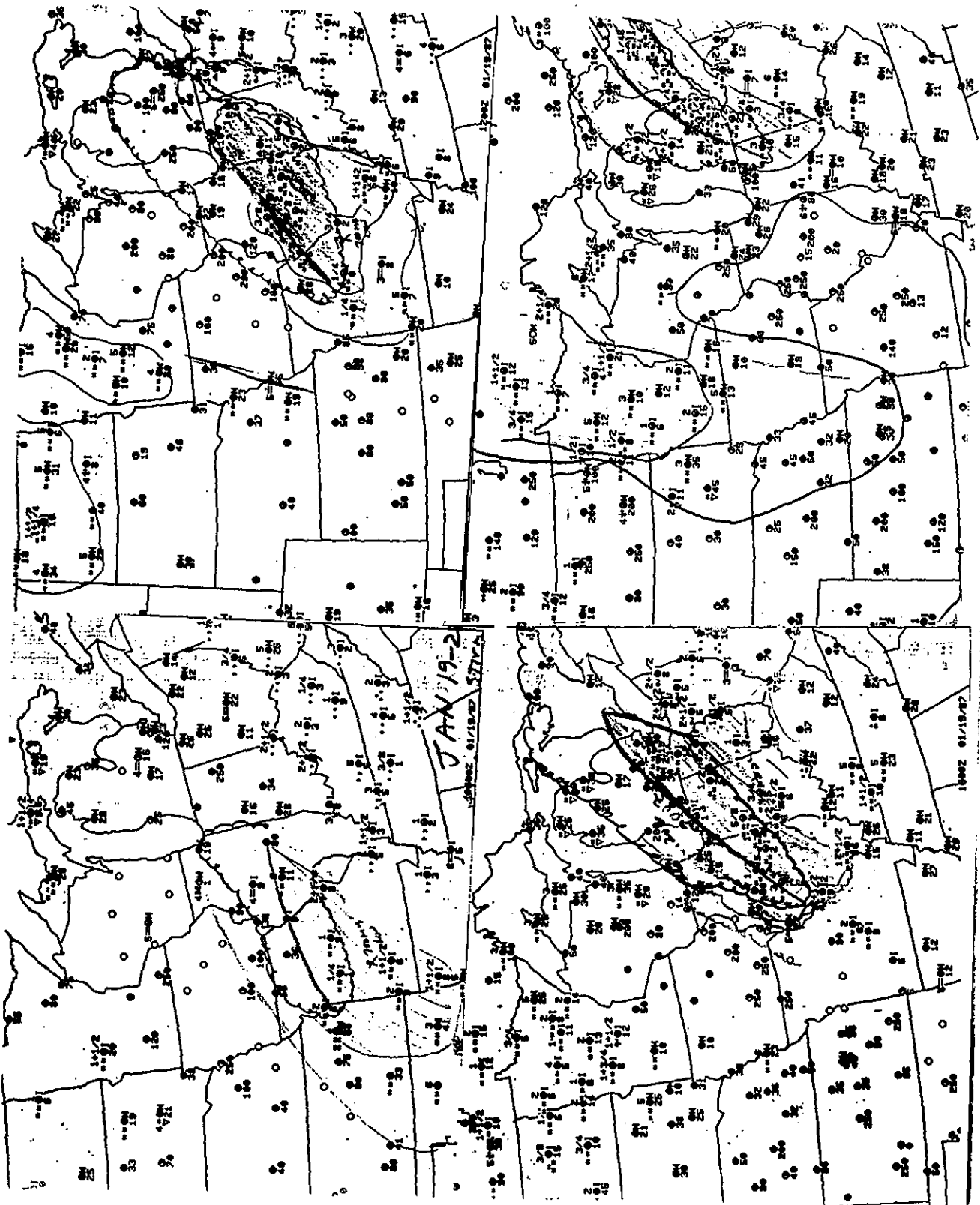


0630Z 19 Jan 87

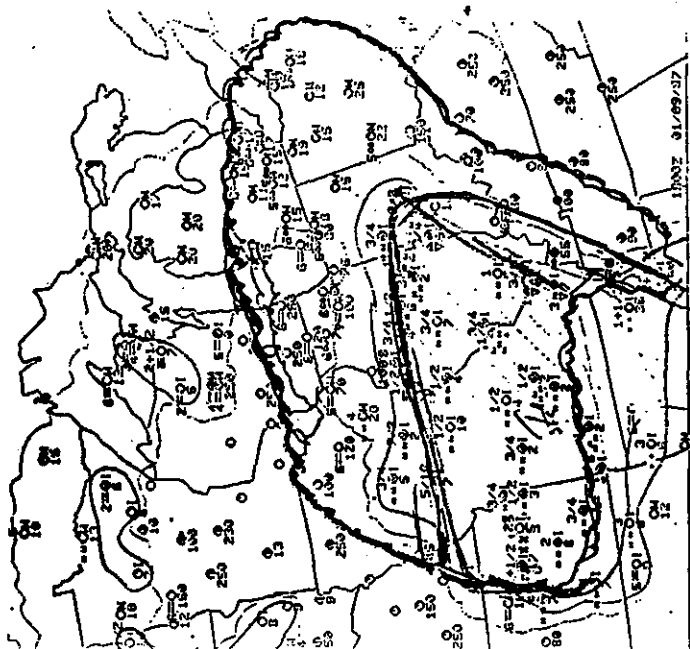
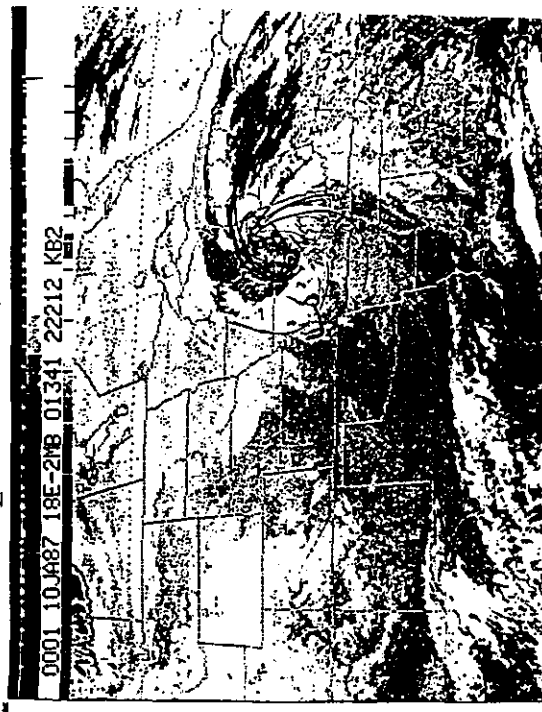
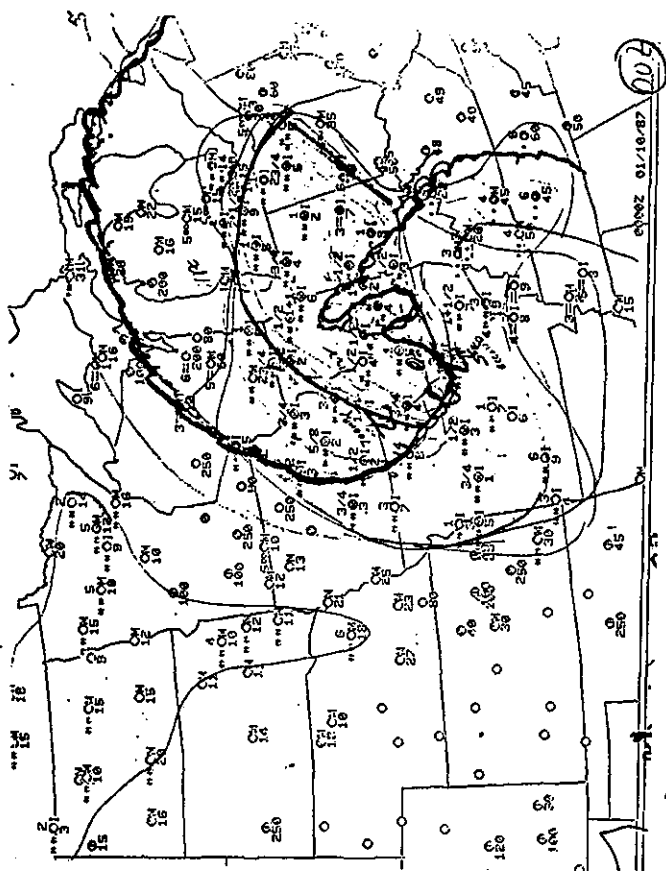


- 71 -

CASE 11



CASE III



WINTER EAST COAST LIGHTNING DATA AND
SURVEY OF LIGHTNING STRIKES IN STORMS

By Carl C. Ewald, Washington ARTCC CWSU

BACKGROUND

The 19 inch color CRT lightning detection monitor was installed by the State University of New York at Albany at the Leesburg CWSU in July 1983. Generally every 50 minutes a map is plotted on the Prism 80 color printer including the lightning strikes for the previous 10 minutes in order to maintain continuity.

The monitor shows the major J routes in green, the adjacent enroute ATC Centers boundaries in red, the important location points in blue, and the cloud-to-ground (CG) lightning strike location as a + or  in one of six changing colors. The + signs indicate where a positive charge is towered to the ground, while a  shows where a negative charge descends to the ground. Cloud-to-cloud lightning discharges are electronically eliminated from the display. Generally, negative strikes are associated with stronger thunderstorms while weak or embedded thunderstorms lower positive charges to the ground. Thunderstorms over the Washington ARTCC airspace and the Mid-Atlantic coastal waters have an operational impact so lightning plots having strikes only in the ocean were sometimes discarded.

WINTER LIGHTNING CLIMATOLOGY

The lightning printouts were reviewed for December 1986 through February 1987 and December 1987 through February 1988. A count of the number of positive versus negative strikes by state and over the ocean was obtained as well as the number of hours/plots that a strike occurred in each state and over the ocean. The Washington Center area (ZDC CTLA) was also divided into three sections: Mountains, Coastal and Central. The results, in tabular form show four conclusions:

1. Stronger thunderstorms with negative CG lightning strikes are most prevalent over the ocean, south of Norfolk and over North Carolina.
2. Weaker thunderstorms with positive CG lightning strikes occur frequently over the ocean and North Carolina and occasionally over Virginia and West Virginia.
3. The least number of CG lightning strikes occur in January which is the only month with more positive than negative strikes.
4. Thunderstorms over the mountains are weak (mostly positive strikes) and are most prevalent during January.

These numbers represent a "rough" count because of the 10 minute data overlap and the under-estimation of the number of lightning strikes over the ocean since some ocean strike plots were discarded.

THREE EAST COAST STORMS

Besides viewing the distribution of strikes by state/ocean a survey of strikes during three East Coast Storms were conducted. The strikes help to locate the front/trough and often the associated low. They also can show movement and intensity changes of the low. This data is a most effective aid as thunderstorms form over the warmer Gulf Stream waters.

NUMBER OF STRIKES / NUMBER OF HOURS

AREA		DEC	JAN	FEB	TOTAL	PERCENTAGE	
POSITIVE STRIKES	NC	178/24	3/3	26/13	207/40	14.2%/15.9%	
	VA	87/16	12/3	8/5	107/24	7.3/9.5	
	WV	1/1	9/7	16/6	113/14	7.8/5.6	
	MD	6/2	8/2	0/0	14/4	1/1.6	
	DE	3/2	0/0	0/0	3/2	.2/8	
	NJ	12/4	0/0	0/0	12/4	.8/1.6	
	PA	3/3	11/3	0/0	14/6	1/2.4	
	CHSPK BAY	4/2	1/1	0/0	5/3	.3/1.2	
	OCEAN {	N OF ORF	171/31	99/10	119/23	389/64	26.8/25.4
		S OF ORF	259/35	35/8	301/48	595/91	41/36
TOTAL		724/120	262/37	470/95	1456/252	100%/100%	
ZDC CTLA {	MTNS	19/6	56/5	8/2	83/13	23.3/16.5	
	CNTRL	146/26	7/3	14/6	167/35	46.9/44.3	
	CSTL	90/19	3/3	13/9	106/31	29.8/39.2	
	TOTAL	255/51	66/11	35/17	356/79	100%/100%	
AREA		DEC	JAN	FEB	TOTAL	PERCENTAGE	
NEGATIVE STRIKES	NC	1071/26	1/1	151/15	1223/42	19.5%/15.6%	
	VA	201/17	0/0	59/7	260/24	4.1/8.9	
	WV	16/3	40/6	7/5	63/14	1/5.2	
	MD	6/2	1/1	1/1	8/4	.1/1.5	
	DE	0/0	0/0	0/0	0/0	0/0	
	NJ	42/3	1/1	0/0	43/4	.7/1.5	
	PA	15/6	7/4	0/0	22/10	.4/3.7	
	CHSPK BAY	11/3	2/2	2/2	15/7	.2/2.6	
	OCEAN {	N OF ORF	337/36	67/10	202/19	606/65	9.6/24.2
		S OF ORF	1069/47	41/11	2934/41	4044/99	64.4/36.8
TOTAL		2768/143	160/33	3356/90	6284/269	100%/100%	
ZDC CTLA {	MTNS	34/7	21/4	2/2	57/13	3.8/14	
	CNTRL	915/27	3/2	136/10	1054/39	69.7/41.9	
	CSTL	332/27	3/3	66/11	401/41	26.5/44.1	
	TOTAL	1281/61	27/9	204/15	1512/93	100%/100%	

CASE STUDY #1: FEBRUARY 23, 1987

At 06 UTC only a few strikes were associated with a low near HAT. Within an hour strikes developed to the east-southeast of HAT showing the location of the associated warm front. Around 08 UTC as the low approached the Virginia Capes, strikes appeared along the Maryland eastern shore due to the east-southeasterly onshore flow north of the low.

The number of strikes greatly increased in the warm air sector after 08 UTC as the low and frontal system approached the warmer waters of the Gulf Stream. For the same reason after 09 UTC as the low moved eastward away from the Virginia Capes the number of strikes north and east of the low center increased.

As the low moved away from the SUNYA lightning detection network coverage the number of strikes greatly diminished. The strikes formed a linear pattern northwest of the low associated with a shortwave trough on the 12 UTC 500 mb analysis from ART across ACY to the low center.

CASE STUDY #2: DECEMBER 24-25, 1986

This case study represented a heavy rain event over North Carolina and eastern Virginia. A low near RWI along with a warm moist air mass having dewpoints in the low 60's, triggered negative CG lightning strikes over central North Carolina between 1900 and 2030 UTC.

A few strikes lingered over southeastern Virginia between 21 and 24 UTC but not much happened until 02 UTC.

At 02 UTC the low center, indicated by two positive strikes, was about 50 miles northwest of SBY and a cold front south of the low was delineated by a band of almost 40 negative strikes. As the eastward moving cold front slowly approached the warmer waters of the Gulf Stream, the number of mostly negative strikes tripled.

At 04 UTC several strikes near the mouth of Delaware Bay placed the low near Cape Henlopen, Delaware. Between 0400 and 0600 UTC the number of strikes greatly increased over New Jersey indicating a period of intensification of the low as it moved northward to ACY at 0630 UTC.

After 0630 UTC, the 15 mostly negative strikes over central New Jersey diminished to 3 positive strikes over northern New Jersey indicating the low was no longer intensifying as it moved northward to CYN VOR (about 15 miles east northeast of McGuire AFB/WRT).

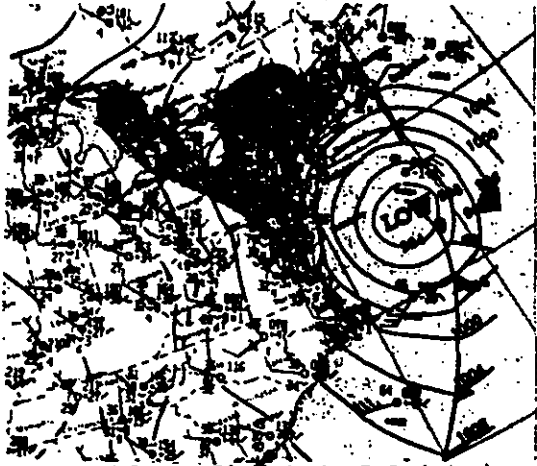
CASE STUDY #3: JANUARY 22, 1987

A developing low was forming over the Virginia capes and most of the strikes were just northeast of the low center over the ocean with several also over northern Chesapeake Bay. The area of strikes northeast of the low center moved fairly rapidly northeastward indicating that the center was moving northeastward through 22 UTC before turning northward.

After 22 UTC a band of negative strikes increased south of the low over the warmer Gulf Stream waters delineating a trough or cold front associated with the low pressure system/storm.

CASE STUDY #1

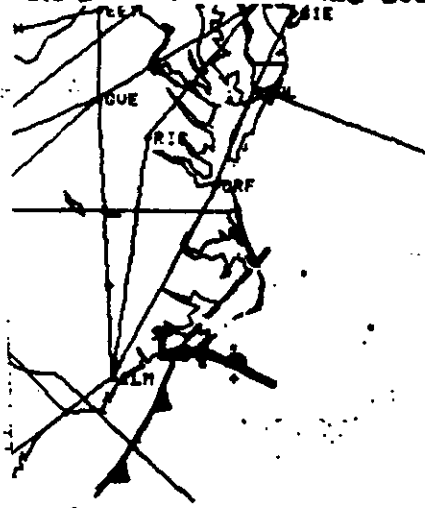
FEB. 23, 1987 05Z THRU 13Z



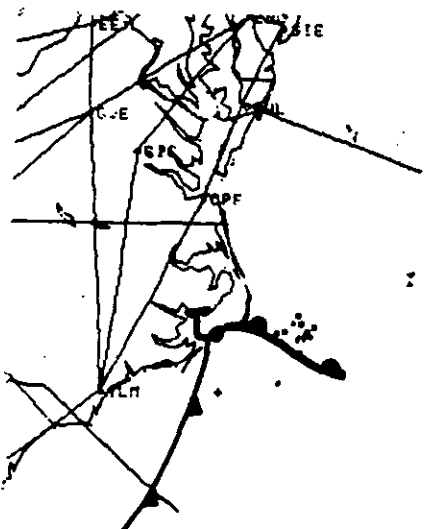
12Z SURFACE ANALYSIS (2/23)



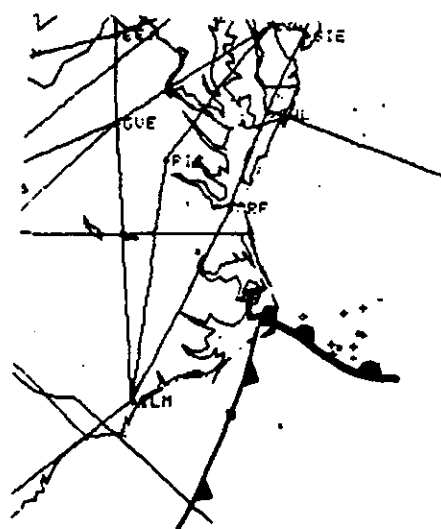
12Z 500MB ANALYSIS (2/23)



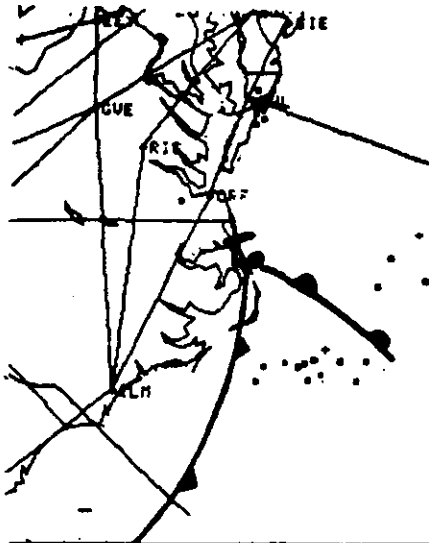
05:20:13 TO 06:04:50 23-FEB-87 FLASH
← TIME KEY →



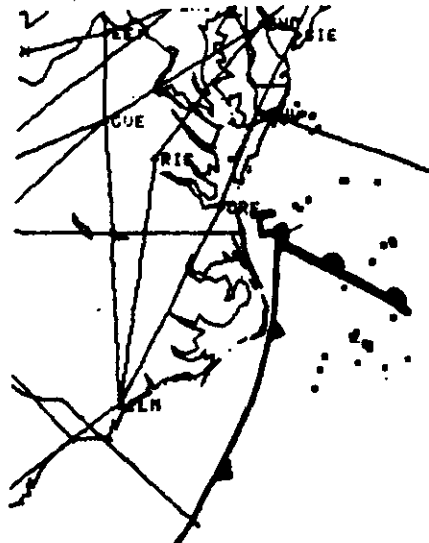
06:04:50 TO 06:54:58 23-FEB-87 FLASH
← TIME KEY →



06:54:58 TO 07:44:13 23-FEB-87 FLASH
← TIME KEY →



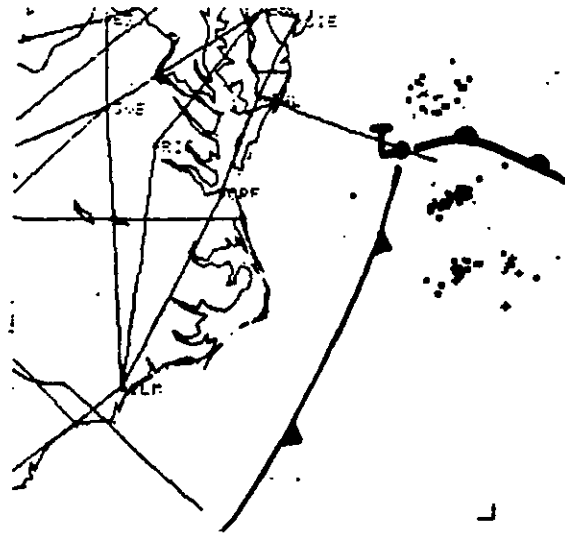
07:44:19 TO 08:33:35 20-FEB-67 FLASH 24
 ● ← TIME KEY → +



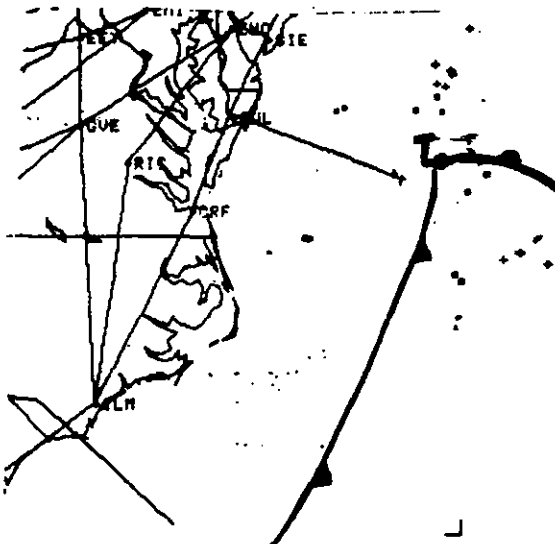
08:37:46 TO 09:24:45 20-FEB-67 FLASH 37
 ● ● ← TIME KEY → + +



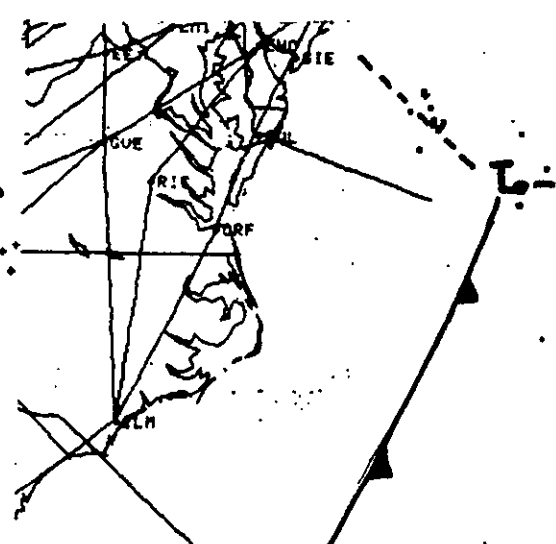
09:24:45 TO 10:14:24 20-FEB-67 FLASH 64
 ● ● ← TIME KEY → + + + +



10:14:24 TO 11:04:56 20-FEB-67 FLASH TOTAL 101
 ● ● ● ← TIME KEY → + + + + +



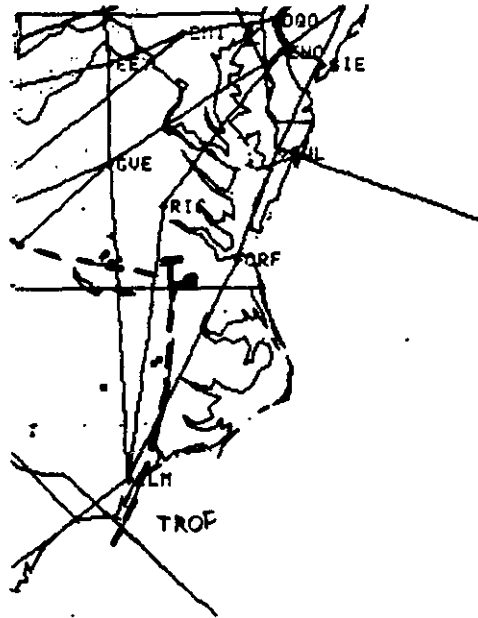
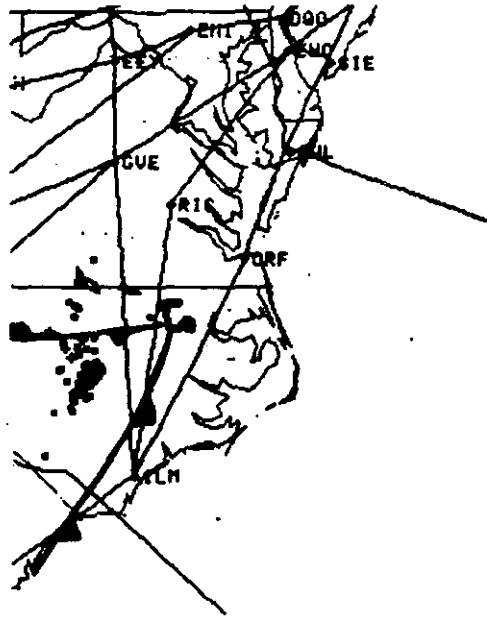
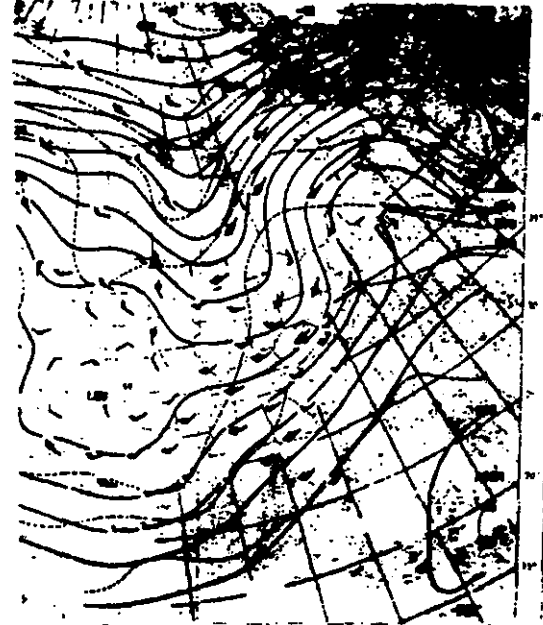
11:04:41 TO 11:52:19 20-FEB-67 FLASH TOTAL 22
 ● ● ← TIME KEY → + + + +



11:59:08 TO 12:42:35 20-FEB-67 FLASH TOTAL 19
 ● ● ● ← TIME KEY → + + +

CASE STUDY #2

DEC. 24-25, 1986 18Z THRU 08Z



18:00:07 TO 19:02:56 24-DEC-86 FLASH 81

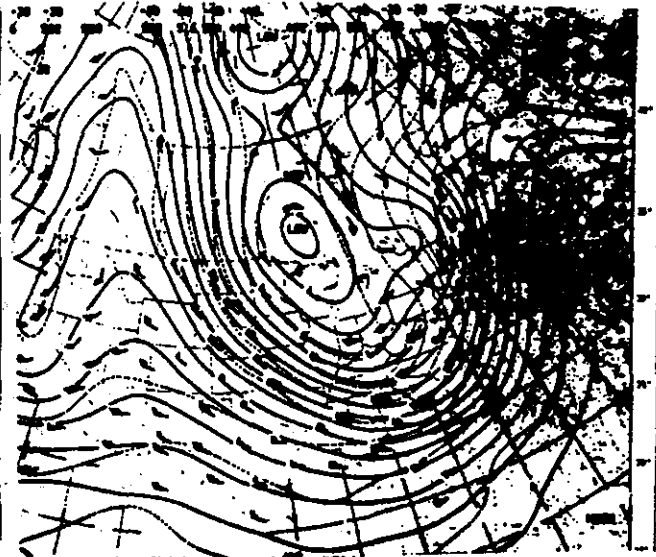
19:59:20 TO 20:25:42 24-DEC-86 FLASH 9

CASE STUDY # 3

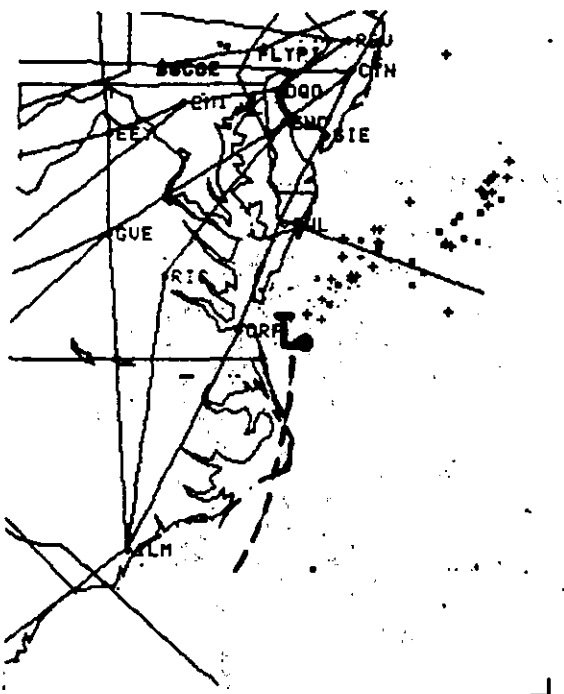
JAN. 22, 1987 18Z THRU 24Z



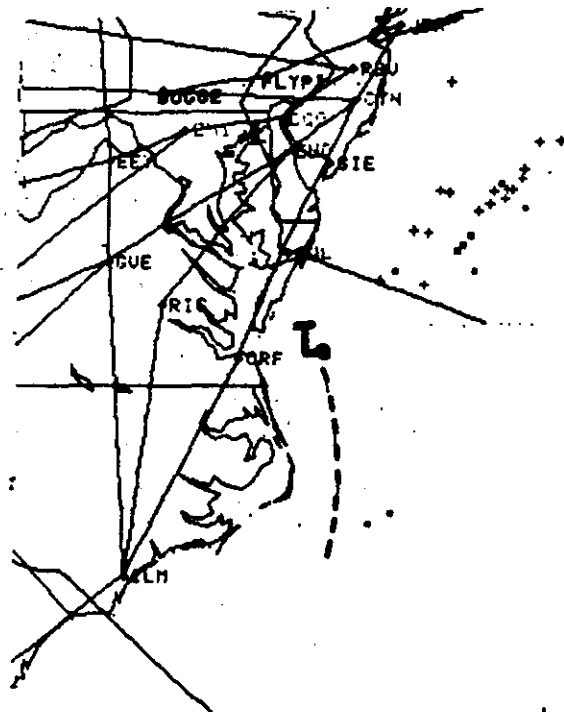
12Z SURFACE ANALYSIS (1/23)



12Z 500MB ANALYSIS (1/23)



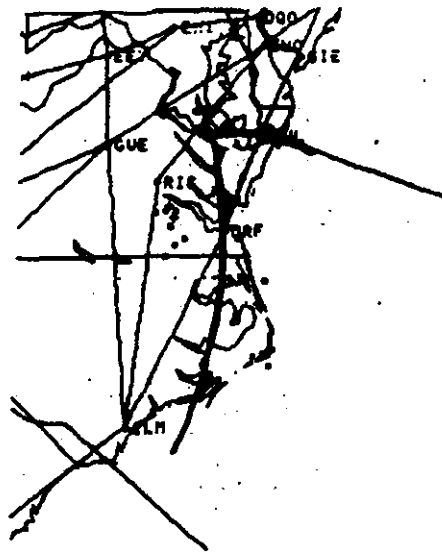
17:43:28 TO 19:40:26 22-JAN-87 FLASH



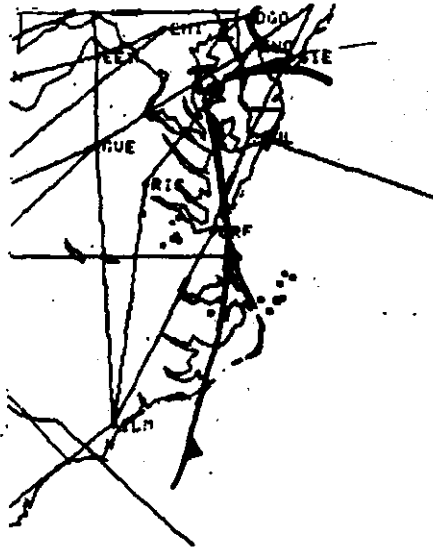
18:30:10 TO 19:31:51 22-JAN-87 FLASH



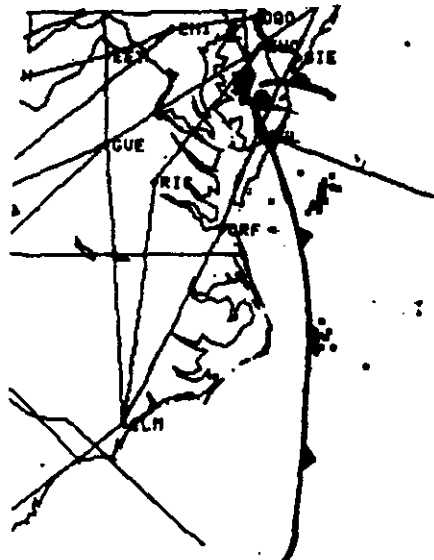
21:27:16 TO 22:19:31 28-DEC-66 FLASH II
 ..B <- TIME KEY >-



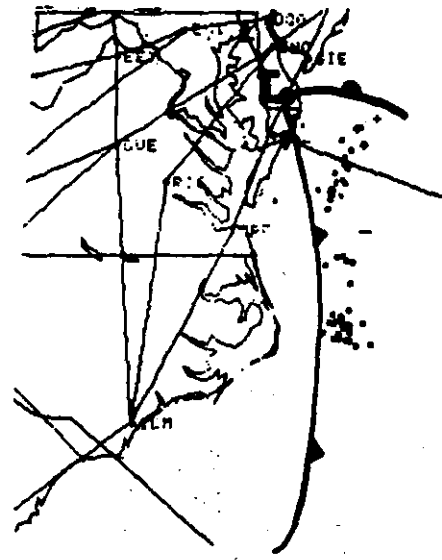
22:17:04 TO 23:12:30 28-DEC-66 FLASH IC
 ..B <- TIME KEY >-



23:10:39 TO 23:53:49 28-DEC-66 FLASH IB
 ..B <- TIME KEY >-



01:43:57 TO 02:31:47 28-DEC-66 FLASH MB
 ..B <- TIME KEY >-



02:23:09 TO 03:21:29 28-DEC-66 FLASH NB
 ..B <- TIME KEY >-



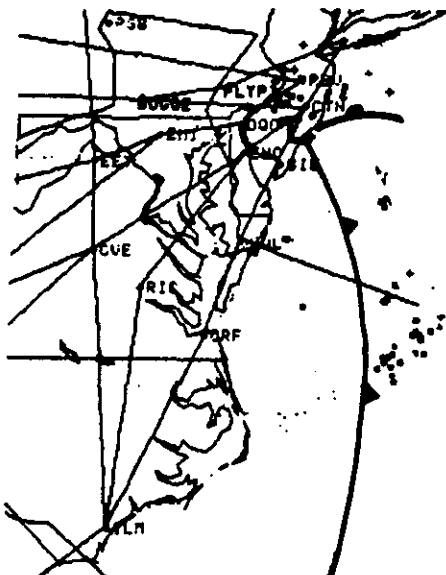
03:13:05 TO 04:11:43 25-002-00 FLASH III



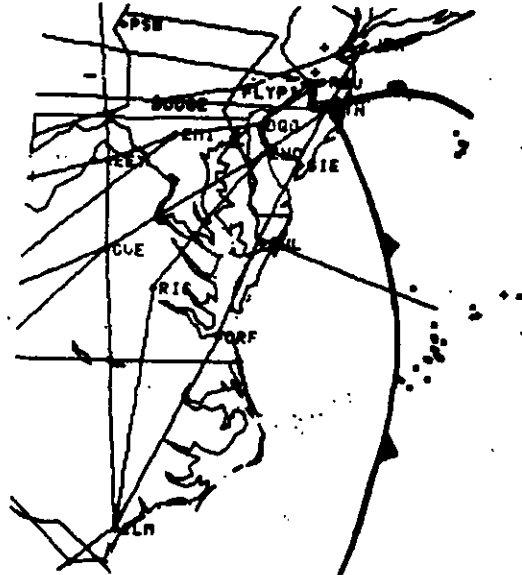
04:03:46 TO 05:01:32 25-002-00 FLASH 105



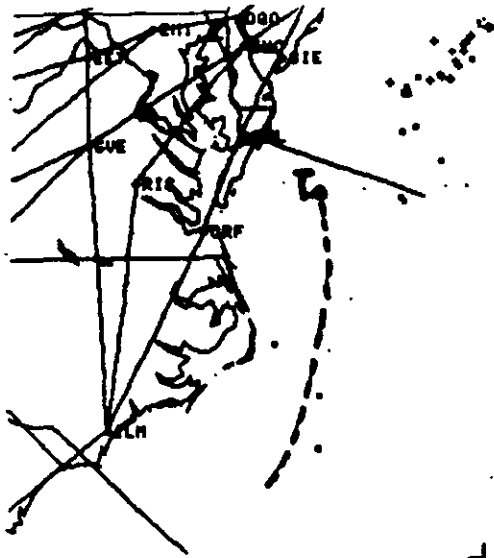
04:53:04 TO 05:52:40 25-002-00 FLASH 05



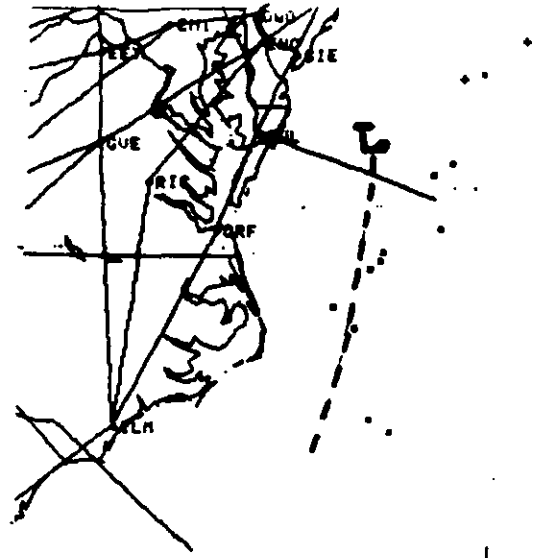
05:43:23 TO 06:39:34 25-002-00 FLASH 32



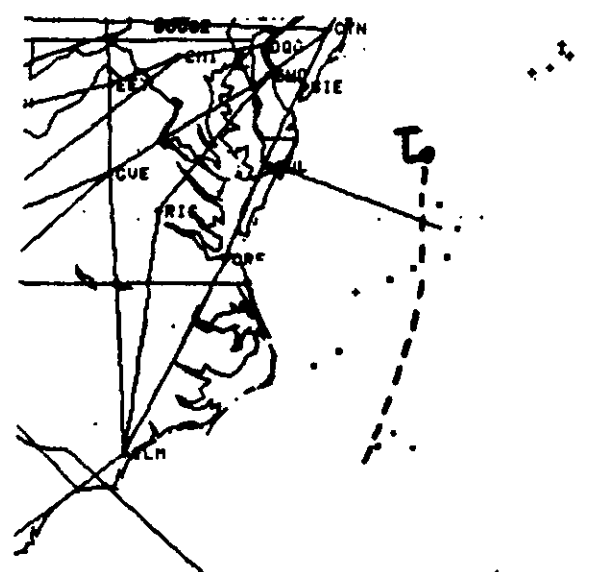
06:39:24 TO 07:29:46 25-002-00 FLASH TC 33



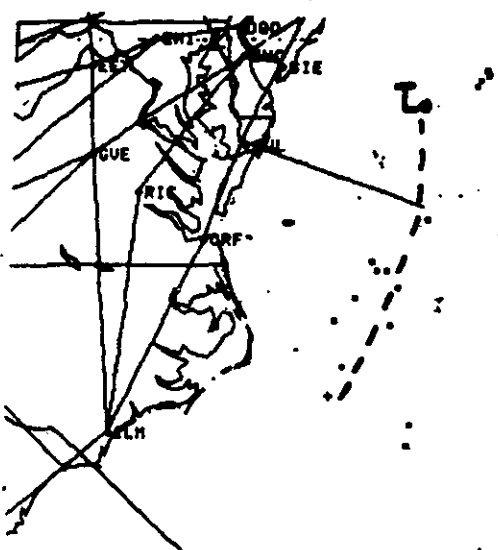
19:25:17 TO 20:16:57 22-JUN-87 FLASH TOTAL 17
 *B ← TIME KEY → *



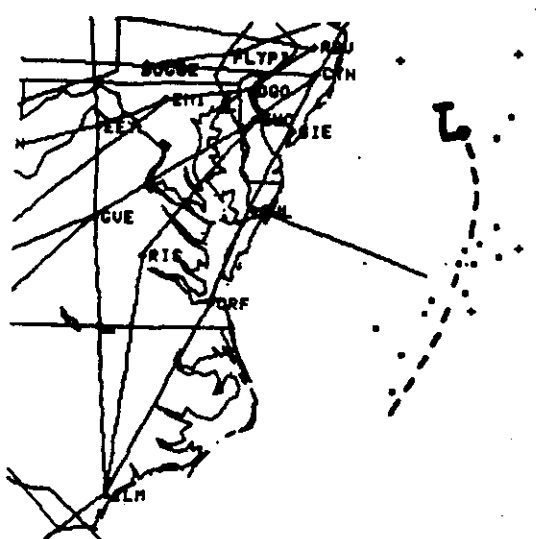
20:13:04 TO 21:12:54 22-JUN-87 FLASH TOTAL 17
 *B ← TIME KEY → *



21:04:35 TO 22:02:53 22-JUN-87 FLASH TOTAL 18
 *B ← TIME KEY → *



22:08:53 TO 22:50:52 22-JUN-87 FLASH TOTAL 16
 *B ← TIME KEY → *



22:44:51 TO 23:10:57 22-JUN-87 FLASH TOTAL 18
 *B ← TIME KEY → *

SKILL IN PREDICTION OF EXPLOSIVE CYCLOGENESIS
OVER THE WESTERN NORTH ATLANTIC OCEAN, 1987-1988:
A FORECAST CHECKLIST AND NMC DYNAMICAL MODELS

Frederick Sanders
9 Flint Street
Marblehead MA 01945

and

Eugene P. Auciello
NOAA, NWS Forecast Office
Boston MA 02128

Analyses and predictions of explosive cyclogenesis over the western North Atlantic Ocean during the 1987-1988 cool season were compared. The analyses were the manual and automated series produced at the National Meteorological Center (NMC). The forecasts were those produced by the Nested Grid Model (NGM) and the "aviation run" of the global spectral model (AVN) at NMC, and also by a simple checklist employed the NWS Forecast Office, Boston.

Skill of the forecasts has evidently improved since the preceding year. Probability of detection of the event in a specified 24-h period, with the manual analyses used as verification, approached was 72% for the NGM in the range from 0-24 h with a false alarm rate of 17%. In the range 36-60 h the values for the AVN forecasts were 42% and 30%. When the automated analyses were used for verification, forecast performance was somewhat better.

Skill of the checklist forecasts was comparable to that of the AVN forecasts but not as good as that of the NGM predictions, in the small sample available for comparison.

Deepening in the NGM forecasts over the range 12-24 h was 2 mb less than in the manual analyses, with a correlation of 0.55. The skill was limited mainly by errors in timing, with the model failing to represent well the initial analyzed deepening but catching up later. The automated analyses displayed a similar failure, with a correlation of 0.49 between analyses. More certain analyses and better boundary-layer modeling are needed.

Table 1

For the 1986-1987 and 1987-1988 seasons, events (E), hits (H), and false alarms (FA); probability of detection (POD), false-alarm rate (FAR), and Critical Success Index (CSI).

12-h			24-h			36-h			48-h		
E	H	FA									
POD	FAR	CSI									

1987-1988 NGM Western Atlantic vs NH

40	29	6	42	26	3	41	15	4			
.72	.17	.63	.62	.10	.58	.37	.21	.33			

1986-1987 NGM C-grid vs NH

36	18	11	35	17	7	35	9	5			
.51	.38	.39	.49	.29	.40	.26	.36	.22			

1987-1988 AVN Western Atlantic vs NH

44	25	2	45	18	4	33	14	6			
.57	.07	.54	.40	.18	.37	.42	.30	.36			

1986-1987 AVN Atlantic and North America vs NH

44	22	7	43	15	7	36	7	7			
.50	.24	.43	.35	.32	.30	.19	.50	.16			

1987-1988 NGM Western Atlantic vs FH

34	28	8	36	25	3	33	17	3			
.82	.22	.67	.69	.11	.64	.52	.15	.47			

1987-1988 AVN Western Atlantic vs FH

38	25	2	37	19	3	26	15	6			
.66	.07	.62	.51	.14	.48	.58	.29	.47			

Fig.1. Positions of cyclones at the center of 24-h periods when explosive deepening was analyzed in the NH series or was predicted by one or both of the NMC models. Positions for overlapping periods for the same cyclone are connected by solid line. Parentheses indicate that explosive deepening occurred in a forecast but not in the analysis.

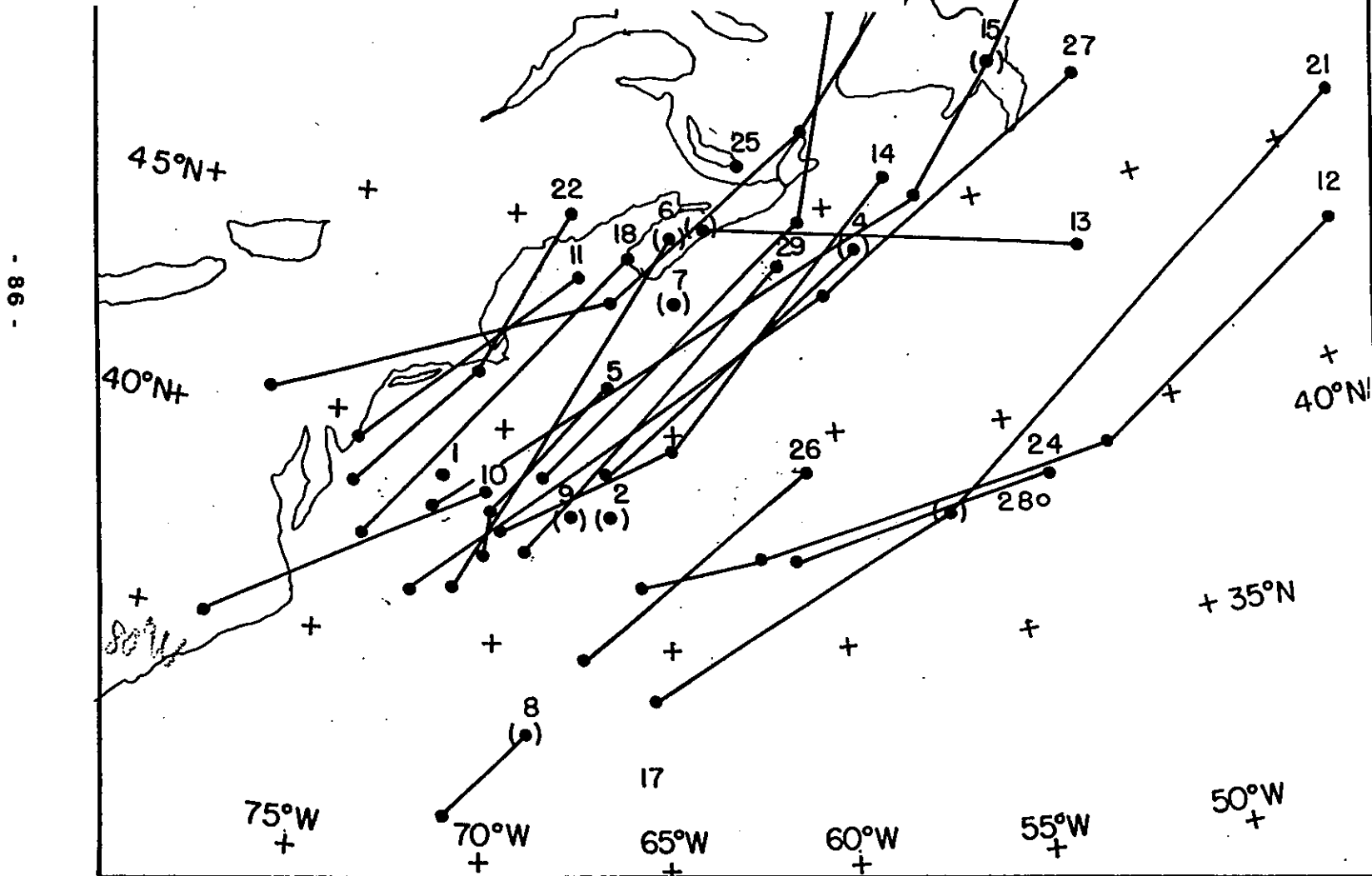
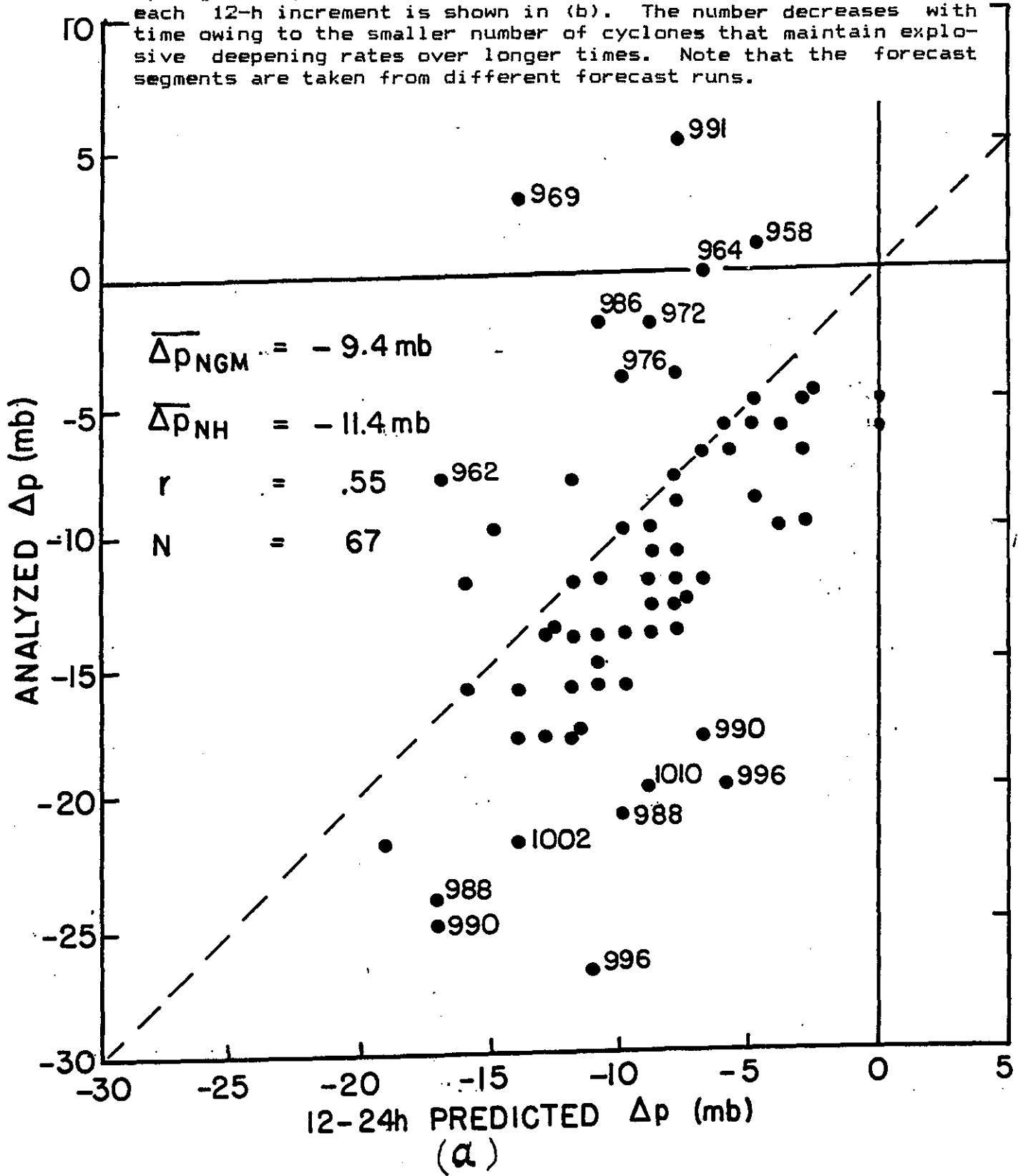
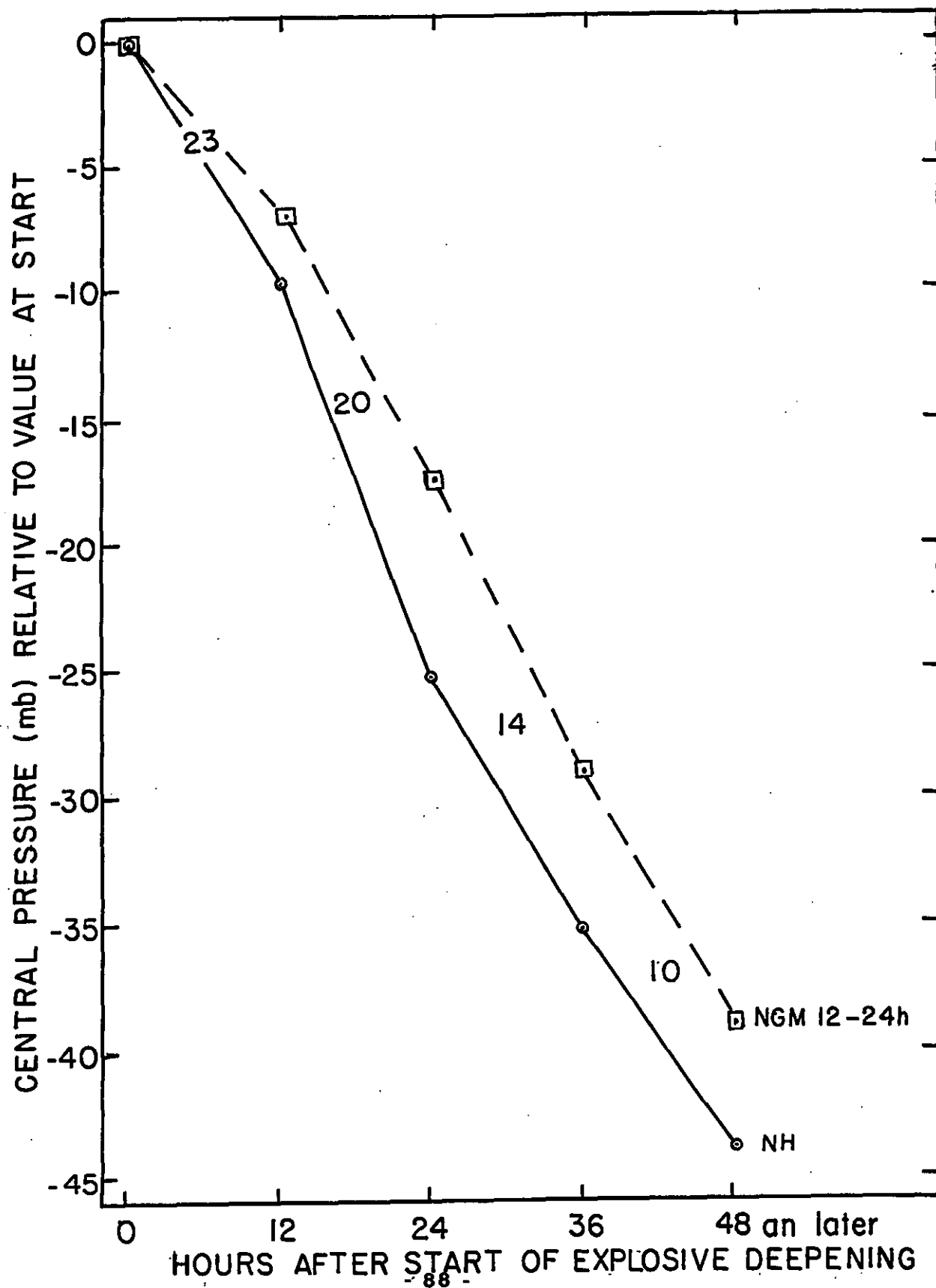


Fig.2. (a) Scatter diagram of 12-h deepening in NH analyses vs in 12-24 h segments of NGM forecasts. (b) Mean central pressure vs time, relative to the central pressure at the start of explosive cyclogenesis, for the FH and NH analyses. The number of pairs for each 12-h increment is shown in (b). The number decreases with time owing to the smaller number of cyclones that maintain explosive deepening rates over longer times. Note that the forecast segments are taken from different forecast runs.



(b)



PATTERNS OF THICKNESS ANOMALY FOR EXPLOSIVE CYCLOGENESIS
OVER THE WEST-CENTRAL NORTH ATLANTIC OCEAN

Frederick Sanders
Marblehead, Massachusetts 01945

and

Christopher A. Davis
Center for Meteorology and Physical Oceanography
Massachusetts Institute of Technology
Cambridge, Massachusetts 022139

Hemispheric anomaly patterns of 1000-500 mb thickness were obtained for 67 cases of explosive cyclogenesis over the western North Atlantic Ocean in December-February during 1962-1977, beginning between latitudes 30-40°N and between longitudes 70-80°W.

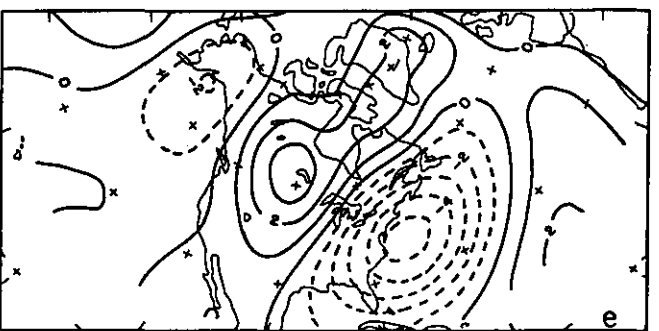
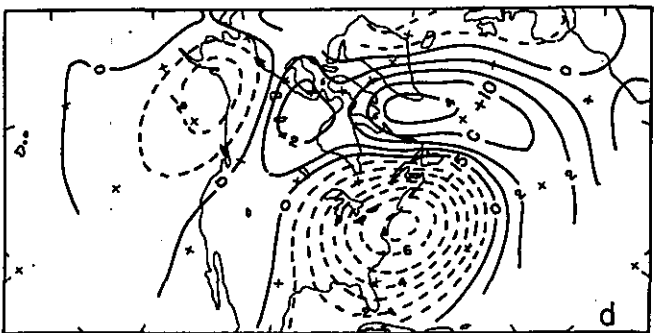
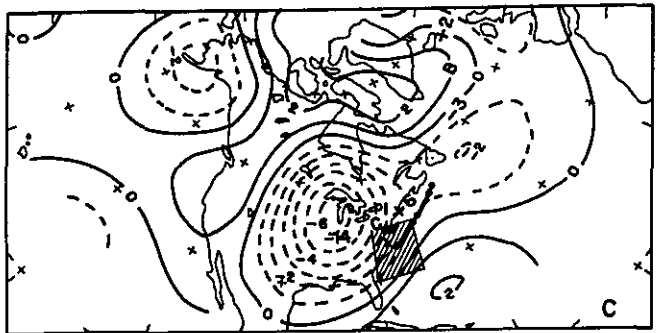
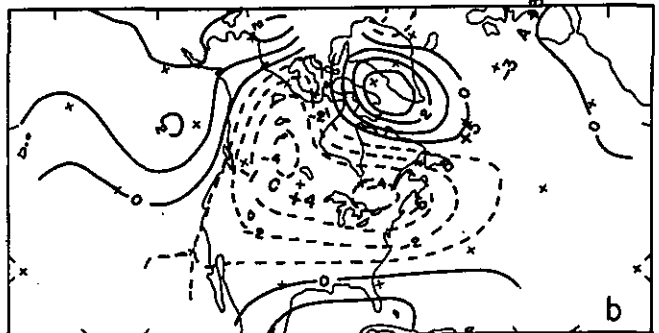
Composite patterns for the 26 strongest cases of cyclogenesis differed markedly from those for the 22 weakest. After a filtering to remove the shortest waves, those for the strongest developments showed a prominent negative anomaly area of large scale, centered over western Canada 5 days before the event, moving southeastward to the western Atlantic days after cyclogenesis. No such pervasive anomaly pattern was seen for the weakest cases.

The most intense cyclogenesis occurred when the air over the region of development was slightly colder than the 15-year average, while the least intense occurred in slightly anomalous warmth.

In the zonal average from 25°W to 125°W, the strongest cases occurred with warmth in polar latitudes, coldness in middle latitudes and anomalously strong westerly thermal wind in the cyclogenetic area. The weakest cases occurred with cold polar latitudes, warmth in upper middle latitudes, and slightly cold anomalies but no excessive thermal wind in the latitudes of cyclogenesis.

It is implied that both baroclinic forcing and heat and moisture flux from the sea surface were enhanced in the strongest cases, but neither effect was obviously dominant.

Fig. 1. Composite patterns of departure of thickness of the layer 1000-500 mb from the long-term mean, for the strong cases of explosive cyclogenesis. Isopleths are at intervals of 2 dam, those for negative values being dashed. a) Day -4, b) Day -2, c) Day 0, d) Day +2, e) Day +4. The regions of cyclogenesis and the mean positions of the cyclones in the sample are indicated in c). Heavy signed values show values and positions of selected local maxima and minima of 24-h change of unfiltered composite thickness, in dam, associated with the implied mobile synoptic systems denoted by letters.



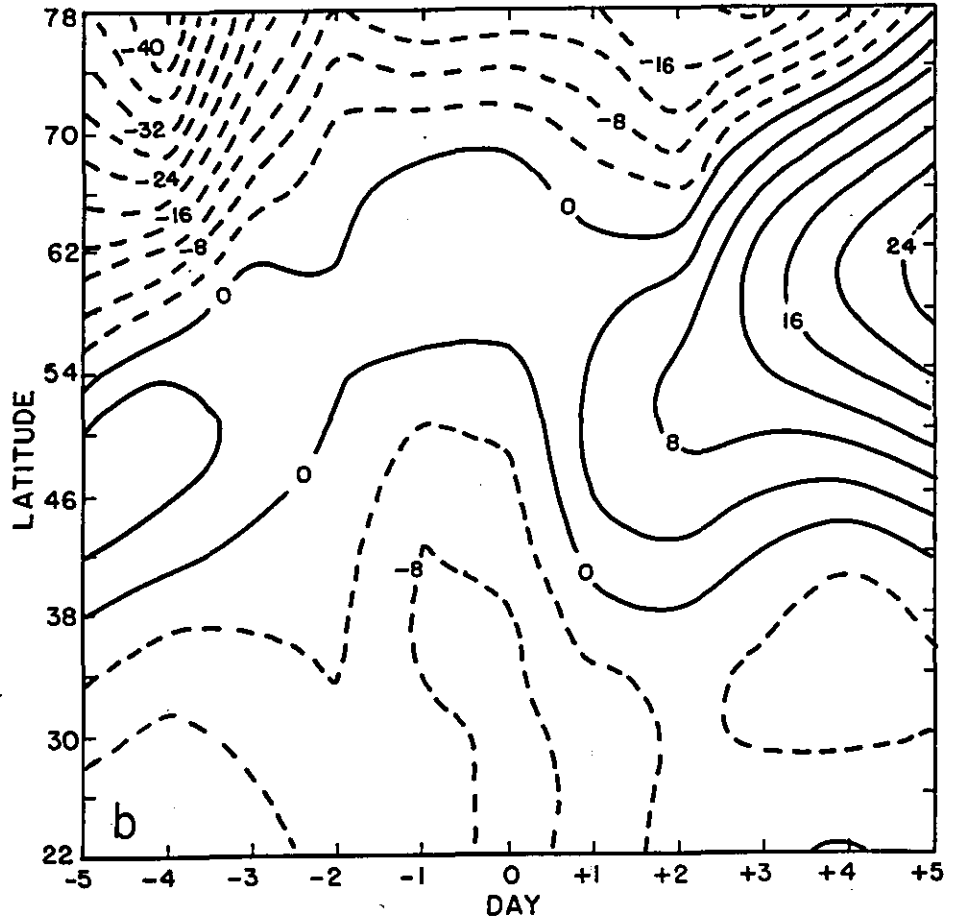
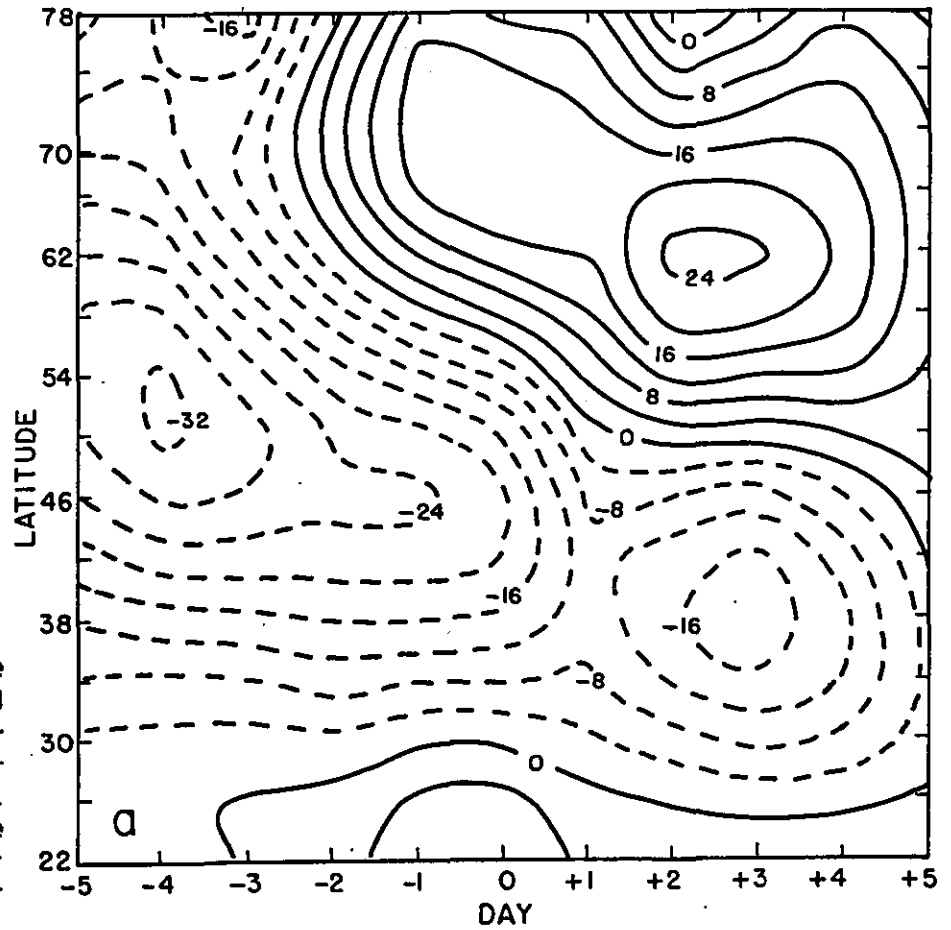


Fig.2. Time series of the zonal mean of the filtered thickness anomalies, averaged from longitude 25°-25°W. Isopleths are at intervals of 4 m, negative values being dashed. a) For the strong cases, b) for the weak cases.

THE ROLE OF MELTING IN DETERMINING PRECIPITATION TYPE IN EASTERN NEW YORK DURING THE STORM OF OCTOBER 4TH 1987

Kenneth D. LaPenta

National Weather Service Forecast Office
Albany, NY 12211

ABSTRACT

On 4 October 1987, an unprecedented early season storm dumped large amounts of snow on Eastern New York. The storm was not well forecast. The numerical guidance was poor, underestimating the storm's intensity, totally underforecasting the quantity of precipitation that fell, and predicting rain not snow.

The local change in temperature is dependent on horizontal thermal advection, changes due to vertical motions, and temperature changes due to non-adiabatic processes. One non-adiabatic process is cooling due to melting. Since the latent heat of fusion is nearly an order of magnitude less than the latent heat of evaporation, it is often overlooked in precipitation type forecasting. The Albany upper air soundings showed significant cooling between 0000 UTC and 1200 UTC 4 October 1987. During that time about an inch of rain fell before precipitation changed to snow. Calculations show cooling due to melting was a critical factor in turning the rain to snow, accounting for nearly two thirds of the observed temperature change in the lower troposphere.

1. Introduction

On 4 October 1987, an unprecedented early season snowstorm dumped large amounts of snow on Eastern New York, causing many deaths, injuries and enormous property damage. Heavy wet snow piled up on trees that had not yet lost their foliage. Numerous trees and limbs collapsed under the weight of the snow taking power lines with them. In New York, over 200,000 homes lost power, some for over a week. Two New Yorkers were killed by falling trees. Twelve other deaths were attributed directly or indirectly to the storm in the state. Over 300 people were injured and property losses were staggering. Parts of western New England were hit just as hard.

Albany had just over 6 inches of snow with one to two feet in the nearby hills to east, and in the Catskills (Fig. 1). In the previous hundred years, Albany's greatest October snowfall was 2 inches in 1952.

The snowstorm was not forecast. The numerical guidance was poor in many respects. The models underestimated the intensity of the system, and totally underforecast the quantity of precipitation that fell. They were also too warm, predicting rain and not snow. Forecasters adjusted the guidance in the right direction, but didn't go far enough. The date on the calendar made it hard for anyone to believe there could be a big snowstorm.

Post analysis helped explain the storm's development and progress. One often overlooked physical process, cooling due to melting, played an important role in determining the type of precipitation that fell. This paper will examine the role melting played in the storm.

2. Background

Forecasting precipitation type is one of the most difficult tasks a meteorologist faces. Small changes in the state of the lower troposphere can have a major impact on the character of a storm. Routine radiosondes sense the atmosphere twice a day, and on a rather broad scale. A correct precipitation type forecast is dependent on assessing changes in the lower atmosphere between sounding times.

The equation for determining the local change in temperature with time is derived from the first law of thermodynamics. Penn (1957) used the following form of the equation for local temperature change:

$$\frac{\partial T}{\partial t} = -V \cdot \nabla T - w (\gamma_d - \gamma) + \frac{1}{C} \frac{dQ}{dt} \quad (1)$$

where:

- T is temperature
- t is time
- V is horizontal wind velocity
- w is vertical wind velocity
- γ_d is the dry adiabatic lapse rate
- γ is the actual lapse rate
- C_p is the specific heat at constant pressure
- Q is heat

If the airmass is saturated and condensation occurs, the latent heat released must be accounted for, and equation (1) is modified. According to Haltiner and Martin (1957), the dry adiabatic lapse rate is replaced by the saturated adiabatic lapse rate and the third term in the equation is replaced by:

$$\frac{dQ}{dt} = \left(c_p + m \frac{L^2}{R_v T^2} \right) \quad (2)$$

where:

- m is the mixing ratio
- L is the latent heat
- R_v is the gas constant for water vapor

The first term in the equation represents temperature change due to horizontal thermal advection. The second term is the change due to vertical motions and the final term change due to non-adiabatic processes.

Horizontal advection is usually the most important factor in determining local temperature change, though under certain circumstances the other two terms can become significant. When precipitation occurs with warm advection, there is large scale upward vertical motion. Under these conditions the vertical motion term is opposite in sign to the horizontal advection term and according to Austin (1949) and Fleagle (1947), about half the magnitude.

Non-adiabatic effects can play a critical role in determining precipitation type. Evaporative cooling is the most important. When precipitation falls through unsaturated air between the cloud and the ground, evaporation occurs. It takes nearly 600 calories of heat from the atmosphere to evaporate 1 gram of water. The amount of cooling is even greater if sublimation is involved. The drier the subcloud air, the greater the cooling. A rapid five, or even 10 degree, drop in surface temperature is not uncommon (Penn, 1957). When the subcloud air reaches saturation, cooling stops.

Non-adiabatic cooling can also occur when snow melts, though the latent heat of fusion is nearly an order of magnitude less than the latent heat of evaporation. About 80 calories of heat are needed to turn a gram of snow to liquid. (Some additional cooling occurs in raising the temperature of the snowflakes to freezing.) For melting to be important, there would have to be significant precipitation, and at the same time little or no warm advection to counteract it. Unlike evaporative cooling, cooling due to melting is not dependent on the degree of saturation. McGuire and Penn (1953) did find a case (13 April 1953, in Boston) where melting was a key factor in determining precipitation type, though few such cases have been documented.

3. Synoptic situation

On 30 September and 1 October 1987, a vigorous short wave dug southeast across western Canada. By 1200 UTC 1 October, the associated surface low pressure (992 mb) reached extreme western Ontario. It then slowed considerably and was over northern Lake Huron at 1200 UTC 2 October, maintaining its intensity. The cold front trailing the low moved through the mid Mississippi valley, and behind it an unseasonably cool airmass moved into the Plains states and Midwest. The upper level trough also slowed, and sharpened as it moved into the Great Lakes.

During the next 24 hours the primary surface low (1012 mb) filled and moved northeast. It was north of Quebec City at 1200 UTC 3 October (Fig. 2). Cold air behind it had spread as far east as the Hudson River Valley. Very warm, moist air (surface dewpoints +10 to +15 deg C) lay over New England, ahead of the cold air. The upper trough continued to sharpen with a strong vorticity maximum swinging through its base. By 1200 UTC 3 October it was in Kentucky. In response to it, a secondary surface low (1011 mb) had formed well east of the coast near latitude 36 north, longitude 71.5 west.

The secondary low moved nearly due north during the day, deepening rather slowly. By 0000 UTC 4 October (Fig. 3) it was east of Cape May, New Jersey (1007 mb). The cold front had moved to eastern New England. Over New York surface temperatures were generally between +5 and +8 deg C. From Cape Cod to Maine surface temperatures and dewpoints remained between +10 and +15 deg C. Pressures were rising slightly from Chesapeake Bay north into eastern New York.

At 500 mb (Fig. 4) an upper low had closed off along the Virginia-West Virginia border and a very strong vorticity maximum moved to south-east Virginia. The greatest height falls (140 m) were over the Delmarva peninsula. The 850 mb analysis for 0000 UTC 4 October (Fig. 5) showed a low east of New Jersey with a large temperature gradient across the northeast. Chatham was +12 deg C, Albany 0 deg C with Buffalo at -6 deg C. 850 mb dewpoints of +8 to +12 deg C over Eastern New England and Nova Scotia indicated copious moisture was present.

After 0000 UTC 4 October, energy from the intense vorticity maximum really began to feed the coastal low and it deepened at better than a millibar per hour. The surface low (1000 mb) continued nearly due north and was at about 40 N and 71 W at 0600 UTC 4 October (Fig. 6). Pressures were falling most rapidly over southeast New England, but had also begun to fall west and northwest of the storm center. Primarily rain was falling, although there was some snow in the Catskills and at Montpelier, Vermont.

By 0900 UTC 4 October, the low had moved to the southeast Massachusetts coast and deepened 5 more millibars. Rain had mixed with, or changed to snow in many parts of northeast Pennsylvania and eastern New York.

At 1200 UTC 4 October, the center of the closed low at 500 mb was near the junction of New York, New Jersey and Pennsylvania (Fig. 7). It tracked northeast, almost directly over Albany and was in western Maine at 0000 UTC 5 October. At 850 mb (Fig. 8), the thermal gradient had tightened further. Portland's temperature had risen to +11 deg C with +14 deg C readings over Nova Scotia. To the west, Albany had fallen to -4.5 deg C with Buffalo at -7 deg C. The system was growing more vertical and the 850 mb low was near Boston. Large quantities of moisture (850 mb dewpoint +10 deg C at Portland) were feeding west over the cold air.

At 1200 UTC 4 October the surface the low was just west of Boston (Fig. 9). It had deepened to 992 millibars (15 mb in 12 hours), and was close to its maximum intensity. It was raining through most of New England with snow in eastern New York. Some places had thunderstorms.

The surface low (992 mb) moved to southeast New Hampshire at 1500 UTC 4 October and to just east of Portland, Maine, at 1800 UTC (Fig. 10). At that time precipitation in eastern New York tapered off.

4. The role of melting in turning the rain to snow

Equation (1) stated the local rate of change in temperature is a function of horizontal advection, change due to vertical motions and change due to non-adiabatic processes. It is almost impossible to quantitatively evaluate each term over the course of the storm since vertical soundings were taken only every 12 hours. Still, by calculating the potential cooling due to precipitation melting, and qualitatively examining the vertical motion and advection terms, we can evaluate the role of melting cooling in determining the precipitation type. It is assumed that cooling due to other non-adiabatic processes such as radiation and conduction was small.

Wexler et. al. (1954) calculated the rate of cooling due to melting. The cooling rate is inversely proportional to the thickness of the layer

cooled, and directly proportional to the precipitation rate. They showed one inch of precipitation (water equivalent) melted in a layer 200 mb thick would produce a 2.5 deg C. drop in temperature over the layer.

Figure 11 shows the Albany sounding for 0000 UTC 4 October. Since the atmosphere was nearly saturated, evaporative cooling was not a factor. The freezing level was at 5200 feet and the surface temperature was +6 deg C. All rain fell from 0000 UTC to 0649 UTC when sleet started to mix in. At 0706 UTC the first snowflakes began to fall, but until 1000 UTC the precipitation was predominantly rain. Between 0000 UTC and 1000 UTC total melted precipitation was 1.00 inches. Figure 12 gives hourly temperature, precipitation and snowfall for Albany.

Figure 13 shows the 0000 UTC 4 October Albany sounding modified for cooling due to melting. It was assumed the cooling was equally distributed within the lowest 200 mb of the atmosphere. Based on our assumptions, melting cooling alone would have brought the freezing level down from 5200 feet ASL to about 2500 feet ASL. Penn (1957) stated that on the average, snow must fall through 1200 feet of above freezing air to melt. That would bring snow down to 1300 foot ASL, low enough for snow in the hills around the Hudson Valley. In reality, as the freezing level fell, cooling was probably concentrated closer to the surface. This would mean melting cooling alone would have brought snow level down even closer to sea level.

Figure 13 also shows the observed 1200 UTC 4 October sounding for Albany. Since 0000 UTC 4 October there had been significant cooling below about 780 mb. Based on our calculations, almost two thirds of the cooling was due to melting. Above 780 mb, temperatures had actually risen, indicating overrunning warm air from the east was helping to generate the precipitation.

Low level cold advection was responsible for much of the remaining cooling between 0000 UTC and 1200 UTC. The 850 mb analysis for 0000 UTC 4 October (Fig. 5), showed a fairly steep temperature gradient with isotherms oriented northnortheast to southsouthwest. At Albany, a north wind of 20 knots indicated some cold advection, although the cross isotherm component of the wind was small. Much stronger cold advection was evident at Atlantic City and Pittsburg. The surface map for the same time (Fig. 3) also indicated some cold advection.

By 1200 UTC 4 October, the 850 mb analysis (Fig. 8) showed the wind flow at Albany had become northnortheast in response to the rapidly deepening low over eastern New England. There was an extremely tight thermal gradient between Albany and the coast. Again, the cross isotherm component was small, but there was at least some warm advection at this time, indicating cold advection had ended some time between 0000 UTC and 1200 UTC 4 October.

Figure 14 gives a time cross-section of surface observations in eastern New York. If cold advection was the prime factor in cooling the lower atmosphere, we would have seen a change to snow upstream of Albany first. The low level flow was north to northwest. Still, snow began mixing in with the rain at Albany before it did at Glens Falls. In fact some snow began falling at Poughkeepsie hours before any snow fell at Glens Falls. Twenty-four hour (1200 UTC 3 October to 1200 UTC 4 October) precipitation at Glens Falls was 0.36 while 1.30 fell at Albany.

The amount of temperature change due to vertical motions, is difficult to assess. At 0000 UTC 4 October, the lapse rate in the lower atmosphere was nearly moist adiabatic, indicating this term was small. At 1200 UTC 4 October the lapse rate between the surface and 800 mb had decreased as slightly greater cooling had occurred near the ground than between 900 and 800 mb. There was a marked inversion between 800 and 750 mb. The sounding had warmed above 780 mb. No data was available above about 680 mb.

The 500 mb low passed almost over Albany about 1500 UTC 4 October. The combination of warm advection between 850 mb and 700 mb, and strong cooling above 600 mb, reduced atmospheric stability enough to produce thunderstorms after about 1100 UTC. The thunderstorms certainly helped generate localized strong vertical motion fields as indicated by precipitation rates of .3 to .4 inches per hour. Thus, after 1200 UTC cooling due to vertical motions was important in keeping the precipitation snow.

Elevation played a key role in the snowfall distribution for the storm. The terrain rises steadily east and west of the Hudson Valley. In Albany 6.5 inches of snow fell, but with an astounding water equivalent of over an inch and a half! After 0000 UTC 4 October the water equivalent of all precipitation was better than 3 inches. So it is not at all surprising that nearby communities such as Averill Park (elevation about 900 feet) and East Jewitt (elevation about 2000 feet) had 1 to 2 feet of snow.

5. Conclusions

Analysis of the 4 October 1987 snowstorm indicated melting played an important role in cooling the lower troposphere and causing rain to change to snow. Calculations showed melting accounted for almost two thirds of the cooling at Albany, between the surface and 800 mb, from 0000 UTC to 1200 UTC.

Numerical models did a poor job of assessing the situation. As stated, they underestimated the deepening of the storm system, and the precipitation forecasts were horrible. The NGM 1200 UTC 3 October run forecast no precipitation at Albany. Better than 3 inches fell. The 0000 UTC 4 October run did not do much better. It predicted 0.03 after 1200 UTC, and over an inch and a half fell. The LFM did about as poorly forecasting 0.14 at 1200 UTC 3 October. The 0000 UTC 4 October LFM called for 0.06 inches with MOS indicating only a 20 percent chance of precipitation after 1200 UTC 4 October.

Guidance favored rain rather than snow, although the choice was not clear cut. On some model runs, forecast thickness and boundary temperatures were marginal. MOS indicated snow probabilities as high as 20 percent on the 1200 UTC 3 October run, and 20 percent on the 0000z 4 October run. Since significant, unforecast rain (and hence melting cooling) occurred between 0000 UTC and 1200 UTC 4 October, forecasters could have assumed a much higher probability of snow.

Documented cases where melting cooling played an important role in determining precipitation type are rare. Thus it is difficult to create a set of guidelines defining when it is important. Still, under the right circumstances it can be critical. Forecasters should be alert to melting cooling when the following conditions are present:

- 1) rain at the surface with a relatively cold lower troposphere (freezing levels 1000-6000 feet).
- 2) precipitation rate (melted) exceeding 0.1 inch/hour (Penn, 1957) or lighter rates for an extended period.
- 3) weak or no warm advection

Surface temperatures should be watched carefully. A slow drop in temperature with the above conditions, indicates melting cooling may be significant.

It is highly doubtful anyone could have forecast the 4 October 1987 snowstorm with significant lead time. However, recognizing significant melting cooling was taking place could have led to an earlier recognition of the hazard present and more timely updates.

REFERENCES

- Austin, J. M., et al, 1949: Research on Atmospheric Pressure Changes. Technical report No. 5, Massachusetts Institute of Technology.
- Fleagle, R. G., 1947: The Fields of Temperature, Pressure, and Three Dimensional Motion in Selected Weather Situations. Journal of Applied Meteorology, 4, 165-185.
- Haltiner, G. and Frank L. Martin, 1957: Dynamical and Physical Meteorology. McGraw Hill Book Co, 206-207.
- McGuire, J. and S. Penn, 1953: Why Did It Snow at Boston in April? Weatherwise, 6, 78-81.
- Penn, Samuel, 1957: Forecasting Guide No. 2 - The Prediction of Rain vs. Snow. U.S. Department of Commerce Weather Bureau, 5-8.
- Wexler, R., R.J. Reed and J. Henig, 1954: Atmospheric Cooling by Melting Snow. Bulletin of the AMS, 35, 48-51.

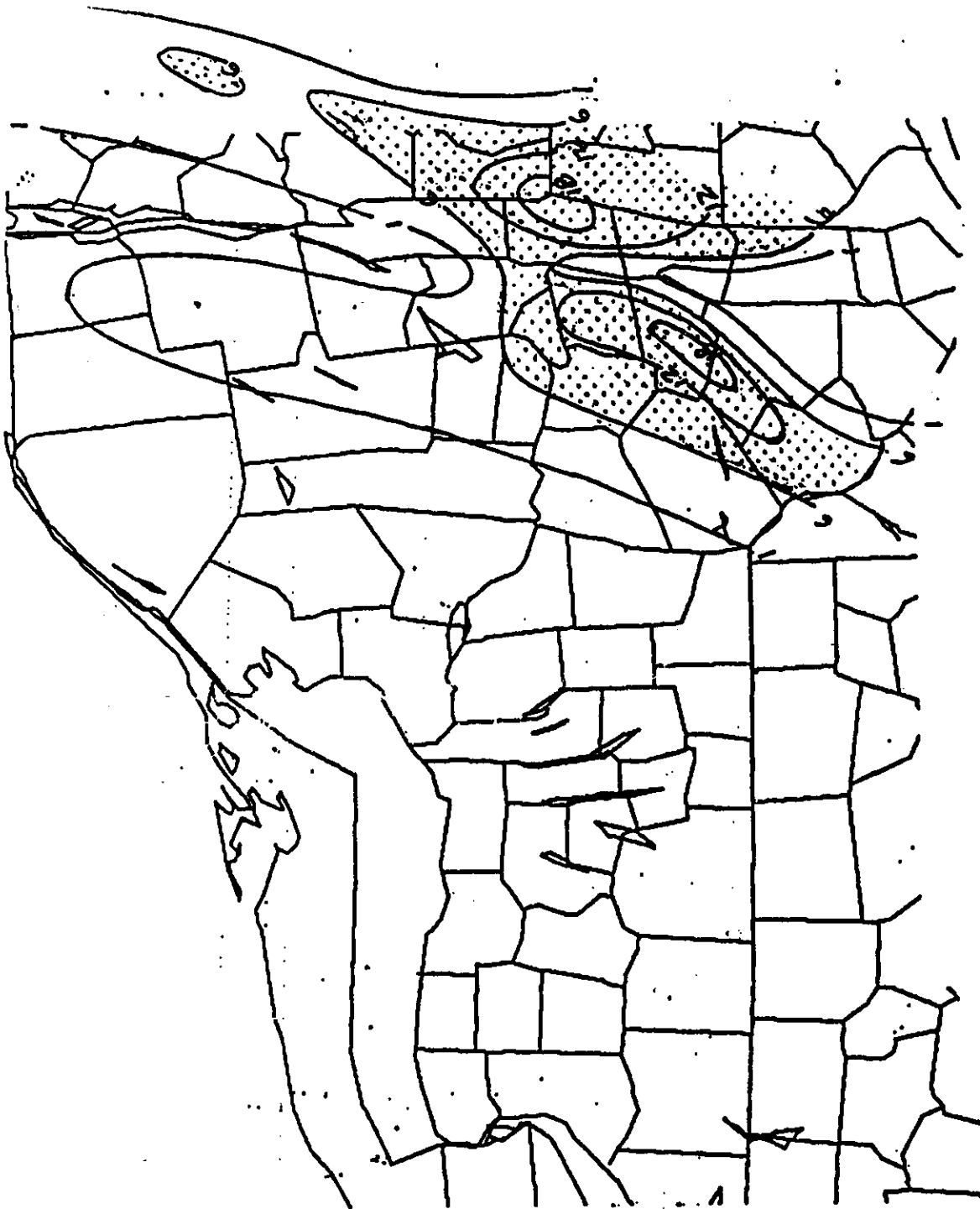


Figure 1. Storm snowfall, 4 October 1987.

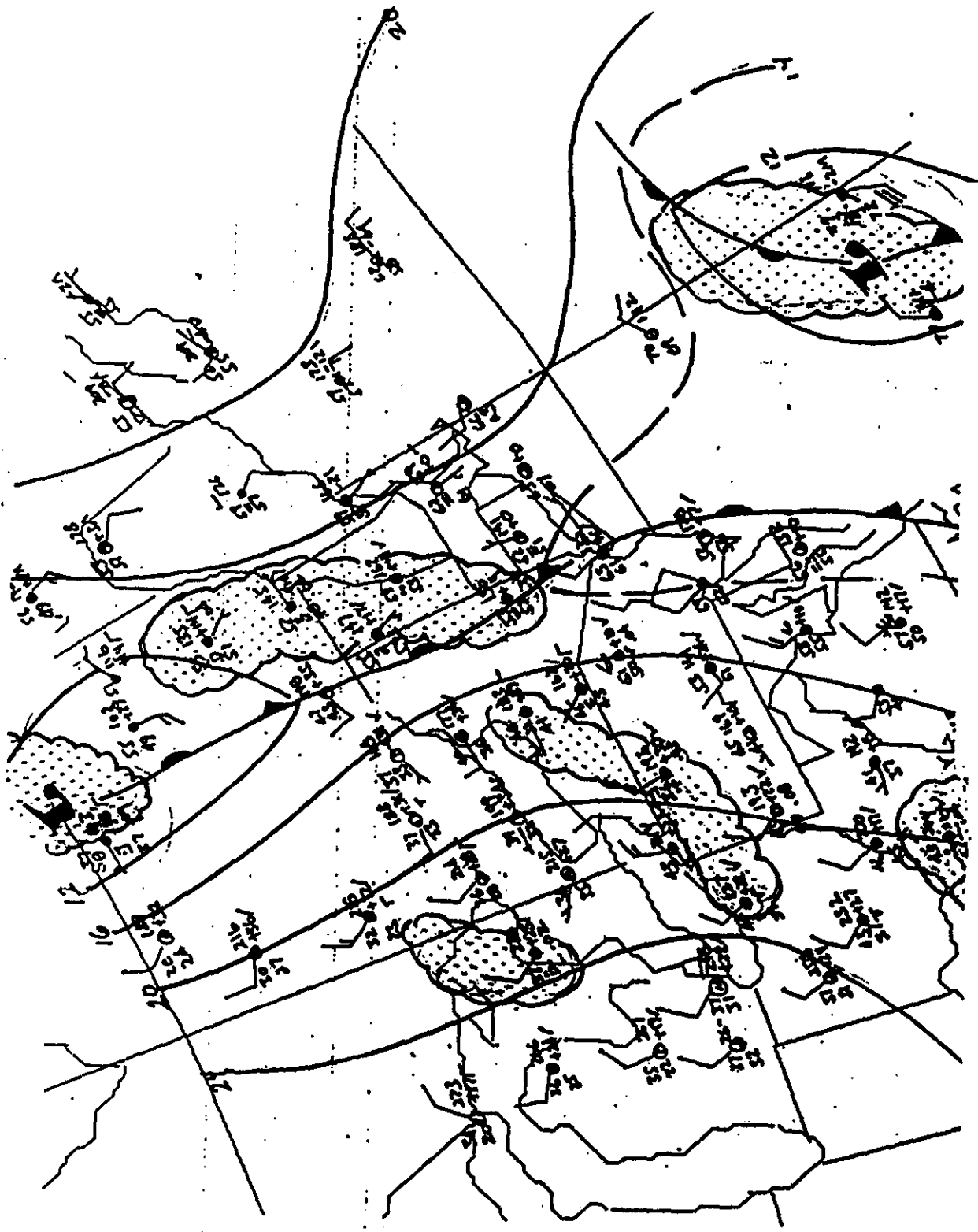


Figure 2. Surface analysis
1200 UTC 3 October 1987.

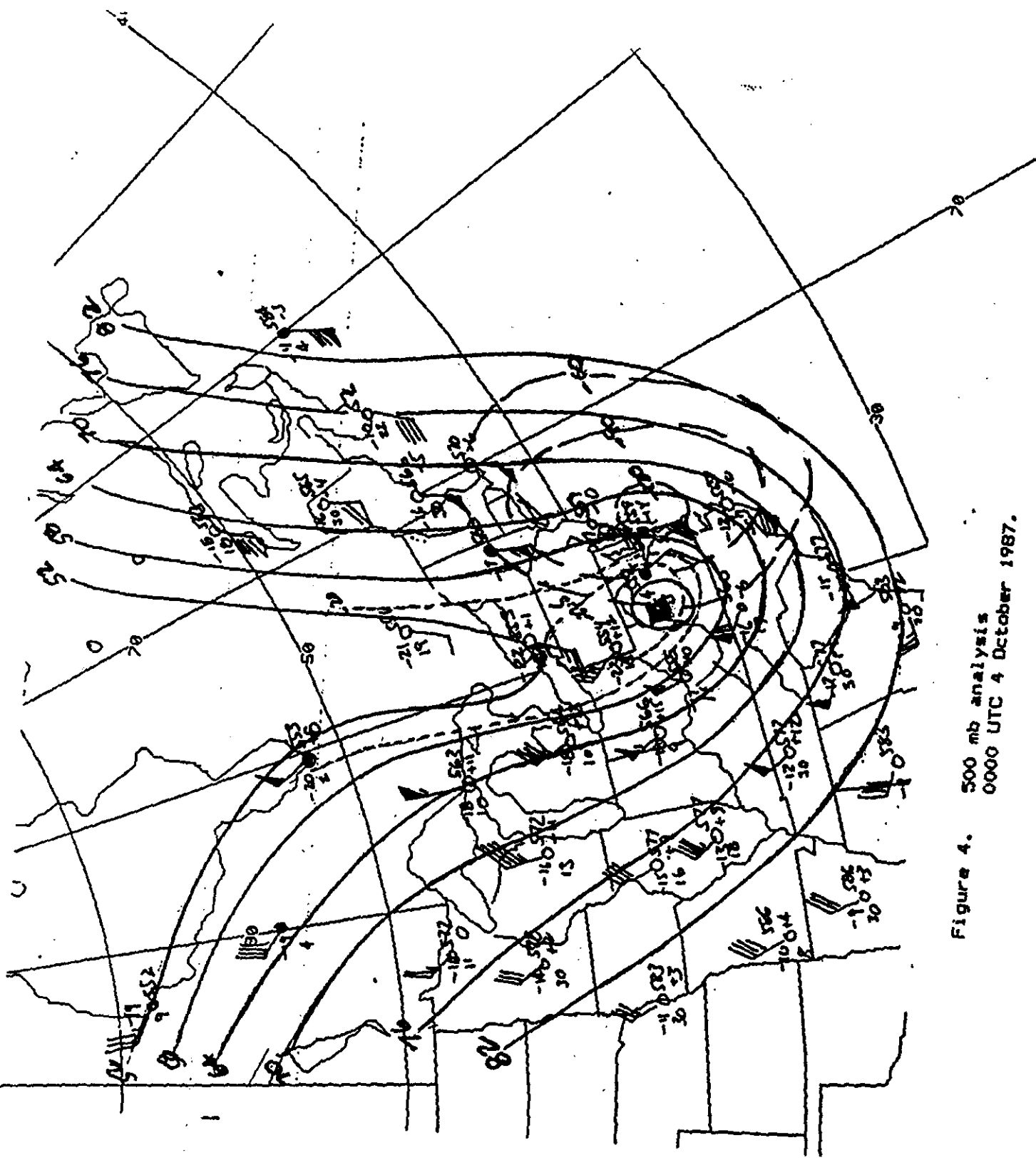


Figure 4. 500 mb analysis
0000 UTC 4 October 1987.

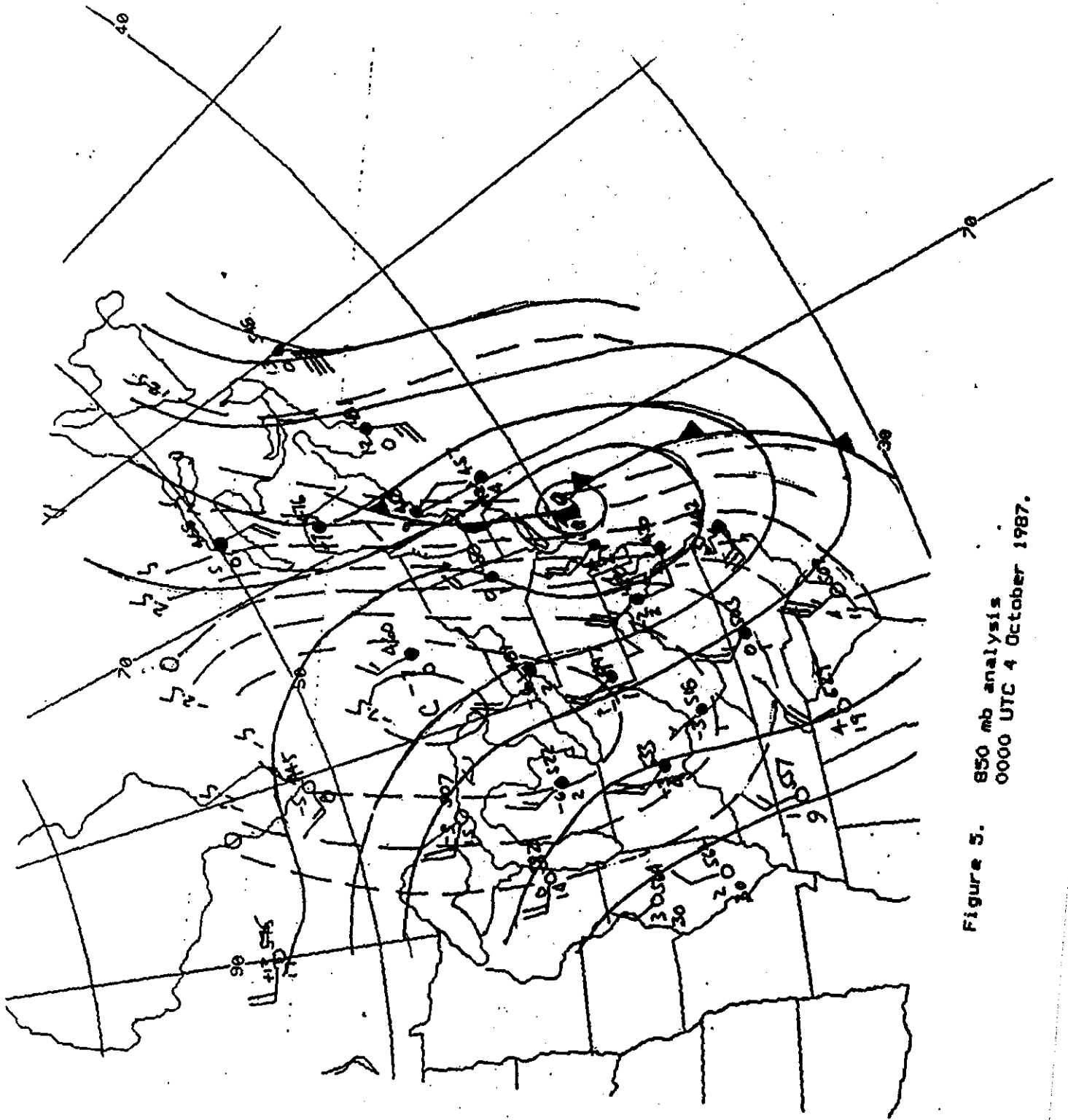


Figure 5. 850 mb analysis
0000 UTC 4 October 1987.

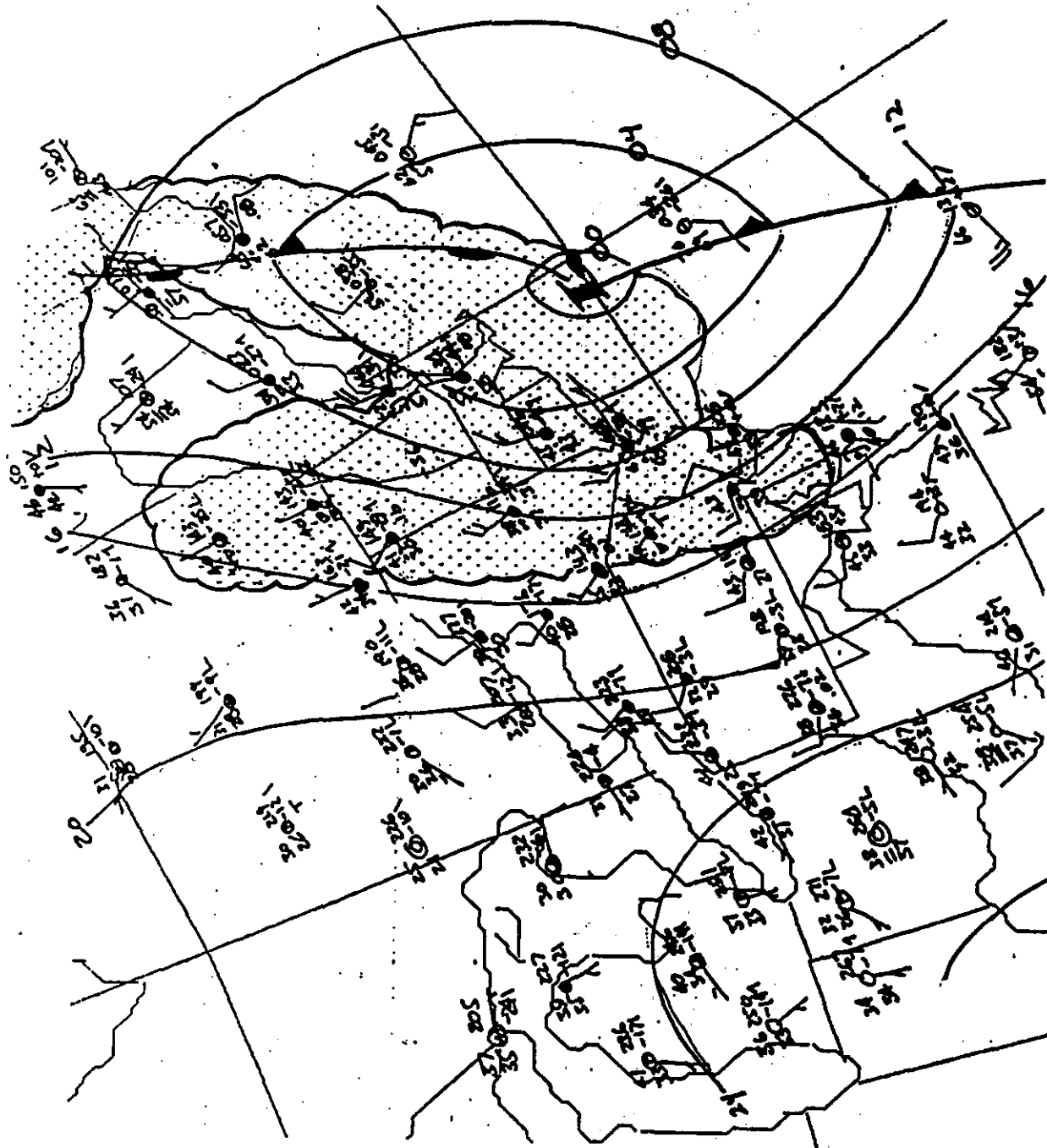


Figure 6. Surface analysis
0600 UTC 4 October 1987.

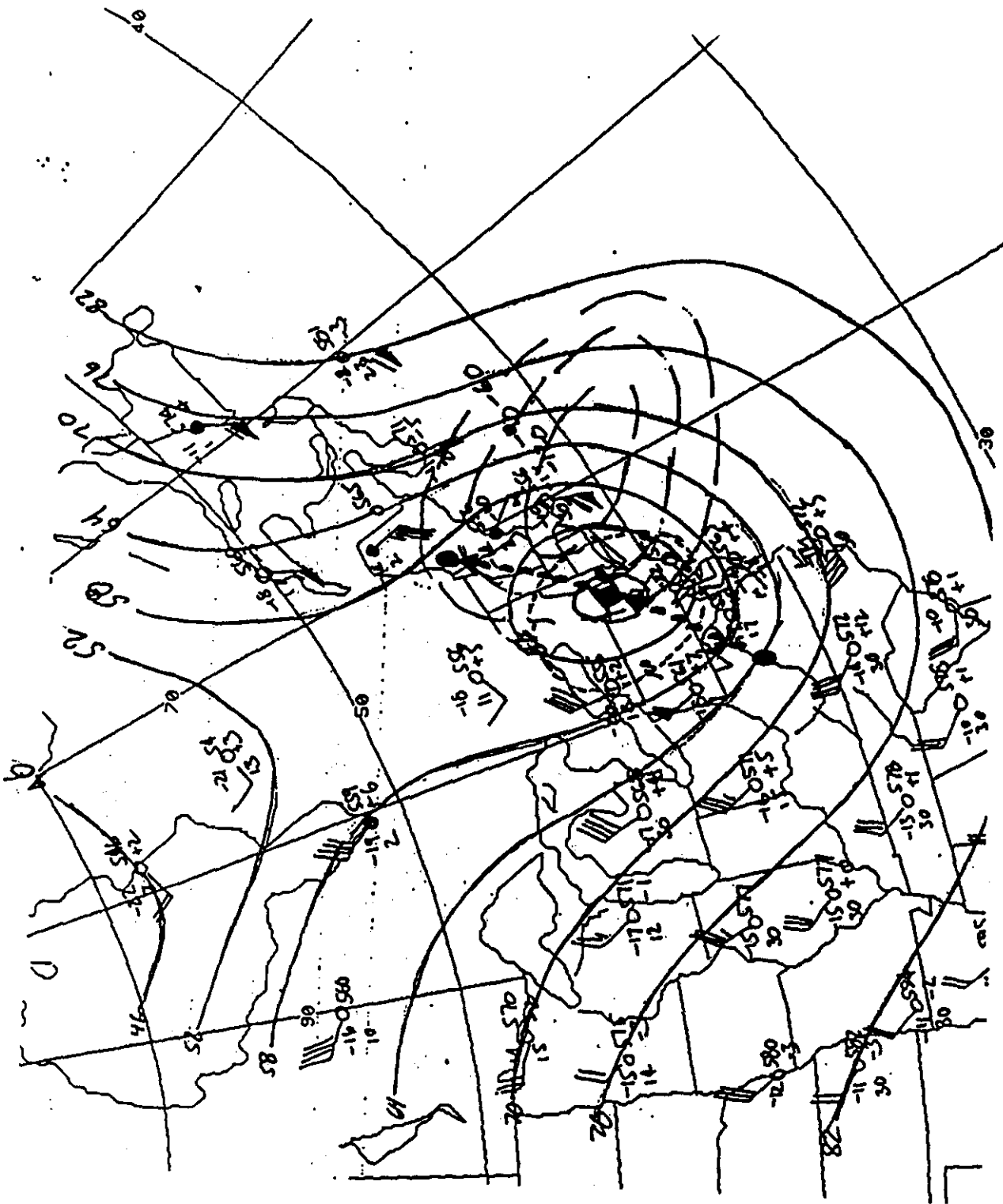


Figure 7. 500 mb analysis
1200 UTC 4 October 1987.

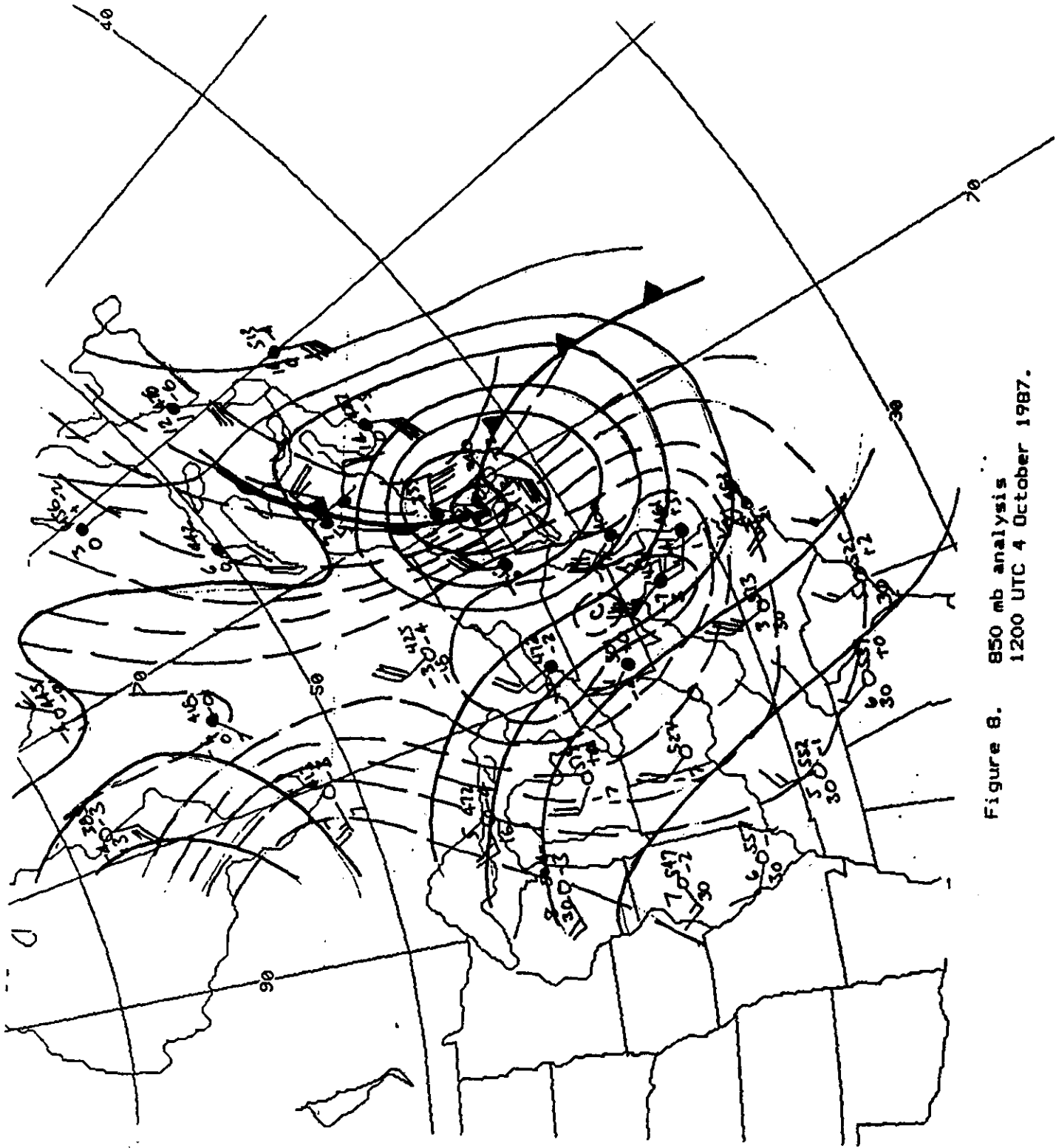


Figure 8. 850 mb analysis
1200 UTC 4 October 1987.

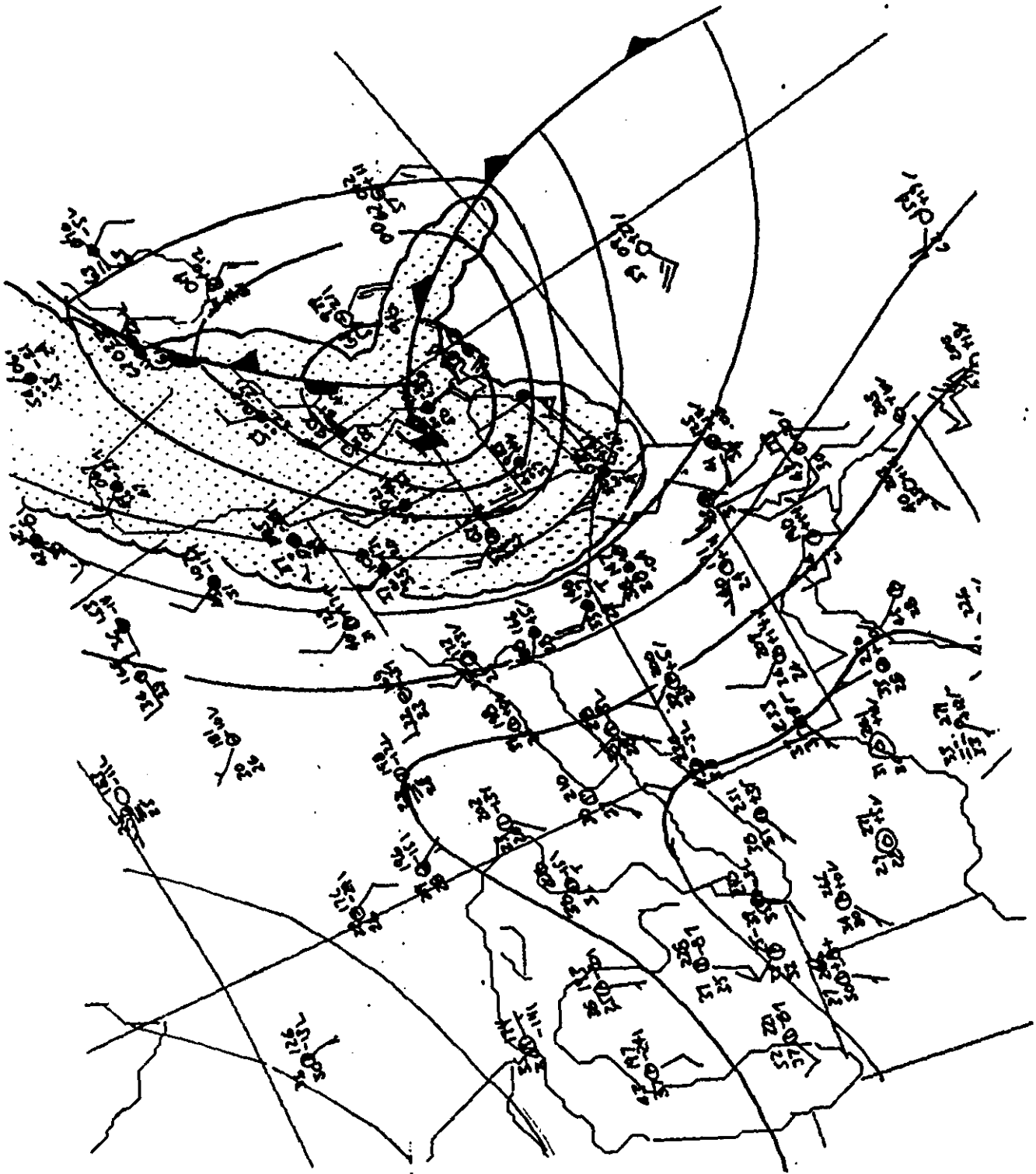


Figure 9. Surface analysis
1200 UTC 4 October 1987.

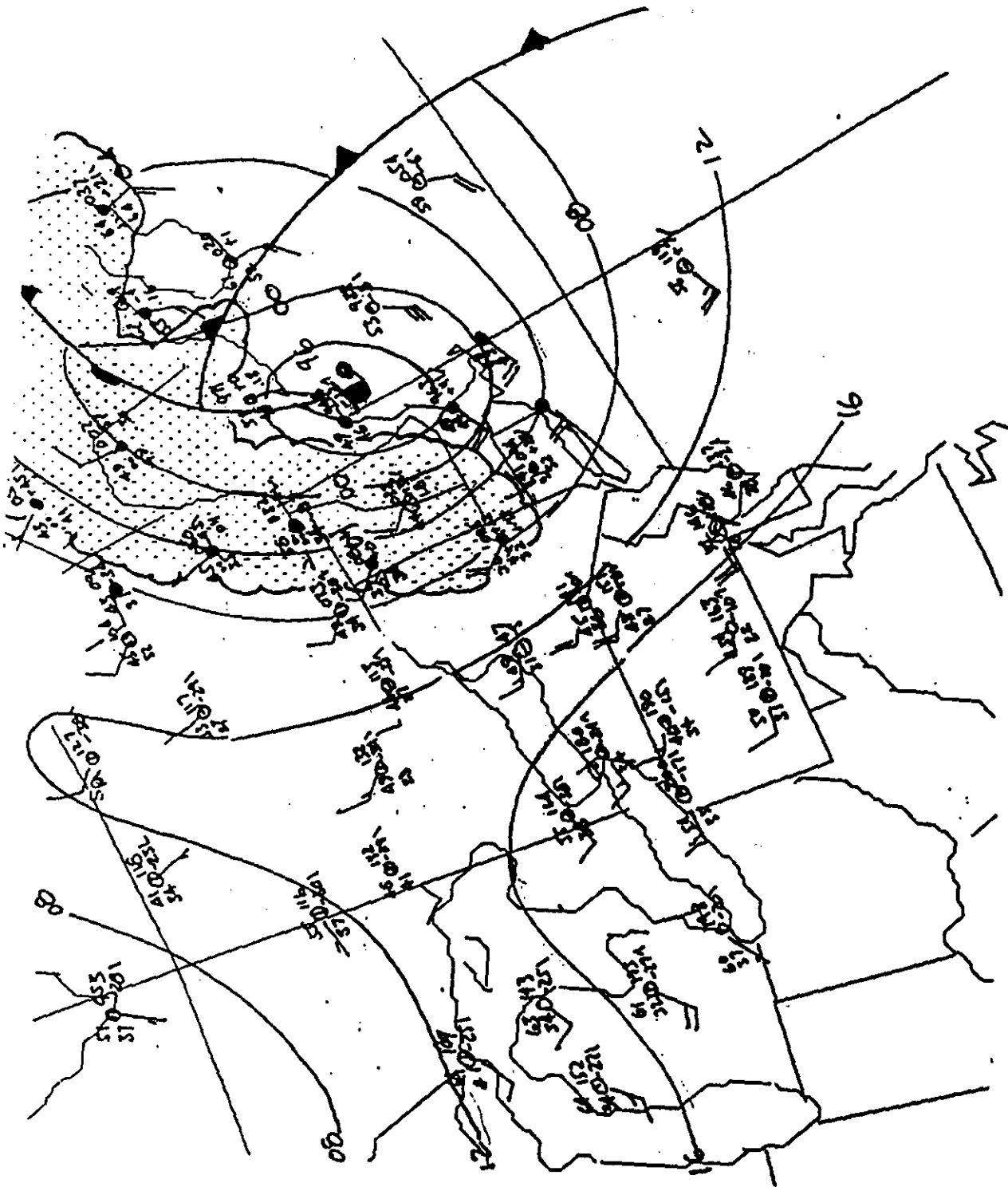


Figure 10. Surface analysis
1800 UTC 4 October 1987.

HOURLY TEMPERATURES AND PRECIPITATION FOR ALBANY

(October 4, 1987)

Time	Temperature	Precipitation hourly -total	Snowfall (cumulative)	
00z	43	0.12	0.56*	
01z	43	0.06	0.62	
02z	43	0.03	0.65	
03z	42	0.02	0.67	
04z	40	0.05	0.72	
05z	39	0.04	0.76	
06z	38	0.10	0.86	
07z	35	0.11	0.97	
08z	35	0.17	1.14	
09z	34	0.16	1.30	
10z	34	0.26	1.56	
11z	33	0.11	1.67	
12z	33	0.19	1.86	1.0
13z	33	0.37	2.23	2.0
14z	33	0.35	2.58	3.0
15z	33	0.34	2.92	4.0
16z	33	0.25	3.17	
17z	33	0.36	3.53	
18z	36	0.05	3.58	6.5
19z	38	T	3.58	

* includes 0.44 that had fallen since 05z on October 3, 1987

Figure 12. Hourly Temperature and precipitation for Albany, NY.

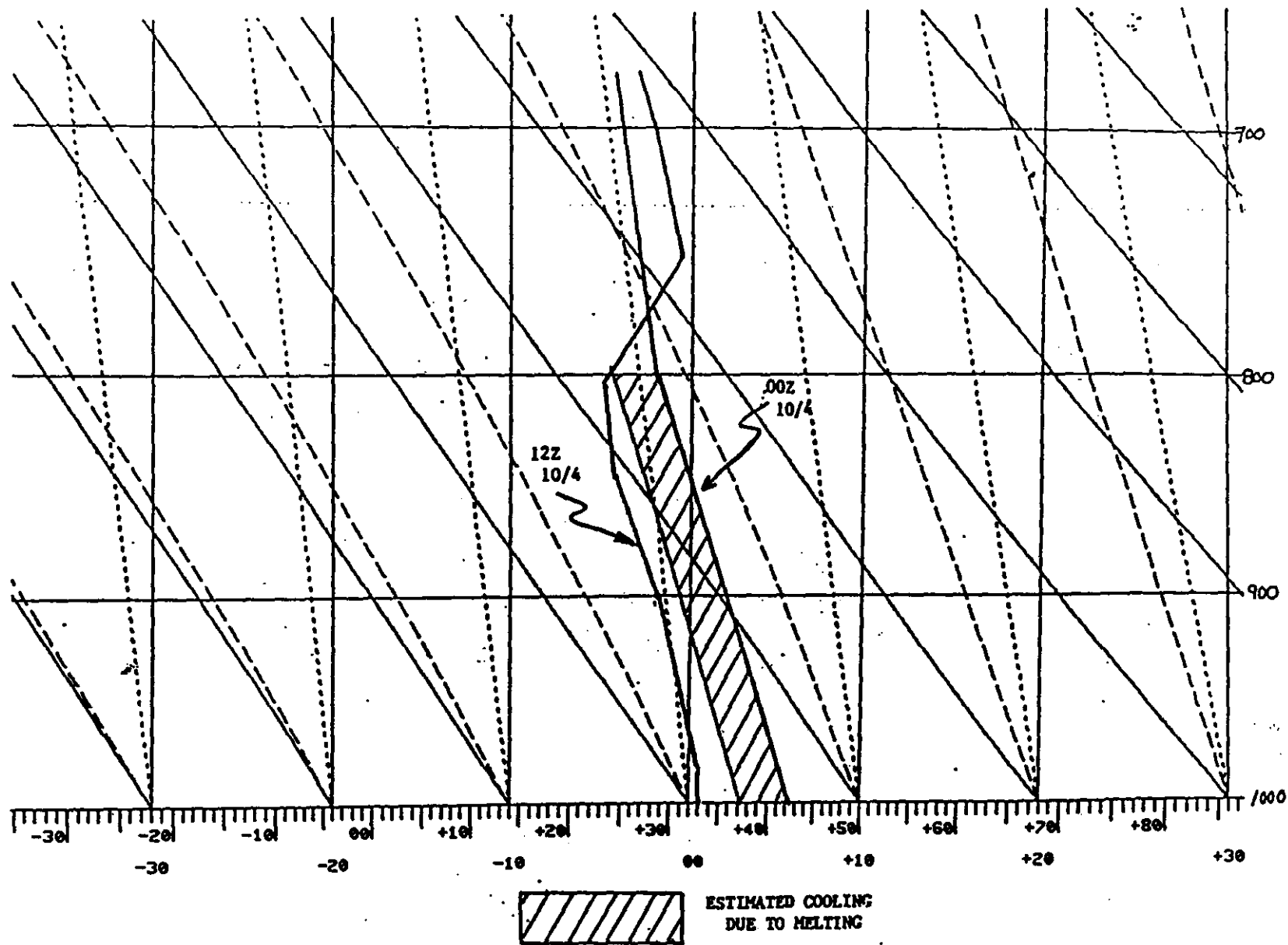


Figure 13. Albany soundings for 0000 UTC and 1200 UTC 4 October 1987. Hatched area indicates cooling due to melting.

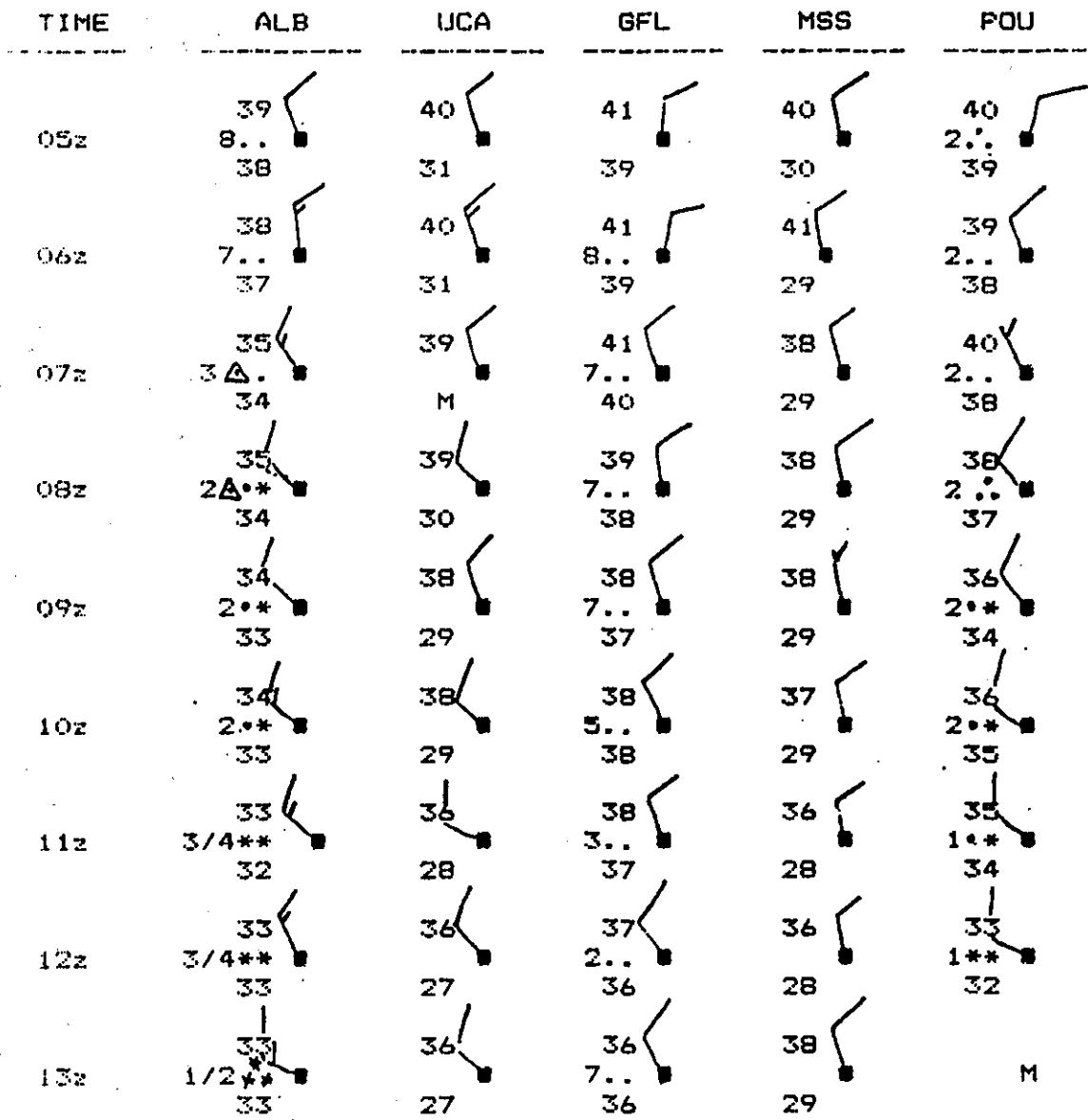


Figure 14. Time cross-section of surface observations across Eastern New York, 0500 UTC-1300 UTC 4 October 1987.

A Procedure for Forecasting Precipitation Type Using NGM Low Level Temperatures and LFM MOS Frozen Precipitation Forecasts ¹

ABSTRACT

Nested Grid Model (NGM) forecasts are available primarily in graphics form and secondarily in alphanumeric form as a FOUS message for selected locations. No Model Output Statistics (MOS) are available from the NGM and won't be in the near future. A procedure is presented for using NGM low level temperature forecasts to determine precipitation type. Also, a technique is presented for combining the results of the procedure with MOS Probability of Frozen (POF) precipitation values from the Limited Fine-mesh Model (LFM) to determine precipitation type.

INTRODUCTION

The NGM has been producing operational 0-48 hour numerical forecasts for the North American continent twice daily since late March 1985. Evaluations, objective and subjective, demonstrated that the Regional Analysis and Forecast System (RAFS) taken from the NGM contained both an improved objective analysis and an improved model. A full complement of RAFS prognostic charts were made available to forecasters in November 1985. The NGM FOUS message had become available in October 1985.

Since it will take a few years to develop MOS guidance from the NGM, some method of using the NGM FOUS message to make objective forecasts was needed in order to have better use of that model now. Also, any techniques or procedures developed will give a measure of goodness of the model and allow a means to measure changes that may be made to the model.

Precipitation type is dependent on the temperature of the atmosphere, especially in the lower levels. Since the NGM FOUS message gives a temperature forecast at three of those lower levels, it was decided to use these forecast temperatures to develop a method to forecast precipitation type out to 48 hours.

PROCEDURE

The relative frequency of precipitation type (frozen, liquid, mixed) was determined for cases of similar temperature values at each of the lower levels contained in the NGM FOUS message for October 1985 through March 1986. All six hourly output (0-48 hours) of the NGM were combined for this study. The results are shown in Tables 1, 2, and 3. For this study frozen precipitation was defined as snow, sleet, or a mixture of the two. Liquid precipitation was defined as rain or freezing rain. Mixed precipitation was defined as any combination of frozen and liquid precipitation occurring at the same time.

Since there was a great range of temperature values, especially for the lowest layer (T1), a combination of temperatures at all three levels was deemed the best approach to determining precipitation type.

To get the data from three variables (T1, T3, T5) into a two dimensional table all T5 equals zero data was analyzed for similar values of T1 and over ranges of T3. The ranges of T3 were determined by

¹ Joseph A. Ronco, Jr., National Weather Service Forecast Office, Portland, ME.

selecting ranges that had a high frequency of liquid precipitation at one extreme to a high frequency of frozen precipitation at the other extreme as determined from Table 2.

The resultant data (Table 4.) was grouped into four categories: one high in frequency of liquid precipitation, one close to a 50 percent frequency of liquid precipitation, one close to a 50 percent frequency of frozen precipitation, and one high in frequency of frozen precipitation. These groups were defined as:

CATEGORY ONE	T1>01
CATEGORY TWO	T1=01 01>T1>95 & T3>01
CATEGORY THREE	01>T1>97 & T3<02 98>T1>95 & 02>T3>97 96>T1>89 & T3>97
CATEGORY FOUR	98>T1>89 & T3<98 T1<90

With the threshold values found for T1 and T3 the four categories were used to determine the frequencies of frozen, liquid, and mixed precipitation for similar values of T5.

Combined data for four stations located in New Hampshire and Maine were used to preserve geographic homogeneity and at the same time yield sufficient cases from which to arrive at conclusions. The four stations chosen were Concord, New Hampshire; and Portland, Bangor, and Caribou, Maine.

The NGM forecast temperatures for the 00Z forecast cycle were combined with the 12Z forecast cycle. This combining could mask out any diurnal effects that may exist, but a preliminary evaluation of the data indicates that diurnal variations are small.

RESULTS

The results are shown in Table 5. Some subjectivity was necessary in developing the table especially where little or no data were available. Note that the frequency of liquid (rain) precipitation is highest at the top of each category and lowest at the bottom. Also, the frequency of liquid (rain) precipitation is highest in category one and the lowest in category four. The opposite is true of frozen (snow) precipitation.

How well did the MOS preferred Probability of Precipitation Type (POPT) forecast perform in comparison to the NGM FOUS temperature method of forecasting precipitation type? The use of the NGM FOUS message lower level temperatures in forecasting precipitation type was superior to the MOS POPT preferred category forecasts. The precipitation type forecasts from the NGM FOUS message were converted to categorical forecasts and verified (Table 6). A frequency greater than or equal to 50 percent for frozen precipitation was considered a categorical

forecast of frozen precipitation. A frequency less than 50 percent was considered a categorical forecast of liquid precipitation. Regardless of the score used, the NGM FOUS temperature method for typing precipitation was superior to MOS POPT preferred category forecasts.

ADDITIONAL PROCEDURE

Since this study found that NGM FOUS lower level temperatures could be used to forecast precipitation type, an additional study using MOS POPT category and NGM FOUS precipitation type (Table 5.) was planned for the winter of 1986-87. However, a detailed comparison of preferred POPT category and POF showed that POF was a more accurate predictor of precipitation type. So POF was substituted for preferred POPT.

Observed precipitation type was stratified by POF ranges (<6, 6-15, 16-25, 26-35, 36-45, 46-55, 56-65, 66-75, 76-85, 86-95, and >95) for the winters of 1985-86 and 1986-87. The results are shown in Table 7. The same definitions for liquid, frozen, and mixed precipitation were applied as used earlier in this study.

Since the NGM precipitation type frequencies in Table 5. were already in four categories by increments of T1 and T3 for all values of T5, it was decided to examine the ranges of POF in each of the four categories for the winters of 1985-86 and 1986-87 (October through March).

The same four locations were used and the 00Z and 12Z forecast cycles combined. Again, a preliminary check of the data indicated any diurnal variations to be small.

ADDITIONAL RESULTS

The results are shown in Table 8. Some subjectivity was used in developing the table, especially where little data were available.

How well did the NGM precipitation type forecasts perform in comparison to the combined NGM/POF method of forecasting precipitation type? The combined NGM/POF forecasts were superior to the NGM type forecasts. The precipitation type forecasts from each were converted to categorical forecasts and verified. All definite forecasts (probabilities greater than 98 percent for either rain or snow) were deleted from the verification process. These accounted for 889 cases, which were almost 25 percent of the total 3663 cases used in developing the tables used to forecast the precipitation type. The verification results are shown in Table 9. The same definitions were used for categorical forecasts of frozen and liquid precipitation types as were used earlier in this study. Regardless of the score used, the combined NGM/POF method of typing precipitation was superior to the NGM FOUS temperature method by itself.

CONCLUSIONS AND COMMENTS

This study has developed a technique for improving precipitation type forecasts by objectively using NGM FOUS lower level temperatures and MOS POF values. Even though the data sample is small and for a particular area, it clearly points the way toward additional studies.

Several changes were made to the NGM since operational forecasts began. Two significant changes took place that could affect the results of this study.

From the time of its beginning operational forecasts, objective and subjective evaluations of the NGM demonstrated that the modeling system produced reliable forecasts. However, systematic errors in the forecasted temperatures, caused by the omission of certain physical processes in the model, were identified.

In July 1986 a more complete formulation of physical processes were introduced into the NGM. Longwave and shortwave radiation, including a diurnal cycle, surface fluxes of heat and moisture over land, and a new turbulent mixing process were added to the model. Important modifications were also made to the representation of cumulus convection by the model.

Implementation of the new physics was to improve the NGM's forecasts of sensible weather such as precipitation, low level temperatures, surface induced circulations such as land/sea breezes, the diurnal variation of low level winds, and maximum and minimum temperatures.

The radiational heating calculations that were introduced in the NGM in July 1986 also produced a progressively colder temperature field, at the rate of about -1.5 degrees in 48 hours, at almost all levels. The cold error continued for more than a year.

In 1987 two modifications, one major and one minor, were introduced into the NGM to reduce errors in the forecast temperatures:

1. In August a change to the near-surface air temperatures used to calculate radiation.
2. In October at each level, the hemispherically-averaged potential temperature was kept constant during the forecast, at its initial value.

The results of these two changes were to reduce the cold bias of NGM forecast temperatures and a small reduction in the areas of precipitation.

The results of this study could be altered by these changes. However, the changes in July 1986 had no discernible impact on the use of the NGM FOUS lower level temperature method of determining precipitation type during the winter of 1986-87. That method of forecasting precipitation type performed very well in Maine and New Hampshire.

The changes made to the NGM in 1987 could also alter the results of this entire study. However, in using both methods (NGM and NGM/POF) during the winter of 1987-88 (October through March) no deterioration was noticed as both performed very well. If anything they seemed to perform even better, as the number of definite forecasts (probabilities

greater than 98 percent) increased to 34.0 percent of all the precipitation events when using the NGM lower temperature method and to 56.2 percent when using the combined NGM/POF method. The frequency of rain or snow occurring remained close to the average frequency for the two previous winter seasons.

A computer program has been written at WSFO Portland, Maine that selects the proper probabilities at six hour intervals (0-48 hours) each time a new NGM FOUS message is received. During the winter of 1987-88 the forecast offices in Boston, Massachusetts and Albany, New York used the program to aid in forecasting precipitation type in their forecast areas. The forecast staffs at those offices found that the NGM and NGM/POF probabilities developed for Maine and New Hampshire performed very well in their forecast areas as well.

The computer program is available from the Scientific Services Division of the National Weather Service's Eastern Region Headquarters. However, caution is advised when using it as it was developed from data for one geographical area. The technique should work in other areas, but it may require developing forecast probabilities from forecast parameters (T1, T3, T5, POF) and observations of precipitation type in those areas.

T1	FROZEN	LIQUID	MIXED
>09	.000	1.000	.000
09	.038	.962	.000
08	.051	.949	.000
07	.066	.934	.000
06	.075	.925	.000
05	.095	.889	.016
04	.109	.848	.043
03	.167	.729	.104
02	.227	.681	.092
01	.328	.590	.082
00	.527	.400	.073
99	.638	.297	.065
98	.778	.162	.060
97	.807	.136	.057
96	.818	.128	.054
95	.833	.116	.051
94	.876	.038	.032
93	.937	.018	.025
92	.959	.018	.023
91	.965	.015	.020
90	.970	.006	.015
89	.987	.000	.013
88	.988	.000	.012
87	.988	.000	.012
86	.997	.000	.003
<86	1.000	.000	.000

Table 1. Relative frequency of precipitation type for temperature T1 from NGM FOUS messages.

T3	FROZEN	LIQUID	MIXED
>10	.000	1.000	.000
10	.027	.973	.000
09	.037	.963	.000
08	.041	.945	.014
07	.045	.940	.015
06	.052	.928	.020
05	.067	.905	.028
04	.085	.880	.035
03	.163	.764	.073
02	.250	.629	.121
01	.297	.578	.125
00	.577	.338	.085
99	.591	.333	.076
98	.748	.178	.074
97	.834	.115	.051
96	.919	.041	.040
95	.945	.033	.022
94	.970	.014	.016
93	.988	.000	.012
92	.990	.000	.010
91	.996	.000	.004
90	.997	.000	.003
<90	1.000	.000	.000

Table 2. Relative frequency of precipitation type for temperature T3 from NGM FOUS messages.

T5	FROZEN	LIQUID	MIXED
>06	.000	1.000	.000
06	.045	.955	.000
05	.047	.953	.000
04	.049	.941	.010
03	.093	.874	.033
02	.188	.770	.042
01	.213	.705	.082
00	.391	.522	.087
99	.460	.448	.092
98	.719	.205	.076
97	.799	.127	.074
96	.809	.124	.067
95	.859	.101	.040
94	.925	.053	.022
93	.959	.030	.011
92	.968	.022	.010
<92	1.000	.000	.000

Table 3. Relative frequency of precipitation type for temperature T5 from NGM FOUS messages.

	T3>01		02>T3>99		00>T3>97		98>T3>95		96>T3>93		T3<94	
T1	RAIN	SNOW	RAIN	SNOW	RAIN	SNOW	RAIN	SNOW	RAIN	SNOW	RAIN	SNOW
>09	2	0	0	0	0	0	0	0	0	0	0	0
09	7	0	0	0	0	0	0	0	0	0	0	0
08	4	0	0	0	0	0	0	0	0	0	0	0
07	7	0	0	0	0	0	0	0	0	0	0	0
06	13	1	0	0	0	0	0	0	0	0	0	0
05	11	0	0	0	1	0	0	0	0	0	0	0
04	6	0	1	0	1	0	0	0	0	0	2	1
03	11	0	0	0	2	3	0	0	0	0	2	0
02	11	0	0	0	2	0	0	0	0	0	4	0
01	5	0	1	1	1	0	1	0	0	0	0	3
00	3	1	2	0	0	3	2	3	0	0	1	3
99	1	1	1	2	2	2	0	1	0	0	1	1
98	1	0	0	2	3	3	2	4	0	0	0	3
97	1	0	0	0	1	0	0	1	0	0	0	0
96	0	0	1	2	2	0	0	2	0	1	0	1
95	1	0	0	0	0	3	0	0	0	0	0	1
94	0	1	0	0	1	0	0	0	0	0	0	0
93	0	0	0	0	1	1	0	0	0	0	0	0
92	0	0	0	0	0	0	0	0	0	0	1	0
91	1	0	1	0	0	0	0	2	0	0	0	0
90	0	0	1	0	0	1	0	0	0	1	0	0
89	0	0	0	0	0	0	0	0	0	0	0	0
88	0	0	0	0	0	0	0	0	0	0	0	0
87	0	0	0	0	0	1	0	0	0	1	0	0
<87	0	0	0	0	0	0	0	0	0	0	0	0

Table 4. Number of precipitation events by type (RAIN=LIQUID and SNOW=FROZEN) for temperature T1 and ranges of T3 from all NGM FOUS messages where T5 equals zero.

CATEGORY ONE frequencies....RAIN .935, SNOW .054, MIXED .011
 CATEGORY TWO frequencies....RAIN .538, SNOW .231, MIXED .231
 CATEGORY THREE frequencies...RAIN .384, SNOW .548, MIXED .068
 CATEGORY FOUR frequencies....RAIN .067, SNOW .800, MIXED .133

	T1>1			T1=1 1>T1>95 & T3>1			1>T1>97 & T3>2 98>T1>95 & 2>T3>97 96>T1>89 & T3>97			98>T1>89 & T3<98 T1<90		
T5	RAIN	SNOW	MIX	RAIN	SNOW	MIX	RAIN	SNOW	MIX	RAIN	SNOW	MIX
>06	1.000	.000	.000	1.000	.000	.000	1.000	.000	.000	1.000	.000	.000
06	.981	.019	.000	.967	.032	.000	.750	.250	.000	.700	.300	.000
05	.977	.023	.000	.952	.048	.000	.727	.273	.000	.600	.400	.000
04	.975	.025	.000	.929	.071	.000	.500	.340	.160	.450	.500	.050
03	.973	.027	.000	.925	.075	.000	.463	.370	.167	.300	.600	.100
02	.968	.032	.000	.810	.095	.095	.409	.409	.182	.100	.700	.200
01	.871	.072	.049	.720	.160	.120	.361	.532	.107	.096	.793	.111
00	.861	.082	.057	.662	.200	.138	.317	.578	.105	.060	.877	.063
99	.650	.200	.150	.625	.214	.161	.258	.638	.104	.043	.922	.035
98	.587	.288	.125	.564	.295	.131	.183	.714	.103	.032	.936	.032
97	.556	.344	.100	.529	.353	.118	.168	.736	.096	.022	.948	.030
96	.521	.399	.080	.364	.545	.091	.136	.775	.089	.019	.954	.027
95	.500	.467	.033	.214	.714	.072	.113	.825	.062	.017	.961	.022
94	.450	.550	.000	.156	.783	.061	.099	.844	.057	.014	.967	.019
93	.333	.667	.000	.080	.866	.054	.071	.881	.048	.012	.971	.017
92	.200	.800	.000	.038	.925	.033	.033	.926	.041	.011	.989	.000
<92	.000	1.000	.000	.000	1.000	.000	.000	1.000	.000	.000	1.000	.000

Table 5. Relative frequency of precipitation type (RAIN=LIQUID and SNOW=FROZEN) for temperature T5 from NGM FOUS messages by category of T1 and T3.

	NGM	POPT
P.O.D.	.920	.858
F.A.R.	.111	.171
C.S.I.	.825	.729
PERCENT CORRECT	88.9	82.9
BIAS	1.035	1.036

Table 6. Skill of precipitation type forecasts from NGM lower level temperature forecasts and MOS POPT preferred category.

POF	LIQUID	FROZEN	MIXED
<6	.979	.018	.003
6-15	.796	.152	.052
16-25	.613	.320	.067
26-35	.505	.413	.082
36-45	.382	.539	.079
46-55	.307	.624	.069
56-65	.248	.687	.065
66-75	.207	.737	.056
76-85	.097	.869	.034
86-95	.045	.931	.024
>95	.001	.998	.001

Table 7. Relative frequency of precipitation type for MOS POF ranges for the winters of 1985-86 and 1986-87 (October through March).

POF	CATEGORY ONE			POF	CATEGORY TWO		
	RAIN	SNOW	MIXED		RAIN	SNOW	MIXED
<6	.981	.017	.002	<6	.859	.084	.057
6-15	.904	.083	.013	6-15	.776	.153	.071
16-25	.844	.119	.037	16-25	.654	.247	.099
26-35	.801	.149	.050	26-35	.615	.266	.119
36-45	.736	.190	.074	36-45	.558	.308	.134
46-55	.718	.201	.081	46-55	.523	.356	.121
56-65	.651	.253	.096	56-65	.400	.506	.094
66-75	.571	.353	.076	66-75	.384	.535	.081
76-85	.472	.513	.015	76-85	.330	.600	.070
86-95	.222	.771	.007	86-95	.295	.636	.069
>95	.100	.900	.000	>95	.110	.875	.015

POF	CATEGORY THREE			POF	CATEGORY FOUR		
	RAIN	SNOW	MIXED		RAIN	SNOW	MIXED
<6	.875	.083	.042	<6	.700	.200	.100
6-15	.566	.320	.113	6-15	.500	.333	.167
16-25	.327	.543	.130	16-25	.240	.720	.040
26-35	.290	.611	.099	26-35	.124	.846	.030
36-45	.232	.682	.086	36-45	.055	.920	.025
46-55	.188	.729	.083	46-55	.025	.956	.019
56-65	.171	.754	.075	56-65	.020	.962	.018
66-75	.158	.782	.060	66-75	.019	.968	.013
76-85	.123	.827	.050	76-85	.018	.976	.006
86-95	.083	.877	.040	86-95	.014	.983	.003
>95	.007	.986	.007	>95	.000	.999	.001

Table 8. Relative frequency of precipitation type for NGM lower level temperature categories and MOS POF ranges combined.

	NGM/POF	NGM
P.O.D.	.940	.929
F.A.R.	.107	.122
C.S.I.	.845	.823
PERCENT CORRECT	88.6	87.0
BIAS	1.052	1.058

Table 9. Skill of precipitation type forecasts from combined NGM/POF forecasts and NGM lower level temperature forecasts.

Local Objective Guidance for Predicting Precipitation Type (LOG/PT) in North Carolina...An Alternative to MOS Guidance

by

Kermit K. Keeter(1), Joel W. Cline(2), and Robert P. Green(3)

- (1) National Weather Service Forecast Office, Raleigh-Durham, NC
- (2) National Hurricane Center, Coral Gables, FL
- (3) National Weather Service Office, Charlotte, NC (Retired)

1. Introduction

There is considerable variability in snowfall amounts across North Carolina. The normal annual snowfall ranges from less than 2 inches in the coastal areas to over 40 inches in the northern mountains (Fig 1). Snow/rain boundaries frequently occur within the state; broad transition zones with a mixture of snow, sleet, freezing rain, and rain are not uncommon. Even small amounts of snow cause traffic accidents, school closings, and a general disruption of community activities and services. Small wonder that the National Weather Service Forecast Office (WSFO) at Raleigh-Durham (RDU) places an important emphasis on forecasting precipitation type.

Forecasting experience at RDU has shown that there is no one single method or technique which consistently and accurately predicts the distribution of precipitation type across the state. The Model Output Statistics (MOS) Probability of Precipitation Type (PoPT) guidance (Bocchieri, 1979) generated from the Limited Area Fine Mesh (LFM) Model is available for several sites across North Carolina (Fig 2); however, this guidance is of limited value when the LFM has significant synoptic scale forecast errors. When such errors occur, another source of objective guidance for predicting precipitation type is desirable.

2. LOG/PT...Experimental Design

2.1 General Description/ Predictand

The Local Objective Guidance for Predicting Precipitation Type (LOG/PT) is generated by the WSFO, RDU. The guidance is produced from regression equations and predicts the conditional (i.e. given the event of precipitation) probability of measurable frozen precipitation (i.e. snow and/or sleet) at ten sites scattered across the climatological regions of North Carolina (Fig 2). The regression equations are supplemented by nomograms used to forecast freezing rain. The focus of this paper is the regression portion of the guidance used to predict frozen precipitation. In this paper the terms snow(rain) and frozen(unfrozen) are used interchangeably.

2.2 Dependent Data Set/ Choice of Predictors

The regression equations were developed from seven winters (1970-77) of data. Precipitation type at each of the ten prediction sites was coupled with the routine (00z and 12z) radiosonde (raob) observations from the National Weather Service Office (WSO) at Greensboro (GSO), North Carolina. The raob observations were concurrent with, or taken just prior to, the onset of precipitation at each site. GSO was chosen as the prediction raob site since it is well located for monitoring the lower tropospheric thermal structure of the prevailing airmass over North Carolina, and in particular the intrusion of cold, dry Canadian air (Fig 3).

From the raob data, four predictors were screened by a stepwise linear regression analysis. The low level thickness (1000/850 mb) and the mid level thickness (850/700 mb) proved to be the best combination of predictors accounting for roughly 40 to 50 percent of the total variance at each site. The multiple correlation coefficients squared (percent of total variance) were not significantly improved by the two additional raob predictors, 1000/700 mb thickness and the 850 mb temperature. The best single predictor was the 1000/700 mb thickness.

2.3 Predictand/ Classification of Mixed Precipitation Events

Since relatively small amounts of snow have a large social impact upon communities in the Southern U.S., the critical question for the forecaster becomes whether there will be measurable amounts of snow during the forecast period. Hence, precipitation type was not verified for a specific hour as does MOS guidance; rather verification was done for the entire 12 hour forecast period between raob reports over the lifetime of the precipitation event. Only measurable precipitation events were included in the dependent data. Using this format, mixed precipitation events were further classified as frozen, provided measurable snow fell, while trace amounts of snow together with measurable amounts of rain were classified as unfrozen.

2.4 Derivation of Regression Equations

The Logit Model provides a curve of best fit suitable for the derivation of regression equations used to predict precipitation type (Glahn and Bocchieri, 1975). As shown (Fig 4), the logit curve is S-shaped and asymptotically approaches 100(0) percent chance of snow as the thickness becomes increasingly lower(colder) higher(warmer).

However, logit regression has limitations when used with a relatively small data set. Specifically, logit regression can not be accomplished by regressing each precipitation case and its corresponding thicknesses singularly since the denominator in the equation of the logit curve would then equal zero; therefore, logit regression requires grouping the data into class intervals and using relative frequencies. A minimum of 20 to 30 precipitation cases per 20 meters of thickness is recommended (Bocchieri, 1984).

For each LOG/PT prediction site, the number of precipitation cases was less than the recommended logit regression minimum over the range of thickness values where there was the most precipitation type uncertainty. Consequently, a linear curve was adapted to approximate the logit (Fig. 5). To insure that the adapted linear curve was a good approximation of the logit, the end points of the linear curve were anchored at the thickness values where precipitation type is no longer in doubt (values of certainty)

(Fig 5). For each of the ten LOG/PT prediction sites, the certainty thickness values were determined by subtracting(adding) the standard raob error of 10 meters to the lowest(highest) observed 1000/700 mb thickness associated with rain(snow).

In the Southern U.S, it is especially important to establish the critical thickness value for rain, to eliminate the influence of the large number of rain cases at relatively warm thicknesses on the slope of the adapted linear curve.

2.5 Verification of Dependent/Independent Data

Verification scores for the dependent data (winters 1970-77) were calculated for each of the prediction sites. Real time GSO raob data was used to predict precipitation type for a first period forecast (i.e. 0-12 hours). A resulting conditional probability ≥ 50 percent was defined as a forecast of measurable frozen precipitation.

The prefigurance or probability of detection (POD) is the ratio of the number of correct snow forecasts to the total number of snow events. POD scores provide the percent of snow events detected or forecast. The scores were generally consistent from station to station and ranged from the low 60s to the low 70s.

The false alarm ratio (FAR) provides the percent wrong of the total number of snow forecasts made. Again, the scores were consistent from station to station ranging from the mid teens to the mid 20s.

It was likely that a good portion of the forecast errors were due to significant changes in the GSO raob temperature profile during the 12 hour forecast period. Operationally, at RDU the precipitation type forecasts are made for a shorter period (0-6 hours) since GSO raobs are available every 6 hours when there is precipitation type uncertainty in North Carolina.

The POD/FAR scores for an independent data set (winters 1977-80) for Charlotte (CLT) were similar to the dependent data scores. This implies that the regression equation for CLT is stable and it is reasonable to assume that the other stations in Western North Carolina receiving as many or more snow events as CLT (i.e. AVL, HKY, GSO, RDU) have stable regression equations as well; however, for those stations east of RDU where snow is less frequent, more snow cases from a larger independent data sample are needed before definitive independent verification scores can be specified.

3. Operational Uses of LOG/PT by RDU

3.1 As a Short-Fused Forecast/As a Perfect Prog Forecast

When precipitation type in North Carolina is uncertain, RDU requests raobs from GSO every six hours. The raob thickness values are then used with the regression equations to produce a site-specific, short-fused forecast (0-6 hours) of precipitation type at each of the ten prediction sites.

When used in a perfect prog sense with the projected thicknesses from the Nested Grid Model (NGM), a 12-48 hour forecast of precipitation is obtained. The projected heights for GSO at 850, 700, and 500 mb are interpolated values taken from the appropriate NGM graphic products. The 1000 mb height is the difference between the 500 mb height and the 1000/500 mb thickness.

The focus for the remainder of this paper is the use of LOG/PT in the perfect prog sense with NGM projected thicknesses to produce a 12-36 hour forecast of precipitation type.

3.2 Use of LOG/PT to Forecast Snow/Rain Boundaries...Case of Jan 21-22 1987

Operationally, LOG/PT has been used to forecast the general location of the snow/rain boundary 12-36 hours prior to the onset of precipitation. An especially accurate forecast was for the heavy snow event of January 21-22, 1987, when up to 20 inches of snow fell over the western half of North Carolina (Fig 6). The snow was associated with a surface low in the Western Gulf of Mexico which deepened while moving northeast to a position off the coast of South Carolina (Figs 7,8). Prior to the arrival of the low, a continental polar air mass was in place resulting in a relatively cold and extremely dry GSO sounding (Fig 9). As is usually the case in North Carolina, evaporative cooling played an important role in the resulting snow event.

Typically, surface lows developing in the Gulf of Mexico and tracking northeast produce precipitation type problems in North Carolina. In this particular case, there was only the primary low, with no secondary low development. Generally, the transition zone of mixed precipitation is relatively narrow (≤ 30 miles) when associated with primary lows tracking east of the Appalachian Mountains; therefore, primary lows are more ideal for predicting the location of a snow/rain boundary.

Table 1 shows the 36 hour projected heights and thicknesses from the NGM for GSO and the resulting frozen precipitation probabilities (in percent) at each LOG/PT prediction site for the 12 hour period of 00-12z, Jan 22, 1987.

Table 1
 LOG/PT as a 36 Hour Forecast of Frozen Precipitation
 Using Projected Thicknesses From the NGM

Input..... NGM 36 Hour Prog For GSO From 1/20/87 00z Run

Projected Heights in Meters

1000 mb Ht..... 75
 850 mb Ht.....1365
 700 mb Ht.....2915

Projected Thicknesses in Meters

1000/850 mb Thkn.....1290
 850/700 mb Thkn.....1550
 1000/700 mb Thkn.....2840

Output..... Conditional Probability of Frozen Precipitation for
 the 12 Hour Period 00-12z 1/22/87

<u>Prediction Site</u>	<u>Probability in Percent</u>
Asheville (AVL).....	50
Hickory (HKY).....	69
Greensboro (GSO).....	68
Charlotte (CLT).....	57
Raleigh-Durham (RDU).....	50
Norfolk (ORF).....	38
Rocky Mount (RWI).....	24
Fayetteville(FAY).....	23
Goldsboro (GSB).....	15
New Bern (EWN).....	0

Table 1. Shows the LOG/PT forecasts used to predict the location of the snow/rain boundary associated with a heavy snow event in Western North Carolina on Jan 22, 1987.

Snow began falling in Western North Carolina around 04z on the 22nd. The snow/rain boundary (0.5 inches <= snow < 2 inches) at 12z on the 22nd (Fig 6) shows a typical climatological orientation for North Carolina associated with Gulf waves with the boundary extending parallel to the Atlantic coast. The 50% probability isopleth was defined to be the perfect prog prediction of the snow/rain boundary. The final position of the boundary was made by interpolating from the site specific probabilities. The predicted snow/rain boundary was very accurate, falling within 25 miles of the actual boundary (Fig 6).

Forecast experience has shown that all winter storms are not equally well suited for attempting an advance forecast of a snow/rain boundary as definitive as that of January 22nd. Those storms involving the development of a secondary low, after the primary low occludes, are especially difficult for forecasting the distribution of precipitation type. Such storms are more likely to involve a relatively broad transition zone of mixed precipitation with multiple precipitation changes at individual

sites. Those storms involving only a primary low whose track is steady and smooth (i.e. without jumps or redevelopment) provide the best opportunity for an accurate forecast of a snow/rain boundary, as such storms usually produce a narrow transition zone of mixed precipitation.

4. Forecast Performance of LOG/PT and MOS (Period Jan '87- Apr '88)

Tables 2 and 3 summarize the POD and FAR verification scores for precipitation type forecasts made by LOG/PT and MOS. The forecasts were made with nine separate storms that brought snow and/or freezing rain to North Carolina over the period of Jan '87 through Apr '88. The forecasts were typically for 24 hour projections.

Table 2
Summary of POD Scores (1/87 - 4/88)
for
LOG/PT and MOS
as
Perfect Prog (24 Hour Forecast)

<u>Prediction Site</u>	<u>No. of Snow Events</u>		<u>POD Scores</u>	
	<u>LOG/PT</u>	<u>MOS</u>	<u>LOG/PT</u>	<u>MOS</u>
<u>All</u>	35	26	0.9	0.7
<u>Western NC</u>	23	20	0.9	0.6
AVL	5	5	0.6	1.0
HKY	6	5	1.0	0.4
GSO	5	4	1.0	0.5
CLT	3	3	1.0	0.3
RDU	4	3	1.0	0.7
<u>Eastern NC</u>	12	6	0.8	1.0
EWN	2	2	1.0	1.0
ORF	2	2	1.0	1.0
POB	2	2	1.0	1.0
GSB	3	x	0.7	x
RWI	3	x	0.3	x

Table 2. Summary of POD verification scores for snow events impacting North Carolina over the period of Jan '87 through Apr '88. The number of snow events for LOG/PT and MOS differ at some sites due to verification differences between the two forecast systems. Western North Carolina refers to the piedmont west through the foothills to the mountains. The POD scores were rounded off to the nearest tenth and represent the percent of snow events detected or forecast.

Table 3

Summary of FAR Scores (1/87 - 4/88)
for
LOG/PT and MOS
as
Perfect Prog (24 Hour Snow Forecasts)

Prediction Site	NO. of Snow Forecasts		FAR Scores	
	LOG/PT	MOS	LOG/PT	MOS
All	38	19	0.2	0.1
<u>Western NC</u>	27	13	0.2	0.1
AVL	3	6	0	0.2
HKY	6	2	0	0
GSO	6	2	0.2	0
CLT	6	1	0.5	0
RDU	6	2	0.3	0
<u>Eastern NC</u>	11	6	0.2	0
EWN	2	2	0	0
ORF	3	2	0.3	0
POB	3	2	0.3	0
GSB	2	x	0	x
RWI	1	x	0	x

Table 3. Summary of FAR verification scores for snow forecasts made by LOG/PT and MOS for the period Jan '87 through Apr '88. The FAR scores were rounded off to the nearest tenth and represent the percent of snow forecasts that were wrong.

Probabilities of snow $\geq 50\%$ were defined as a snow forecast for both LOG/PT and MOS. Snow also was defined as the MOS forecast if the probability of snow was $< 50\%$ but the PoPT best category for precipitation type was frozen. A snow event was defined as the occurrence of snow at a prediction site at the time of forecast verification. Due to the verification differences between LOG/PT and MOS, the number of snow events for each differed at some sites. Moreover, MOS forecasts verify at a specific hour while LOG/PT forecasts verify over a 12 hour period. Consequently, a MOS forecast valid at 00(12z) verified as snow, provided only snow was falling at 00(12z); the LOG/PT forecast verified as snow, only if measurable snow fell during the ensuing 12 hour period from 00-12z(12-00z). Due to these verification differences, a direct comparison of LOG/PT to MOS can not be made; however an examination of the forecast performance of each can point to the relative strengths and weaknesses of the two forecast systems.

Table 2 shows LOG/PT predicted 90% of all snow events that occurred at the ten prediction sites while MOS accounted for 70%. In Western North Carolina, LOG/PT predicted all of the snow events in the foothills (HKY), and in the piedmont (CLT, GSO, RDU). Snow events not forecast by LOG/PT in

the mountains (AVL) included springtime snows associated with 500 mb cutoff lows that moved along or just west of the North Carolina mountains- one of a few synoptic patterns that produce snow in North Carolina while the airmass over the prediction site at GSO remains much too warm for snow throughout the precipitation event.

The springtime mountain snows were predicted by MOS and that accounts for its higher POD score at AVL relative to LOG/PT; but MOS significantly underforecast the snow events at all of the other Western North Carolina sites. MOS's tendency to underforecast snow was due to synoptic errors by the LFM in moving the cold air surface high eastward too quickly and prematurely warming the thicknesses. From this study's limited sample of winter storms and from past forecast experience, this well known LFM error appears to occur more often when the cold air high is entrenched along the eastern seaboard well before the gulf wave tracks northeast with the onset of precipitation in North Carolina.

In Eastern North Carolina where LOG/PT and MOS share three common prediction sites, the number of snow events was limited. Both LOG/PT and MOS predicted the two snow events occurring at EWN, ORF, and FAX. MOS may not underforecast snow in Eastern North Carolina to the same extent it does in Western North Carolina. Perhaps, when the cold air is far enough south to produce snow in Eastern North Carolina, the surface high is generally stronger and MOS is less likely to move the cold air out of the region as quickly.

LOG/PT has two prediction sites in Eastern North Carolina for which there is no MOS guidance (GSB,RWI). The POD score for RWI was especially low and out of line with the scores at the other sites. Errors were found in the entry of the dependent data used to develop the RWI regression equation and that accounts for a large portion of the POD error.

Table 3 (FAR scores) shows LOG/PT with a much larger percentage of snow forecasts that were wrong than does MOS. This was true for both Western and Eastern North Carolina sites. Operationally, LOG/PT's tendency to overforecast snow can be seen in a given storm as bringing the snow too far east and south into North Carolina. This error was largely due to the cold air bias of the NGM as seen in a mean error of -16 meters in the 1000/850 mb thickness for seven separate storms.

As indicated by the low FAR scores, MOS showed little tendency to overforecast snow. MOS did slightly overforecast snow in the mountains when cold air from the backside of a passing low was not sufficient to change rain to snow before the precipitation ended. The full extent of this type of overforecast error is not indicated here since only those storms that actually produced snow or freezing rain in North Carolina were examined. Further, forecast experience at RDU has shown that MOS does have a tendency to change rain to snow before the precipitation ends, in a post-frontal fashion, an infrequent scenario in North Carolina, especially east of the mountains.

5. Summary

LOG/PT is generated by the WSFO RDU and is based upon regression equations that predict the conditional probability of measurable snow at ten sites scattered across the climatological regions of North Carolina.

From GSO raob data, stepwise linear regression selected the low (1000-850 mb) and mid (850-700 mb) level thicknesses as the best predictors of precipitation type. The predictors accounted for approximately 40 to 50% of the total variance at each prediction site. GSO was used as the prediction raob site since it is well located for monitoring the lower tropospheric thermal structure of the prevailing airmass over North Carolina, and particularly the intrusion of cold, dry Canadian air.

LOG/PT was designed to address the major problems inherent in forecasting precipitation type in the Southern U.S., where snow is relatively infrequent and where even small amounts make a large social impact.

Because of the limited number of snow cases, the derivation of the LOG/PT regression equations could not be based upon the Logit Model, whose S-shaped non-linear curve is ideally suited for the prediction of precipitation type. Instead, the thickness values associated with the certainty of rain(snow) were determined and used to adapt a linear curve as a close approximation of the logit over the range of values where there is the greatest degree of precipitation type uncertainty. This approach allowed for maximum utilization of a limited dependent data base.

Because of the large social impact of even small amounts of snow upon North Carolina communities, LOG/PT was designed to maximize its capability to detect a snow event. This was accomplished by verifying precipitation type over the forecast period instead of verifying at a point in time, as does MOS. Using this format, LOG/PT further classifies a mixed precipitation event as snow, provided measurable snow fell, while those mixed events with only a trace of snow were classified as rain.

LOG/PT was developed to supplement MOS by providing another source of objective guidance when there are synoptic errors in the LFM. Operationally LOG/PT provides a site-specific short-fused forecast (0-6 hours) of precipitation type when used with real-time GSO thicknesses. When used in a perfect prog sense with projected thicknesses from the NGM, LOG/PT produces a 12-48 hour forecast of precipitation type.

Due to verification differences, a direct comparison between LOG/PT and MOS can not be made; however, the forecast performance of each was examined for 9 separate storms that produced snow and/or freezing rain in North Carolina from January 1987 through April 1988. The POD scores represent the percent of snow events forecast, while the FAR score represent the percent of snow forecasts that were wrong. The POD(FAR) errors can be interpreted as an under(over) forecast of snow. The POD(FAR) scores indicated that LOG/PT excelled in predicting snow events, but with a tendency to overforecast snow too far east beyond its climatologically preferred location in the mountains and foothills of North Carolina. This overforecast error was due to a cold air bias in the NGM's prediction of the low level thickness (1000-850 mb). LOG/PT showed little tendency to underforecast snow except for springtime mountain snows associated with 500 mb cutoff lows tracking along or just west of the North Carolina mountains.

MOS was found to significantly underforecast snow due to the LFM prematurely warming the thicknesses as it erroneously pushed the cold air surface high eastward too quickly. This LFM synoptic error occurred most often when the cold air was entrenched along the eastern seaboard well before the gulf wave tracks northeast and the onset of precipitation in North Carolina. MOS showed less tendency to underforecast snow in Eastern

relative to Western North Carolina. This suggests that the LFM may be less apt to move the cold air surface high offshore too quickly, when the high is strong enough to push cold air far enough south for the relatively infrequent event of snow in Eastern North Carolina. MOS showed little tendency to overforecast snow; however forecast experience has shown that MOS does have a tendency to change rain to snow before the precipitation ends, an infrequent scenario in North Carolina.

On a few occasions, LOG/PT has been used to forecast the general location of the snow/rain boundary 12-36 hours prior to the onset of precipitation. Forecast experience has shown that perhaps the most favorable synoptic pattern for an accurate forecast of a snow/rain boundary is associated with primary gulf waves tracking northeast without any secondary low development. Such storms generally produce a relatively narrow transition zone of mixed precipitation, provided that their track shows little variation and is without significant jumps or redevelopment.

6. Conclusions

Refinement and verification of LOG/PT continues as an ongoing process, with efforts to both improve the LOG/PT guidance and the forecasters use of the guidance.

Of particular interest is the recent change made in the NGM to reduce its cold air bias and how that might impact upon the NGM's forecast of the low level thickness and LOG/PT's tendency to overforecast snow. Further, there is a need to verify more storms and to include storms that only produce a cold rain in North Carolina since this study's sample was skewed toward snow producing storms.

Consideration has been given toward adding more predictors to the regression equations, but this would likely require an extensive dependent data base suitable for logit analysis. The current adapted linear model restricts the full range of thickness values by establishing specific values associated with the certainty of rain(snow). This approach is not well suited for adding other predictors, since their range of values would also be restricted and their influence upon the predictands variability would not be fully sampled.

The forecasters judicious use of LOG/PT may be further enhanced by verifying its performance with a larger sample of storms covering the full range of synoptic patterns associated with precipitation type forecast problems in North Carolina. Also the possibility of generating separate regression equations for each of the major synoptic types holds promise and will be explored.

As more technological advances are brought into operations (e.g wind profilers), more forecasters will become involved in the development of algorithms. It is essential that objective techniques such as LOG/PT not be used as black boxes, but that their judicious use be maximized through an extensive knowledge of synoptic and meso-scale meteorology. At RDU, any success LOG/PT has enjoyed has been due to its wise use by a skilled and knowledgeable forecast staff.

7. Acknowledgements

This project is dedicated to operational forecasters in general, and to the forecast staff at RDU in particular. Few local studies are accomplished on station without the labor of many. So many thanks go to the entire RDU staff and management for all their extra work and help in making this ongoing project a reality. Thanks are extended to Joe Bocchieri of NWS's Techniques Developmental Laboratory (TDL), whose many well written articles on objective forecasting of precipitation type, were invaluable. Thanks to Scientific Services of the Eastern Region of NWS for providing the funding needed to obtain archived data. Thanks to Bob Muller, Meteorologist in Charge of the WSFO RDU, and to Dr. Gerald Watson, Professor of Meteorology at North Carolina State University, who arranged a cooperative research agreement between the University and the WSFO, RDU. The initial involvement of one of the co-authors, Joel Cline, was a result of that agreement. Also from the WSFO RDU thanks go to the Deputy Meteorologist in Charge Joe Pelissier, and lead forecasters Larry Lee, Jan Price, and Jon Valentine for their critical review of this paper.

Special thanks to Larry Lee and Jan Price, whose encouragement were instrumental in this paper being written.

Most of all, the principal author thanks his wife Louane and their four children Kara, Brian, Leah, and Myra for sharing our family time with this project; and thanks to Louane for the help that only an English major could provide.

8. References

- Bocchieri, J.R., 1979: A new operational system for forecasting precipitation type. Mon. Wea. Rev., 107, pp. 637-649.
- Bocchieri, J.R., 1984: personal communication, Techniques Development Laboratory, NOAA, Silver Spring, MD. 20910
- Glahn, H.R. and J.R. Bocchieri, 1975: Objective estimation of the conditional probability of frozen precipitation. Mon. Wea. Rev., 103, pp. 3-15.

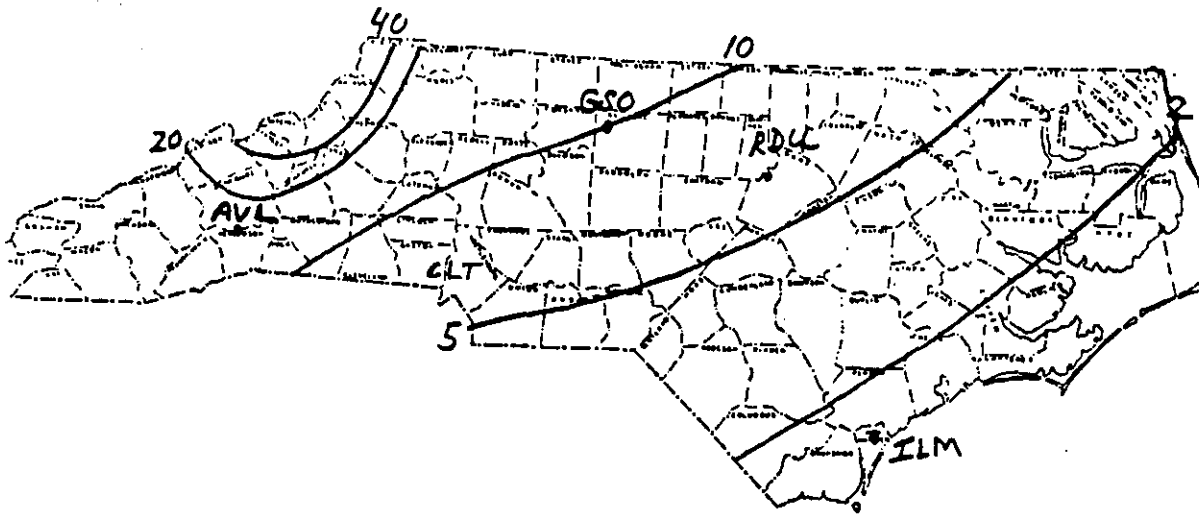


Fig 1. Shows the normal annual snowfall (inches) across North Carolina ranges from less than 2 inches in the coastal areas to over 40 inches in the northern mountains. The locations shown are National Weather Service stations: Asheville (AVL), Charlotte (CLT), Greensboro (GSO), Raleigh-Durham (RDU), Wilmington (ILM).

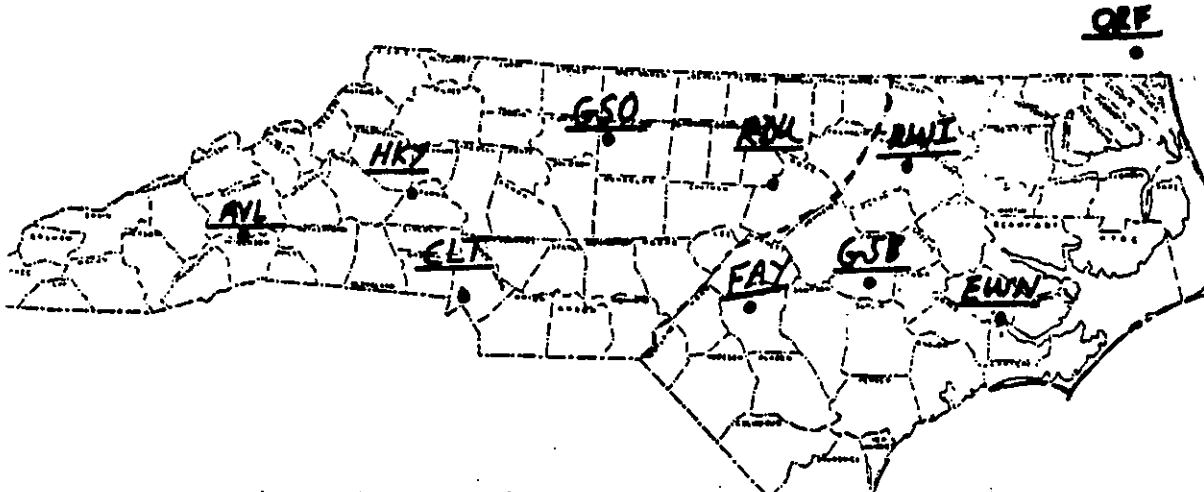


Fig 2. LOG/PT and MOS guidance are available at eight common sites scattered across the climatological regions of NC. LOG/PT is also available at two additional sites (GSB, RWT). The dashed line separates Western NC from Eastern NC. Western NC is from the piedmont west through the mountains. The individual sites and associated climatological regions are:

Western NC

AVL-Asheville-Mountains
 HKY-Hickory-Foothills
 CLT-Charlotte-S. Piedmont
 GSO-Greensboro-Nw. Piedmont
 RDU-Raleigh-Durham-Ne. Piedmont

Eastern NC

FAY-Fayetteville-Sandhills
 RWT-Rocky Mount-N. Coastal Plain
 GSB-Goldsboro-Central Coastal Plain
 ORF-Norfolk,VA-N.Coastal Area
 EWN-New Bern-Central Coastal Area

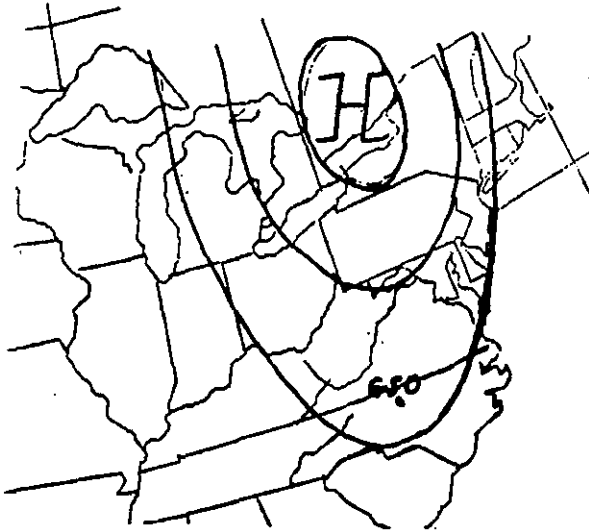


Fig 3. Typically, the center of the cold air high is located between the Great Lakes and New England when there are precipitation type problems in NC. The GSO raob site is well located for monitoring the lower tropospheric thermal structure of the prevailing airmass over NC.

Fig 4. The logit curve is well suited for predicting a binary predictand such as the occurrence or non-occurrence of snow. This S-shaped non-linear curve asymptotically approaches 100(0) percent chance of snow as the thickness becomes increasingly lower (colder) higher (warmer).

PROB OF SNOW

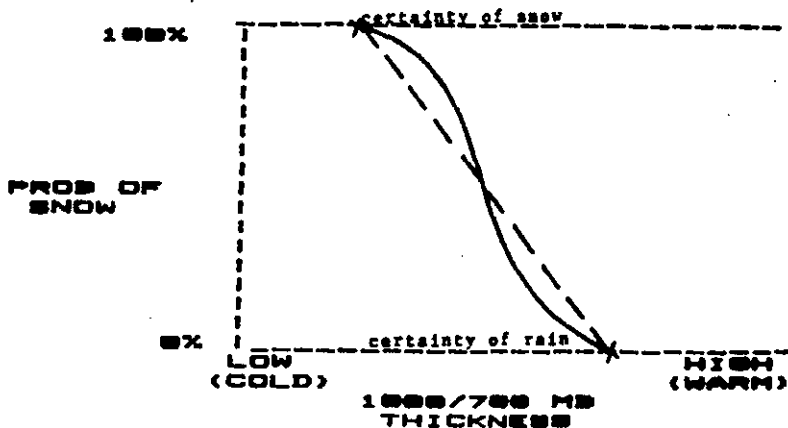
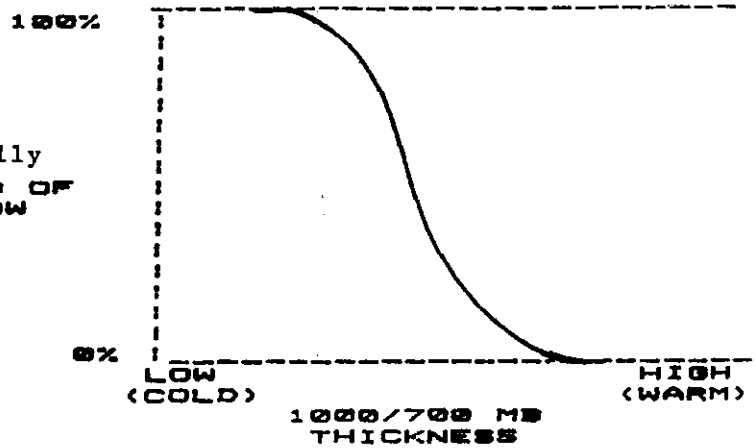


Fig 5. A linear curve (dashed line) was adapted as a good approximation to the logit by anchoring its end points at the thickness values where the precipitation type is no longer in doubt (values of certainty).

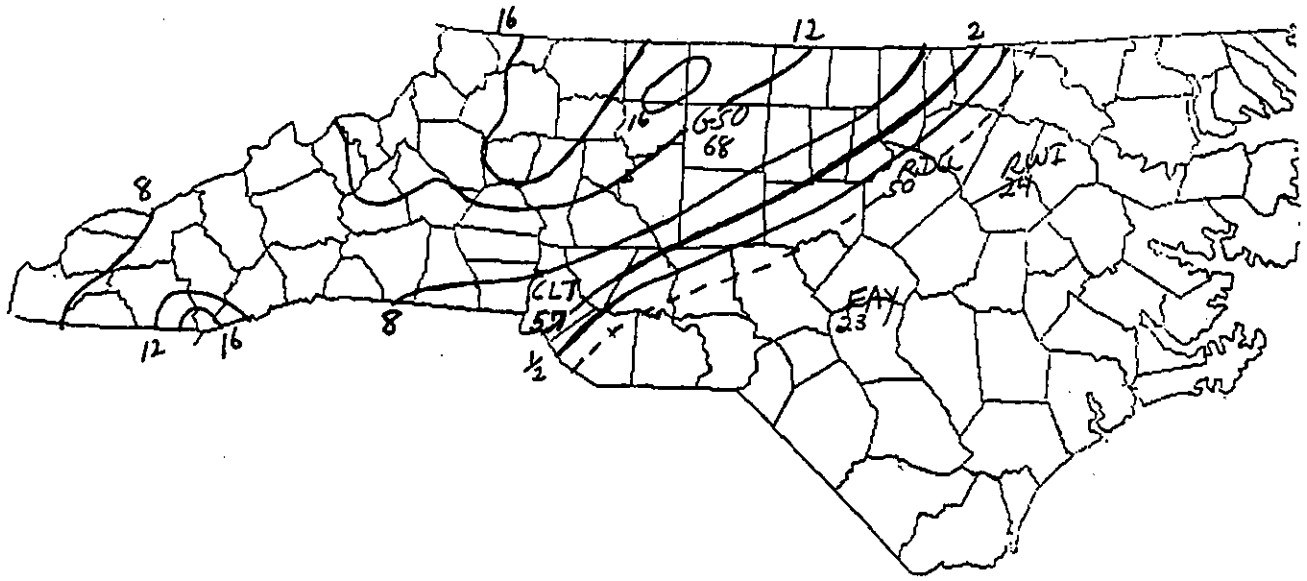


Fig 6. The dashed line is the 36 hour forecast by LOG/PT of the snow/rain boundary valid at 12z January 22, 1987. The site probabilities for snow are shown for CLT, GSO, RDU, RWI, and FAY. The 50 percent probability isopleth was used as the snow/rain boundary forecast position. The actual snowfall amounts (inches) are shown as solid lines. The actual snow/rain boundary was operationally defined as the area between the 1/2 and 2 inch snowfall isopleths. For this case, the predicted snow/rain boundary was exceptionally accurate falling within 25 miles of the actual boundary.

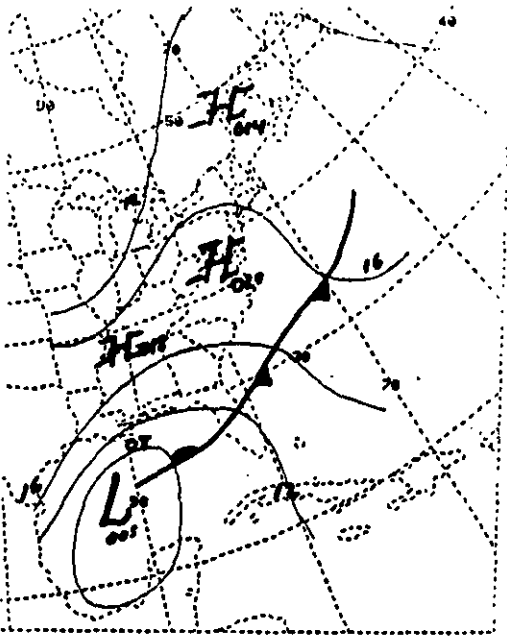


Fig 7. Shows the surface map valid at 00z January 22, 1987. The incipient low was developing in the Western Gulf of Mexico. Isobars shown are for every 4 mb.

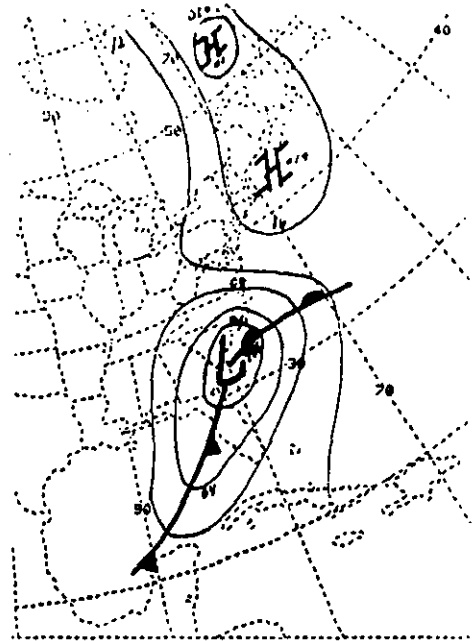


Fig 8. Shows the surface map valid 12z January 22, 1987. The low has tracked from the Western Gulf of Mexico to a position along the South Carolina coast. Heavy snow has been falling in Western North Carolina since 06z. The low has deepened to a central pressure of 996 mb. Isobars are shown for every 4 mb.

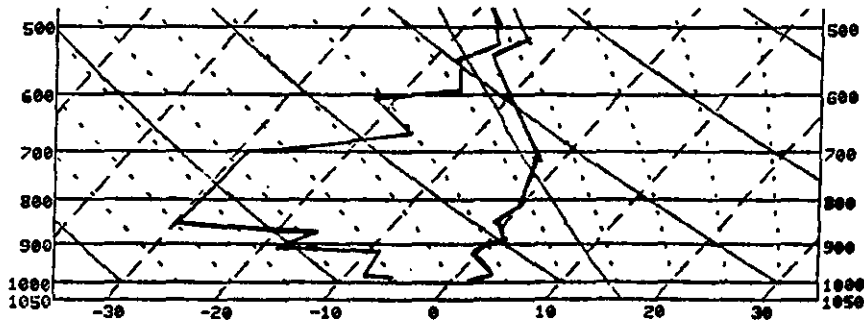


Fig 9. Shows the GSO raob sounding valid at 00z January 22, 1987. The dry bulb and dewpoint temperatures are shown on a standard Skew-T. Note how dry the airmass is below 600 mb and the large potential for evaporative cooling.

WINTER PRECIPITATION TYPE

by

Richard P. McNulty
WSFO Topeka Kansas

1. Introduction

Winter weather forecasting brings many interesting and challenging situations, not the least of which is forecasting precipitation type, i.e., rain versus snow versus freezing precipitation. Presented below is a brief summary of the physical aspects of winter precipitation type. It is hoped that this discussion will lead to a better understanding of winter precipitation processes, and thus to better rain versus snow versus freezing precipitation forecasts.

2. Rain versus Snow

The rain versus snow forecast (without the complicating issue of freezing precipitation) is one of the simpler precipitation type forecasts to face the winter forecaster. This does not mean that locating the rain-snow line in time and space is easy, but the physics of this forecast situation is less complicated than those involving freezing rain or sleet (ice pellets).

The key to the rain-snow question lies in the lower tropospheric thermal structure. In the typical case, temperature decreases with height away from the surface. The type of precipitation at the surface depends upon the thermal structure between the layer where the precipitation is formed (usually as snow during winter) and the ground.

If the entire layer is below freezing (Figure 1A), the snow remains as snow from the formation layer to the ground. On the other hand, if an above-freezing layer exists near the surface, the potential exists to melt the snow to rain (Figure 1B/1C). Penn [1] states that this warm layer must be sufficiently deep to provide enough heat to melt the snow to rain. Studies have found that this melting depth varied from 750 feet to 1500 feet, depending upon snowflake type, melted drop size and lapse rate. Another study expressed the probability of snow in terms of the depth of the warm layer (Table 1).

The variation of precipitation type with change in lapse rate ($G = -dT/Dz$) is shown in Figure 1B/1C. The rate of heat transfer is proportional to the temperature difference between the melting snow flake (at 0 C) and the surrounding air. Thus the larger the temperature difference the faster the snow will melt. In terms of lapse rate, shallow layers with large lapse rates (Figure 1B) can melt snow to rain with the same efficiency as deeper layers with smaller lapse rates (Figure 1C). On the average, the freezing level must be at least 1200 feet above the surface to insure that the snow will melt to rain.

TABLE 1: chance of snow versus warm layer depth

chance of snow: 50 %	warm layer depth: 35 mb/920 ft
70 %	25 mb/660 ft
90 %	12 mb/315 ft

If the depth of the melting layer can be predicted, precipitation type can be anticipated. This vertical structure is observed at least twice a day, but must be inferred between rawinsonde runs. Factors affecting these changes will be discussed in Section 5.

A typical cross-section through a rain-snow boundary might look like Figure 2. Where all temperatures above a point are below freezing, snow is indicated. Where the freezing level is higher than some critical level, rain occurs. There also exists a zone with the freezing level between the critical level and the ground where either rain, or snow, or both occur.

In work done by the AES, Stewart [2] found that for saturated conditions, the temperature profile near the rain-snow boundary tends to be associated with deep isothermal layers which have temperatures close to 0 C.

3. Freezing Rain and Ice Pellets

A discussion of freezing rain or ice pellets needs to start with the definition of these precipitation types from the Glossary of Meteorology [3]:

a. freezing rain: rain that falls in liquid form but freezes upon impact to form a coating of glaze upon the ground and on exposed objects (this implies a surface air temperature of 0 C (32 F) or less;

b. ice pellets (sleet): transparent or translucent pellets of ice, 5 mm or less in diameter; they form from the freezing of rain drops or the refreezing of largely melted snowflakes when falling through a below-freezing layer of air near the earth's surface.

The vertical temperature profiles associated with both freezing rain and ice pellets are similar. Both involve an elevated warm (above freezing) layer and a below-freezing layer between the ground and the elevated warm layer. The physical processes occurring differ, however.

With both precipitation types, snow falls into the elevated warm layer and begins to melt. In the case of freezing rain, the snow completely melts to liquid before falling into the below-freezing layer. In order for liquid droplets to freeze, freezing nuclei and temperatures generally below -10 C must be present (heterogeneous nucleation). In the typical freezing rain case, temperatures are

warmer than -10 C and the number of freezing nuclei are not significant to initiate the freezing process. The droplets remain liquid and become supercooled. Upon striking the below-freezing ground, these liquid droplets freeze and glaze the surface.

This discussion implies that the depth of the below-freezing layer near the ground is not as important as the temperature of that layer. If the cool layer temperature is less than -10 C (and freezing nuclei are sufficiently abundant), either snow or sleet could occur, depending upon the degree of refreezing (related to the depth of the cold air). If the cool layer temperature is warmer than -10 C , the liquid droplets will be supercooled and freezing rain will occur.

In the case of ice pellets, the snow falling into the elevated warm layer partially melts before entering the lower cool layer. This partial melting produces an ice crystal surrounded by liquid water. As this combination falls into the below-freezing layer, it begins to refreeze immediately (due to the presence of the ice crystal). This results in ice pellets (sleet) at the surface.

The key difference in the above situations is the degree of melting that the snow undergoes in the elevated warm layer. Stewart and King [4] used a model to study the melting of snow in an elevated warm layer. They found that if the maximum temperature in the warm layer exceeded 3 to 4 degrees C, snowflakes melted completely to liquid resulting in rain or freezing rain (depending upon the surface temperature) (Figure 3). If the maximum temperature in the warm layer was less than 1 C, only partial melting occurred, followed by complete refreezing in the cool layer, and snow at the surface. Warm layers with maximum temperatures between 1 and 3 degrees had a mixture of partially melted and completely melted snowflakes. This resulted in ice pellets, or more commonly a mixture of snow, rain (or freezing rain) and ice pellets. These results imply that the maximum warm layer temperature can serve as a guide for proper interpretation of a sounding in terms of freezing rain versus ice pellet potential.

Stewart [5] also examined the changes in the elevated warm layer due to the melting snow, in the absence of other factors (such as thermal advection). Melting snow requires latent heat to change phase. This heat is extracted from the surrounding environment. If snow falls through the warm layer for a sufficient length of time, the layer will slowly erode (cool) and finally disappear. As the maximum temperature of the warm layer decreases, the resulting precipitation type will evolve from freezing rain to ice pellets to snow (with a mixture of the various types likely during the transition). As a result Stewart [5] refers to freezing rain as a "self-limiting" process, in the absence of other factors.

Figure 4 illustrates a typical cross-section through a freezing rain/ice pellet event.

4. Sounding Examples

Even though two cases do not a generality make, an example of an

ice pellet sounding and a freezing rain sounding will lend support to the conclusions of Stewart and King [4].

The sounding for November 27, 1987, (Figure 5) shows an elevated warm layer between 860 mb and 775 mb with a maximum temperature of +2.2 degrees C at 852 mb. The 40 mb deep above-freezing layer at the surface precludes freezing rain in this case. However, the +2.2 degree C maximum fits Stewart and King's [4] criterion for ice pellets. Note that the lower portion of the sounding is essentially saturated, thus satisfying the assumptions of the Stewart and King model.

Table 2 lists the precipitation type on hourly and special soundings that occurred at Topeka on November 27th. Although the precipitation was mainly liquid (rain), intermittent periods of ice pellets did occur before changing completely to snow during the evening. One could speculate that the warm layer at the surface was a strong factor in making rain the predominant precipitation type, completely melting some of ice pellets falling into the layer from above.

(As a point of information, the evening sounding was entirely below freezing except for a 50 mb above-freezing layer at the surface.)

Table 2: Precipitation Occurrence at Topeka on 11-27-87

GMT	Precip	GMT	Precip
1430	R-IP-	2053	R-
1450	R-IP-	2114	RIP-
1510	R-	2151	R-IP-S-
1535	...	2238	R-
1550	...	2254	R-
1650	...	2351	R-
1750	L-	0051	R-
1835	L-	0125	R-S-
1851	L-IP-	0150	R-S-
1950	R-	0250	S-
2035	R-	0350	S-

The sounding for the morning of December 13, 1984, is shown in Figure 6. The elevated warm layer runs from 890 mb to 740 mb with a maximum temperature of +3.4 degrees C at 793 mb. The layer below the warm layer is below freezing from 890 mb to the surface. Although the sounding is not saturated through the entire depth, the +3.4 degree maximum and the freezing temperature at the surface indicate freezing rain potential. Light freezing rain did occur at Topeka from 7:03 AM to 2:45 PM, at which time the surface temperature rose above freezing.

5. Changes in the Vertical Profile

As alluded to in an earlier section the forecaster gets a detailed look at the lower tropospheric thermal structure twice a day. Between

these times, changes in structure must be inferred from other factors.

Penn [1] provides an excellent discussion of those factors which affect local temperature change in the lower troposphere away from the surface. These factors are:

- (a) thermal advection by the horizontal wind;
- (b) temperature changes due to vertical displacement; and
- (c) effects of non-adiabatic heating or cooling.

Studies have shown that the horizontal thermal advection is the dominant process in the lower troposphere. Its effect is somewhat reduced by the change due to vertical displacement. Specifically, warm temperature advection is usually associated with upward vertical motion. Upward motion causes cooling during adiabatic ascent. The net effect is to reduce the warming expected from advection alone by about one-half. If a forecaster can determine what type of advection is occurring, vertical profile changes can be inferred, and precipitation type anticipated.

Even though the advection factor is generally dominant, there are situations where non-adiabatic effects can be significant. Two effects are important in rain-snow situations. The first is evaporational cooling. When precipitation (particularly rain) falls through an unsaturated layer between the cloud and ground, precipitation will evaporate, particularly if the below-cloud air is rather dry. When this occurs the air cools. As the air becomes saturated, its temperature approaches the wet-bulb temperature of the original drier air. If this wet-bulb temperature is below freezing, the precipitation at the surface may change from rain to snow as the freezing level lowers toward the surface. The evaporational cooling in this case overpowers any warm advection that may be occurring, and can cool the air by 5 to 10 degrees C in an hour. Once the layer becomes saturated, this non-adiabatic effect ceases and advection again becomes dominant.

A second non-adiabatic effect is the melting of snow to rain. As mentioned earlier, snow extracts heat from the surrounding environment when it melts. In the typical situation this cooling effect is not large enough to offset warming due to advection. However, in very heavy precipitation events, R+ may change to S+ due to lowering of the freezing level by latent heat absorbed by the melting snow.

The above discussion indicates that thermal advection is the dominant factor affecting temperature change in the lower troposphere. It should be asked then: What information is routinely available to the forecaster to analyze the lower tropospheric thermal advection? The answer is: the surface chart and the 850 mb chart. However, a lot can happen between the surface and the 850 mb level that may or may not be obvious from either level. What is needed is a more detailed analysis system for the lower troposphere. The current rawinsonde message has an abundance of information just waiting to be tapped. For example, using the entire temperature profile, the pressure-altitude

data, and the PIBAL (wind) data, plots and/or analyses at 500 ft, 1000 ft, 1500 ft, etc. (AGL), could be generated. From these charts the interlaced thermal advection patterns frequently associated with winter storms could be better diagnosed. Such information would enhance a forecaster's ability to infer changes in the vertical temperature profile, and its subsequent impact on precipitation type.

Figures 7 through 9 illustrate this concept for March 3, 1988. At the surface (Figure 7) weak to moderate cold air advection extended across Missouri, Kansas and Oklahoma. No warm air advection is evident. At 5000 feet (AGL) (Figure 8), cold air advection is minimal or absent while warm air advection is moderate to strong across Missouri. Examination of charts every 1000 feet down to the 2000 feet level (AGL) (Figure 9) shows this same pattern of warm air advection. Temperatures across Northern Missouri warmed during the day and the rain/snow line moved north before the precipitation ended as an upper level short wave trough moved over the area during the afternoon.

6. Concluding Remarks

The discussion in this note is not meant to imply that the only information available to the forecaster for forecasting rain versus snow versus freezing precipitation is the vertical temperature profile. Some very useful techniques involving thickness values are available. Also, MOS produces a precipitation type forecast. Either of these topics could be a topic for an extensive discussion by itself.

Nevertheless, the information presented here should improve a forecaster's understanding of the physical processes involved in winter weather precipitation forecasting. In particular, the results of Stewart and King [4] which relate warm layer strength to precipitation type should be useful operationally. These new values should enhance the forecaster's ability to correctly anticipate precipitation type.

References

1. Penn, S., 1957: The Prediction of Snow vs. Rain. U.S. Dept. Commerce (Weather Bureau), Forecasters Guide No. 2, 29 pp.
2. Stewart, R.E., 1987: Nowcasting rain/snow transitions and freezing rain. Proc. Symp. Mesoscale Anal. & Fcstg., Vancouver, 155-161.
3. Huschke, R.E., 1959: Glossary of Meteorology. Amer. Meteorological Society, 638 pp.
4. Stewart, R.E. and P. King, 1987: Freezing precipitation in winter storms. Mon. Wea. Rev., 115, 7, 1270-1279.
5. Stewart, R.E., 1985: Precipitation types in winter storms. Pure Appl. Geophys., 123, 597-609.

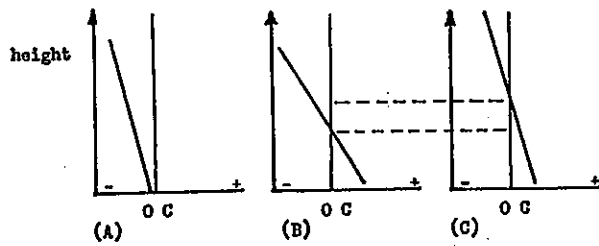


FIG 1: Example of a rain-snow sounding

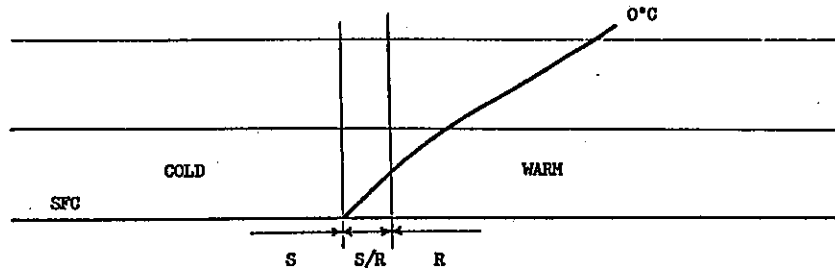


FIG 2: Typical rain-snow cross-section

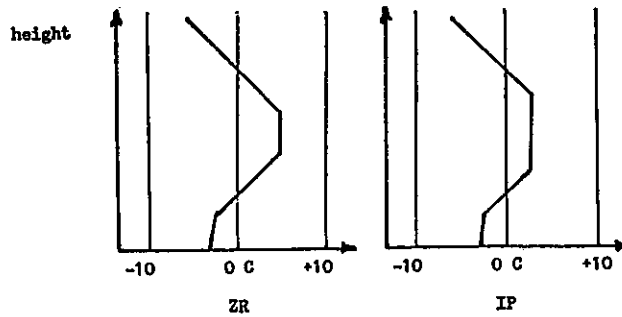


FIG 3: Example of freezing rain and ice pellet sounding

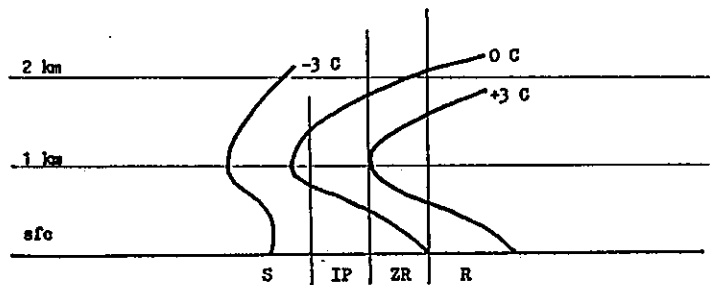


FIG 4: Typical freezing rain/ice pellet cross-section

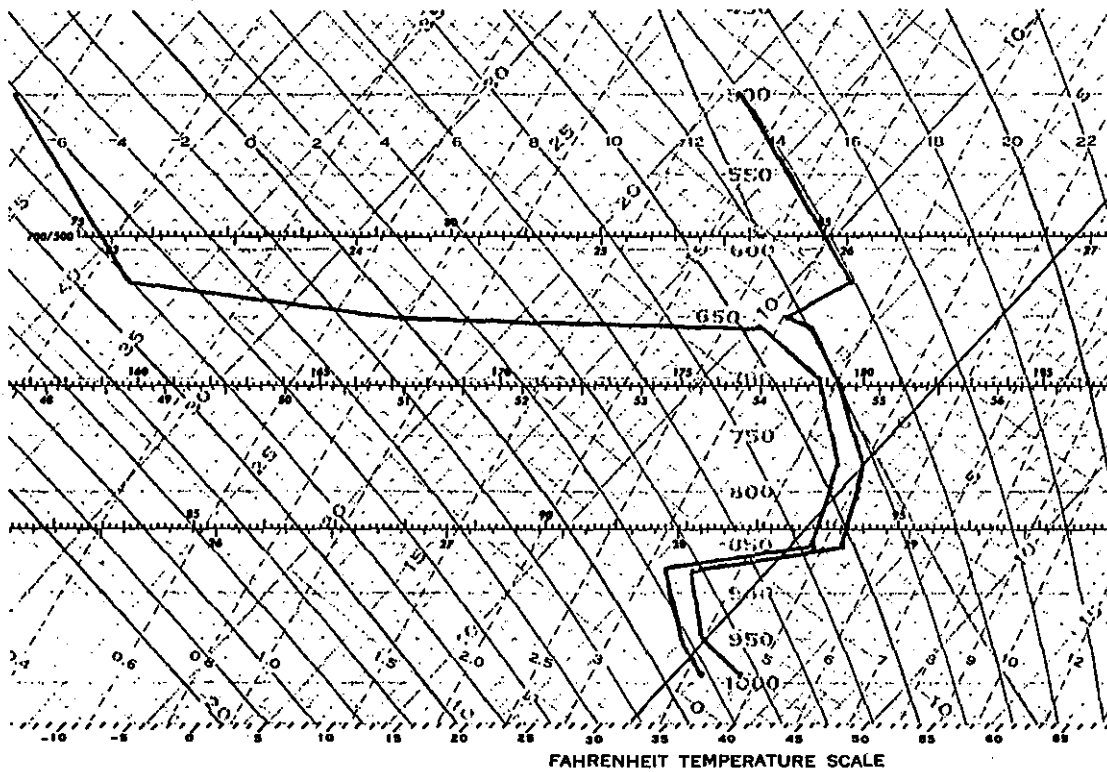


FIG 5: Topeka, KS, sounding for 11-27-87

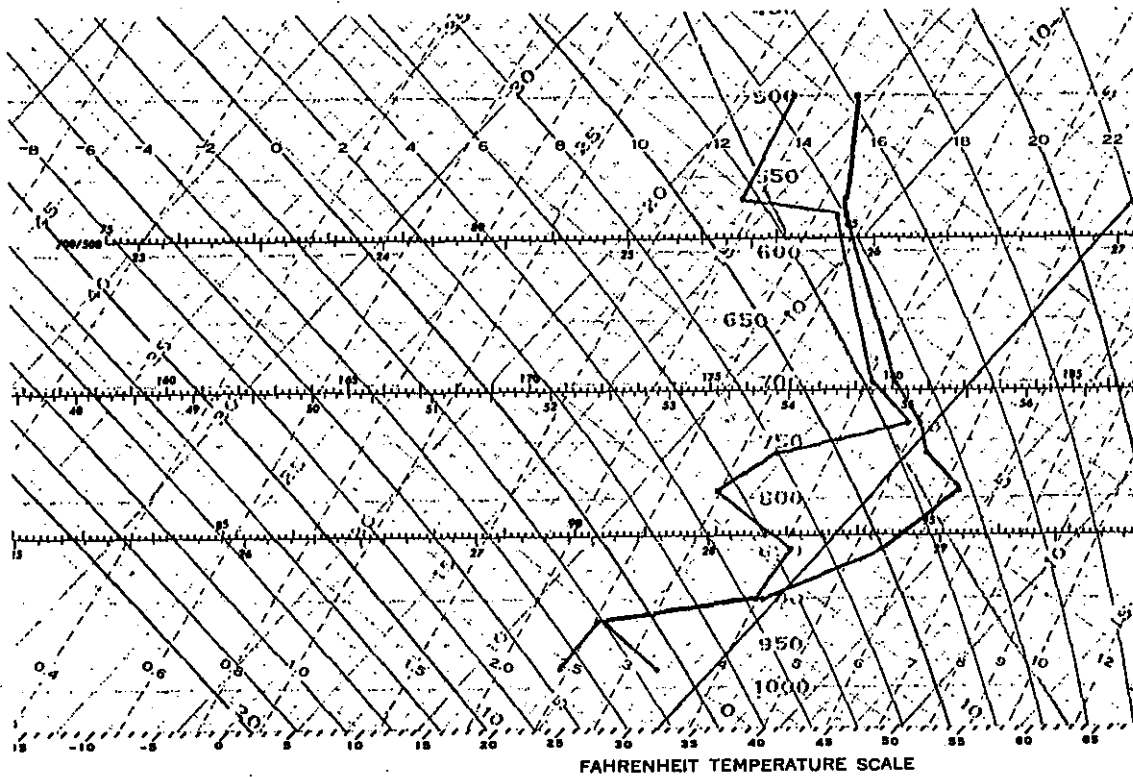
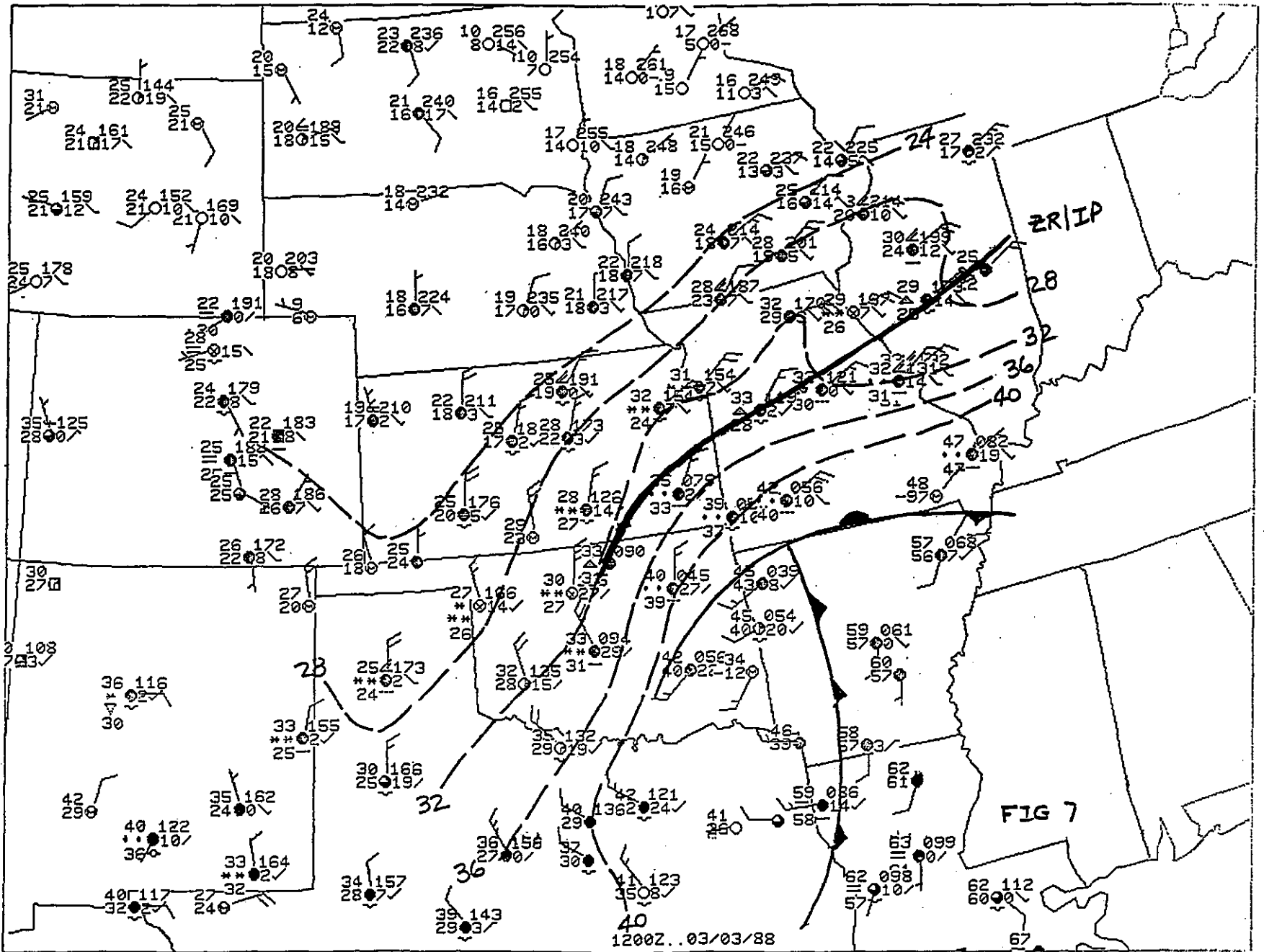


FIG 6: Topeka, KS, sounding for 12-13-84



THE OPERATIONAL DILEMMA OF HUGE NUMERICAL MODEL DIFFERENCES

Frank C. Brody
National Meteorological Center
Forecast Branch
Camp Springs MD

1. INTRODUCTION

Weather forecasters in the U.S. have access to three sophisticated short-range numerical prediction models. This can be a blessing and a curse. The models often arrive at very different solutions, especially in the 36 to 48 hour time frame during the cool season. This leads to forecaster confusion and frustration, which ultimately affects the forecast users. This paper will show examples of huge differences between LFM and NGM solutions, and will discuss the impact of these differences on forecast decisions. NMC's efforts to deal with this problem will also be outlined.

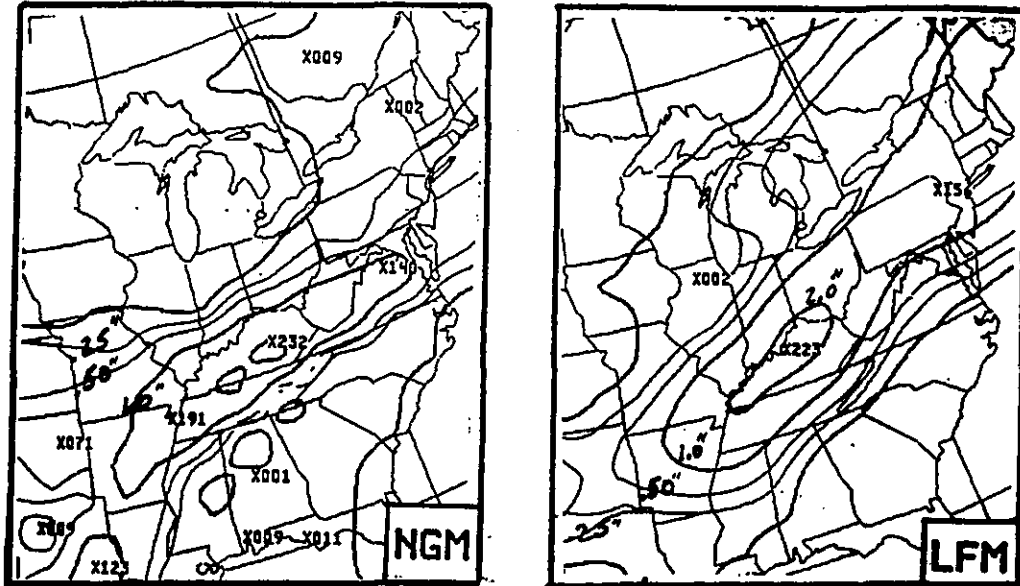
2. CASE 1: DECEMBER 26, 1987

Figure 1a shows the NGM and LFM accumulated 24 to 48 hour QPFs (Quantitative Precipitation Forecasts), for the 24 hour period ending 12Z December 26, 1987. These forecasts were generated from the 12Z December 24, 1987 model runs.

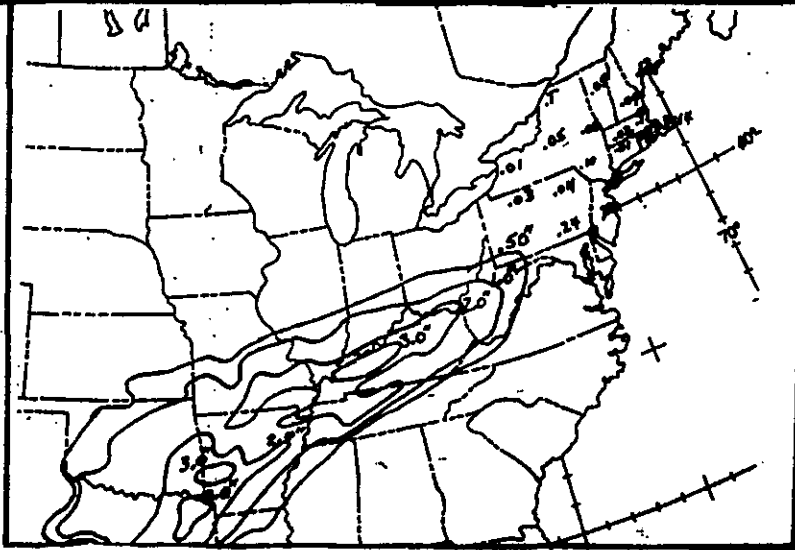
Both models forecast substantial rainfall over the Tennessee and Ohio Valleys. However, their QPFs for the northeastern states differed drastically. The LFM forecast **ONE INCH OR MORE** for much of Pennsylvania, New York, and New England; the NGM forecast **.25 INCH OR LESS** for most of that region. Fortunately, this was not a snow situation. If it were, forecasters would be faced with with a gut-wrenching decision: 1 to 3 inches of snow versus 10 to 15 inches of snow!

Observed precipitation isohyets for this 24 hour period (Figure 1b) showed the NGM clearly outperformed the LFM in the Northeast. Observed amounts across New England were generally $\leq .15$ inch. The simplistic "rule of thumb" of reducing the LFM QPF by one-half would have backfired, since the LFM was overdone by a factor of ten in the Northeast. However, the LFM was fairly accurate for the Lower Ohio and Tennessee Valleys, as was the NGM.

FIGURE 1a



**24 THRU 48 HR QPFS
VALID 12Z DEC 26 1987**



**OBSERVED PCPN
24 HRS ENDING 12Z DEC 26 1987**

FIGURE 1b

3. CASE 2: FEBRUARY 12, 1988

The 12Z February 10, 1988 model runs yielded the 48-hour forecasts in Figure 2a. The most important difference was the surface pressure and thickness patterns in the Mid-Atlantic area. The LFM was much faster and deeper than the NGM in moving the coastal low northward off the East Coast. This timing difference implied significantly different weather conditions for 12Z February 12. The NGM forecast **WARM ADVECTION and EASTERLY FLOW**, with moderate to heavy precipitation implied (though not actually forecast) for the Richmond-to-New York City megalopolis. The LFM forecast **COLD ADVECTION and NORTHWEST FLOW** for Richmond to Philadelphia, implying that most of the precipitation would have ended by 12Z February 12.

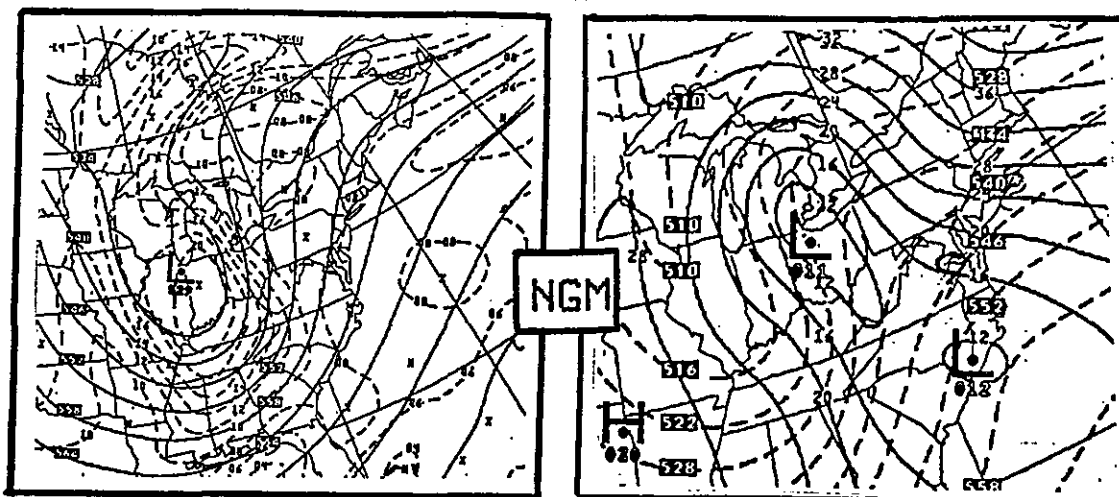
The verifying objective analysis (Figure 2b) showed the NGM was too slow and weak, while the LFM was a bit too fast and intense with the surface low at 12Z February 12. The NMC manual surface analysis (not shown) placed the surface low just southeast of Atlantic City, New Jersey, with a 1004 mb central pressure. This would place the surface low even closer to the LFM position. The actual instantaneous weather at 12Z February 12: rain had mostly ended along the Mid-Atlantic coast, except for moderate rain falling at New York City.

Figure 3a shows the 48 hour QPFs valid for the 12 hour period ending 12Z February 12. The NGM forecast maximum amounts of less than .50 inch, with **no precipitation along the coast northeast of Delaware**. The LFM forecast **widespread .50 and 1.00 inch amounts from the Mid-Atlantic area into New England**. This gave the February 10 day shift forecasters a choice of forecasting either little or no precipitation/low POPs (NGM) or heavy precipitation/high POPs (LFM) for the 3rd period ("tomorrow night") valid 00Z through 12Z February 12, 1988.

Observed precipitation isohyets (Figure 3b) showed widespread amounts of one inch or more across the Mid-Atlantic region (24 hour amounts are shown, but most fell in the final 12 hours ending 12Z February 12). Significant snow (4 to 10 inches) fell from northeast Pennsylvania into southeast New York and western New England (Figure 3c).

The LFM QPF outperformed the NGM QPF in this case. The rule of thumb of reducing the LFM QPF by one-half would have again backfired for the Mid-Atlantic region (though it would have worked for parts of New England and upstate New York). In contrast to Case 1, though, this "halving" procedure would have resulted in a drastic **underforecasting** of precipitation amounts for most of the Mid-Atlantic area.

FIGURE 2a



48 HR FCSTS VALID 12Z FEB 12 1988

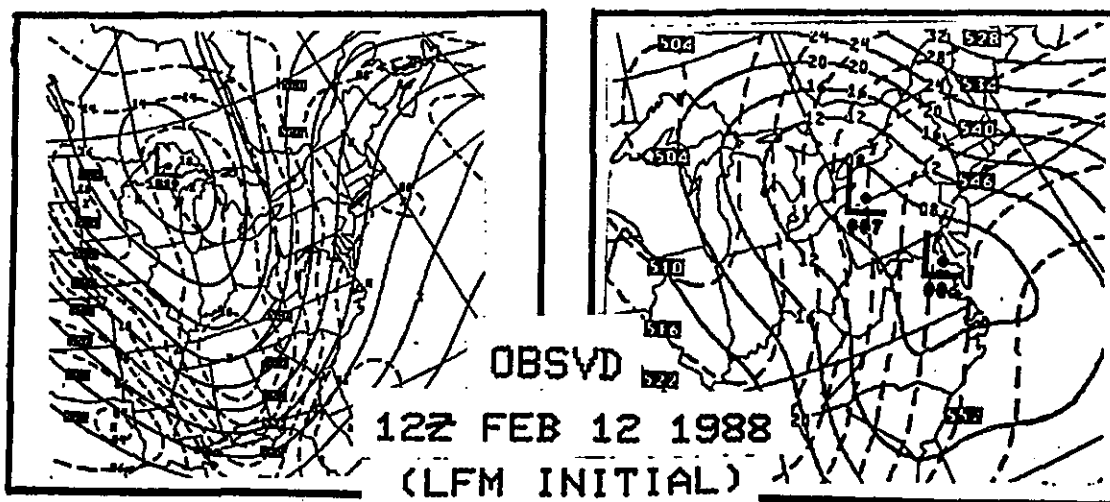
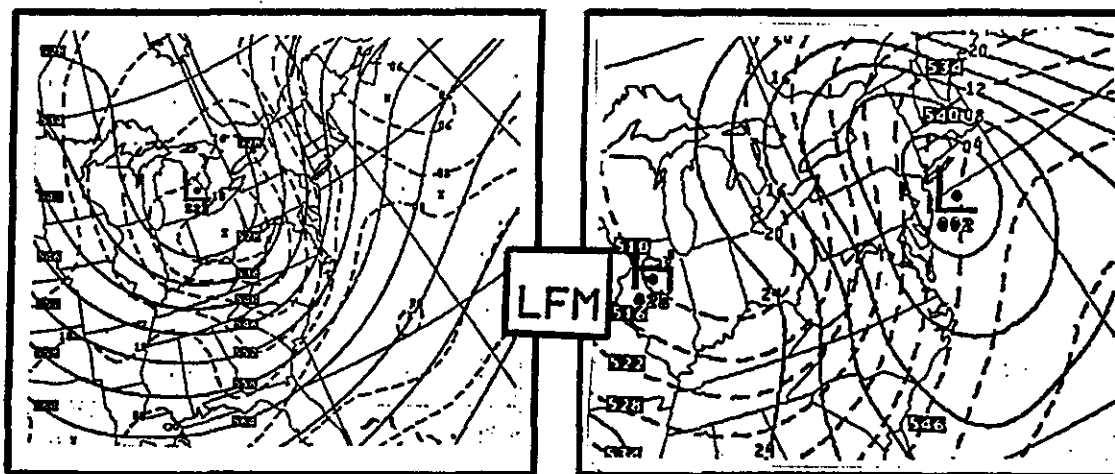
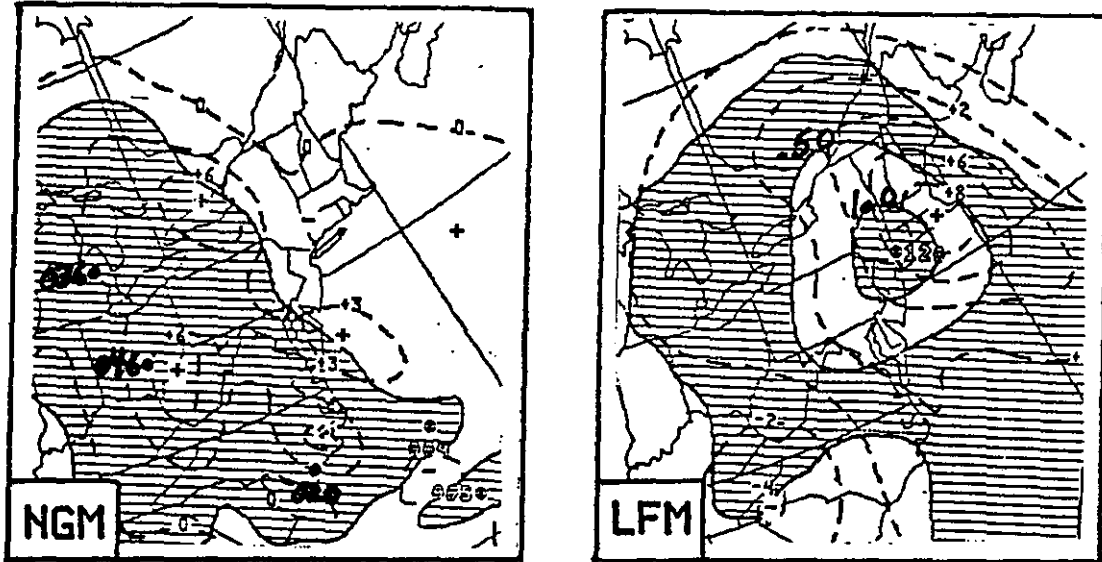
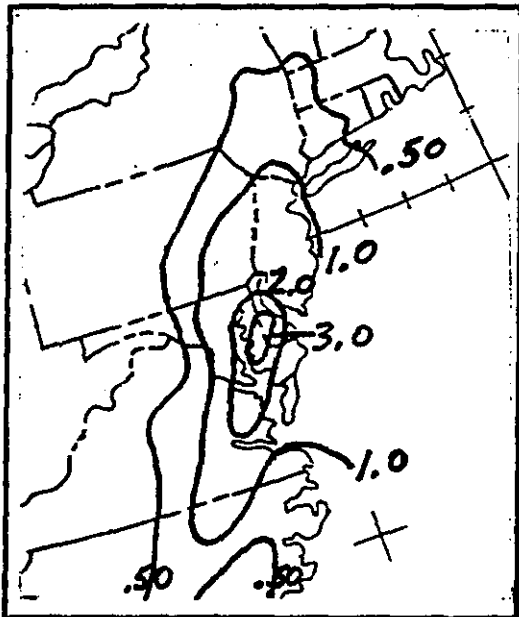


FIGURE 2b

FIGURE 3a

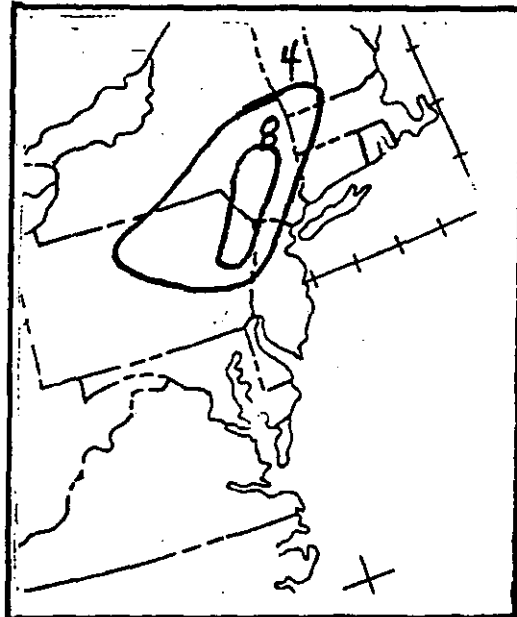


48 HR QPFS: 12 HOURS ENDING
12Z FEB 12 1988



24 HR PCPN
ENDING 12Z FEB 12 1988

FIGURE 3b



12 HR SNOWFALL
ENDING 12Z FEB 12 1988

FIGURE 3c

This example illustrates systematic errors noted subjectively by NMC forecasters. The NGM is often too slow, too weak, and too dry with East Coast cyclogenesis, while the LFM is too quick, especially at 36 to 48 hours.

4. CASE 3: MARCH 11, 1988

This was an epic snowstorm for Wyoming and western Nebraska. Ten inches of new snow fell at Chadron in northwest Nebraska during the 12 hours ending 12Z March 11. Three-day storm totals of 20 to 35 inches occurred over parts of Wyoming and western Nebraska (Storm Data).

Figure 4a shows the NGM and LFM 48 hour forecasts valid 12Z March 11, 1988. The day shift forecasters on March 9 were faced with **nightmarish** model differences. The NGM forecast a deep closed upper low over Nebraska with a 988 mb surface low over southeast South Dakota. The LFM forecast a much weaker upper low over New Mexico, with a 998 mb surface low over central Texas (800 miles from the NGM's low position!). The two model solutions implied drastically different weather scenarios for the Great Plains states.

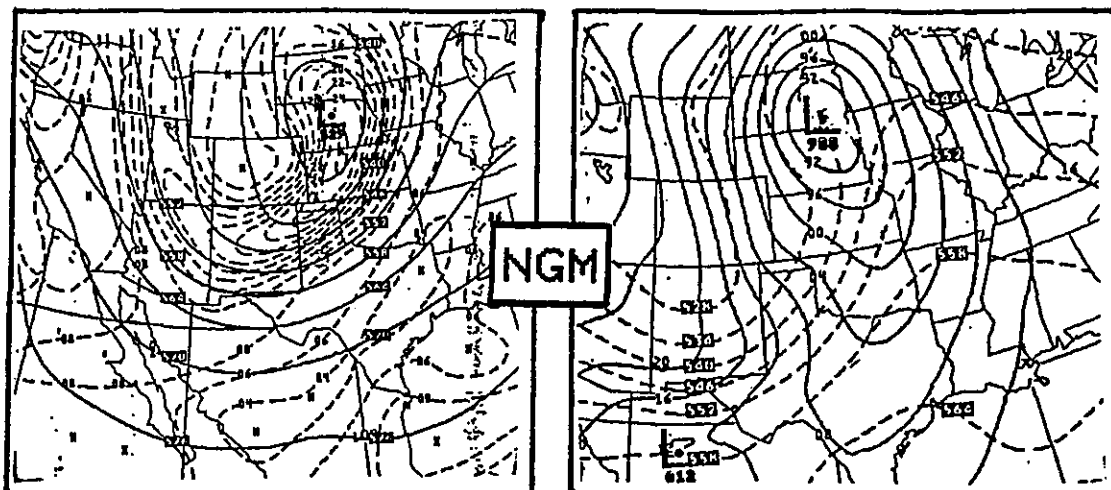
Verifying analyses (Figure 4b) show the NGM was the clear "winner" with the circulation forecasts, despite being a bit too fast and intense with the surface and upper low centers. A forecaster who had correctly anticipated an NGM "victory" might have been tempted to favor the NGM QPF over the LFM QPF. Ironically, that seemingly logical reasoning would have proved incorrect (Figure 5b). While the LFM QPF was too extensive, it pinned down the **axis** of the heaviest amounts quite well through the High Plains and central Rockies. The NGM QPF was centered too far north, implying the heaviest snow would fall in the Dakotas. However, the NGM was more realistic with the **areal extent** of half-inch amounts.

This paradox has been noted before by NMC forecasters. A superior circulation forecast by one model does not necessarily imply a better QPF by that model (Brody, 1986).

5. CASE 4: JANUARY 18, 1988

The 12Z model runs from January 16, 1988 generated the 48 hour forecasts shown in Figure 6a. The NGM and LFM differed greatly in handling the 500 mb vort max over Michigan, with correspondingly large 500 mb height differences. Surface forecasts also differed dramatically. While the LFM forecast a 999 mb low over Ontario, the NGM forecast only an inverted trough. The LFM forecast **NORTHERLY FLOW** and **COLD**

FIGURE 4a



48 HR FCSTS VALID 12Z MARCH 11 1988

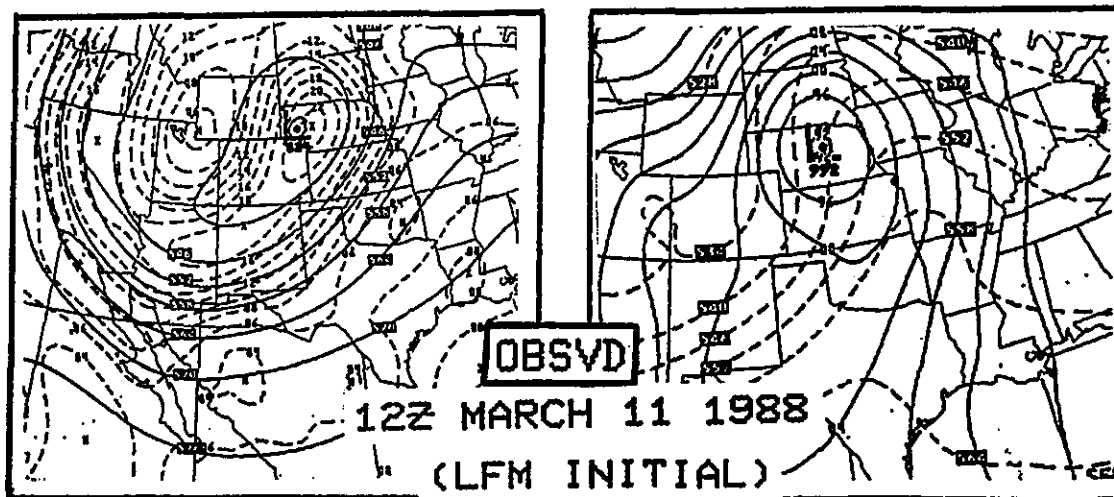
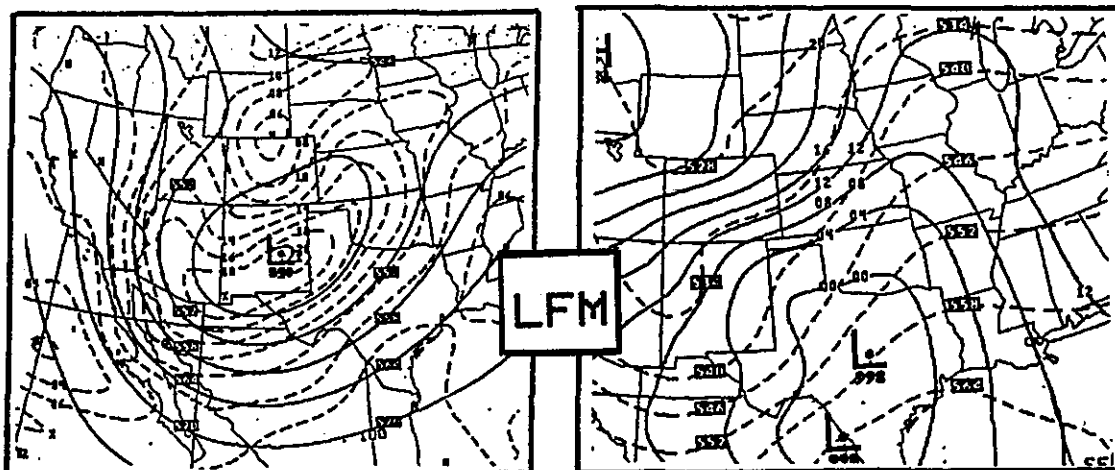
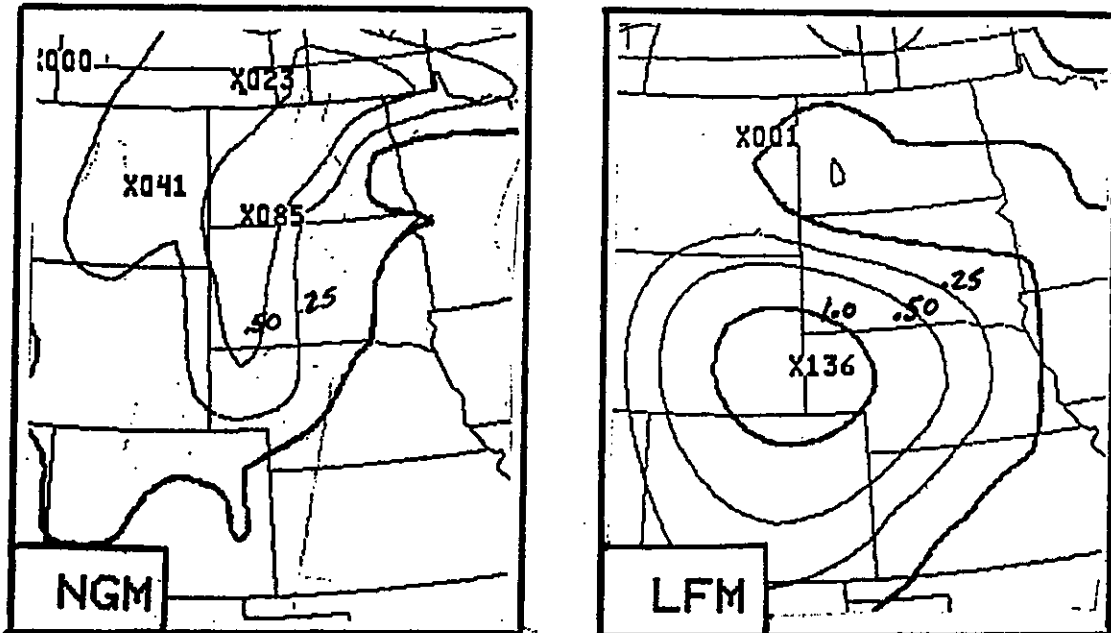
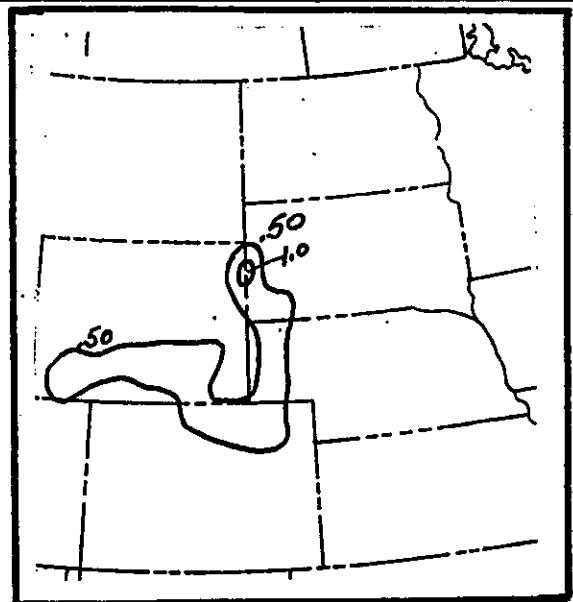


FIGURE 4b

FIGURE 5a



24 THRU 48 HR QPF
ENDING 12Z MARCH 11 1988



OBSERVED PCPN
24 HRS ENDING 12Z MARCH 11 1988

FIGURE 5b

ADVECTION over the Great Lakes and Ohio Valley, while the **NGM** forecast **SOUTHERLY FLOW** and **WARM ADVECTION** across the same area! These differences obviously gave forecasters quite a range of wind and temperature forecast possibilities across the region.

Verification (Figure 6b) showed that a "compromise" between the two models would have yielded a reasonable solution. The **LFM overforecast** the intensity of the vort max and surface low. The **NGM underforecast** the intensity of these features. The verifying thermal advection fields and low level flow patterns were generally a **compromise** (though leaning toward the LFM) between the two model forecasts. Widely differing QPFs (not shown) were also generated by the two model runs. As with the circulation forecasts, a compromise or "averaging" of the model QPFs would have yielded the best results.

This example further demonstrates the importance of considering **all** models when making a forecast, despite the general superiority of one model.

6. DISCUSSION

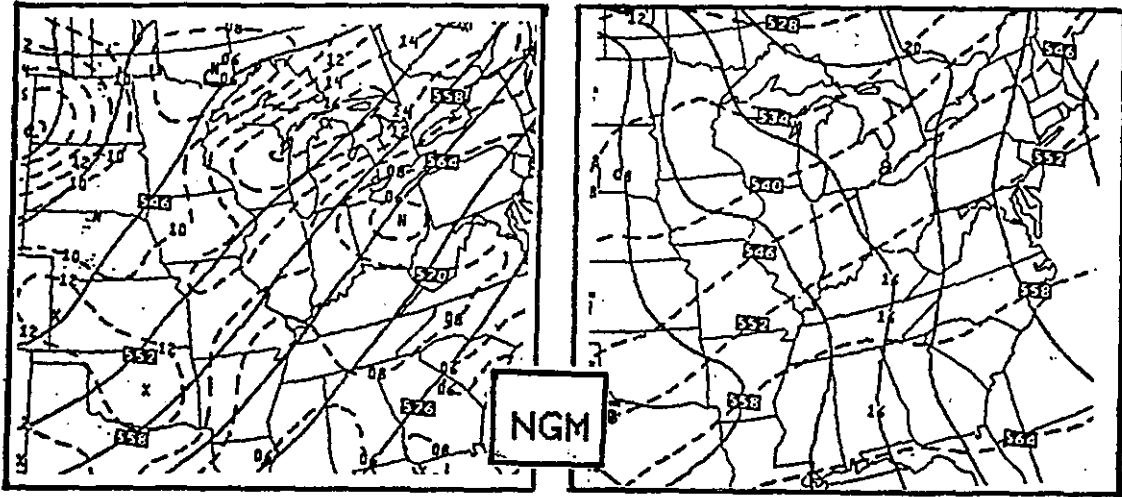
Each cool season will produce many more situations of huge numerical model differences. As demonstrated in the examples, no one model **consistently** outperforms the others. While not displayed in the examples, the Aviation model (AVN a.k.a. Spectal/MRF) model often provides a reasonable compromise between the NGM and LFM, or it may "side" with one model. Thus, the AVN model often serves as an operational "arbitrator" when forecasters encounter large differences between NGM and LFM model solutions.

Other tools to help assess model differences include (but are not limited to):

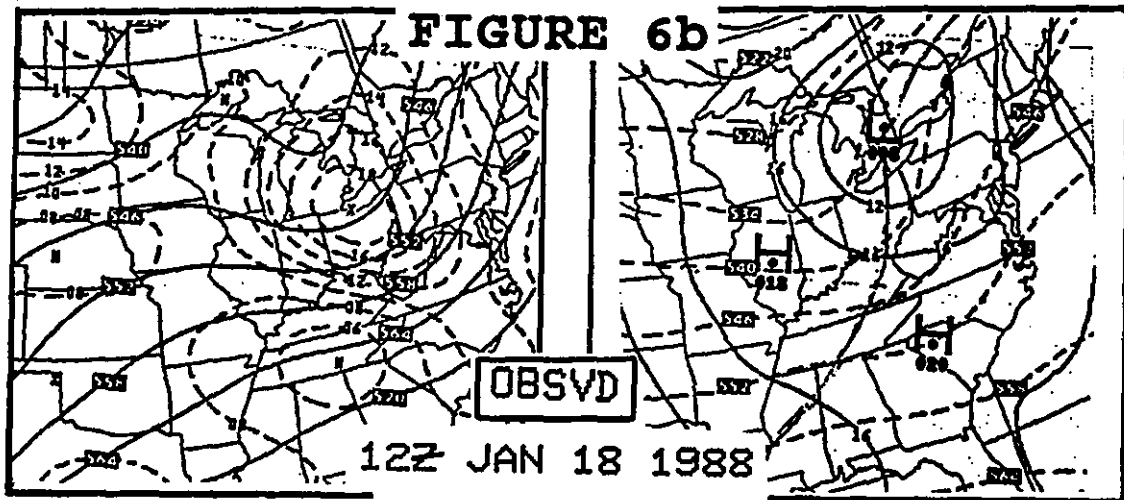
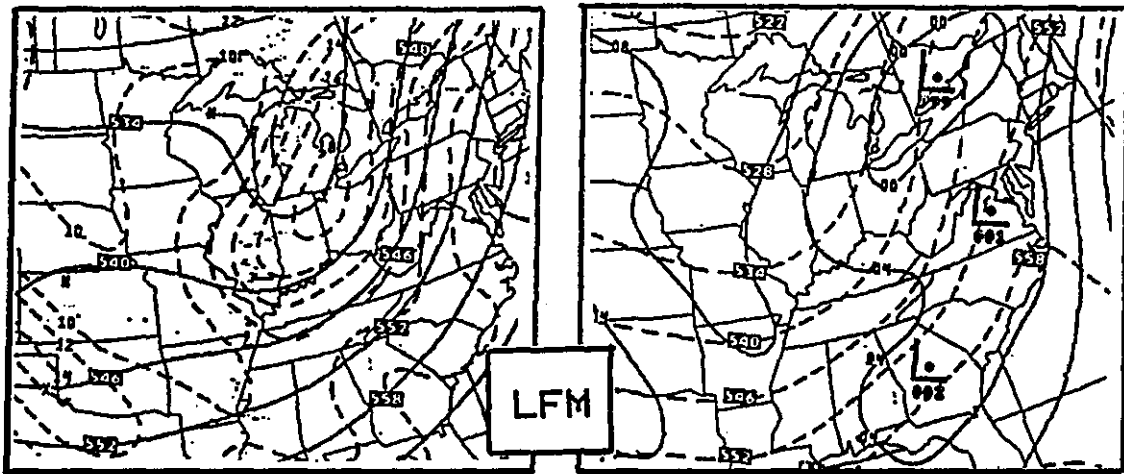
- knowledge of systematic model errors, especially as a function of synoptic regime
- evaluation of model initializations
- degree of agreement between different models
- consistency between consecutive runs of the same model
- recent model performance characteristics

At NMC, the European Model (ECMWF) and United Kingdom Met Office Model (UKMET) are also available for comparisons.

FIGURE 6a



48 HR FCSTS VALID 12Z JAN 18 1988



12Z JAN 18 1988

(LFM INITIAL)

NMC also has the capability to run the LFM from the NGM analysis, and vice versa. This can sometimes help diagnose whether model differences are rooted in **initialization differences** or in **systematic errors**. This model re-run capability may eventually be available to NMC forecasters in real time.

On a daily basis, NMC issues several technical reasoning discussions to accompany graphical forecast products. These discussions often highlight model differences and forecaster preferences and interpretations. The Hemispheric Prognostic Discussion (AFOS heading CCCPMDHMD, WMO heading FXUS3 KWBC) specifically addresses short range (0 to 48 hr) and medium range (3 to 5 day) model differences.

To deal effectively with model differences, it is imperative to know **how models perform in different synoptic patterns**. More research must be aimed in this direction by forecasters and modelers if weather forecasters hope to face this problem intelligently in the 1990s.

7. ACKNOWLEDGMENTS

The author would like to thank Ron McPherson, Jim Hoke, Sondra Young, and Mike Schichtel for their helpful suggestions in preparing the original workshop presentation and this written version. Special thanks also to Linda Burroughs for word-processing assistance.

8. REFERENCES

- Brody, F., 1986: Model performance of 500 mb closed lows and associated QPFs in the western U.S. Postprints, First National Weather Service Winter Weather Workshop, Denver, Colorado.
- Storm Data, March, 1988, NOAA, National Climatic Data Center, Asheville, NC

SNOW FORECASTING USING PHYSICAL PARAMETERS

D.Bachand, J.Morissette and V.Turcotte

Quebec Weather Centre (QWC)
100 Boul.Alexis-Nihon, St-Laurent
P.Qué., Can., H4M 2N8

Abstract. A technique has been developed to help forecasting snow amounts. This technique is the result of a systematic study of 15 synoptic systems that affected the province of Quebec. For these systems, we related together the snow amounts observed at different stations to the quantitative assessment of the physical parameters directly responsible for precipitation, using the quasi-geostrophic theory. The parameters used were the 500 mb vorticity advection by the thermal wind (1000-500 mb thicknesses), the precipitable water, the 1000 mb vorticity and its tendency, the 1000-500 mb thicknesses tendency.

1- INTRODUCTION

To forecast snow accumulations we must first evaluate the synoptic features responsible for the formation of precipitation. These elements include the vertical velocity and the available moisture in the atmosphere. Also we must evaluate related parameters that are more difficult to quantify, as stability and local effects. Finally we must evaluate precipitation duration and take into account the possible changes in precipitation types.

As the purpose of this paper is to deal with snow episodes and related accumulations, we will from now assume that the precipitation type is known or determined by other techniques.

The usual tools available operationally to forecast snow accumulations are:

- the QPF from the numerical models, which are nowadays quite good but nevertheless not always reliable.
- statistical and empirical techniques. These often give relevant indications but do not forecast precise quantities.

We then need to have a technique to complete the information obtained by the above mentioned tools and to assess the NWP QPF's for each particular case.

2- THE TECHNIQUE

To achieve this goal, a systematic study of synoptic systems which affected the province of Quebec was undertaken. We tried to link the snow episodes and amounts observed with these systems to the values of the physical parameters directly responsible for precipitation, using the quasi-geostrophic theory.

To assess the vertical velocity in the mid-troposphere, we used Trenberth's formulation of the omega equation which states that vertical velocity can be accounted for by evaluating the advection of vorticity by the thermal wind. (Trenberth,1977)

Secondly, the parameter used to evaluate the low level vertical velocity is the 1000 mb geostrophic vorticity and its tendency. (Holton,1972; Zwack et al.,1984)

A qualitative assessment of the temperature advections and air mass stability is done by taking into account the 1000-500 mb thicknesses tendency.

Finally the available moisture is directly accounted for by the quantity of precipitable water.

A- TECHNIQUE DEVELOPMENT

In order to understand the technique, we will examine briefly how it was developed.

Database

Fifteen meteorological systems that affected the province of Quebec were used. From these 15 weather systems, we could extract about 175 snow episodes of about 12 hours at different observation stations.

Types of systems

Because of the type of synoptic situations studied, the results of the technique apply with more reliability in cases where:

- the weather systems are in translation with a mean speed of the order of 25 knots.
- the systems are supported aloft by a well defined vorticity centre which maintains its identity in time.

Parameter variations

With this type of systems, we can usually identify a maximum of Vorticity Advection by the Thermal Wind (VATW). This maximum may vary in intensity but maintains its identity in time so that we can track it.

Then we can relate together the snow episodes and the parameters used in two kinds of situations:

- when VATW is increasing in time, i.e. the maximum of VATW is approaching a region.
- when VATW is decreasing, i.e. the maximum of VATW is moving away from a region.

Data extraction

For the sake of brevity, we will examine only the more important snow episodes corresponding to increasing VATW during 12 hour periods.

For these periods, the snow amounts were related to the following features:

- the MAXIMUM values of VATW, Qg (1000 mb geost. vorticity) and PCPTW (precipitable water) reached during the periods.
- the variation of Qg during the period (usually an increase in this case).
- the sign of the 1000-500 mb thicknesses tendency.

With surface lows moving at about 25 knots, the correlations above could be made for snow episodes of about 12 hours duration. This is not really a limitation, since we can then adjust the accumulations given by the resulting tables to the speed of the systems.

We will now examine how the different parameters are evaluated operationally and their link with "snow amounts".

B- EVALUATION OF THE PHYSICAL PARAMETERS

a) Vertical velocity in the mid-troposphere (fig.1)

To visualize and evaluate the VATW (Vorticity Advection by the Thermal Wind), we use, as proposed by Trenberth, the superimposition of the 1000-500 mb thickness lines to the absolute vorticity field at 500 mb.

To quantify the advection values, we defined a "surface advection unit" to which we arbitrarily assigned the relative value of 100. (This surface advection unit is shown on fig.1)

We verified that, in fact, this advection surface of 100 corresponds approximately to a real advection value of 2.75×10^{-9} /sec/sec.

To give an idea of the representative values of advection, we can note, as indicated in the table at the bottom of the figure, that, when sufficient moisture is available, maximum values of VATW of the order of 100 moving through a region correspond frequently to accumulations of 10-15 cm (4-6 inches) of snow whereas when the maximum reaches or exceeds 200, we usually observe snow amounts exceeding 15 cm (6 in.).

(Note that V_t in the table is a shorter symbol for VATW).

We recall that these correlations are for 12 hour periods where VATW is increasing.

b) Precipitable Water (PCPTW) (fig.2)

To estimate the available moisture in the atmosphere, we use fields of precipitable water.

We can see on figure 2 a field of precipitable water which is an analysis based on the Canadian RFE (Regional Finite Elements) model, showing contours of precipitable water at every 5 mm. These fields are available on an operational basis at analysis and prognosis times, as are also the other fields in (a) above and (c) below.

The critical lines are the 10 and 15 mm contours. In summary, we can say that, when vertical velocity is sufficient, snow amounts of 15 cm or more generally require a quantity of precipitable water of at least 10 mm. On the other hand, when precipitable water is less than 7 mm, we rarely observe accumulations reaching 10 cm. Finally, when precipitable water exceeds 15 mm, the potential of moisture for snow amounts is maximised.

c) Low level vertical velocity (fig.3)

Finally the low levels vertical velocity is accounted for in our technique by the 1000 mb geostrophic vorticity (Q_g) and its variation $[D(Q_g)]$.

The fields used are analysis and prognosis of 1000 mb geostrophic vorticity in units of 10^{-5} /sec and contoured at every 2 units.

Maxima of geostrophic vorticity are well associated to surface lows. The instantaneous values of Q_g are proportional to the vertical velocity in the boundary layer. (Holton,1972; Zwack et al.,1984)

What is mainly considered is the local time variation of 1000 mb vorticity during the snow episodes, as this represents convergence and vertical velocity at low levels. (Zwack et al., 1984)

Snow amounts are generally somewhat less sensitive to this parameter than they are to VATW and PCPTW. But it is nevertheless important as it allows to refine the snow amounts.

To give an idea of the representative values, we can note that, if sufficient moisture and mid-tropospheric vertical velocity are available, then a variation of Q_g exceeding 5 units during the period considered indicates accumulations approaching 10 cm, whereas an increase of Q_g of more than 10 units makes it favourable to amounts of 15 cm or more.

C- RESULTS (fig.4)

Figure 4 shows the correlations obtained between the MAXIMUM values of VATW, MAXIMUM values of PCPTW, and SNOW AMOUNTS for 12 hour periods of snow when VATW is increasing.

On the right-hand side of the figure, we consider cases where thicknesses (DZ) are rising, whereas on the left-hand side, we deal with cases where thicknesses (DZ) are falling.

In first approximation and to facilitate the demonstration, we ignore the 1000 mb geostrophic vorticity predictor.

The snow amounts indicated are in centimeters (Cm).

So, for example, in the case where the predictors reach the highest values for the correlations established, i.e. VATW greater than 200 and PCPTW greater than 15 mm, we generally observe 12 hour accumulations of 25 cm (10 inches) or more.

On the other hand, we note that, as expected, for equivalent conditions of PCPTW and VATW, the snow accumulations will be larger when DZ (thicknesses) are rising during the period than when they are falling, which may correspond, for example, to occluding systems.

The influence of the 1000 mb geostrophic vorticity (Q_g) and its variation is shown in the table at the bottom of the figure. We can see that, for important increases of Q_g , especially for increases of 10 units or more, snow accumulations will be larger than the means indicated in the figure.

3- CASE STUDY - NOVEMBER 25-26, 1987

a) Synoptic situation and events (fig. 5)

In this period, a low which had formed earlier in SWRN US, tracked through the lower Great Lakes towards the east coast, with a reformation taking place by 18Z november 26.

Before this reformation took place, the central MSL pressure of the low had been rising in time up to a value of 1024 mb when it came nearest to our regions of responsibility by 18Z november 26.

With this system, that seemed to be weakening, we nevertheless observed very important snow accumulations over extreme SWRN Quebec. The snow amounts were generally between 20 and 30 cm, with a maximum of 48 cm (18 inches) in YSC (Sherbrooke). Moreover, this was the very first snow storm of the winter over southwestern Quebec.

The rain-snow boundary, which was well associated to the thickness line 540 dam, just slid along the Canada/US border.

Our technique, which was applied in real time to that case, allowed a very good forecast of this snow storm, which, at first glance, might look inoffensive.

b) Synoptic evolution and assessment of parameters

Without getting into development details, we can see that there were some indications showing that this low pressure system was really intensifying even though its central pressure was rising.

1- Surface (figs.8,12)

First, at the surface, the ridging that took place over ERN Quebec between 25/12Z and 26/00Z, along with the approaching low over lower Great Lakes, caused the pressure gradient to increase in the Northeast quadrant of the low, indicating an increase in convergence.

The advantage of the technique is to allow objective measurement of that increase, with the 1000 mb geostrophic vorticity parameter (Qg). We can see from figures 8 and 12 that:

- the Qg centre increased from +8 to +10 during this period
- the gradient of Qg also significantly increased in the northeast quadrant of the low, indicating more important time changes of Qg taking place.

2- 500 mb (figs. 7,11)

At 500 mb, the persistence of the intense vorticity centre between 25/12Z and 26/00Z while moving along in a confluent flow toward a region of stronger circulation, caused the vorticity advection by the thermal wind to increase ahead of the system. At 25/12Z, the stronger VATW was behind the surface low complex (in the northwest quadrant). By 26/00Z, it had moved ahead the system (in the northeast quadrant).

Again the technique could give some measure of this increase of VATW ahead of the surface low, showing VATW of the order of 200 now present at 26/00Z (fig. 11).

3- Available moisture (figs.9-13)

The available moisture, in the region of snow type precipitation and as measured by the precipitable water reached a maximum of 15 mm over extreme southwestern Quebec.

4- Composite Charts (figs. 13-14)

Composite charts at 26/00Z show that the area of MDT/HVY snow at that time is very well correlated to the region where:

- VATW is larger or increasing (fig.13)
- PCPTW is of the order of 15 mm. (fig.13)
- Qg is increasing (fig.14)

In summary, the 12 hour period mainly considered here is the one from 25/18Z to 26/06Z. In that period, over southwestern Quebec, Qg was increasing, VATW and DZ were rising for about the first six hours and then remained constant for the rest of the period.

The snow amounts correlation figure (fig.4) shows that, in the case of rising DZ, with PCPTW of 15 mm or more and VATW increasing to 200 or more, one can associate a 12 hour period of 25 cm of snow or more. This figure was very representative of the situation.

Finally, a 24 hour evolution chart of the predictors (fig.6), shows that the technique helps to refine the area which will be affected by the larger accumulations. It is obvious from the figure that the parameters are maximum over extreme southwestern Quebec. So the critical sector is well delineated by the technique.

4- LIMITATIONS

The limitations to the technique are of two kinds:

a) Representativity of the parameters

Some phenomena are not well represented by the parameters used:

- Local effects like orography and on-shore flow must be evaluated from experience or other techniques.
- The warm air advection is not always well represented by the VATW in the way we look at it right now. Sometimes, when the warm air advection at low levels is far ahead of the system and the 500 mb vorticity centre, then there are no vorticity lines in the area of temperature advection so that there is no advection of vorticity shown because the vertical velocity is all accounted for below 500 mb.

b) Accuracy of the forecast parameters

The accuracy of the forecast parameters also limits sometimes the usefulness of the technique.

The Qg, DZ and PCPTW parameters are generally reliable forecast parameters. But on the other hand, the reliability of the 500 mb forecast vorticity depends on the synoptic situation. In some particular cases, like channeled jets and vorticity lobes in a strong circulation, vorticity centres and gradients are often poorly predicted by the numerical models.

5- CONCLUSION

- Advantages

On the other hand, the advantages of the technique include the following:

- it allows the evaluation of individual physical parameters for each weather system
- it allows to assess the NWP model's QPF
- it gives directly snow amounts forecasts
- being a "Perfect Prog" approach, it is applicable to any NWP model.

- Future development

- First of all, we intend to increase the statistical sample by studying new cases.
- We also intend to program the calculations of VATW, which will facilitate the use of the technique.
- Further case studies should allow to refine the interpretation of the parameters in different synoptic situations.
- We already began to use the VATW at 850 mb to assess the vertical velocity at that level. This added feature has the advantage to complete the information given by VATW as evaluated with the 500 mb vorticity and the 1000-500 mb thicknesses. It particularly and efficiently helps in cases of warm air advection not related to 500 mb vorticity, as pointed out in the limitations section above.

Finally, we can say, as a general evaluation of the consequences of the use of this technique at QWC, that it is definitely a positive contribution to the accuracy of snow amounts forecast and of the swath of the larger accumulations associated to a system track and intensity.

6- REFERENCES

- 1- Holton, J., 1972: An introduction to dynamic meteorology, Academic Press, New-York and London, 319pp.
- 2- Trenberth, Kevin, E., 1977: On the interpretation of the Diagnostic Quasi-geostrophic Omega equation, Monthly Weather Review, Jan. 1978, Vol. 106, No. 1, p. 131-137.
- 3- Zwack, P. and G. Babin, 1984: Using Quasi-geostrophic theory to understand lower troposphere synoptic scale vertical motion, 10th Conf. on Wea. For. and Anal., Amer. Meteor. Soc., Clearwater Beach, Fla., June 1984, p. 256-264.
- 4- Zwack, P. and M. Kabil, 1988: Estimating Lower Tropospheric Vertical Motion from Surface Pressure and Pressure Tendency Data Alone, Monthly Weather Review, March 1988, Vol. 116, No. 3, p. 795-803.

Fig.2

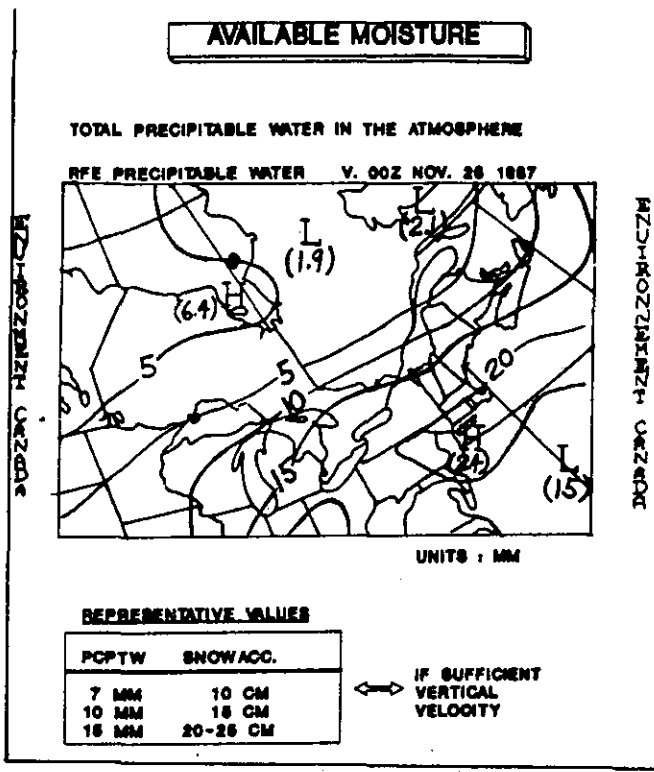


Fig.1

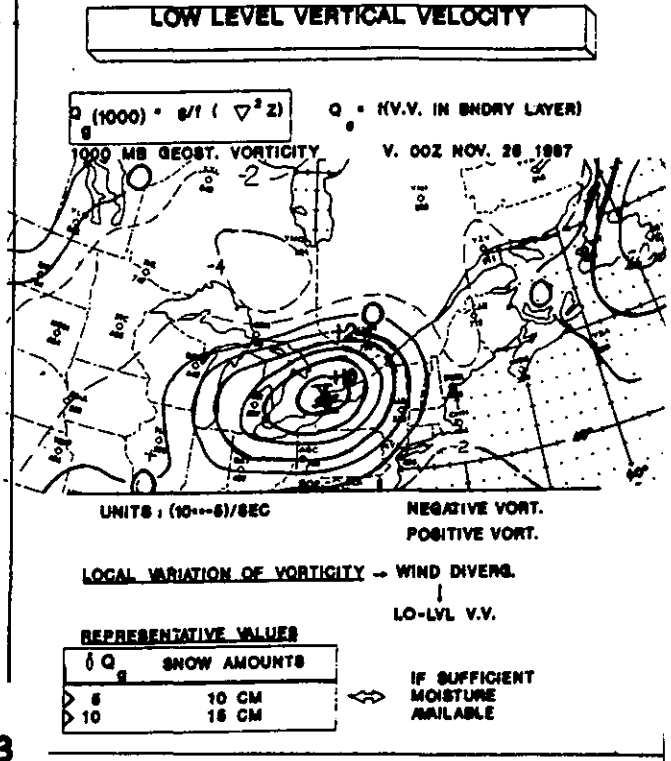
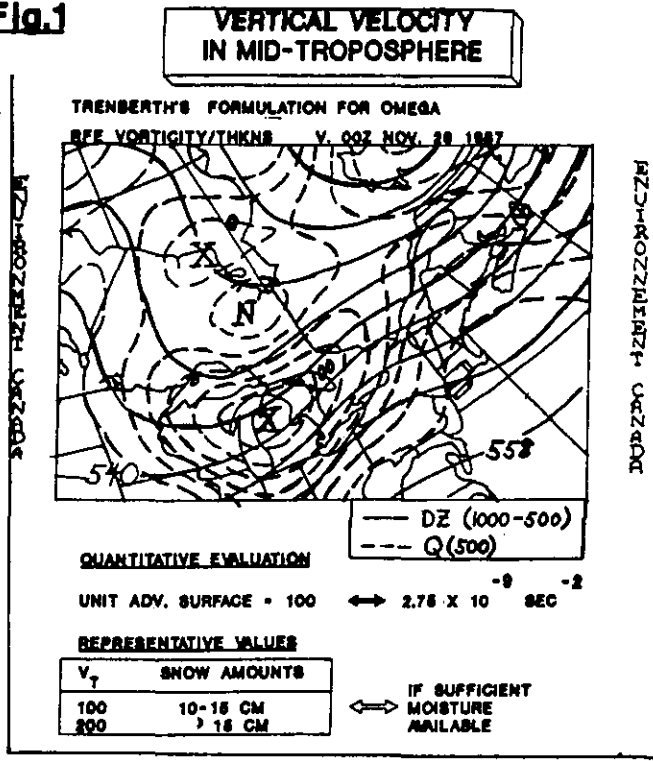


Fig.3

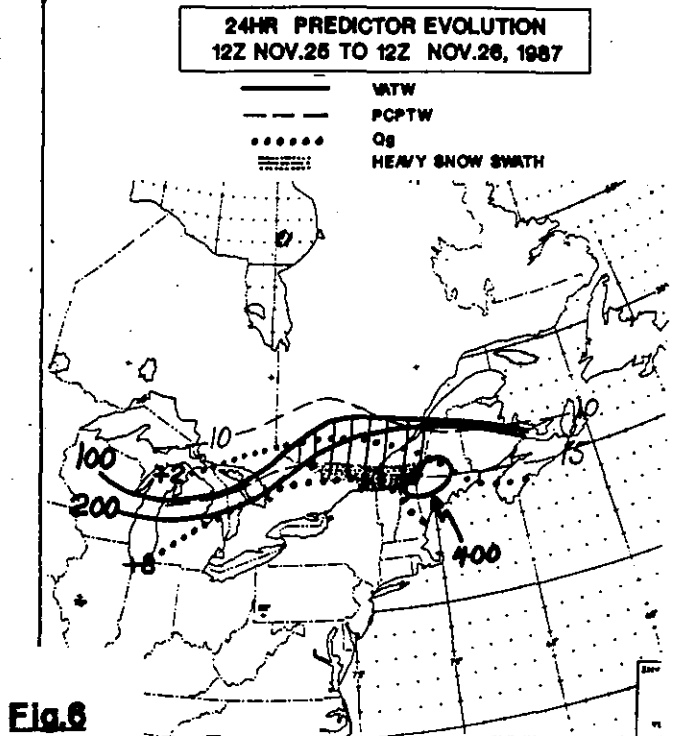
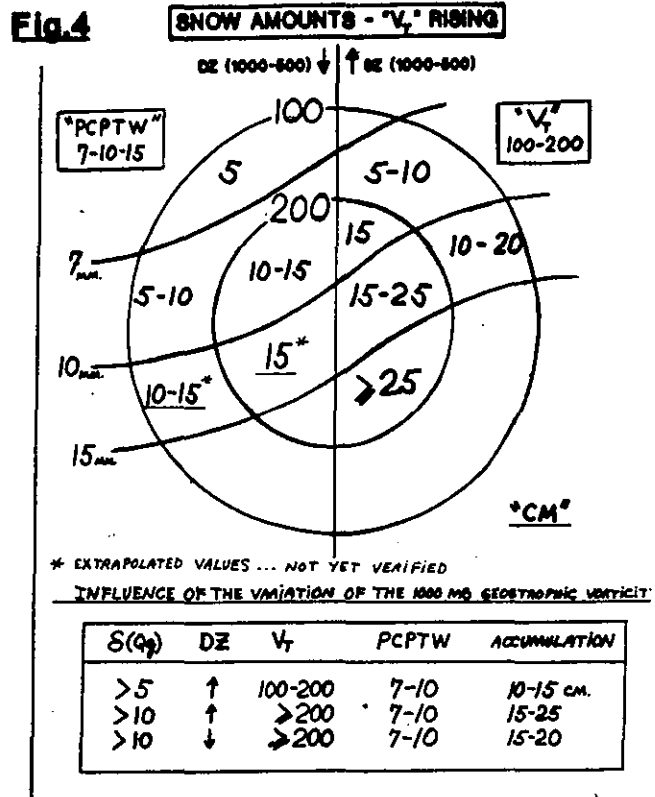
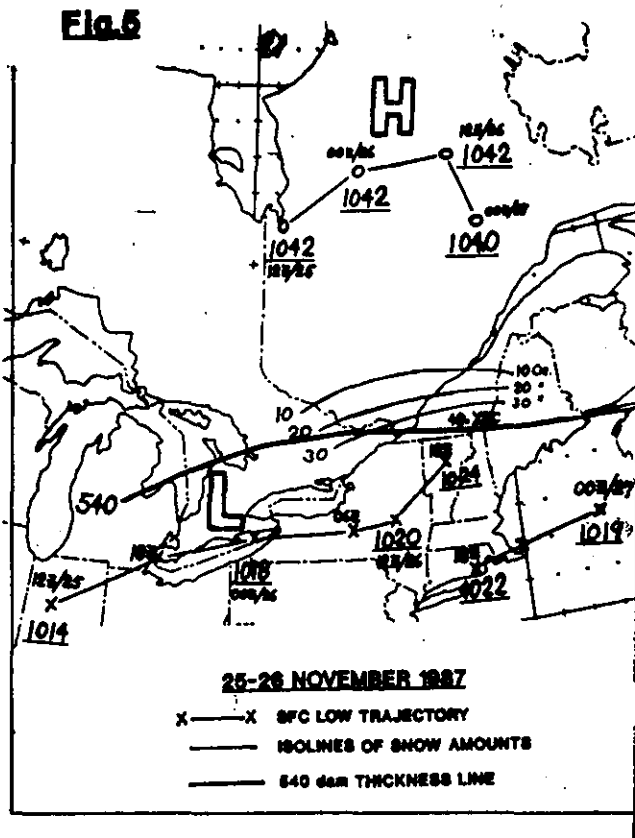


Fig.6

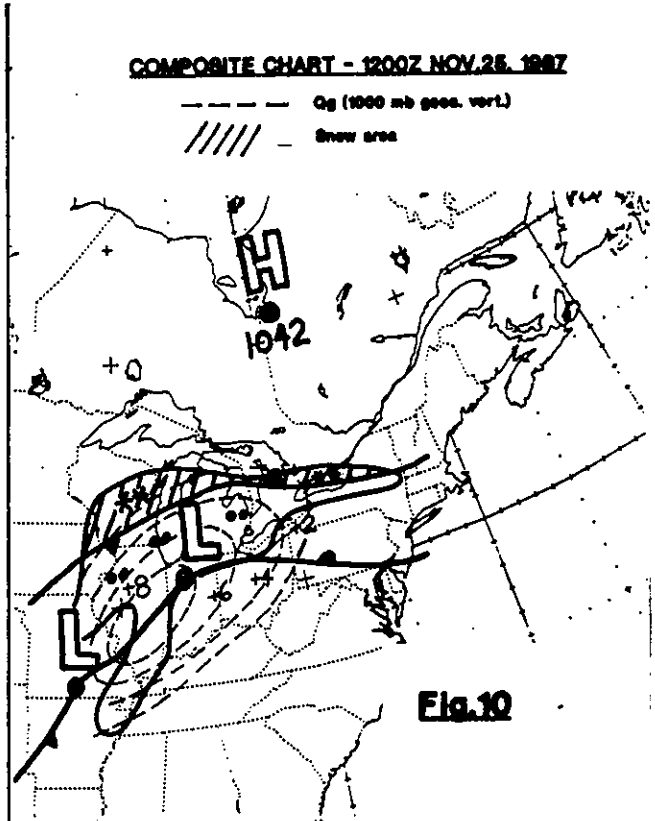
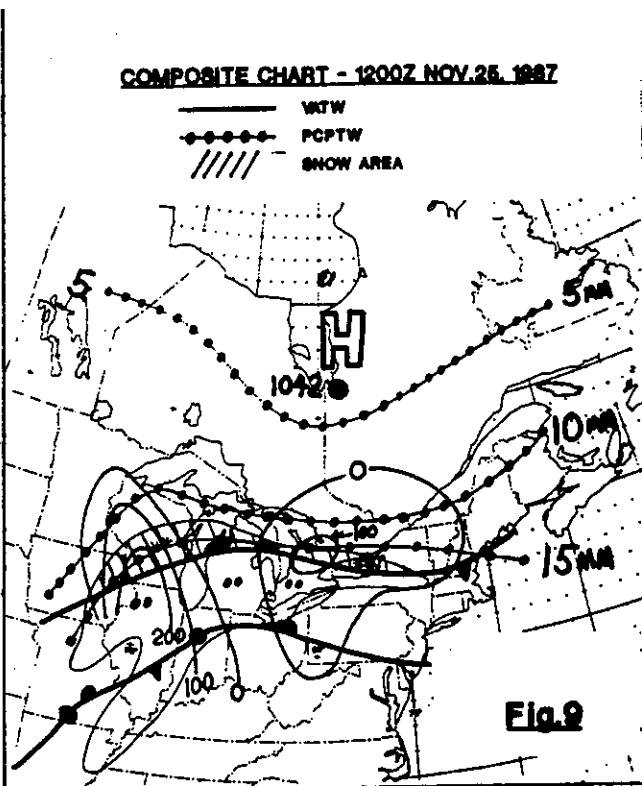
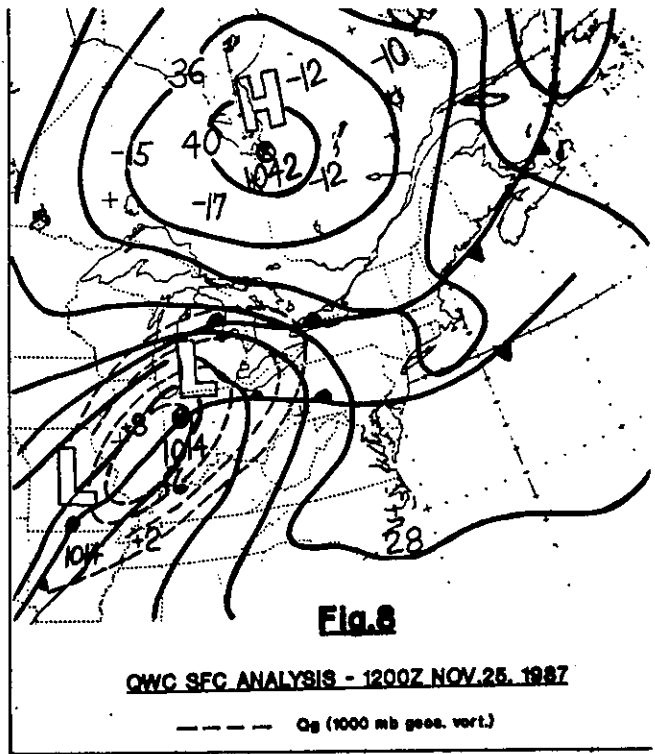
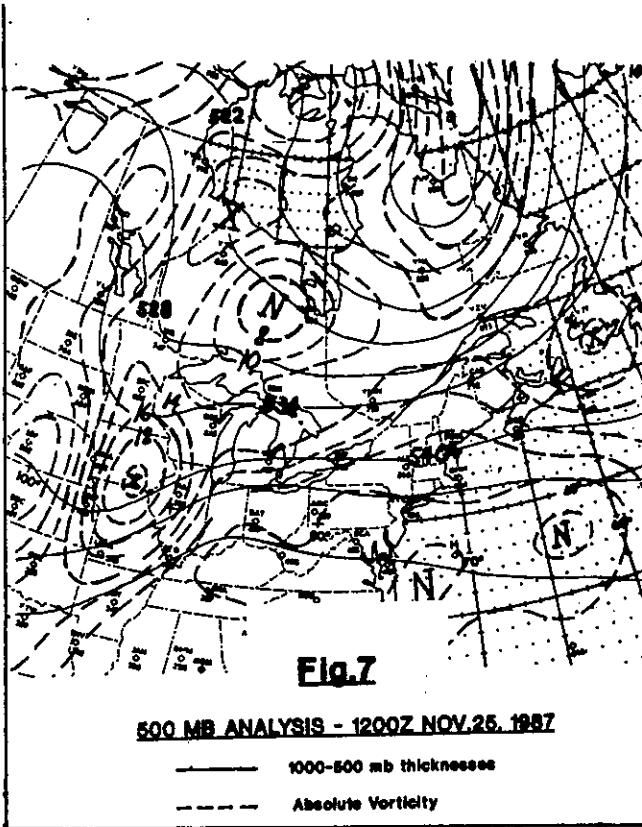


Fig.11

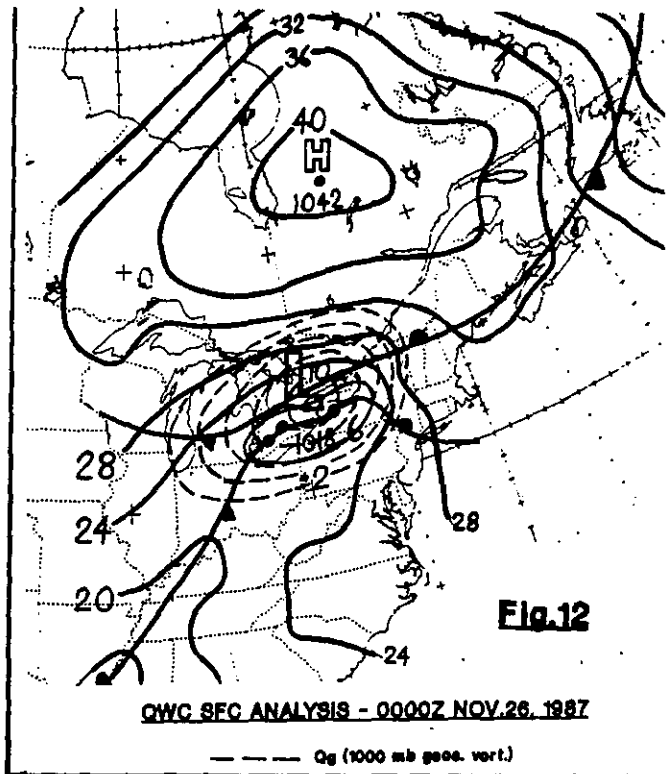
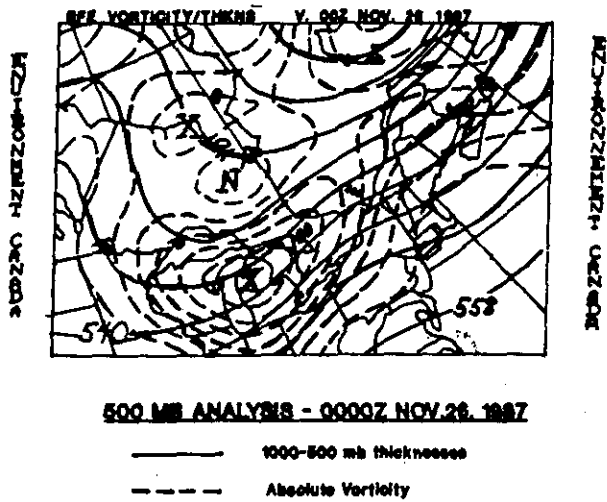


Fig.12

COMPOSITE CHART - 0000Z NOV.26. 1987

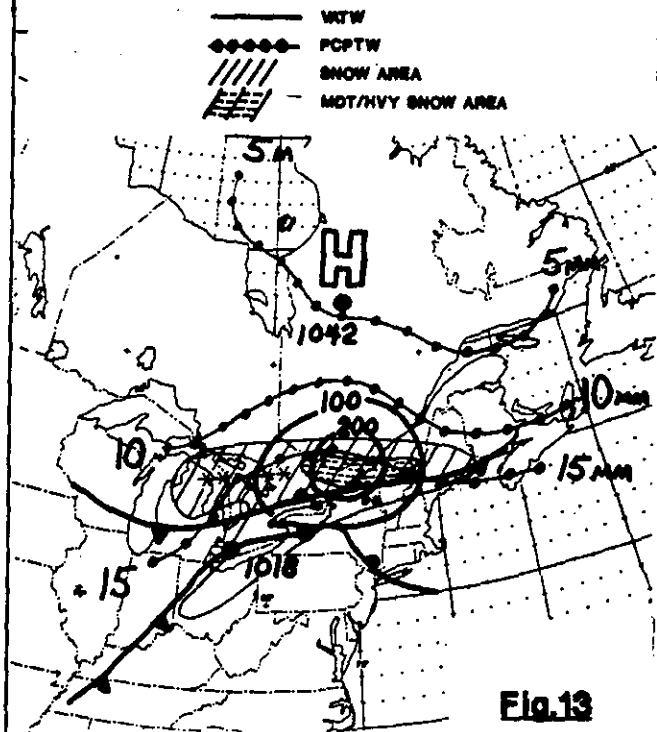


Fig.13

COMPOSITE CHART - 0000Z NOV.26. 1987

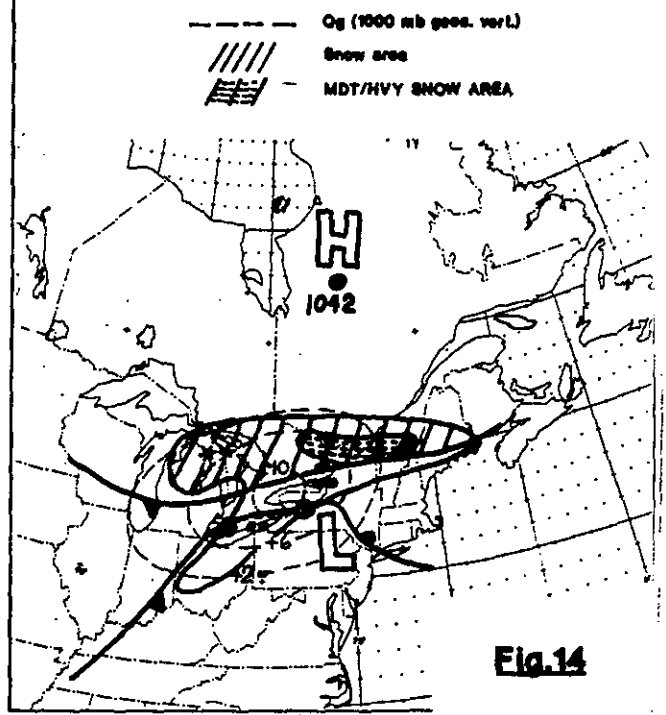


Fig.14

CONCERNING Q-VECTORS

Notes by F. Sanders, 1988.

References

Hoskins, B. J., I. Draghici and H. C. Davies, 1978: A new look at the omega-equation. Quart. J. Roy. Meteor. Soc., 104, 31-38.

Hoskins, B. J. and M. A. Pedder, 1980: The diagnosis of middle latitude synoptic development. Quart. J. Roy. Meteor. Soc., 106, 707-720.

Thorpe, A., 1985: The cold front of 13 January 1983. Weather, 40, 34-42.

Hoskins and Pedder (1980) show that the omega-equation can be written as

$$\sigma \nabla^2 \omega + f^2 \frac{\partial^2 \omega}{\partial p^2} = -2 \frac{R}{P} \left(\frac{P}{P_0} \right)^\kappa \nabla \cdot \underline{Q},$$

where the left-hand side is identical to the familiar one that has been used for a couple of decades, and the right-hand side is exactly equivalent to the familiar expressions involving the vertical derivative of the vorticity advection (leading to the "PVA-rule") and the horizontal Laplacian of temperature advection, (leading to the "warm-advection rule"). (Sigma is static stability.) It's nice and compact. The vertical motion is upward when the Q-vector field is convergent, and, in addition, Q itself is proportional to the low-level ageostrophic wind and proportional but opposite in direction to the high-level ageostrophic wind. The problem comes when we look at what Q is:

$$\underline{Q} \equiv \left[\frac{\partial \underline{V}_g}{\partial x} \cdot \nabla \left(\frac{\partial \Phi}{\partial p} \right), \frac{\partial \underline{V}_g}{\partial y} \cdot \nabla \left[\frac{\partial \Phi}{\partial p} \right] \right],$$

where the expressions separated by a comma on the right-hand side are the components in the x- and y-directions, phi is the geopotential, gz, and

$$\frac{\partial \underline{V}_g}{\partial x} = \frac{\partial u_g}{\partial x} \underline{i} + \frac{\partial v_g}{\partial x} \underline{j}$$

$$\frac{\partial \underline{V}_g}{\partial y} = \frac{\partial u_g}{\partial y} \underline{i} + \frac{\partial v_g}{\partial y} \underline{j},$$

where \underline{i} and \underline{j} are the unit vectors along the x- and y-axes. As it stands, I don't know any way to make sense out of Q by visual inspection of charts. However, as pointed out by Hoskins

and by Thorpe (1985), there is a way of doing it. The trick is to take the x-axis along the isotherms at whatever point you are interested in.

Then

$$\nabla \left(\frac{\partial \Phi}{\partial p} \right) = \frac{\partial}{\partial y} \left(\frac{\partial \Phi}{\partial p} \right) \hat{j}.$$

Using hydrostatics, we can write

$$\frac{\partial}{\partial y} \left(\frac{\partial \Phi}{\partial p} \right) = \frac{R}{p} \nabla \left(-\frac{\partial T}{\partial y} \right),$$

so that

$$\underline{Q} = \frac{R}{p} \left(-\frac{\partial T}{\partial y} \right) \left[\frac{\partial v_g}{\partial x} \hat{i} + \frac{\partial w_g}{\partial y} \hat{j} \right].$$

Now, since geostrophically, with a constant value of f ,

$$\frac{\partial v_g}{\partial y} = -\frac{\partial u_g}{\partial x},$$

and we can write

$$\underline{Q} = \frac{R}{p} \left(-\frac{\partial T}{\partial y} \right) \left[\frac{\partial v_g}{\partial x} \hat{i} - \frac{\partial u_g}{\partial x} \hat{j} \right]$$

or, using a vector identity,

$$\underline{Q} = \frac{R}{p} \left(-\frac{\partial T}{\partial y} \right) \left[\hat{k} \times \frac{\partial \underline{V}_g}{\partial x} \right]$$

where \hat{k} is the unit vertical vector. This says that the \underline{Q} -vector can be obtained by marching along the isotherm with the cold air on your left hand and noting the vector change of the geostrophic wind. Rotate this vector change 90 degrees clockwise and you have the direction of the low-level ageostrophic wind. The magnitude is proportional to the magnitude of the vector rate of change and to the strength of the temperature gradient. Once you have obtained a few judicious estimates of the \underline{Q} -vector field, you can see where the convergent and divergent areas are, and so where the regions of ascent and descent are. Applying this to ideal cases of a string of lows and highs along approximately straight isotherms, a string of cold troughs and warm ridges at upper levels, and to a frontogenetical situation gives familiar answers in each case.

MAJOR ARCTIC OUTBREAKS AFFECTING LOUISIANA

Edward B. Mortimer (1)
National Weather Service Forecast Office
Albuquerque, New Mexico

G. Alan Johnson (2) and Henry W. N. Lau (3)
National Weather Service Forecast Office
Slidell, Louisiana 70458

ABSTRACT

This study was designed to provide the forecaster with guidelines to assist in the subjective evaluation of the onset of arctic outbreaks into the deep south several days in advance. After analyzing the synoptic patterns prior to and during an event, it was determined that several classic signatures existed which set the stage for a major arctic outbreak into Louisiana as well as the remainder of the Gulf Coast States.

It was found that a major arctic outbreak occurred about once every five years. Thus, the forecaster has a responsibility to forecast these rare freeze events several days in advance. These significant arctic outbreaks can produce extensive economic losses to agricultural, commercial and public property. There have been 20 major arctic outbreaks during the past 103 years. Ten of these outbreaks have affected some portion of the state since 1948.

1. INTRODUCTION

The Bayou State of Louisiana is subject to major arctic outbreaks which produce severe freezes. These can produce extensive economic losses to agricultural, commercial and public property. The freezes in the early 1980's destroyed most of the orange groves and some of the tropical trees in southeastern Louisiana while also causing considerable commercial and public losses due to power outages and frozen water pipes.

There have been 20 major arctic outbreaks during the past 103 years. Ten (10) of these outbreaks have affected some portion of the state since 1948. Notable outbreaks since 1948 have occurred during 1949, 1951, 1962 (twice), 1963 (twice), 1982, 1983 (twice) and 1985. Of these dates, 4 freezes (1951, 1962, 1963 and 1983) affected the entire state.

Although the frequency of occurrence is only about once every five years, the forecaster has a responsibility to forecast these freeze events several days in advance in order to allow agricultural interests, utility companies and the public to take necessary precautions to protect the property and prevent potential losses. Pattern recognition is an important tool in helping forecasters determine when conditions exist for a surge of arctic air into the southeastern U. S. This additional tool can help forecasters decide when the potential exists for a southward surge of an arctic air mass.

This study was designed to provide the forecaster with guidelines to assist in the subjective evaluation of the onset of arctic outbreaks into the deep south several days in advance. After evaluating the past 10 major arctic outbreaks, for which upper air data was available, several significant patterns (signatures) were recognized which led to the onset of an arctic outbreaks into Louisiana as well as the Gulf Coastal States.

2. CLIMATOLOGY

A. GENERAL.

Louisiana lies roughly between latitude 29.5N and 33.0N and between the 94th meridian and the Pearl River in the extreme southeast and Mississippi River elsewhere. Elevation across the state increases gradually from the coast northward, with the highest point of only 535 feet in the northwestern section.

The principal influences that determine the climate of Louisiana are its subtropical latitudes and the Gulf of Mexico. The primary air mass affecting the state is Maritime Tropical which develops in the Atlantic high pressure anticyclone. This spreads warm humid air across the state from the Gulf of Mexico for considerable periods of time during the winter season. (This influence is evident from the fact that the average water temperature of the Gulf along its northern shore ranges from 57 to 63 degrees Fahrenheit most of the winter season.) However, for varying periods of time surges of polar and arctic air spread southward from the Canadian provinces (Continental Polar air mass) or from the eastern Pacific (Maritime Polar air mass) (Fig. 1). During this portion of the year, the region experiences extreme minimum temperatures lower than those in any other comparable area of the world (Trewartha, 1961).

The minimum temperatures (in degrees Fahrenheit) across the state normally average in the 30s north to the low and mid 40s south during the winter months of December through February and in the lower 40s north to near 50 south in November. However, average temperatures are somewhat deceptive as minimum temperatures in the lower teens across the north and in the lower 20's across portions of the south are not uncommon for short periods during the winter season.

The record low temperatures for the state range from a (-) 16 degs F at Minden in northwestern Louisiana to 15 degs F at Boothville and 21 degs F at Burrwood, both in the lower reaches of the Mississippi River Delta. Because of its subtropical influence, the record low temperature in Louisiana is the second warmest (to Florida) of the lower 48 states.

B. ARCTIC FREEZE.

An event was defined as a major arctic outbreak when the temperature dropped to or below a critical value at 2 or more stations in 2 or more climatological divisions. These were generally short term events of 1 to 3 days. The severe winter seasons of the late 70's are not included even though the cold air mass remained entrenched over the state for long periods of time. This was the case because the coldest daily temperatures hovered a degree or two above the critical values which were established for this study.

In order to eliminate all but the most severe freeze episodes, a critical minimum temperature was derived for each of the 67 climatological stations across the state (Figs. 2a and 2b).

Using these values with an areal coverage of at least two stations in two or more climatological divisions, 20 arctic outbreaks were identified in Louisiana since 1885. Of these 20, only 8 affected the entire state while the remainder affected various sections of the state (refer to Table 1). (See Section IV for information on "classical signatures" for recognizing in advance a major arctic outbreak for the Gulf Coast States).

Major arctic outbreaks across Louisiana are generally accompanied by some freezing precipitation and/or snow with the initial surge, but only a few events produced heavy snows (see Johnson and Mortimer, 1986). Major arctic outbreaks also appear to occur in cycles, with occurrences in several seasons and a break of 8 to 11 years before the next occurrence. This appears to fit the solar sun spot cycle best with most episodes occurring during the period between a peak and a lull in sunspot activity as presented in Fig. 3.

3. SIGNATURES

A. GENERAL

Pattern recognition can help a forecaster decide when the conditions exist for a surge of arctic air into Louisiana and when to deviate from numerical guidance. Although numerical guidance has improved over the last several years, the guidance is still based on statistical methods which will not identify most rare or extreme events. The best improvement can be made in the short-medium term (2 to 3 days) forecast. Actual minimum temperatures are not necessarily as important as the cold trend indicated in long-range forecasts (3 to 5 days). However, identifying the potential for a severe freeze threat is sufficient so that it can be communicated to the agricultural community as well as to other businesses, public and private interests. This will allow the "users" to take actions commensurate with the assessed freeze potential. For example, a severe freeze threat even at a low confidence level 3 or 4 days in the future could trigger several low-cost actions such as a review of resources and accelerated harvesting. In southern sections of the state, some businesses and residences are vulnerable to major plumbing repairs if an advance warning of an impending severe freeze is not given. As the confidence level of an impending damaging freeze increases, the actions to decrease losses would become more intense, expensive and widespread.

For example, during the winter season of 1984-85, numerical guidance (even medium range) was exceptionally good in identifying a developing synoptic pattern which was to lead to a damaging freeze over the entire state of Louisiana as well as adjacent Gulf Coast States. Some 3 to 4 days of advance warning was given for the mid-January 1985 major arctic outbreak which significantly reduced the economic losses statewide.

B. UPPER AIR PATTERNS

After analyzing the synoptic patterns prior to and during a major arctic outbreak into the continental United States, it was determined that several similarities existed. Since 1948, there have been 10 major freeze events which brought significant economic losses to the Bayou State. Since upper air data were not available prior to November 1948, the data sample was restricted to these 10 events (according to specified criteria by the authors).

Several features were found to be similar to those presented by McFarland (1976) in his study of freezes affecting the Lower Rio Grande Valley of Texas. However, several subtle differences

were found for events affecting Louisiana. McFarland's study utilized only 3 events which had upper air data available (i.e. since 1948). The study for Louisiana utilized 103 years of data for freezes in Louisiana with 10 events occurring since 1948. Six (6) signatures were noted at times during the arctic outbreaks as described in Table 2. However an additional major signature was common to one or more of the 6 classic signatures (patterns). The dominant signature noted for these 10 events was a strong ridge of high pressure over the eastern Pacific or West Coast of North America. Normally, this feature is in response to a deep, cold trough developing in the central Pacific between longitudes 160W and 180W (Figs. 4 through 9).

The following is a scenario of events which may lead to a major arctic outbreak into Louisiana and adjacent Gulf Coast States.

A week to 10 days before a major arctic outbreak occurred in Louisiana, a deep trough would move into or develop in the central Pacific between longitudes 160W and 180W. In response to this development, a strong ridge would build over the eastern Pacific and extend into northern Alaska or the Arctic Ocean. The ridge axis was generally along or just west of 130W in 8 of the 10 events, with a ridge over the West Coast of North America in two events. A short-wave omega block was superimposed on the long wave ridge in several of the events (Fig. 4). The strength of this ridge was influenced by the intensity of the upstream trough. The strength of the ridge also influenced the transitory speed of downstream troughs over North America. The development of this ridge was present in each event and should alert the forecaster to the potential for a surge of colder air.

In tandem with this strong ridge was a cold, deep low pressure trough from Hudson Bay southward across the Central Plains of the U.S. To help anchor this strong ridge-trough couplet over North America, a strong, deep trough was usually present over the central Pacific (Fig. 6 and 9). The development of this rather stable L/W pattern may be attributed to colder than normal waters over the north-central Pacific in the summer and fall seasons forcing warmer waters northward over the extreme eastern Pacific as described by Namias (1978). Variations of this main synoptic pattern were identified and described as classic signatures in Table 2.

Over North America, there were several mechanisms present which eventually caused an arctic air mass to surge southward. The authors identified 6 additional, though sometimes subtle, upper air signatures conducive to surges of major arctic outbreaks into portions of Louisiana. The beginning signature did not persist throughout the entire event, but would evolve into one or more of the other features, except that an upper level ridge was dominant in all cases.

Seven (7) events were associated with a closed low near Hudson Bay (Figs. 4, 5 and 7). In 3 events, a trough extended east to west across southern Canada or into the northwestern U.S. The trough would remain nearly stationary for several days with a strong northerly flow across Canada and a strong zonal flow south of the trough (Fig. 6). This allowed the cold dome of arctic air to intensify over Canada. The west portion of the trough would then rotate southeastward into the central plains, in response to a series of S/W troughs. This allowed the arctic air to surge southward. There were 3 events with a northeast-southwest trough from the Hudson Bay low which moved eastward to establish a long-wave trough over the central states by the end of the event (Fig. 5). There was one event, 1985, in which the L/W trough was established over the eastern states (Fig. 8).

Three (3) outbreaks were associated with a S/W moving eastward through the southern portion of the ridge into the southwestern states while the northern branch was across southern Canada or the northern tier states (Fig. 7). A split flow pattern was normally located over western North America. These short-waves became in phase with a stationary or slow moving long wave trough and accelerated the southern portion of the trough into the central or eastern states. Cyclogenesis occurred when a strong S/W trough ejected east or northeast from the L/W trough. This usually resulted in discontinuous retrogression of the L/W trough over the western states (Fig. 9).

Three (3) events were associated with a cold, deep low in the Canadian Prairie Provinces with a S/W trough extending into the Pacific Northwest. This trough rotated southeastward into the Central Plains and developed into a full-latitude trough which progressed eastward into the eastern states (Figs. 6 and 8).

Discontinuous retrogression occurred in over half of the events. This occurred when a S/W was ejected east or northeast from the L/W trough as a second S/W approached from the northwest. This would give the L/W trough the appearance of first moving eastward then redeveloping westward with the upstream S/W (Fig. 9).

C. SURFACE PATTERNS

A high pressure system intensified from the Yukon Territories southeastward into central and western Canada under the influence of a strong building upper level ridge and a deep, cold low or trough normally located in the Hudson Bay area. As strong S/W troughs surged south or southeast towards the U.S. the Arctic High would move southeast into the northern Rockies and Plain States. On a few occasions the pressure would reach 1050 mb or higher from the Yukon to the northern Rockies (Fig. 10).

For the arctic air to spread southward to Louisiana and the western Gulf Coast States, the arctic surface high would have to move or build south into eastern Texas. If the high moved east or southeast through the mid-Mississippi Valley or into Mississippi/Alabama the coldest air would be shunted more eastward.

An important factor for the development of record-breaking low temperatures in mid-winter was an extensive blanket of snow from the Plains States north and northwest through Canada. By mid-winter the frigid arctic air and the fronts combined to form snow rather than rain from the northern and central Rockies eastward to the East Coast. While amounts were usually not heavy, snow persisted on the ground owing to persistent cold air outbreaks far to the south along the Gulf Coast. This often would lead to snow far south of normal. The snow cover in turn helped to refrigerate the arctic air in its southward transit, partly through an increased albedo. The cover remained on the ground and was maintained by the frequent arctic air surges and replenished by storms moving along the south and eastern seaboard as discussed by Namias (1978). A recent example of this phenomena was in December 1983 when 2 record-breaking events clobbered the Bayou State within a one week period. During this event economic losses were widespread statewide but more devastating over southern Louisiana. An extensive snow cover was normally as far south as extreme northern Texas, Arkansas, northern Mississippi during record-breaking arctic outbreaks in Louisiana (Fig. 10).

4. ADDITIONAL FORECAST GUIDELINES

- 1) Follow 24-hour 500 mb high fall/rise couplets. Superimpose on 500 mb map to correlate with deepening troughs or amplifying ridges.
- 2) Check pressure of surface high (generally 1050 mb or higher) and temperature of air mass (generally [-] 20 degs F or colder) in western/central Canada (mainly inland areas away from marine influence).
- 3) Thickness patterns can be deceiving when examining arctic air masses.
- 4) Also note extent of snow cover from Canada southward into U.S.
- 5) Cross-sections can be used to depict the major arctic air from the polar type air.
- 6) Major arctic outbreaks are usually associated with two or more synoptic patterns (signatures) over a period of several days to a week or more.

7) The majority of the events were associated with signatures 2 and 3 in addition to the major signature which was common to all events (strong ridge).

8) If the southern branch of the westerlies becomes a dominant pattern for the Gulf Coast States, the coldest air mass will be shunted eastward away from Louisiana or overrunning conditions will develop. This was the case back during the winter of 1979. This particular winter season was one of the coldest on record in many areas of Louisiana. However, for the reasons discussed above the critical temperatures for a major arctic outbreak were not reached.

5. CONCLUSIONS

This study was designed to provide the forecaster with guidelines to assist in the subjective evaluation of the onset of arctic outbreaks into the deep south several days in advance. After analyzing the synoptic patterns prior to and during an event, it was determined that several classic signatures existed which set the stage for a major arctic outbreak into Louisiana as well as the remainder of the Gulf Coast States.

It was found that a major arctic outbreak occurred about once every 5 years. Thus, the forecaster has a responsibility to forecast these rare freeze events several days in advance. This allows the agricultural business interests, utility companies and other interests to take the necessary precautions to reduce their potential losses. Even though numerical guidance has improved over the last several years, the forecaster must recognize those situations which will lead to the intrusion of arctic air into the state. With the timely recognition of these classic signatures, the forecaster should be able to greatly curtail the economic losses in the state.

NOTES AND REFERENCES

1. Johnson, G.A. and Mortimer, Edward (1986): Synoptic Climatology for Heavy Snowfall across Louisiana. 11th Conf. Weather Forecasting and Analysis, pp 99-105.
2. McFarland, Marshall J. (1976): Useful Relationships between 500 MB Features and Major Freeze Events in the Lower Rio Grande Valley of Texas. NOAA TECH. MEMO NWS SR-88.
3. Mississippi River Commission, Lower Mississippi Comprehensive Study, Appendix C, Vol. I, Regional Climatology, Hydrology and Geology, Vicksburg, 1974, pp 1-95.
4. Namias, Jerome (1978): Multiple Causes of the North American Abnormal Winter 1976-77. Mthly Wx Review, Vol. 106, No. 3, Mar 1978.
5. Trewartha, G.T. (1961): The Earths Problem Climates. University of Wisconsin Press, Madison, Ws.

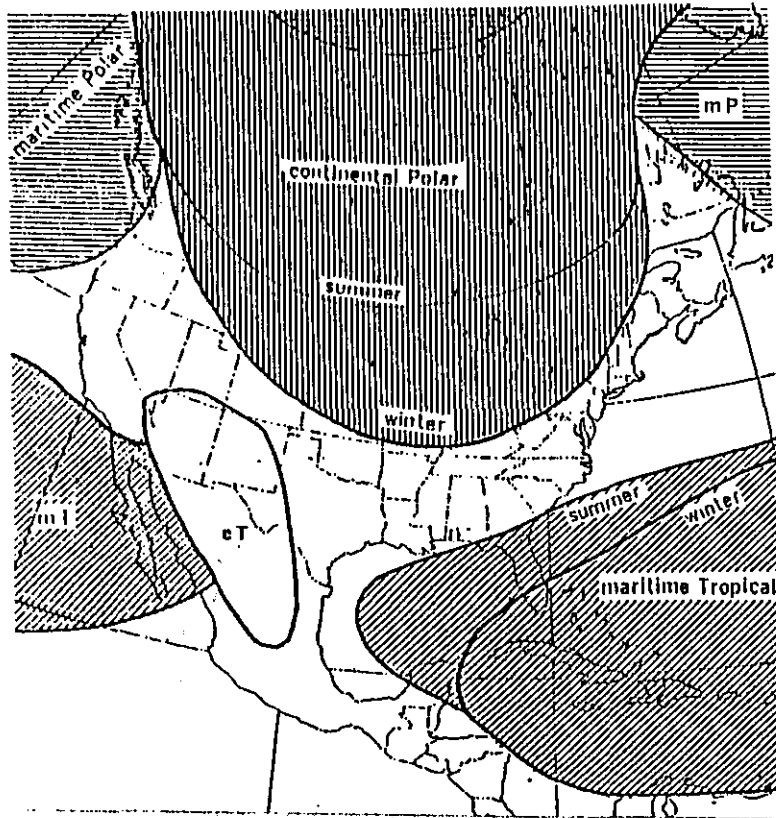


Fig. 1. Air mass locations across North America.

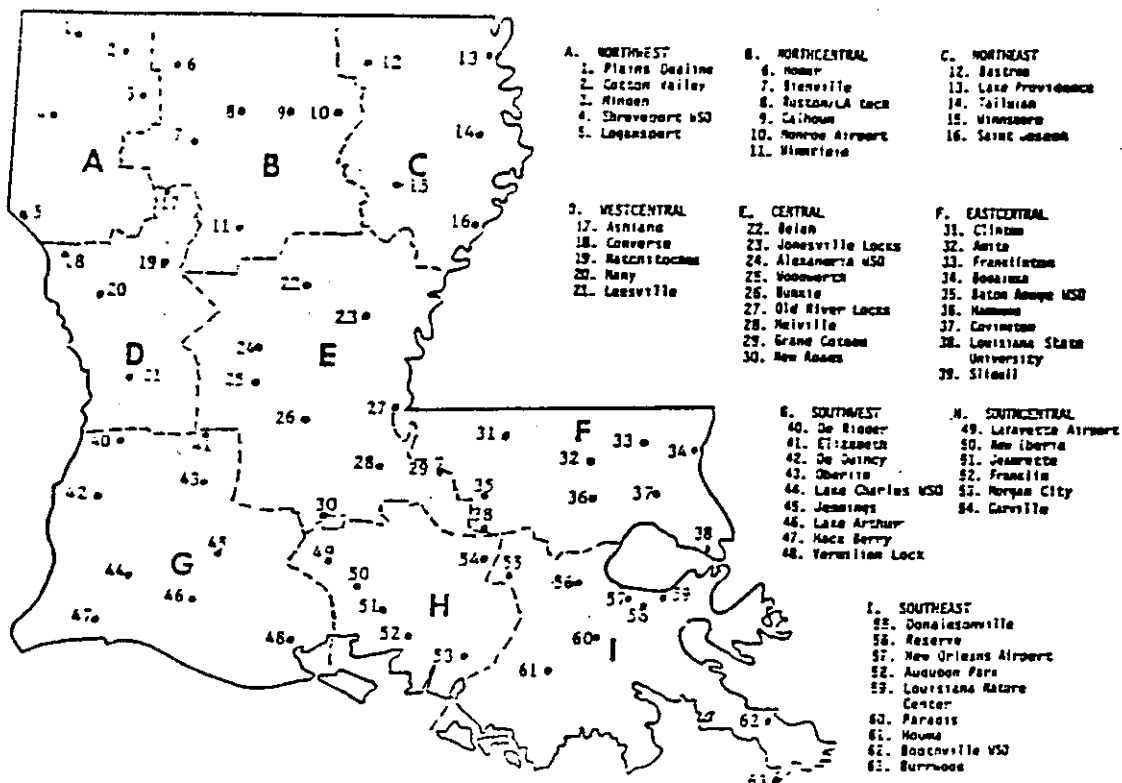


Fig. 2a. List of cities and climatic divisions for Louisiana used in the climatological data.

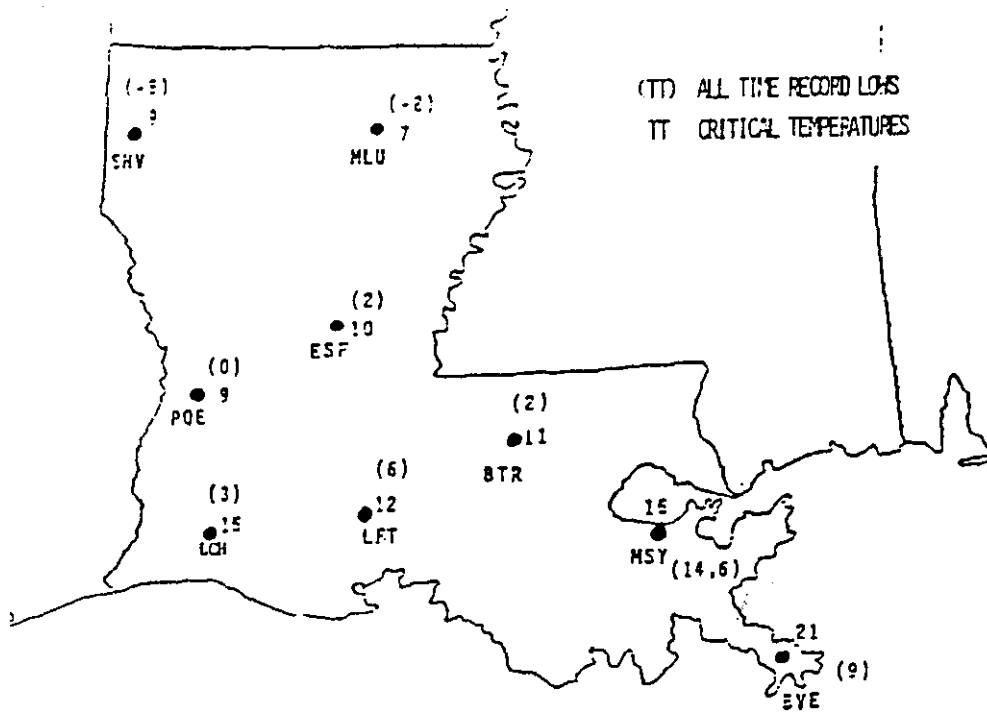


Fig. 2b. Critical temperatures for major arctic outbreaks affecting Louisiana and all time record low temperatures in Louisiana.

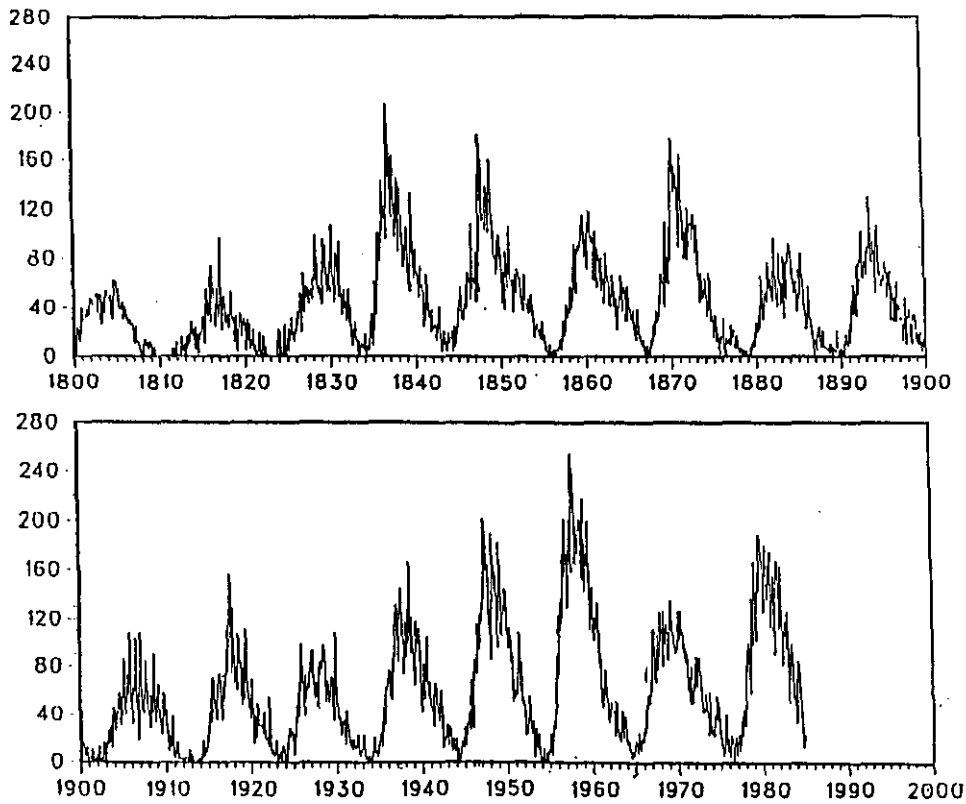


Fig. 3. MONTHLY MEAN SUNSPOT NUMBERS January 1800 - December 1985. Monthly mean numbers reveal the sunspot count's variability. The largest monthly mean (253.8) occurred in October 1957.

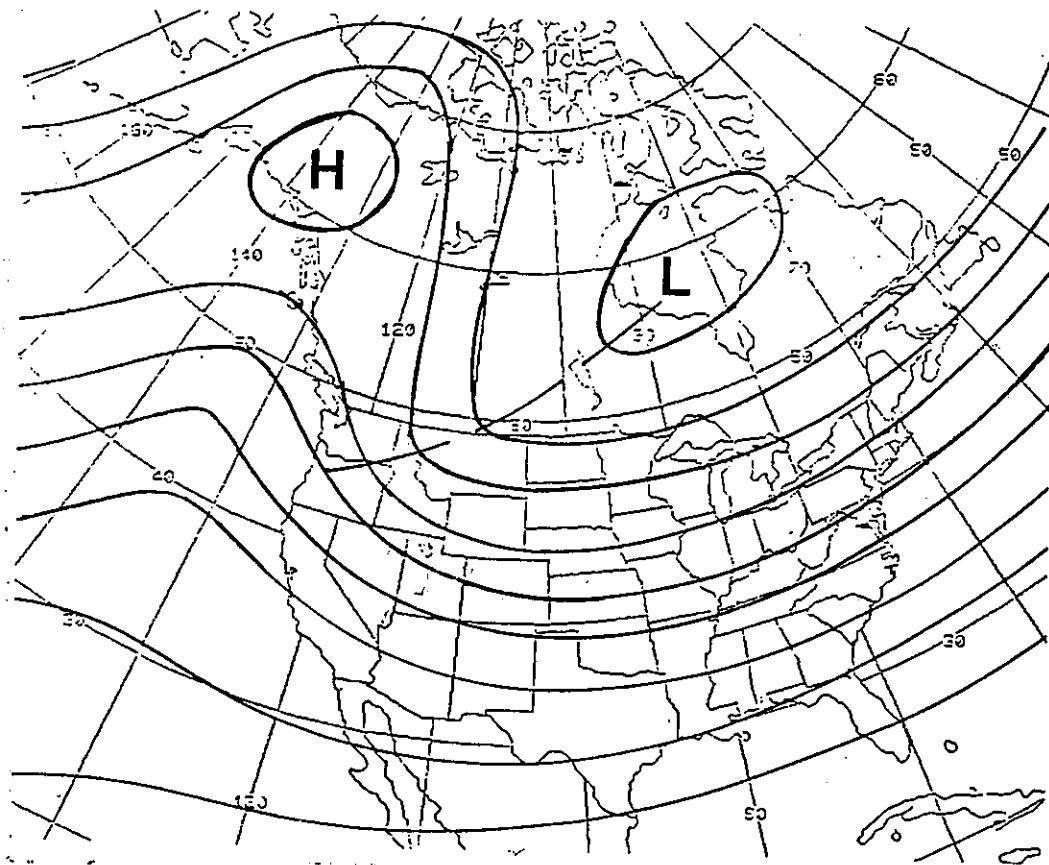


Fig. 4. Low near Hudson Bay with a trough extending west of southwest into southwest Canada or the Pacific Northwest. A series of short-wave (S/W) troughs would cause this trough to surge southward without cyclogenesis.

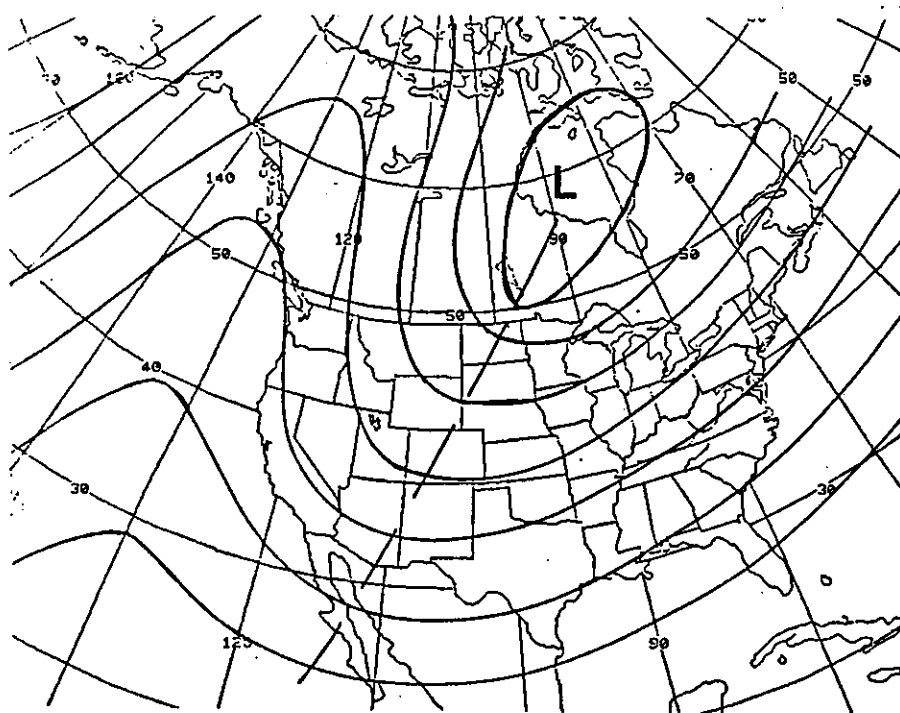


Fig. 5. Low near Hudson Bay with a trough extending into the southwestern U. S., which progresses eastward into the central Plains as a full latitude trough.

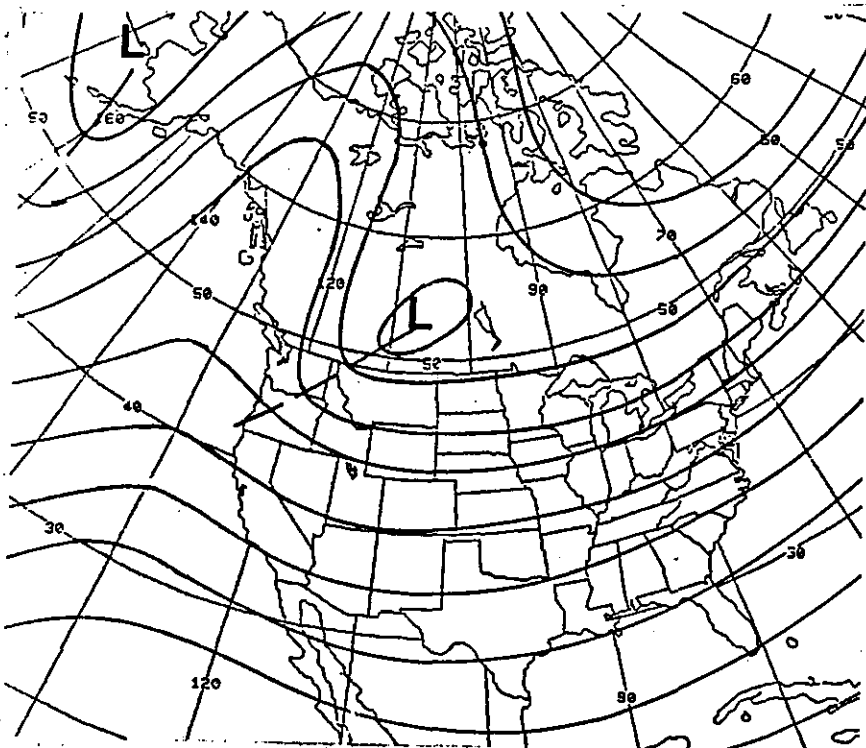


Fig. 6. A closed low moving southward through the prairie provinces of Canada, which develops into a long-wave (L/W) trough without cyclogenesis.

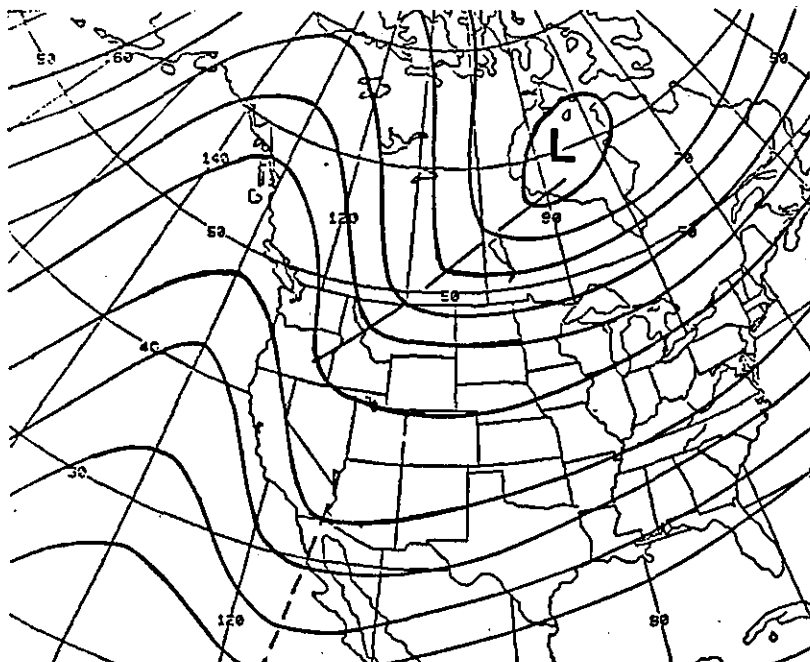


Fig. 7. A S/W trough in the southern branch of the westerlies moves eastward into the southwestern states. In the meantime another S/W trough in the branch of the westerlies moves eastward which frequently becomes inphase with the L/W trough. This pattern is quite typical of a split-flow in western North America.

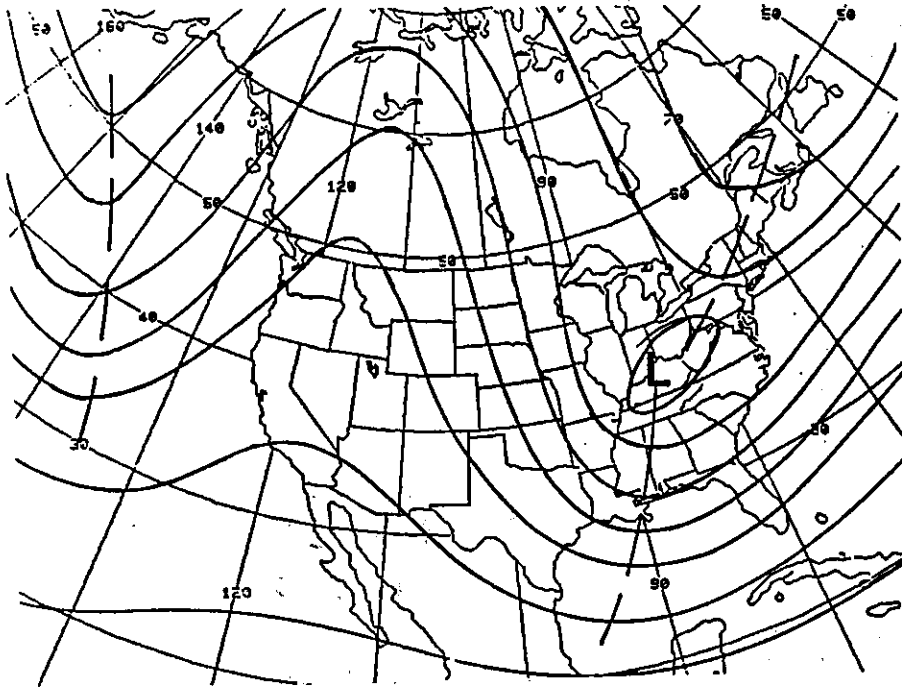


Fig. 8. A deep trough was over the eastern U. S., sometimes accompanied by a closed low.

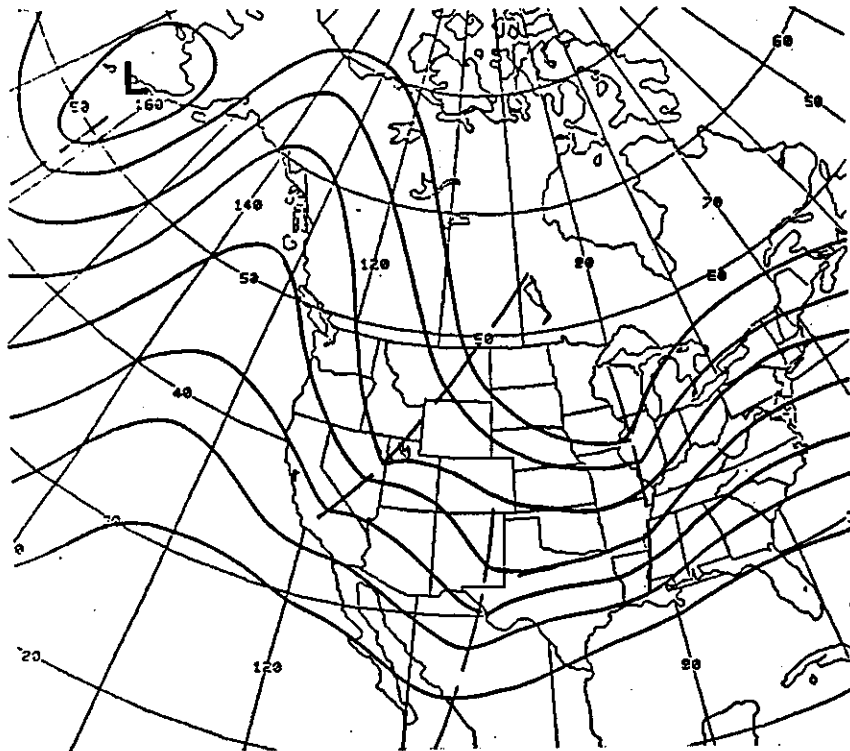


Fig. 9. Discontinuous retrogression of trough over the western U. S.

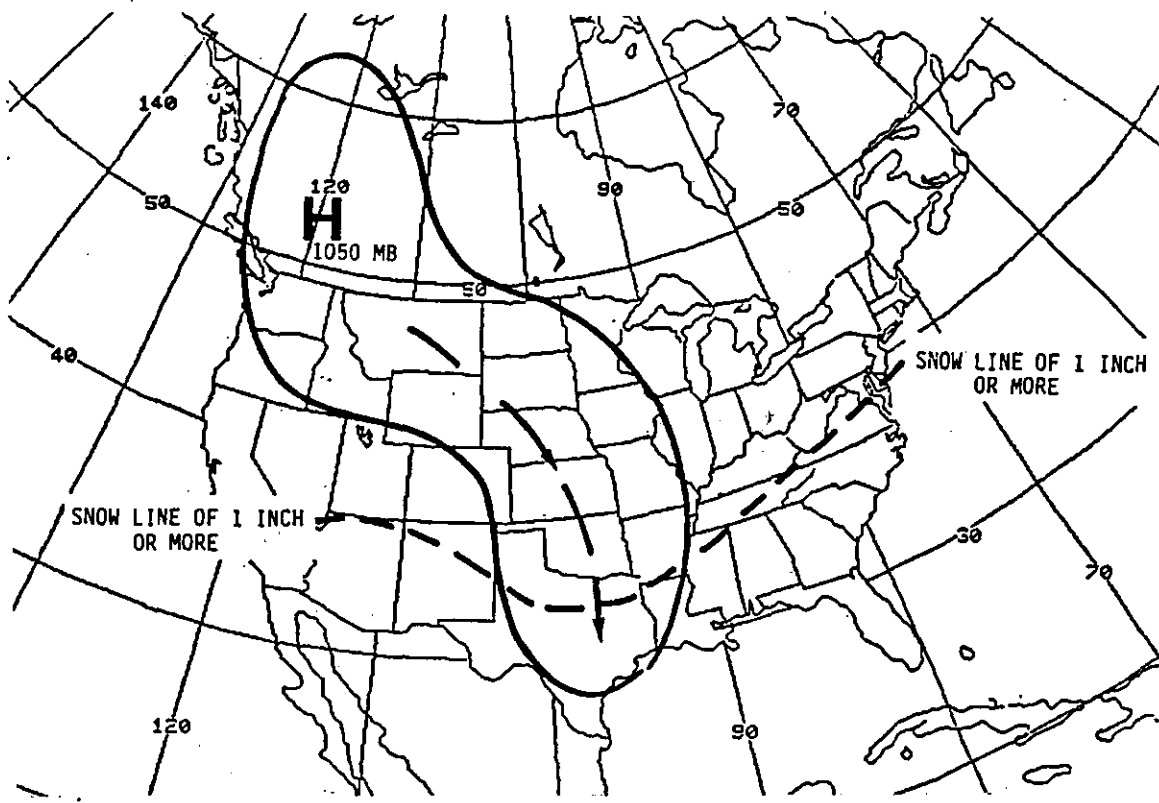


Fig. 10. Mean surface ridge across North America during major arctic outbreaks along with an average snow cover.

Table 1. List of arctic outbreaks affecting Louisiana during the past 103 years and portions of the state affected.

Date	Area	Climate Regions
1-9-1886	entire state	
2-8-1895	entire state	
2-13-1899	entire state	
2-13/14-1905	north	nw-nc-wc
1-12-1918	entire state	
12-23 1929	north & west	nw-wc-sw-ne
1-18/19-1930	north & west	nw-nc-wc-sw
1-17 to 19-1940	north & southwest	nw-nc-ne-wc-sw
1-27-1940	northeast thru east central	ne-c-ec-se
1-18 to 24-1948	all except southeast	nc-ne-wc-c-sw-ec
1-31/2-1-1949	northwest	nw-nc-wc
2-1/2-1951	entire state	
1-11/12-1962	entire state	
12 12/13 1962	East half	ne-c-ec-sc-se
1-24/25 1963	north & southeast	nw-nc-ne-c-ec-se
12 23/24 1963	extreme north	nw-nc-ne
1-9 to 13 1982	entire state	
12-24/25 1983	entire state	
12-30/31-1983	west and north	nw-nc-ne-wc-sw
1 17 to 22 1983	northeast & southeast	

Table 2. Classic signatures associated with arctic outbreaks into Louisiana

- 1) Low near Hudson Bay with a trough extending west or southwest into southwest Canada or the Pacific Northwest (Fig. 4). A series of short-wave (S/W) troughs would cause this trough to surge southward without cyclogenesis.
- 2) Low near Hudson Bay with a trough extending into the southwestern U. S. (Fig. 5), which progresses eastward into the Central Plains as a full latitude trough.
- 3) A closed low moving southward through the prairie provinces of Canada (Fig. 6), which develops into a long-wave (L/W) trough without cyclogenesis.
- 4) A S/W trough in the southern branch of the westerlies moves eastward into the southwestern states. In the meantime another S/W in the northern branch of the westerlies moves eastward which frequently becomes in-phase with the L/W trough (Fig. 7). Occasionally, a closed low was noted in the southern branch. This pattern is quite typical of a split flow in western North America.
- 5) A deep trough was over the eastern U. S., sometimes accompanied by a closed low (Fig. 8).
- 6) Discontinuous retrogression of trough over the western U. S. (Fig. 9).

THE WINTER STORM OF JANUARY 6 and 7, 1988

by Frank Makosky and John G. Hoffner
National Weather Service Forecast Office
Birmingham, Alabama

A major winter storm moved across Alabama beginning the night of January 6 and continuing into the afternoon of January 7. Although the track of the storm center was across the Northern Gulf, up to 11 inches of snow fell across the Tennessee Valley (see figure 1). A total of 11 inches was reported in Bridgeport, in the northeast corner of the state, and 10 inches fell at the Huntsville/Decatur airport. Across Central Alabama, the problem was freezing rain and sleet. Between 1 and 2 inches water equivalent precipitation fell in these areas before diminishing during the afternoon of the 7th. In South Alabama, where it was above freezing during the night, evaporative cooling lowered the temperature and caused some icing problems from freezing rain during the day on the 7th.

Serious icing conditions in the Birmingham area caused major traffic problems and closed down the interstate system as well as causing widespread power outages. Across North Alabama, around 15 million dollars damage occurred to the state's poultry industry. Not only due to the cold temperatures, but also from collapsing chicken house roofs due to the weight of the ice and snow.

After the precipitation ended, temperatures for the next several days did not rise above freezing over North Alabama hindering clean up operations. In some locations, snow remained on the ground for nearly a week.

The guidance and the interpretation of the guidance by the local forecast staff was excellent for this event. Snow was mentioned as a possibility for north Alabama in the extended forecast five days before the event. A Winter Storm Watch was issued for North Alabama on Tuesday, January 5, thirty-six hours before the storm struck, and each forecast was progressively fine-tuned until the precipitation began falling late Wednesday night January 6. Also, special weather statements, radio interviews and NOAA weather radio updates issued by the Weather Service Staffs of the affected areas were excellent throughout the storm.

Since all of the guidance was excellent leading up to the the winter storm, the forecast was dependent only on interpreting how the expected parameters would affect snow, sleet or ice accumulations. This write-up will not attempt to describe the guidance since the LFM, NGM and MRF were consistent and the forecasts were based on the models established twenty years ago by Younkin and others.

We will present one map that typified the excellent guidance referred to above. Figure 2 shows the twenty-four hour surface and thickness progs that verified at 6AM CST Thursday, January 7. This time was about mid way through the worst of the storm. It

shows a pattern that forecasters in the southeast recognize as a producer of winter weather in the Deep South. A strong arctic high (1040mb) was expected to be near Washington D.C., a polar boundary was shown along the Gulf Coast, and there was a suggestion of a surface low forming in South Texas.

The thickness forecast was used to delineate, with some other considerations such as upper air soundings and expected wet bulb temperatures, the area where frozen precipitation was expected. The 5460 meter thickness was used to outline the watch area and all snow was predicted in the Tennessee Valley where the thickness was near 5400 meters.

The verification map (figure 3) shows that snow was being reported across Northern Alabama with temperatures in the 20s. Across Mississippi, freezing rain was occurring at Jackson and Meridian, while snow was falling at Tupelo. Thus, the twenty four hour thickness forecast provided a good objective guess as to precipitation type.

Figure 3 shows a weak stable wave of approximately 1014 mb off the southeast Texas coast. This map is typical of a budding winter storm. A stable wave nearly always develops in this location. The strong contrast between cold air over land and the warm Gulf water temperatures, plus the shape of the coastline, makes this a natural baroclinic zone. Notice that the computer guidance (figure 2) erred in locating the low pressure center over South Texas. The guidance will often err by not showing the low over the Gulf.

After the stable wave in the Gulf forms, it will usually remain stationary, or a series of minor waves will move along the front and dissipate as each moves east of the influence of the primary upper level trough. Although data is sparse in the Gulf, it appears that this sequence of maps (figures 3 through 6) shows that this forming and dissipation of waves was occurring along the polar boundary. As the primary upper level trough digs southeastward, the stable wave will often deepen, and when the upper trough reaches a position approximately five degrees upstream, the frontal wave will move east and north and will usually continue to deepen. Notice the change from figure 6 to figure 7. Although there was no sign of intensification, the low pressure center had definitely moved eastward in response to the approach of the upper level trough.

The series of surface maps shows important local effects that had considerable impact on temperatures and accumulations of snow, sleet and ice. Notice on figure 3, the inverted trough that extended from the Gulf low through Mississippi and northward. Two factors produced the inverted trough. First, the approach of the upper level trough was being reflected or induced at the surface. Second, there was the effect of the terrain. The cold arctic air associated with the high pressure ridge was being dammed east of the Appalachian ridge. The east and southeast low level flow across the mountain ridge produced a lee side trough in Western Alabama. This is more noticeable in figures 4 through 6. Apparently, the adiabatic downslope warming was just enough to raise the temperature to above freezing in Central Alabama from Birmingham westward. In fact, ice accumulations were considerably greater in eastern

sections of the city then in the western sections. Notice the location of the surface freezing line in figures 4 through 6.

This example showing the damming of cold air in Georgia and extreme east and southeast Alabama, and the lee side trough in western Alabama is a typical reaction to this type of synoptic pattern. It usually occurs several times during the winter. As a matter of fact, the only area of the state that was not perfectly forecast was a small area of southeast Alabama near Auburn where ice accumulated south of the watch/warning area. Forecasters did not fully consider the wedging of modified arctic air into this area of the state.

By 6pm Thursday January 7, (figure 7), the surface low had moved into the Eastern Gulf. Except for some drizzle and snow flurries, the precipitation over Alabama had ended. Notice that the inverted trough with the associated warm tongue persisted. This feature continued until the surface low moved to near the Virginia coast the next day. At this time, the low level winds over Alabama shifted to the north and northwest. This is an important consideration for temperature forecasting because, as long as the lee side trough persists, so will the warm tongue.

Let's take a look at the value of interpreting upper level soundings before and during the storm. As previously mentioned, forecast thickness values over Alabama suggested some type of frozen precipitation from the northern border to at least central Alabama. The forecasters were better able to discriminate precipitation type by analyzing soundings. The ones shown in this write-up are those taken by WSMO Centreville, but soundings taken by Jackson, Little Rock and Nashville were also examined. WSMO Centreville also provided intermediate soundings at 18Z January 6, and 06Z January 7. These were immensely helpful.

Figure 8 shows the 18Z January 6, sounding. It was obvious that at this point, the atmosphere was below freezing except for a shallow layer near the surface. If precipitation were imminent, "snow" would have been the forecast for the latitudes near Centreville. However, the upstream sounding at Jackson (not shown) revealed a nose of above freezing temperatures from 750 mb to 900 mb. Winds at this level were south-southwest at 20 to 30 knots. This suggested some warming would take place near 850 mb at Centreville in the next 6 to 12 hours. This information was critical to forecasters since temperatures must be below freezing from near the surface to about 5000 feet for precipitation to be in the form of pure snow.

Figure 9 (00Z January 7) does indeed show that a small nose of above freezing temperatures had formed near 850 mb. Winds aloft at this level were light from the south suggesting some further warming was possible. Now forecasters were thinking more in terms of a mixture of snow, sleet and freezing rain for central Alabama. Other soundings continued to indicate all snow for the Tennessee Valley. These soundings were taken about six hours before the precipitation began at Birmingham. Wet bulb temperatures were near freezing at 850 mb but below freezing at all other levels.

Figure 10 (06Z January 7) shows that the warm bulge had become more pronounced. Above freezing temperatures existed from 900 mb to 700 mb. Winds aloft were

moderate to strong from the south and southwest. Hence continued warming was expected above 900 mb. Low level winds continued from the east and northeast. The wet bulb curve showed that, at least initially, below freezing temperatures could be expected below 5000 feet. Therefore, the precipitation (that was about to start at Birmingham) should begin as snow.

By 12Z January 7, figure 11 shows that the warm nose was most pronounced near 850 mb. Above freezing temperatures continued from 900 mb to 700 mb. Winds aloft above 2000 feet were mostly from the south between 40 and 50 knots in this layer. Again, some continued warming was expected until the upper trough passed. Near the surface the winds continued from the east and northeast, indicating neutral or cold advection. Freezing rain and sleet were occurring in the Birmingham area at this time, but shortly after this, the precipitation changed to rain as Birmingham's temperature rose to 33°F. The sounding showed a cold bulge at around 1000 feet above the ground. Temperatures just above the surface must have continued below freezing throughout the day because ice accumulations at higher elevations and in the trees around Birmingham were heavier.

This was a very interesting winter storm that seemed to behave in a manner that allowed forecasters sufficient time to absorb changes in parameters and to apply tested forecasting techniques.

Also, the results of this study have led to the following conclusions:

1. Winter storms while moving through the Gulf do not fit the Younkin models. The heaviest snow is more apt to be about 400 miles instead of 150 miles north or left of the storm track.
2. Model guidance that positions a surface low away from the favored baroclinic zone on the Gulf should be viewed as suspect.
3. A Gulf storm in the winter often begins with a stable wave forming on an old polar boundary in the western Gulf. Impulses may move along this boundary toward the coast, but the main event does not occur until an upper level trough moves into the Texas area and kicks the storm east or northeast.
4. Cold air damming east and adiabatic downslope warming west of the Appalachian spine have subtle effects on temperatures and resulting precipitation type.
5. An upstream sounding is an invaluable tool for fine-tuning a winter forecast. With a little practice, temperatures, dew points and wet bulbs can be accurately estimated for the critical lowest 5000 feet of the forecast location for 6 to 12 hours. Also, greater accuracy can be obtained if intermediate soundings are requested from observing sites.

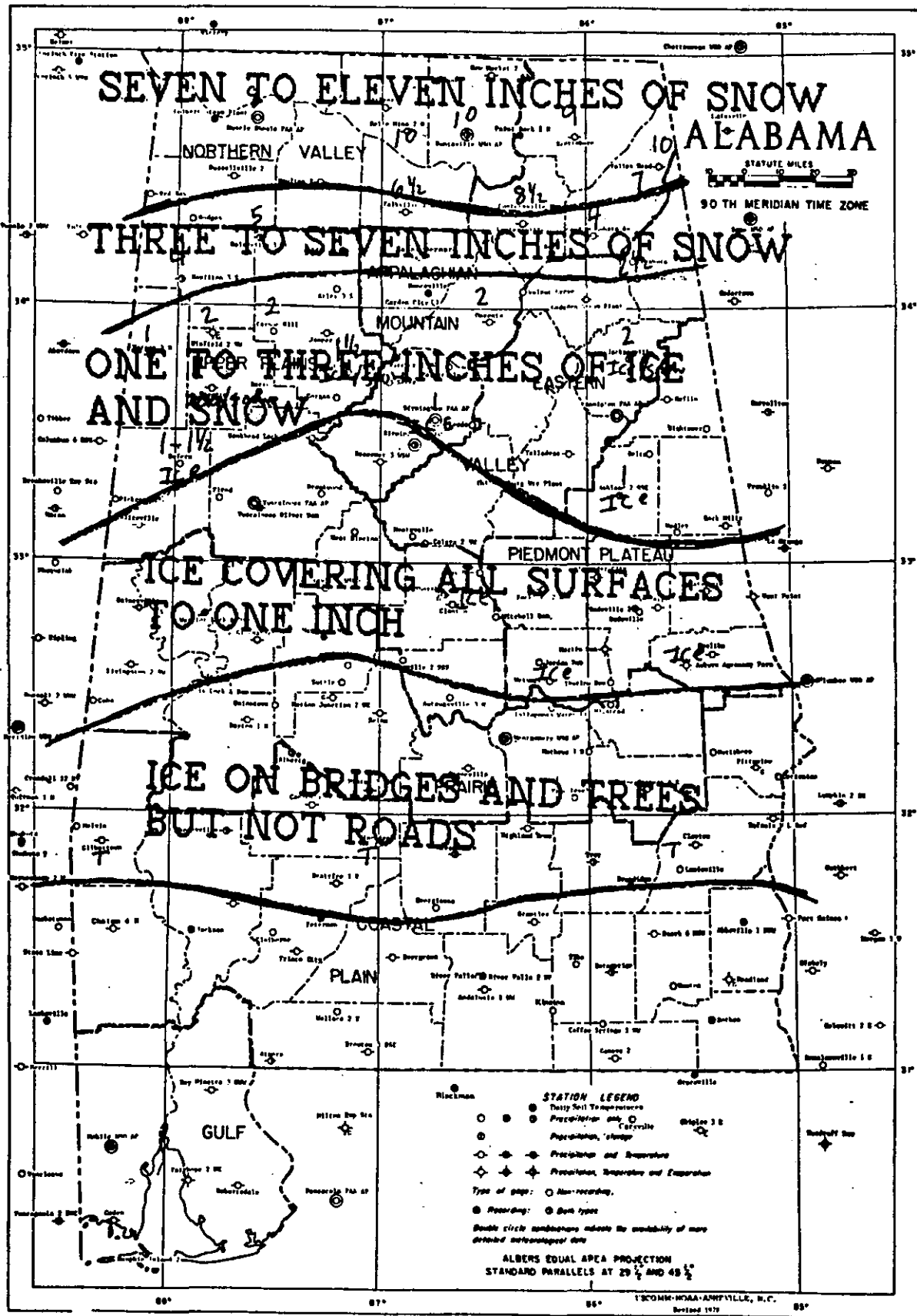


FIGURE 1 TOTAL SNOW FALL ACCUMULATIONS JANUARY 6-7 1988

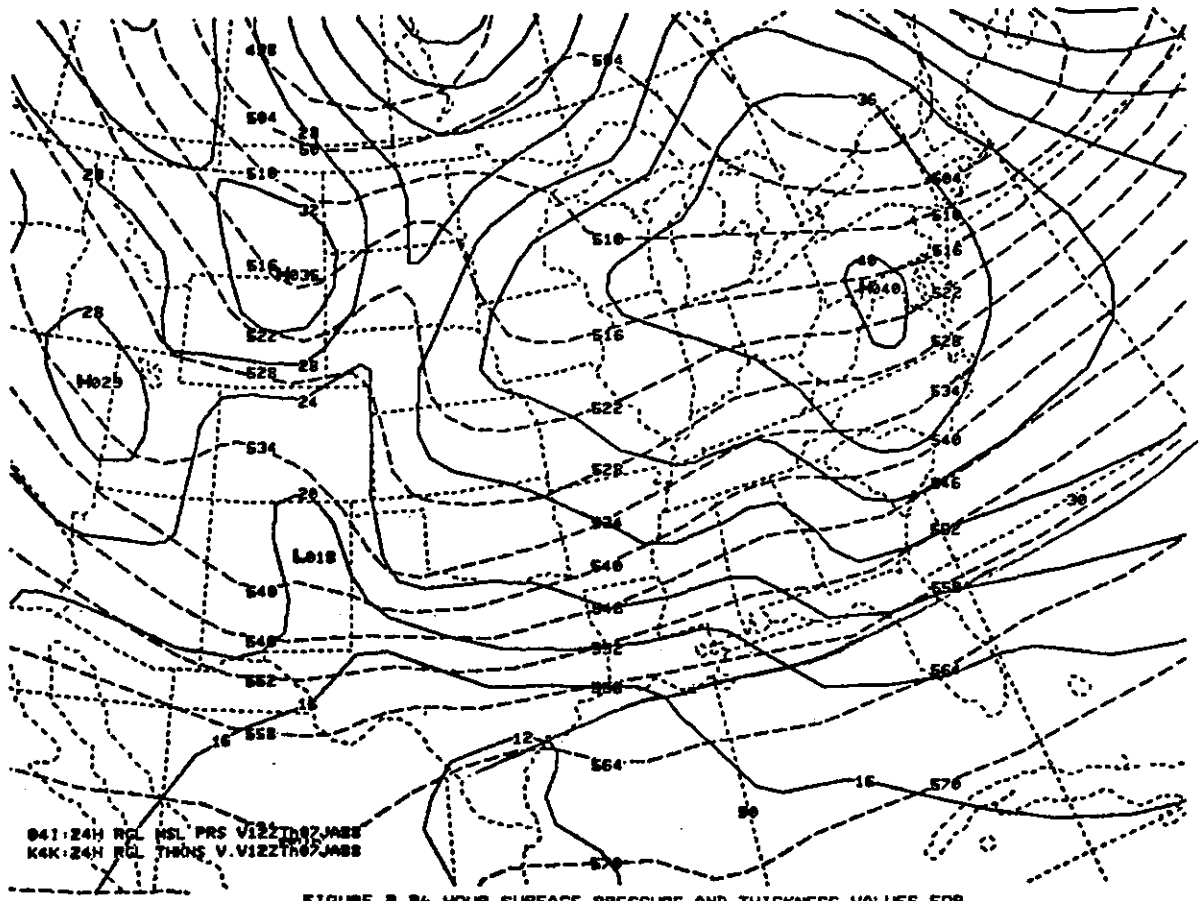


FIGURE 2 24 HOUR SURFACE PRESSURE AND THICKNESS VALUES FOR 122 THURSDAY JANUARY 7 1988

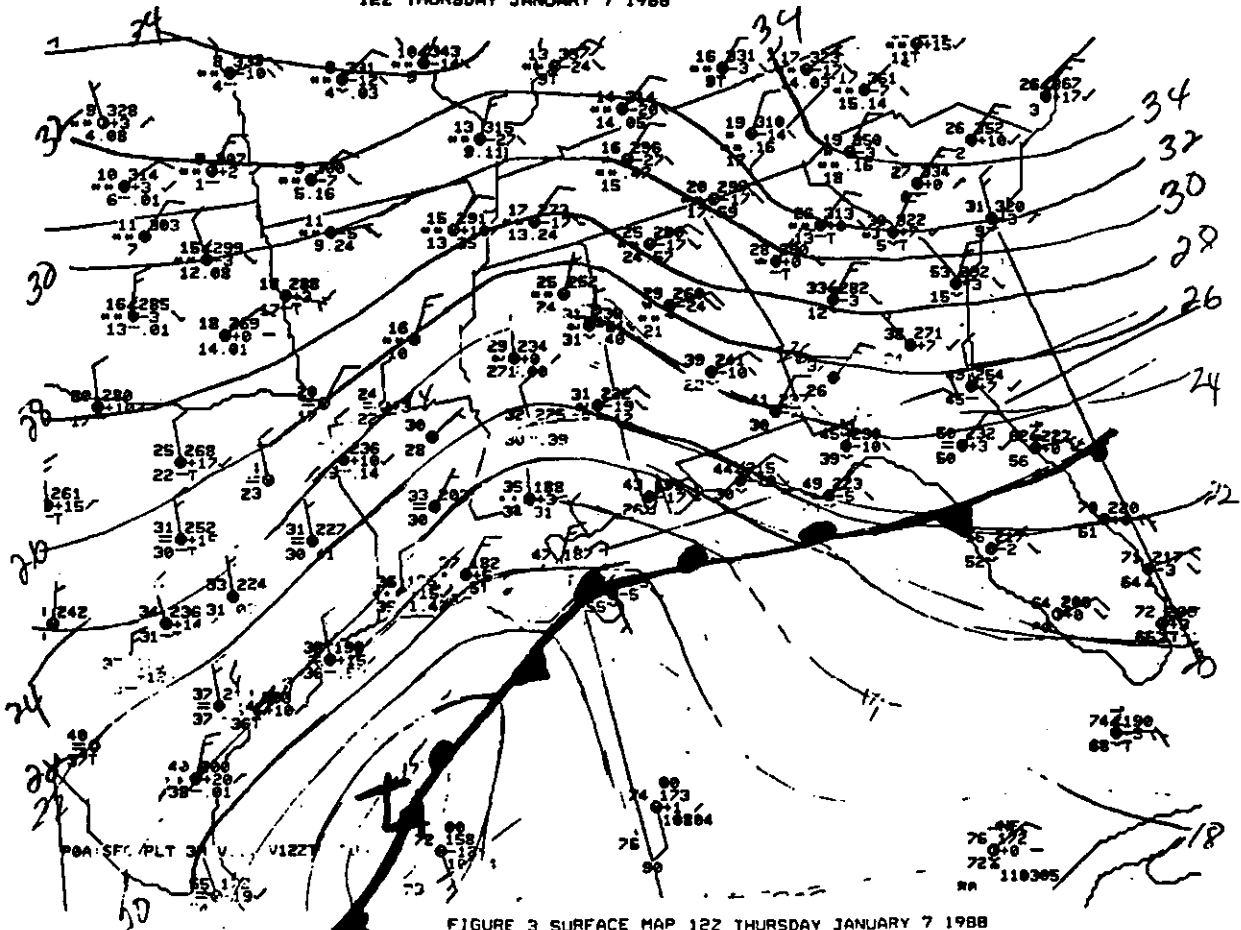


FIGURE 3 SURFACE MAP 122 THURSDAY JANUARY 7 1988

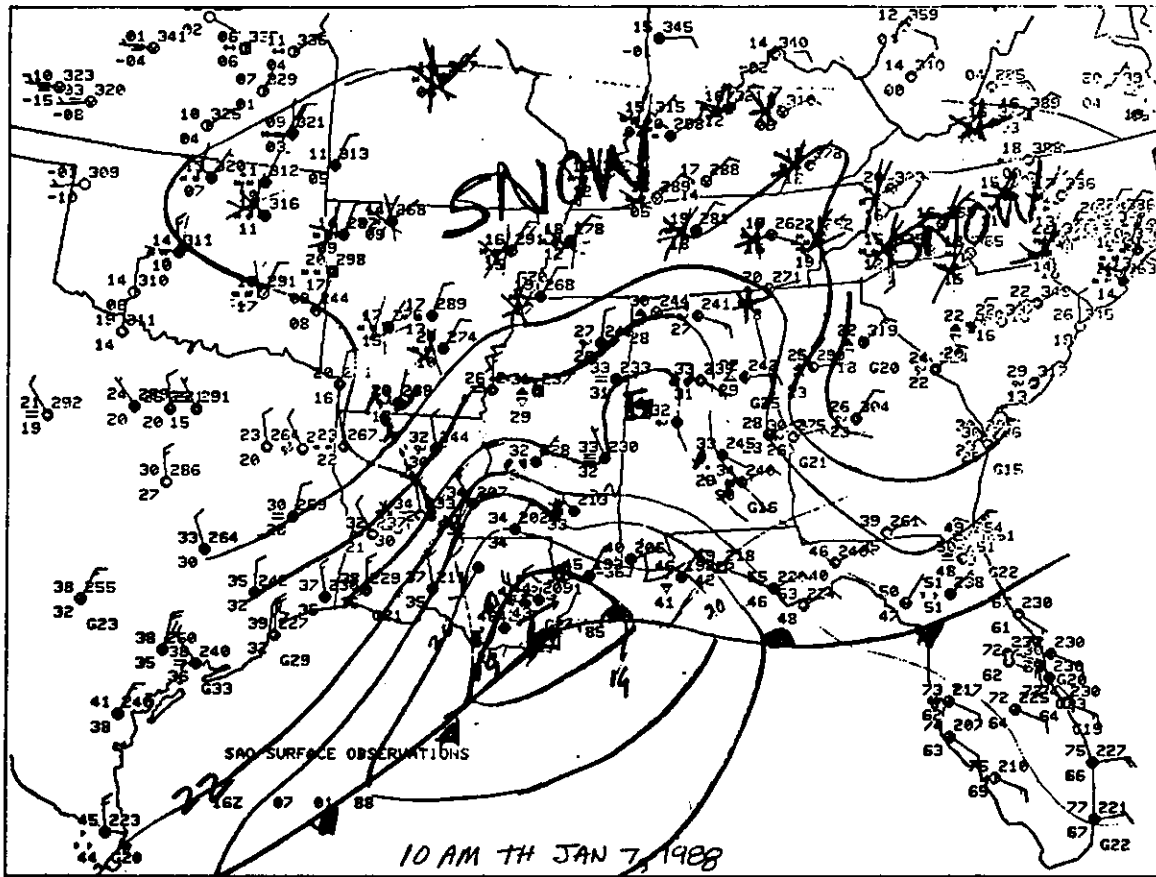


FIGURE 4 SURFACE MAP 16Z THURSDAY JANUARY 7 1988

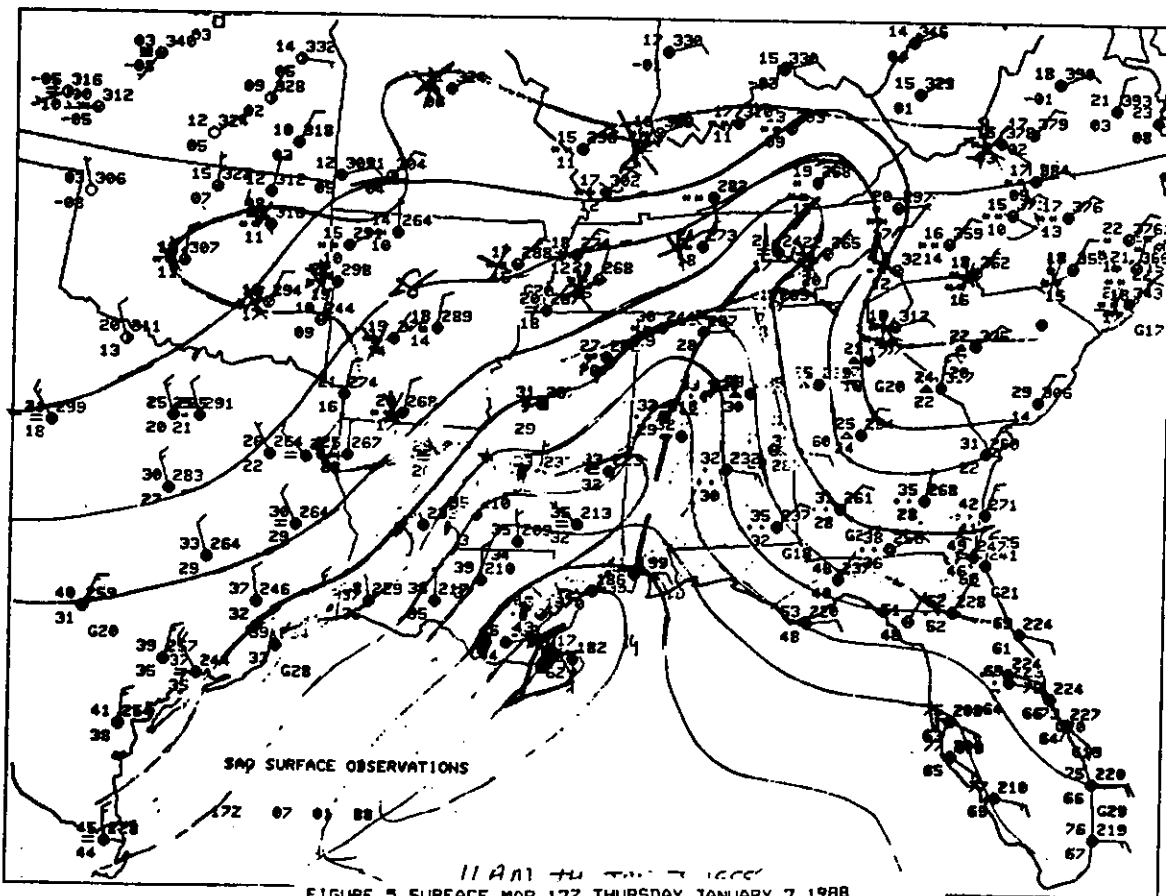
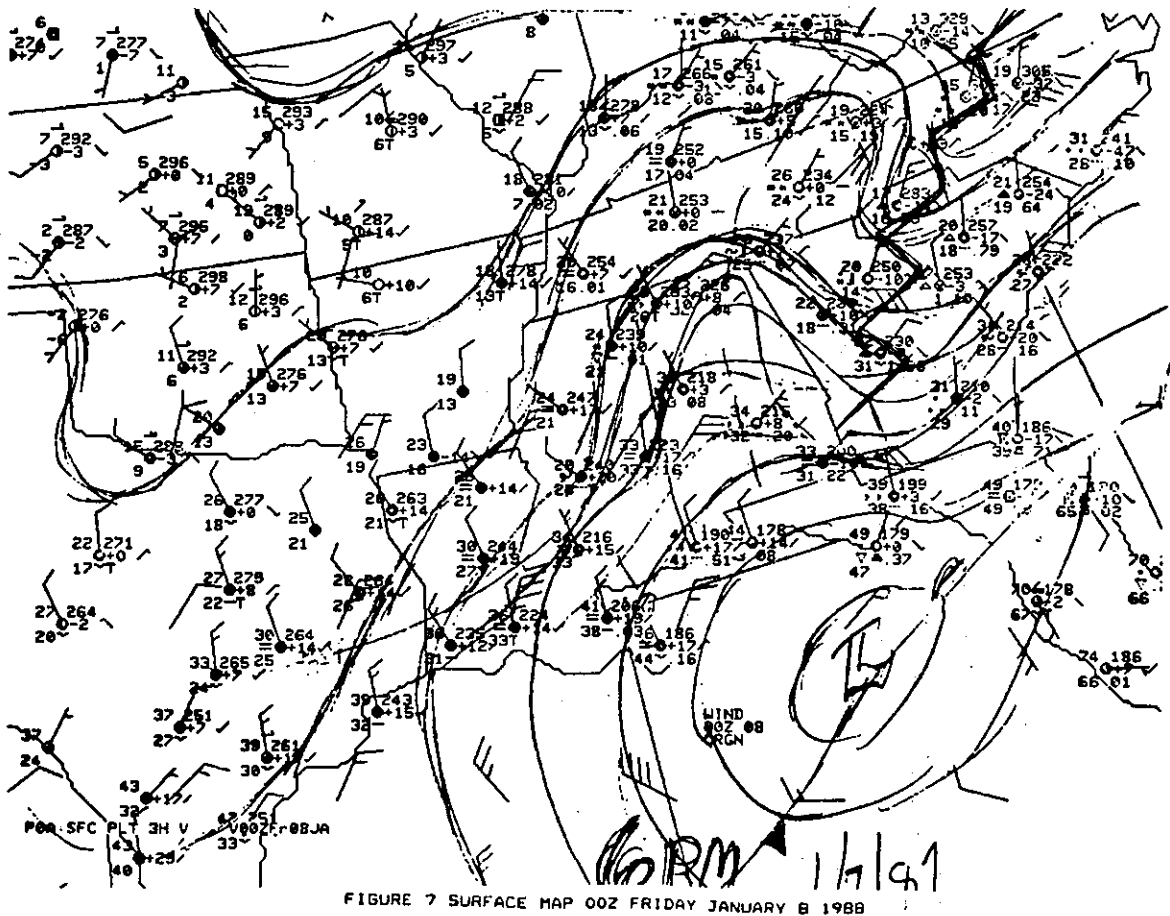
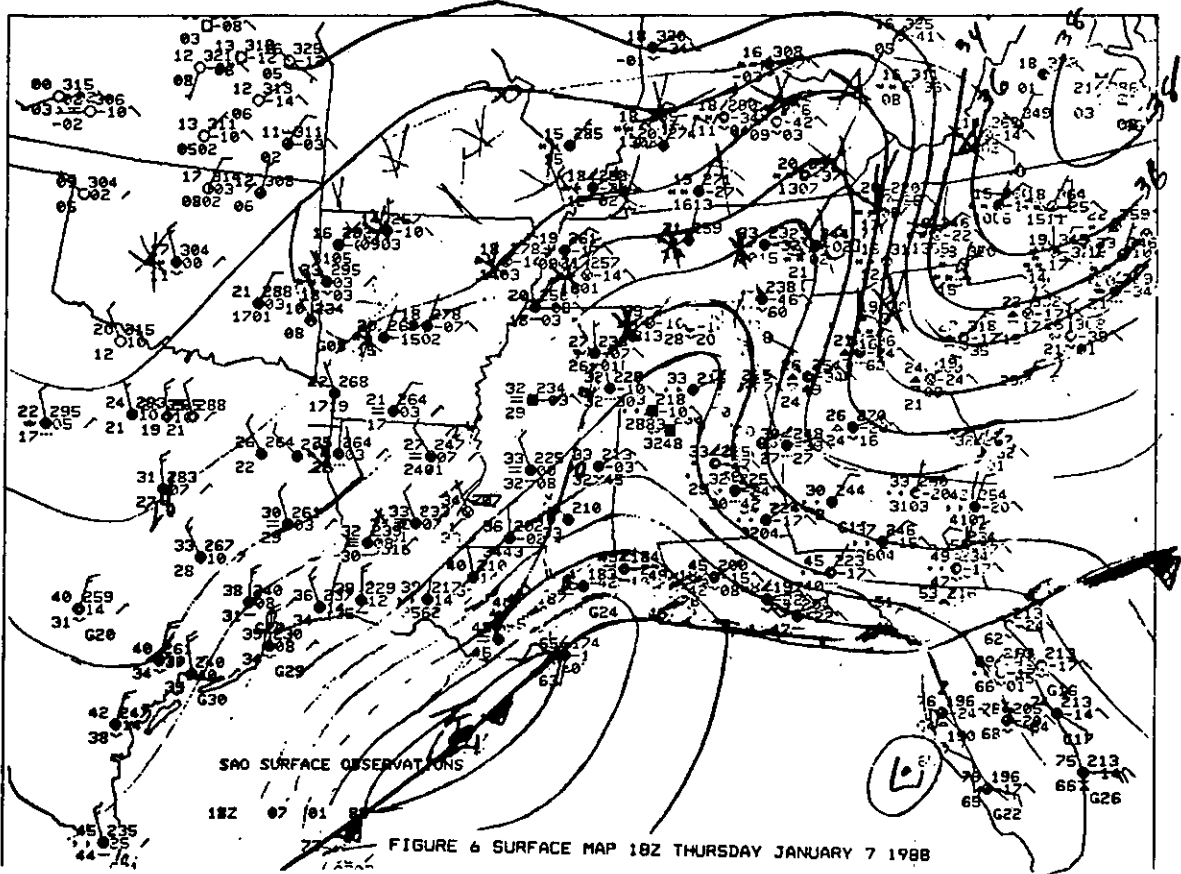


FIGURE 5 SURFACE MAP 17Z THURSDAY JANUARY 7 1988



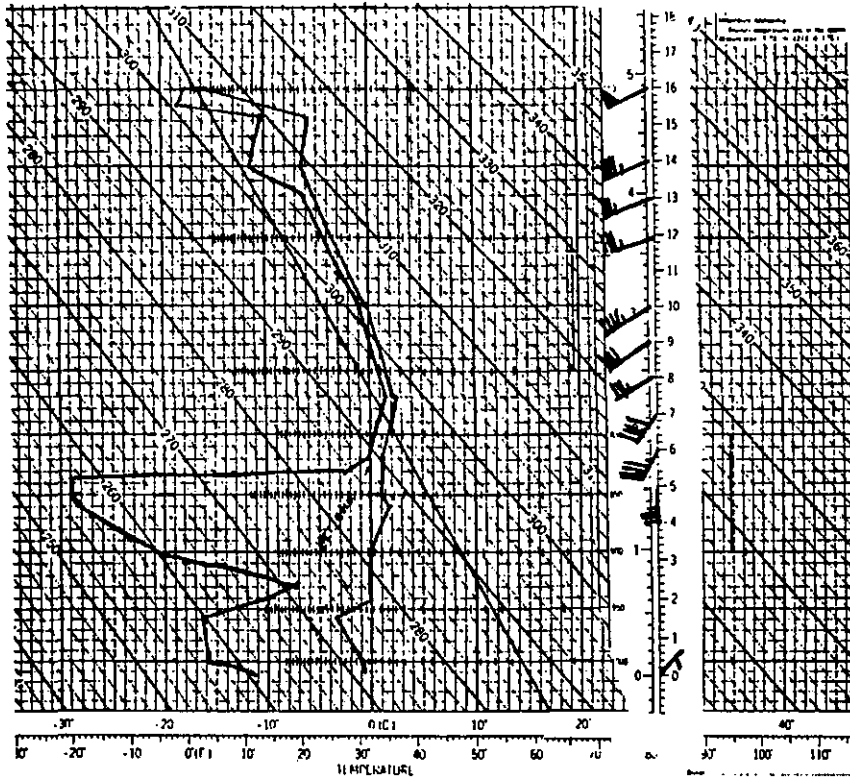
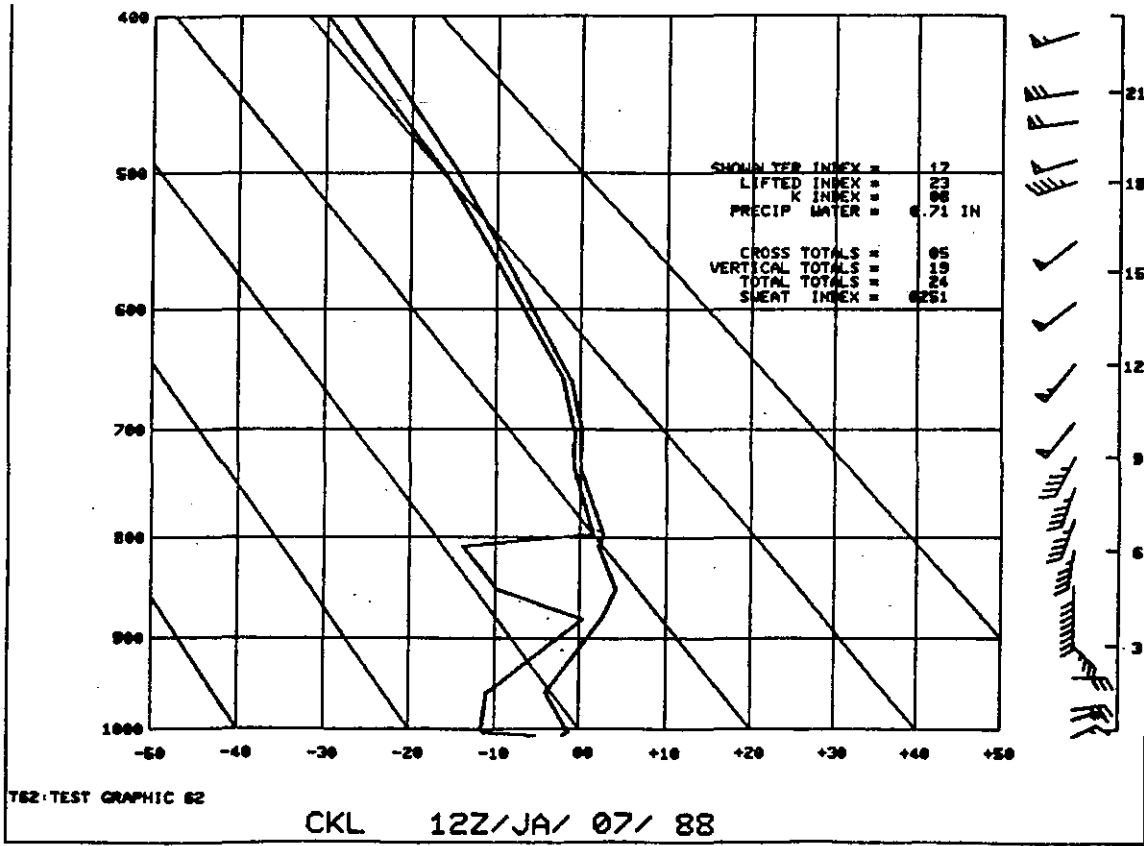


FIGURE 10 UPPER AIR SOUNDING WSMD CENTREVILLE
06Z THURSDAY JANUARY 7 1988



TSZ-TEST GRAPHIC 82

CKL 12Z/JA/ 07/ 88

FIGURE 11 UPPER AIR SOUNDING WSMD CENTREVILLE
12Z THURSDAY JANUARY 7 1988

WINTER STORM EVENT OF JAN 15, 1988 OVER COASTAL SOUTH CAROLINA

Robert W. Kelly & Mary J. Parker (WSFO Columbia SC)

I. Introduction

The winter weather event of January 15, 1988 hit the eastern third of South Carolina with little warning. The purpose of this paper is to discuss the analysis and guidance available to the forecasters and examine how well this event was progged by the models.

A few hours after midnight on January 15, 1988, freezing rain started in some areas of coastal South Carolina. Light rain started at Charleston at 2:39 AM EST and turned to freezing rain at 3:19 AM. AT Myrtle Beach AFB freezing rain started at 3:05 AM and turned to snow at 3:35 AM. The area of freezing and frozen precipitation eventually extended inland to parts of Dillon, Marion, Florence, Lee, Sumter, Calhoun, Orangeburg, Bamberg, and Allendale counties of South Carolina. (FIG 1) The area of precipitation ended during the morning over inland parts of South Carolina and by noon was completely offshore. Total snowfall amounts ranged from a trace inland at Florence up to 5 inches in some parts of northeast South Carolina.

This storm had a serious impact on both interstate travelers as well as local commuters. Interstate 26 between Orangeburg and Charleston was covered with a sheet of ice in many areas. Ice closed bridges in Charleston. Some schools were closed and Myrtle Beach AFB was closed except to essential personnel. Although the precipitation had ended by noon, the ice and snow persisted on some roads into the afternoon.

This paper will analyze the actual weather development from 00Z to 12Z Friday Jan. 15, 1988. We will also analyze the prog packages available to both the day shift forecaster on Thursday, Jan 14, and the evening shift. We will try to determine how well the progs handled the weather development, and what indicators may have proved most critical.

II. 00Z-12Z Transition

How did the atmosphere change from evening with clear skies into freezing rain and snow by morning? What do the observations and analyses show?

The most obvious features are of course the surface data. at 00Z (Thursday evening) temperatures in the eastern portion of the state were ranging from the upper 20s to the low 30s. Dew points were generally in the teens and wet bulb temperatures were below 32F. By 12Z (Friday morning) temperatures were in the 20s throughout the area with freezing or frozen precipitation occurring along the coast and into the eastern midlands.

	00Z		12Z
FLO	250 OVC	29/15/0408	-X 30 OVC 5S- 23/19/0409
CRE	30 SCT 250	-BKN 32/18/0304	-X 20 OVC 1S- 25/22/0108
CHS	150 SCT 250 OVC	36/20/0710	9 OVC 4IP- 27/25/0210

Such a marked difference on the surface must have been reflected aloft as well. Consider the standard level charts (500/850 MB), then the computed/analyzed data derived from the upper air reports.

The evening 500MB chart showed a trough moving into the Mississippi valley, the flow across South Carolina was from about 250 degrees at 60 knots. Temperatures were significantly colder to the north but over the area in question the range was from -21C at AHN to -18C at AYS. The trajectory showed cold advection from the great plains southward to Arkansas and then easterly to the Carolinas and southern Georgia.

By 12Z there was a substantial cooling at this level. the morning raob showed -28C at AHN, -25C at CHS, -19C at AYS. In addition there was a strong vort max over Tennessee with good PVA throughout the Carolinas and coastal Georgia. The trough was moving into the western Appalachians. Such a significant cooling at this level would indicate a destabilization of the atmosphere, and in fact the computed vertical velocities at 00Z and 12Z will reflect this.

At 850MB we had a warm advective pattern, with temperatures rising as much as 5 degrees celsius at CHS, and 3 degrees at both AHN and AYS. More importantly, the southerly winds over the coastal plains increased from 5 knots to 25 knots at CHS while continuing at AYS to be 15 to 20 knots. During this time there was a wind shift at AHN from southerly at 5 knots to northwest 15 knots. This was a good indication of convergence over the coastal plains of SC, coupled with the cooling at the 500MB level.

While this destabilization was occurring in the atmosphere, the surface was not behaving in a convective manner. The cooling was noted above, but what is also most important is the continuing strong northeast flow of cold dense air under the less dense southerly flow aloft. This led to the most hazardous of winter weather situations in South Carolina, overrunning with the cold northeast wedge. This is most often a problem in the northwest part of the state where the cold air becomes entrapped along the eastern slopes of the Appalachians and the less dense flow from the Gulf of Mexico runs over the cool air. The typical response is for precipitation to form along the wind shear line and the evaporating precipitation to cool the surface to the wet bulb temperature, enhancing the density difference and producing freezing precipitation. In this case the surface temperatures were already below freezing except along the south coast and most of the precipitation was in the form of snow. There was a significant freezing rain problem in Charleston as the temperature dropped from 36F to 27F and in the process the precipitation ranged from freezing rain to sleet. Further inland and along the north coast the entire temperature profile was below freezing and hence the snowfall.

Throughout the mixing layer perhaps the most significant change was in the mean RH. at 00Z the mean RH was less than 30% over the entire state, by 12Z the mean RH had increased to more than 70% over the coastal plains and was about 60% inland as far as FLO. The increased flow and convergence at the 850MB level was only part of the story as the RAOB sounding showed dramatic increase in moisture at all levels, and precipitable water increased from .13 inch to .57 inch despite the cold atmosphere.

Vertical velocities more than doubled overnight from approximately +1.5 to slightly more than +3. The analysis showed a VV max of +6 off the coast of SC. This enhanced cloud development, but still the overrunning would seem to be the most dominating driving force for this type precipitation event.

With overrunning precipitation thickness values are not as significant as with cyclogenetic systems, since the character of the precipitation is determined near the ground. Still it does have some value in that it reflects to some extent the temperature in the cloud layer. 5400 meters has been frequently used as a marginal value for precipitation type, and in this case it was not a bad value. Based on the NGM analyses for 00Z and 12Z, the thickness values showed a cooling trend with values close to the threshold over the south coast where the freezing rain and sleet fell, and colder values over northeast SC where the snow fell.

	00Z	12Z
SAV	546	541
CHS	543	537
MYR	540	534
FLO	537	531

We will look at how the models handled this event, and then attempt to determine how predictable this storm event was, and what were the factors which may have been the best predictors.

III. Machine Progs from 12Z Jan 14 (Thu)

Thursday morning the forecasters were faced with a reasonably familiar weather situation. A surface high was in Indiana, 850MB pattern weak, the 500MB pattern a zonal flow with no distinguishing traits. What in the progs would indicate the type weather to expect? We have already discussed the progression of weather during the night of Jan 14-15, but was this pattern predictable, based on the 12Z progs?

The progs showed substantial atmospheric cooling through 24 hours, forecasting 24 hour thickness values ranging from 5340 meters at Myrtle Beach to 5390 meters at Savannah. These values were remarkably close to the actual computed values at the valid time, so atmospheric cooling was accurately predicted.

The 24 hour forecast for mean relative humidity was approximately 60%. In fact, the computed mean RH for 12Z Friday (24 hours) was in excess of 70% throughout the coastal plains, and greater than 60% in the Florence area. Although the actual values are close, this is an area of critical threshold values, and 70% is frequently used as a boundary value by forecasters in precipitation forecasts. This was a case where the progs were on the dry side of the threshold, and reality was on the wet side, a small objective difference, but a remarkably different development.

Vertical velocities were progged to be small. Values ranged from near zero to +1. By 12Z Friday actual vertical velocities were computed to be approximately +3 throughout the coastal plains. The low forecast values for vertical velocity coupled with marginal moisture conditions gave little indication of incipient precipitation.

The 500MB progs were generally good, indicating the strong PVA and trough location. The values were only slightly off in a geographical sense with the prog position slightly slow. One important factor noted earlier was the 500MB temperature in the sense of destabilization. The graphical 500MB progs do not give temperature values, although as we have seen, the thickness values did indicate cooling through the layer.

The 850MB progs were deficient. The progs failed to show either the increasing wind or the warm advection. In fact, the progs for 24 hours at 850MB were as much as 7 degrees celsius too cold. Considering that destabilization is dependent upon the lapse rate, having 850MB levels too cold with cooling thickness values, there is no particular reason to believe that there would be a tendency toward instability. This of course concurs with the prog values for vertical velocities which were underforecast. The weak flow forecast at 850MB also would have made the increase of moisture necessary for precipitation unlikely.

In summary, although the 12Z progs indicated a cooling atmosphere, they missed the low level action of increased advection of temperature and moisture, and therefore missed the vertical motions despite the good forecast of PVA. Moisture was only slightly underforecast, but it was an error made in a critical threshold range. The net result was a forecast of no precipitation (on both the QPF chart and numerical guidance) with lows in the low 20s. The cloud cover at CHS was forecast to be overcast at 12Z, only scattered at 06Z and 18Z. The surface pattern of a northeast ridge was accurately handled, but the low levels, which provided the source for the precipitation, were not well forecast. This poor forecast of the low levels caused the models to miss the event entirely.

IV. Machine Progs from 00Z Jan 15 (Thu eve)

The thicknesses forecast for 12z Friday were all below the 540 value in the area of South Carolina which was hit by the storm. The forecast thickness values for several locations are listed below.

Myrtle Beach	534
Charleston	537
Florence	531
Savannah	540

The 850 mb forecast for 12Z Friday showed temperatures over eastern South Carolina ranged from 0C near Savannah, Georgia to -5C at Wilmington, North Carolina. The model showed a strong northeast surface wind at 00Z Friday and forecast it to continue through 00Z Saturday. For 12Z Friday, the boundary layer wind was forecast to be northeast 20 knots over northeast South Carolina. However, at 850 mb virtually no gradient was forecast.

The 04Q and 02Q showed no precipitation over land and light precipitation offshore. However, the 70 percent relative humidity isoline was forecast at 12Z Friday to encompass the eastern two thirds of South Carolina and the coastal waters. This 70 percent isoline is usually an indication of sufficient humidity to produce precipitation if the right mechanisms are available. By 00Z Saturday, the 50 percent relative humidity isoline was forecast to encompass the coast with the 30 percent isoline approximately encompassing the mountains.

The model forecast a +3 vertical velocity over the entire coastal region for 12Z Friday. For 00Z Saturday the model forecast a negative vertical velocity over land and a +6 vertical velocity well offshore. Finally, for 12Z Friday strong PVA was forecast over South Carolina with the maximum in the vicinity of Atlanta and a trough along the Appalachians. By 00Z Saturday, the maximum vorticity was forecast to be over central North Carolina with the trough over northeastern South Carolina and extending off the coast.

What could the evening or mid shift forecaster have seen to alert him to the weather which developed? There were several indicators pointing to the possibility of frozen precipitation on the NGM run at 00Z Friday. First of all, the forecast temperatures at 12Z Friday were cold enough, as indicated by the thickness values and 850 mb temperatures. Also, sufficient moisture was forecast to be available as shown by the 70 percent RH isoline at 12Z Friday which encompassed the eastern two thirds of South Carolina and the coastal waters. Strong vertical velocities were indicated over eastern South Carolina during the 00Z to 12Z time period as well as strong PVA.

This combination of factors could indicate a forecast of frozen precipitation, but the lead time could only have been a couple of hours at the most. Additionally, since this event was primarily an overrunning precipitation situation, the forecast of weak winds at 850 mb was a critical deficiency in the model.

V. Summary

There was a marked increase in quality from the 12Z run Thursday to the 00Z run Thursday evening. The progs reviewed by the day shift for the forecast for that night gave no indication of the significant weather about to develop. The major contributing factors to this weather event were in the low levels of the atmosphere, but the progs most effectively handled the upper levels. This was not a large scale synoptic storm, but rather a mesoscale winter storm affecting several counties in the eastern part of South Carolina.

Overrunning precipitation is a familiar phenomenon to forecasters in South Carolina, but it most commonly occurs in the northwest part of the state. The clues forecasters look for are cool dry northeast winds on the surface, and warm moist winds from the south at a few thousand feet above ground level. This is exactly what transpired along the coast. Had the forecasters expected the increase in southerly winds at 850 mb, and had the forecasters expected the moisture to increase as much as it did, above the 70% level, then the forecast would have had a completely different character.

This was a case in which the forecaster decided to agree with the computer model of the forecast process, and the model was wrong in the critical areas which determined the weather, but correct in other areas that were less important. While the 00Z run of the model was much more accurate in its forecast of the lower levels, these graphic progs were only available about two hours before the event. This would be around midnight, during the change of forecast shifts and at a time when forecast dissemination is least effective due to the late hour.

It is likely that most forecasters recognize a major bust by a model run, because their experience is still an invaluable asset when dealing with the atmosphere. It is less obvious when the model seems to have a good handle on the overall situation, but minor inaccuracies in a few critical parameters produce significantly different results from the model outputs.

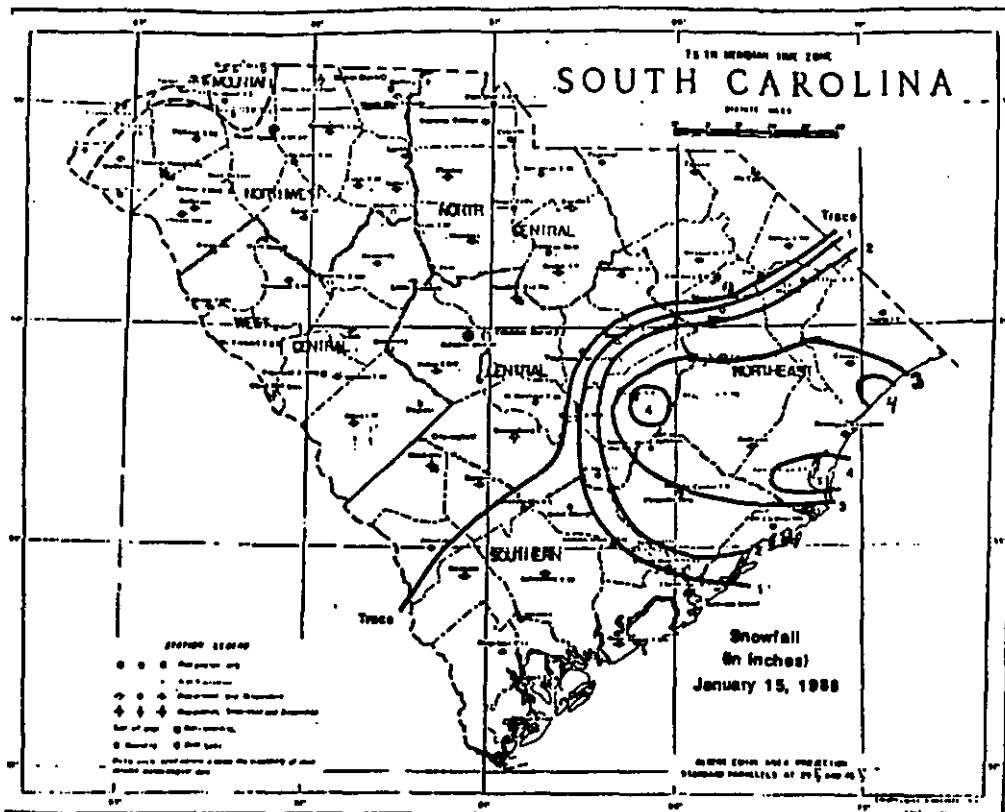
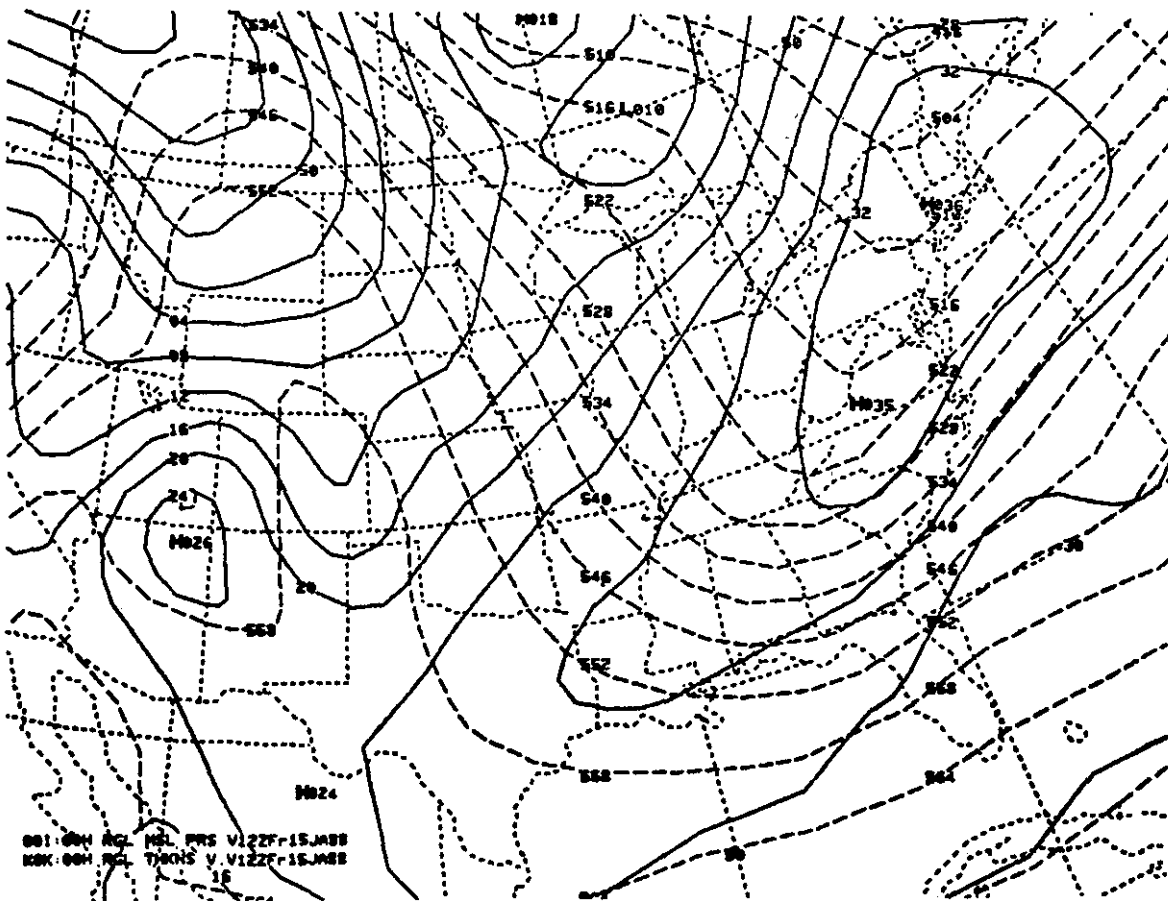


Figure 1



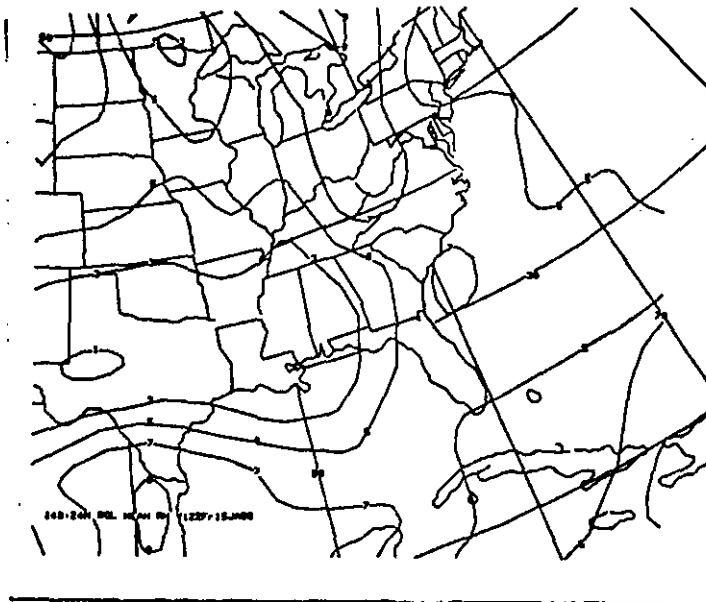
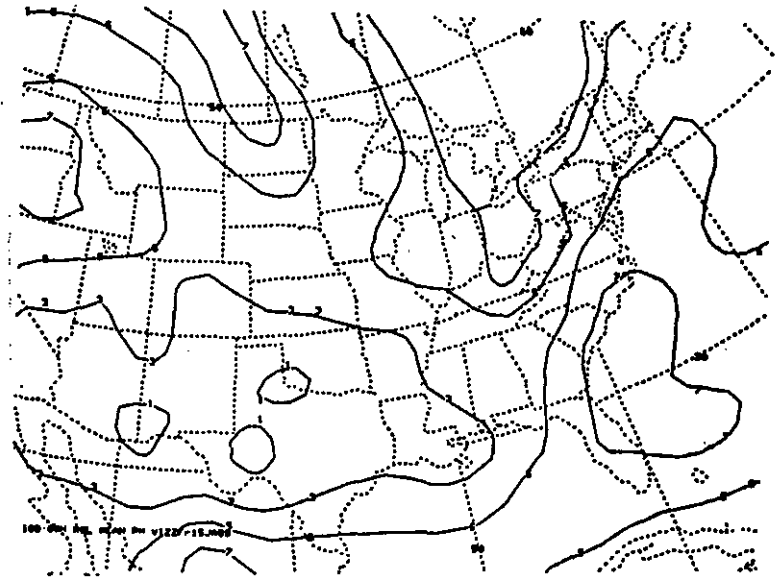


Figure 3

Figure 4



Figures 3 and 4 show the 24 hour forecast of mean relative humidity (FIG 3) and the actual mean relative humidity at 12Z Friday (FIG 4). Although the RH was only slightly underforecast, it was in a critical value area which increased its significance.

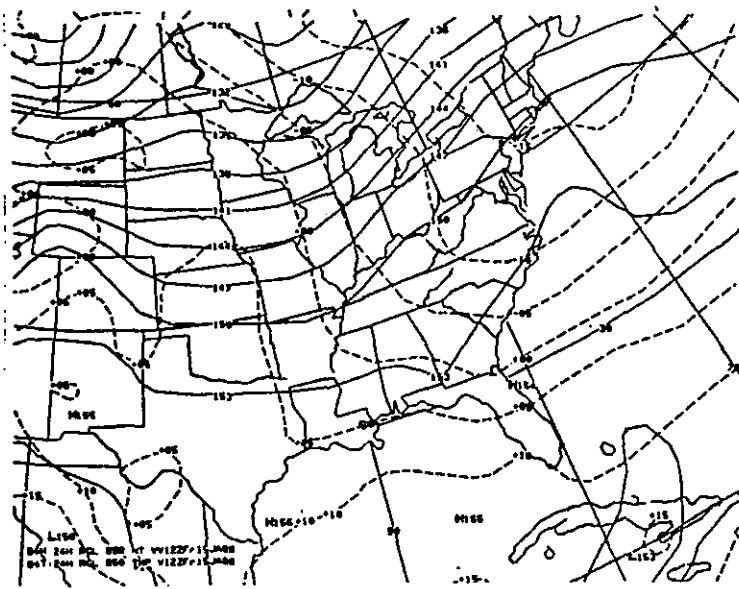


Figure 5

Figure 6

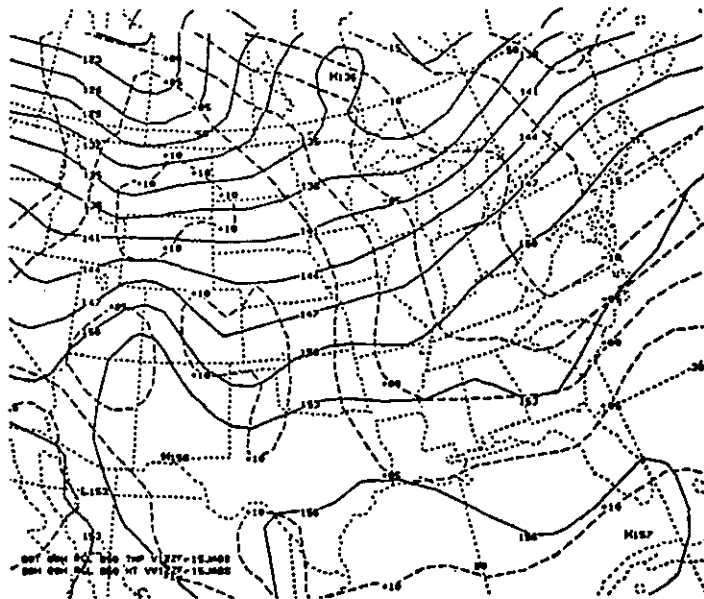


Figure 5 shows the 24 hour forecast for 850 MB heights and temperature, Figure 6 is the actual analysis for the same time. A critical element of this mesoscale precipitation event was the sudden, and unexpected, increase in southerly winds at the 850 MB level along the coast early Friday morning. This led to rapid overrunning development.

A METHOD FOR PREDICTING METEOROLOGICAL BOMBS IN THE
WESTERN NORTH ATLANTIC OCEAN

Eugene P. Auciello
National Weather Service Forecast Office
Boston, Massachusetts

Abstract

An operational checklist for the forecasting of meteorological bombs between 38°-45° N latitude and 55°-75° W longitude was developed by Auciello and Sanders (1986). The checklist incorporates tangible meteorological parameters responsible for the development of explosive maritime cyclones. The intensity, speed, and coastal crossing of 500-millibar vorticity maxima are of primary importance. Marine forecasters at the National Weather Service Forecast Office at Boston have utilized the checklist routinely during the past three cold seasons. The checklist has proven to be a valuable aid in the prediction of meteorological bombs up to 36 hours prior to the event. From 1 October 1987 through 31 March 1988, 15 bombs were observed over the checklist forecast area. The explosive cyclogenesis checklist forecast 18 bombs accounting for 12 hits and six false alarms. Verification for the 1987-88 cold season resulted in a probability of detection of .80, a false alarm ratio of .33, and a critical success index of .57.

1. INTRODUCTION

An explosive cyclogenesis checklist was developed by Auciello and Sanders (1986) as an objective operational technique for the forecasting of meteorological bombs up to 36 hours prior to the event over an area bounded by 38° to 45° N latitude and 55° to 75° W longitude.

A meteorological "bomb" was originally defined by Sanders and Gyakum (1980) as an extratropical surface cyclone whose central pressure falls averaged at least 1 millibar hour⁻¹ for 24 hours at 60° N latitude, normalized geostrophically at other latitudes.

In a later study, Sanders (1986) studied explosive cyclogenesis in the West Central North Atlantic Ocean. A high correlation was found between upper-level cyclonic vorticity advection over the surface cyclone and simultaneous surface deepening rate. Thus, the explosive maritime cyclone is fundamentally a baroclinic disturbance in which the low-level response to a given upper-level forcing is dramatically large. An operational checklist for forecasting explosive cyclogenesis in the Western North Atlantic was based upon this research.

Tracks and central values of surface low pressure centers and 500-millibar absolute vorticity maxima were gathered from operational analyses for 48 cases of explosive cyclogenesis which occurred between January 1981 and November 1984 over an area bounded by 38° to 45° N latitude and 55° to 75° W longitude. Peak occurrence was in January. The months with the next greatest number of bombs were February, December, November, and March in descending order of frequency. These cases were stratified into strong, moderate, and weak categories according to intensity. The sample included 12 strong, 16 moderate, and 20 weak bombs. Weak bombs were omitted since such events do not normally produce storm-force winds. A study of the mean behavior of the remaining 28 strong and moderate bombs lead to the development of the explosive cyclogenesis checklist.

2. CHECKLIST DEVELOPMENT

The original explosive cyclogenesis checklist utilized Limited-area Fine-mesh (LFM) input and was comprised of six questions.

1. Does a 500-millibar absolute vorticity maximum of $15 \times 10^{-5} \text{ s}^{-1}$ or greater exist in the LFM initial analysis over an area bounded by 30° to 50° N latitude and 85° to 110° W longitude?
2. Does this 500-millibar vorticity maximum maintain initial intensity or strengthen on successive 12, 24, 36, and 48 hour LFM charts?
3. Is this 500-millibar vorticity maximum forecast to move an average of 30 knots or greater through 48 hours?
4. Does the initial LFM-produced 500-millibar vorticity maximum cross the coast between 32° and 42° N latitude?
5. Does a jet streak of 120 knots or greater exist at 250 or 300 millibars in a position just south of the initial 500-millibar vorticity maximum?
6. Does the LFM develop a surface low of 995 millibars or deeper during the next 48 hours over an area bounded by 38° to 45° N latitude and 55° to 75° W longitude?

The first four questions deal exclusively with LFM-produced 500-millibar absolute vorticity maxima whose characteristics were inherent to each of the 28 bombs examined. A vorticity maximum of at least $15 \times 10^{-5} \text{ s}^{-1}$ existed as an initial LFM condition within a spawning area bounded by 30° to 50° N latitude and 85° to 110° W longitude. Vorticity maxima between $15 \times 10^{-5} \text{ s}^{-1}$ and $18 \times 10^{-5} \text{ s}^{-1}$ were characteristic of moderate bombs, while strong bombs exhibited initial vorticity maxima of $19 \times 10^{-5} \text{ s}^{-1}$ or greater. With few exceptions, the LFM-produced vorticity maxima maintained initial intensity or strengthened through 48 hours.

Movement averaged 30 knots for moderate bombs and 35 knots for strong bombs. This speed of movement provides the strong baroclinic impetus necessary for explosive development. All initial vorticity maxima crossed the coast between 32° and 42° N latitude, indirectly incorporating the strong sea-surface temperature gradient along the north wall of the Gulf Stream into the analysis. The northern crossing point was extended to 45° N after a review of the 1985-86 cold season.

The fifth question refers to a jet streak which, in the early stages of explosive cyclogenesis, is usually present in a position just south of the initial 500-millibar vorticity maximum. A jet streak threshold of 120 knots was arbitrarily chosen.

The last checklist question refers to the existence of an LFM-produced surface low of 995 millibars or deeper between 38° to 45° N latitude and 55° to 75° W longitude. The LFM usually develops a weak new surface low in the Atlantic along the strong sea-surface temperature gradient of the Gulf Stream in response to upper-level forcing. Of the 28 bombs examined, the vorticity maximum responsible for rapid deepening pre-existed the surface low in each case.

The checklist was completed for each LFM cycle during the 1985-87 cold seasons. If four or more checklist questions were answered affirmatively, the situation was closely monitored for the possibility of explosive cyclogenesis. The four-yes threshold was estimated to be optimal after reviewing checklist performance during the 1985-86 cold season.

3. LFM TO NGM CONVERSION

For the 1987-88 cold season, the explosive cyclogenesis checklist was converted from the LFM to the Nested Grid Model (NGM). Despite a shortfall in predicted deepening, the NGM displays a high degree of skill in forecasting explosive maritime cyclones. Checklist conversion required minor adjustments to specific threshold values due to inherent differences between models.

The NGM-keyed checklist couples an initial 500-millibar absolute vorticity maximum of $17 \times 10^{-5} \text{ s}^{-1}$ or greater with a surface low of 990 millibars or deeper. NGM-produced vorticity maxima between $17 \times 10^{-5} \text{ s}^{-1}$ and $20 \times 10^{-5} \text{ s}^{-1}$ are characteristic of moderate bombs while strong bombs exhibit initial vorticity maxima of $21 \times 10^{-5} \text{ s}^{-1}$ or greater. In addition to model changes, the jet streak threshold was lowered by 10 knots. The NGM-keyed checklist appears below.

1. Does a 500-millibar absolute vorticity maximum of $17 \times 10^{-5} \text{ s}^{-1}$ or greater exist in the NGM initial analysis over an area bounded by 30° to 50° N latitude and 85° to 110° W longitude?
2. Does this 500-millibar vorticity maximum maintain initial intensity or strengthen on successive 12, 24, 36, and 48 hour NGM charts?
3. Is this 500-millibar vorticity maximum forecast to move an average of 30 knots or greater through 48 hours?
4. Does the initial NGM-produced 500-millibar vorticity maximum cross the coast between 32° and 45° N latitude?
5. Does a jet streak of 110 knots or greater exist at 250 or 300 millibars within a 300 nautical mile radius in the semicircle south of the initial 500-millibar vorticity maximum?
6. Does the NGM develop a surface low of 990 millibars or deeper during the next 48 hours over an area bounded by 38° to 45° N latitude and 55° to 75° W longitude?

The checklist was completed for each NGM cycle during the 1987-88 cold season. The four-yes threshold was utilized.

4. CHECKLIST PERFORMANCE

Completed checklists from the 1985-86, 1986-87 and 1987-88 cold seasons were examined for individual cases when four or more questions were answered affirmatively. These were denoted forecast episodes. Consecutive checklists referring to the same cyclone were considered as a single episode. A particular cyclone, whether it qualified as a bomb during a single 24-hour period, or for overlapping periods, was considered as a single event. To be considered an event (E), a cyclone had to qualify as a bomb somewhere within the area bounded by 38° to 45° N latitude and 55° to 75° W longitude.

A hit (H) was scored when a cyclone qualified as a bomb in the forecast area at some time from zero to 36 hours after a forecast episode. If no bomb occurred in the area within the time range of any of the checklists in an episode, that forecast episode was denoted a false alarm (FA). If a bomb occurred and was not within the time range of any checklist with four or more affirmative answers, the event was denoted a miss. A probability of detection, false alarm ratio, and critical success index

was calculated for each cold season to determine overall checklist performance. The probability of detection (POD) is H/E . The false alarm ratio (FAR) is $FA/(FA + H)$. The critical success index (CSI), or threat score, is given by $CSI = [(POD)^{-1} + (1 - FAR)^{-1} - 1]^{-1}$.

4.1 1985-86 Cold Season

Routine completion of the explosive cyclogenesis checklist was instituted at the National Weather Service Forecast Office at Boston in late December 1985. During the period from 19 December 1985 through 31 March 1986 nine events were observed from National Meteorological Center (NMC) analyses as compiled by Sanders (1987a). Peak occurrence was in January accounting for four events. Three events occurred in February, followed by two events in March.

The explosive cyclogenesis checklist forecast 13 episodes accounting for six hits and seven false alarms. The checklist missed three bombs. These statistics resulted in a probability of detection of .67, a false alarm ratio of .54, and a critical success index of .38. Of the seven false alarms, four coincided with gale or storm centers that did not meet meteorological bomb criteria.

The three bombs missed by the checklist exploded east of Sable Island resulting in storm-force winds south of Nova Scotia. Vorticity maxima associated with the three misses crossed the coast north of 42° N latitude. After reviewing checklist performance in these cases, the northern crossing point for vorticity maxima was extended to 45° N latitude for the 1986-87 cold season.

4.2 1986-87 Cold Season

The 1986-87 cold season proved to be considerably more active than the preceding one. From 1 October 1986 through 31 March 1987, 17 events were observed from NMC analyses as compiled by Sanders (1987b). Peak occurrence was during January and February, with each month accounting for five events. The months of November and December each accounted for three events. One event occurred in October.

The explosive cyclogenesis checklist forecast 25 episodes accounting for 13 hits and 12 false alarms. The checklist missed four weak bombs. These statistics resulted in a probability of detection of .76, a false alarm ratio of .48, and a critical success index of .45. Of the 12 false alarms, 11 coincided with gale or storm centers that did not meet meteorological bomb criteria. In earlier studies, Auciello and Sanders (1987a, 1987b) reviewed checklist performance from the 1985-86 and 1986-87 cold seasons in detail.

4.3 1987-88 Cold Season

From 1 October through 31 March 1988, 15 meteorological bombs were observed over the checklist forecast area. Peak occurrence was in December with four events preceded by three events in November. Two

events occurred in January followed by two events in February and three events in March. One event occurred in early October.

The NGM-keyed explosive cyclogenesis checklist forecast 18 episodes accounting for 12 hits and six false alarms. The checklist missed three bombs. These statistics resulted in a probability of detection of .80, a false alarm ratio of .33, and a critical success index of .57. Of the six false alarms, one was a bomb that developed just outside the verification area. Four other false alarms coincided with gale or storm centers that did not meet meteorological bomb criteria.

Skill in the 1987-88 cold season is difficult to compare with the skill for the two preceding cold seasons since the checklist was keyed to different models. The four-yes threshold probably remains optimal. A different threshold would produce changes in opposite directions in the probability of detection and the false alarm ratio. Of the three misses, two bombs were associated with vorticity maxima that never crossed the coast but tracked northeast parallel to the coastline. The third miss resulted from a poor NGM forecast of 500-millibar vorticity.

5. SIGNIFICANCE OF CHECKLIST QUESTIONS

For the 1987-88 cold season, percentages of affirmatively answered questions were computed for all checklists associated with forecast episodes that were scored hits. Question 1, dealing with the existence of a significant vorticity maximum in the spawning area, was answered affirmatively 97 percent of the time. Question 3, dealing with the speed of this vorticity maximum, ranked second and was answered affirmatively 94 percent of the time. Question 4, dealing with the coastal crossing of the vorticity maximum, ranked third and was answered affirmatively 87 percent of the time.

These percentages are not surprising. Sanders (1987a) examined the intensity, speed, and latitudinal crossing of 500-millibar absolute vorticity maxima and associated explosive cyclogenesis in the Western North Atlantic. Research showed that during the 1986-86 cold season, 40 percent of the upper-level vorticity maxima crossing the east coast of North America produced meteorological bombs. The overall likelihood increased to 50 percent at the height of the bomb season.

Jet streaks, once thought to be a unique synoptic signature of explosive cyclogenesis, ranked fourth. Question 5, dealing with jet streaks, was answered affirmatively only 77 percent of the time. Although redundant, since strong baroclinicity is handled by the speed of a vorticity maximum in question 3, the inclusion of the jet streak question serves to reinforce the existence of strong baroclinicity.

Question 2, dealing with subsequent strength of an initial vorticity maximum, ranked fifth and was answered affirmatively 71 percent of the time. This infers that a strong initial vorticity maximum may, within limits, decrease in intensity and still produce a bomb.

NGM development of a surface low 990 millibars or deeper over the checklist forecast area, dealt with in question 6, ranked last and was answered affirmatively 61 percent of the time. The NGM will usually develop a weak new surface low in the Western North Atlantic in response to upper-level forcing. While several checklists associated with explosive development were associated with NGM surface lows in the 991 to 995 millibar range, increasing the checklist threshold by 5 millibars to compensate for the NGM's shortfall in predicted deepening would only increase the number of false alarms.

Upper-level vorticity appears to be the key to forecasting explosive maritime cyclones in the Western North Atlantic. Vorticity maxima responsible for rapid deepening pre-exist a surface low. The motion of a vorticity maximum relative to a surface low is a counterclockwise spiral beginning to the northwest of the nascent bomb and ending to the south of the developed storm. Strong bombs are distinguished from moderate bombs by the substantially greater initial separation distance and the greater relative speed of the vorticity maximum.

6. PROBLEMS AND SOLUTIONS

A problem frequently encountered during completion of the explosive cyclogenesis checklist was the existence of dual initial 500-millibar absolute vorticity maxima in the spawning area. In such cases, checklist completion should be accomplished by handling each vorticity maximum separately. Another problem often encountered was the tracking of merging vorticity maxima. In these cases, checklist completion should be accomplished by following the vorticity maximum created by the merge.

Although the checklist is an objective technique, inconsistencies in checklist completion are common. This is a pitfall that should be avoided. The threshold values assigned to both the LFM- and NGM-keyed checklist questions were systematically chosen. For all checklist questions where a threshold value is not met, a negative answer is required. Close does not count. Subjectivity should not enter into checklist completion and is responsible, in part, for a higher than expected false alarm ratio.

During the 1985-86, 1986-87, and 1987-88 cold seasons, the false alarm ratios were .54, .48, and .33, respectively. This steady decline in the false alarm ratio is due, in part, to increased proficiency in checklist completion. However, a lower false alarm ratio is desirable. False alarm recognition is the key. The absence of an affirmative answer for question 6, dealing with model development of a surface low over the forecast area, should arouse suspicion. In almost all cases, false

alarms can be recognized by the complete absence of a model-produced surface low over or near the checklist forecast area. In defense of the checklist, 80 percent of the false alarms that occurred during the past three cold seasons coincided with gale or storm centers that did not meet meteorological bomb criteria. In fact, one was a bomb that developed just outside the verification area. Overwarning does not appear to be a problem.

The checklist has averaged three misses per cold season. A majority of these misses were associated with weak bombs. Weak bombs were omitted from checklist development since such events do not normally produce storm-force winds. More importantly, during the 1987-88 cold season, two misses were associated with vorticity maxima that never crossed the coast but tracked northeast parallel to the coastline. The checklist relies on the coastal crossing of vorticity maxima and fails to adequately recognize these coastal skimmers. When a checklist produces three affirmative answers coupled with an NGM forecast of a coastal skimmer, the situation should be closely monitored.

7. CONCLUSIONS

The explosive cyclogenesis checklist is an objective operational technique for forecasting meteorological bombs in the Western North Atlantic between 38°-45° N latitude and 55°-75° W longitude. The checklist incorporates tangible meteorological parameters responsible for explosive development. The intensity, speed, and coastal crossing of 500-millibar absolute vorticity maxima are of primary importance.

The purpose of the checklist, as designed, is to increase forecaster awareness as to the potential for explosive deepening. Simply stated: if you, the forecaster, do not suspect a bomb, then you will not be actively searching for one. If you, the forecaster, are not actively searching for a bomb, then you will not find it until it is too late.

During the past three cold seasons, the checklist has proven to be a valuable aid in the prediction of explosive maritime cyclones resulting in increased lead-time of marine warnings. Advanced warning is crucial to a mariner's decision-making process.

8. ACKNOWLEDGEMENTS

Special thanks to my colleague Dr. Fred Sanders for checklist collaboration, and to the forecasters at the National Weather Service Forecast Office at Boston for routine checklist completion.

9. REFERENCES

Auciello, E. and F. Sanders, 1986: An operational checklist for the forecasting of explosive cyclogenesis in the North Atlantic Ocean. Eastern Region Technical Attachment, No. 86-7, National Weather Service, NOAA, U.S. Dept. of Commerce, 5 pp.

_____, and _____, 1987a: Verification of the explosive cyclogenesis checklist. Eastern Region Technical Attachment, No. 87-19, National Weather Service, NOAA, U.S. Department of Commerce, 4 pp.

_____, and _____, 1987b: An operational checklist for the forecasting of explosive cyclogenesis in the North Atlantic Ocean. Preprint of the Second Workshop on Operational Meteorology, Canadian Meteorological and Oceanographic Society, Halifax, Nova Scotia, pp 45-55.

Sanders, F. and J. Gyakum, 1980: Synoptic-dynamic climatology of the bomb. Mon. Wea. Rev., 108:10:1589-1606.

Sanders, F., 1986: Explosive cyclogenesis in the West Central North Atlantic Ocean, 1981-1984. Part I: Composite structure and mean behavior. Mon. Wea. Rev., 114:10:1781-1794.

_____, 1987a: A study of 500-mb vorticity maxima crossing the east coast of North America and associated cyclogenesis. Wea. Forecasting, 2:1:70-83.

_____, 1987b: Skill of NMC operational dynamical models in prediction of explosive cyclogenesis. Wea. Forecasting, 2:4:322-336.

WINTER WEATHER AND THE CENTER WEATHER SERVICE UNIT

WAYNE D. WEEKS, CWSU METEOROLOGIST

BOSTON AIR ROUTE TRAFFIC CONTROL CENTER

NASHUA, NEW HAMPSHIRE

ABSTRACT

Each of the twenty-two enroute air route traffic control centers (ARTCC's) in the United States has a complement of four National Weather Service (NWS) meteorologists to serve the aviation public by advising air traffic controlling and other Federal Aviation Administration (FAA) personnel on weather. The purpose of this article is to inform the general meteorological community of our specialized duties and operations during winter weather.

OUTLINE

- I. "Yes or no" thinking and acceptance rate.
- II. Acceptance rate, wind direction, programs, and delays.
- III. Snowfall and snow removal.
- IV. Center Weather Advisories (CWA's).

I. "YES OR NO" THINKING AND ACCEPTANCE RATE.

Although the briefings, forecasts, and advisories provided by the CWSU are for the benefit of the aviation public, the primary recipients of our products are FAA air traffic control personnel. Their mindset may be entirely different from that of the general public. I say that to provide background for how our products must be worded to achieve the maximum effect. The analogies that best may fit our situation are left-and-right brain thinking or the marriage of an engineer to an artist.

Air traffic control requires a greater degree of precision in forecasting than that which is required by general weather forecasts. Therefore, specificity in forecasting is important in many cases. Those of you who have experienced the dilemma of forecasting for an area the size of several states, while being verified by only a few observation points, can better understand the problem. To illustrate the importance of precision forecasting, a case in point would be an airport where the acceptance rate is cut in half when the runways are wet. To clarify, let me explain acceptance rate. The acceptance rate is the number of air craft that can land at an airfield under given conditions. Because braking action on a wet runway is slower than that on a dry runway, it may take aircraft twice as long to stop on wet runways. Because of the slower braking time, fewer planes can land, stop, and clear the runways in a given amount of time. For the example, let's say that our airport can land one plane a minute, or sixty an hour under dry conditions. On a wet runway, it takes an aircraft two minutes to land, stop and clear the runway. So only thirty aircraft per hour can land there when it's wet. Thus the acceptance rate has been cut in half.

Because of parameters such as wet or dry runways and the effect on the acceptance rate, air traffic personnel do not want to know about scattered showers or a chance of rain. They want to know whether or not the runways will be wet and at what time. The reason for this exactness is that sixty aircraft may be destined for our airfield at a given hour; and if the runway surfaces are wet, thirty of those planes and their passengers will have to wait. Such delay will cause unnecessary fuel to be burned by the aircraft and an increased work load on the air traffic controllers, who will be communicating with the pilots while they circle the airfield awaiting their turns to land. With the proper notice, the aircraft can be delayed at their gates before becoming airborne.

Probability terms such as "chance of," "likely," "occasional," or "slight chance" are of little help in many aspects of air traffic control. It doesn't take too long to realize what kind of accuracy a yes-or-no precipitation forecast will have.

This yes-or-no thinking applies to such things as precipitation type, ceilings, visibilities (will the visibility be above or below one half mile?), and wind direction. Members of the weather forecasting community can see the difficulties that may occur during a New England Nor'easter with liquid, mixed, and frozen precipitation.

II. ACCEPTANCE RATE, WIND DIRECTION, PROGRAMS, AND DELAYS.

On the day after a snowstorm, the visibilities are good, the clouds are often scattered, and the wind is strong from the northwest. This combination would lead one to believe that there would be no difficulties in landing. Admittedly, compared to the low visibilities and blowing snow of the previous day, there are fewer problems; but conditions are still less than ideal.

SEE EXHIBIT 1 FOR A DIAGRAM OF BOSTON'S RUNWAY CONFIGURATION

Looking at the diagram of Boston's airfield, we see runways thirty-three right and left, the ones used when there is a wind from the Northwest. Large aircraft can use only runway 33L, because 33R, at 2557 feet, is not long enough to accommodate their deceleration and braking. So for the purpose of major airliners, when there is a strong Northwest wind, Boston is a one runway airport. Not only does this mean that landing aircraft have only one choice, but departing aircraft have the same choice. Not only do landing aircraft have to wait their turns in line to land, but they must share the runway with planes on the ground taking off.

How does forecasting Northwest winds make a difference? It doesn't. A forecast of wind from three hundred thirty degrees at twenty-five knots gusting to forty in itself is not a great deal of help without a time frame for when it will begin or end. Will the velocity remain the same? Will this wind last through the rush hour? When will the gusts subside? When the wind shifts, will it shift more to the West, or to the North and to the Northeast? These, among others, are the types of questions that we at the CWSU try to answer.

All other conditions being equal, the acceptance rate at Boston is 36 when runways 33R and L are the only ones in use. As the wind direction shifts to a more Westerly direction, aircraft will be able to depart on runway 27. Use of the added runway will increase the acceptance rate to 44. Should the wind shift to a more Northerly direction, or to the Northeast, runways 4R and L can be used, increasing the acceptance rate to 50.

Because Boston's Logan airport is the one we at Boston Center deal with daily, I have used it as an example. Meteorologists at other centers tell me that wind direction causes similar difficulties at New York City, Pittsburg, Detroit, and Washington National airports.

On any given day, the normal rush hour traffic load at major airports approaches the maximum that the airports can handle. Therefore, weather restrictions such as unfavorable wind directions, low ceilings or visibilities, put an additional burden on a nearly saturated system. To prevent overloads on the air traffic system, the FAA traffic management personnel have computer programs to notify facilities nationwide of delays in flights planned to certain airports or areas of the country. These "programs" result in delays which may be in the form of holding on the ground for thirty minutes all aircraft destined for the restricted airport. The delay could worsen to several hours, or, in the worst case, all inbound flights could be cancelled until the weather improves. Another form of program would be in the form of an en route delay by increasing the spacing of aircraft flying over a certain waypoint (e.g. thirty miles in trail over Providence,) in order to allow more time for aircraft to land and clear the runways.

III. SNOWFALL AND SNOW REMOVAL.

Anticipating unfavorable conditions such as strong winds, unfavorable wind directions, snow storms, freezing precipitation events, wet runways, etc. is where the CWSU forecasters provide a great deal of help during winter storms.

Most of the forecasts prepared at the CWSU for traffic planning purposes are shorter in duration than those prepared for the general public. ARTCC personnel focus their planning primarily on the present shift, and then on what conditions can be expected for the next shift. Extra attention is paid to the weather forecast for the next rush hour. These concerns are, first, for anticipating air traffic delays, and, second, for determining personnel to be assigned to the next shift. Additional people can be and have been called in for the next shift because of CWSU weather forecasts. In order to accommodate the work loading of the shift at hand and the next shift, the time frame of our most important forecasts is from twelve to sixteen hours.

Most air traffic personnel usually learn of a forthcoming winter storm several days in advance from general public information, such as the NOAA weather radio. At the Boston Center, a briefing sheet with an outlook to thirty-six hours past the issuance time notifies the aviation community of an impending storm. This far in advance, one of the services we provide the FAA is forecasting the accessibility of remote equipment for periodic maintenance.

The first advisory that we issue is called a Meteorological Impact Statement (MIS), which is valid up to twelve hours. This is the first CWSU issuance notifying our Air Traffic people of the onset of weather hazardous to aviation. It will include forthcoming turbulence, low level wind shear, icing, low IFR conditions, precipitation types and winds. Because of the time period of the MIS, it often is the last advisory issued on our evening shift, or the first one issued during the morning. Twelve hours is adequate time to anticipate an increased workload for the next rush hour, which is either early morning or late afternoon.

With the onset of snowfall, concerns, in addition to the basic terminal forecast information, become important for air traffic operation. These require special purpose forecasts unique to airport operations. Because several inches of snow will require closing runways for snowplowing, snow accumulation is important. During some snowstorms, the primary runways at airports may be closed more than once for snow removal. Anticipating a wind shift, which will require changing the primary runway(s) is extra important when snow removal will be required on the new runway.

IV. Center Weather Advisories (CWA's).

Often a hazard to aviation will occur that is not of sufficient magnitude to warrant an advisory from the National Aviation Weather Advisory Unit (NAWAU) located in Kansas City. This means a condition may not cover a large enough area to justify a Sigmet or an Airmet. The areal extent of this condition, though not large on a national scale, is significant enough to affect air traffic in an ARTCC's boundaries. Low level wind shear, severe icing, and severe turbulence are the most likely conditions for CWA's. At this time, the CWSU meteorologist will issue a CWA. Air traffic controllers will read a CWA to all aircraft on their frequencies. That means this is an en route advisory, as well as a flight planning advisory.

There are also times when a sigmet issued by NAWAU covers such a large area to be confusing to pilots and controllers in an individual center's boundaries. For an example, imagine an aircraft flying from Albany (ALB), New York, to Concord (CON), New Hampshire, at 29,000 feet.

SEE EXHIBIT 2 FOR THE ROUTE FROM ALB-CON.

This flight could be part of a longer one, but this leg of the trip is in the Boston ARTCC airspace. At some point during the flight, the air traffic controller reads that Sigmet Alfa 1 is in effect for moderate or greater turbulence from flight levels 20,000 to 40,000 feet in an area bounded by Nashville (BNA), Tennessee, Portland (PWM), Maine, Cape Hatteras (HAT), North Carolina, Savannah (SAV), Georgia, and back to Nashville.

Does the flight from Albany to Concord cross the line into the area of expected turbulence? The majority of aircraft that ARTCC's deal with do not have a handy map of sufficient scale to determine that answer, which is not obvious. The pilot could ask the air traffic controller, who would then likely ask the CWSU meteorologist.

SEE EXHIBIT 3 FOR THE SIGMET AREA.

In cases such as this one, a CWA could be issued that would more clearly define the turbulence area for air traffic personnel and aircraft within the local boundaries. The CWA would have a heading that cross-references the applicable sigmet. In the example, if the sigmet were worded as such:

SIGMET ALFA 1 131500-131900

FM BNA-PWM-HAT-SAV-BNA.

NC SC GA TN KY VA WV MD DE NJ PA NY CT RI MA VT NH ME AND COASTAL WATERS

MDT-SVR TURBC FL 200-400. CONDS LKLY CONTG BYD 1900Z.

The CWA would be worded as such:

ZBW1 CWA01/ALFA 1 131500-131700

FM HNK-ALB-PWM-HTO-LGA-HNK.

MDT-SVR TURBC FL200-400. CONDS CONTG BYD 1700.

(Note that CWA's can only be valid for two hours.)

SEE EXHIBIT 4 FOR THE CWA AREA.

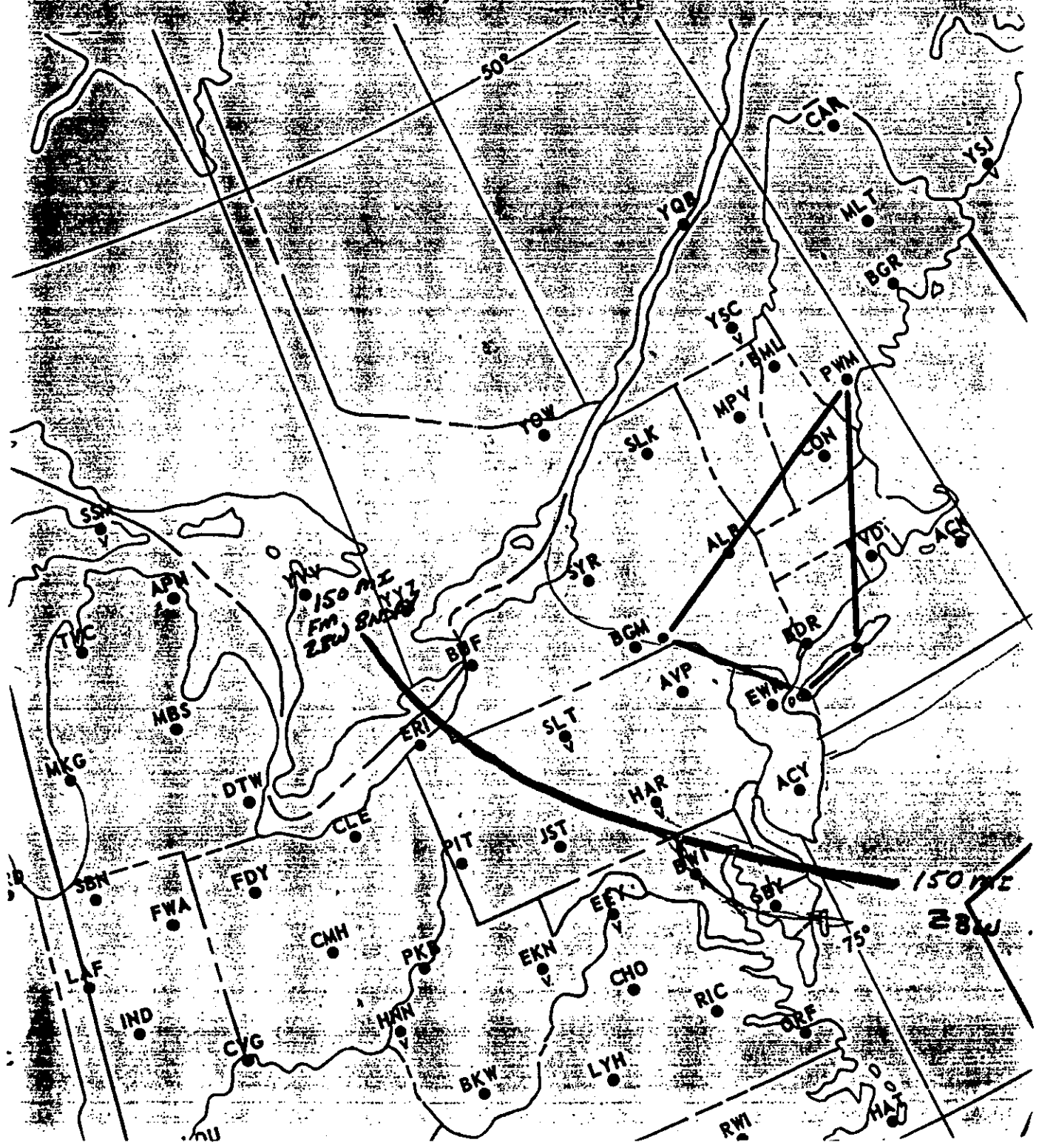
For a pilot whose flying is primarily confined to the Northeastern U.S., the area bounded in the CWA is easier to visualize than that in the Sigmet. As can be seen by looking at exhibits 2 and 4, the entire route from Albany to Concord is within the area of turbulence.

Because the CWSU is located in the same room as our primary consumers, the air traffic controllers, this allows us to be more responsive to the aviation community. We can issue a CWA shortly after receiving a few pilot reports. There have been cases when advisories have been requested by FAA supervisors. Occasionally a CWA will be issued as a leader for a forthcoming sigmet. FAA publications treat CWA's the same as sigmets, as far as dissemination to the aviation community.

During winter storms, a rapid response time can be especially valuable because of the frequently changing types of precipitation, wind speeds and directions.

ZBW1 QUA CI/ALFA I

EXHIBIT 4



LATE SEASON SNOWFALLS IN THE NORTH CAROLINA MOUNTAINS
ASSOCIATED WITH CUTOFF LOWS

Michael E. Sabones
and
Kermit K. Keeter

WSFO Raleigh NC

I Introduction

Late season snowstorms are a significant forecast problem in any part of the country. Late season snowfall events that occur with upper level cutoff lows pose some unique problems for the North Carolina mountains. Vertical temperature differences can result in snowfall during events that had no previous history of snow at lower elevations. Orographic effects from upslope flow during these events, as well as the dynamics associated with cutoff lows, help sustain enough cold air over the area to produce snowfall, while meteorological factors favor a rainfall event at lower elevations.

Two cutoff low events will be examined, April 2-5, 1987, and April 12, 1988. These were distinctly different events in some respects while quite similar in others. One element common to both cases was surface temperatures prior to each event. Daytime temperatures one day prior to each event were quite warm, generally in the 60s (F). A major snow event in April is a climatologically unlikely event in the North Carolina mountains, and warm surface temperatures prior to onset only made a major snowfall event seem more unlikely.

This paper will explore some of the problems forecasters had to deal with in a brief analysis of each event.

II April 2-5, 1987

This was a rather long lived episode that occurred when an open trough over the Mississippi valley, became a cutoff low over Kentucky and Tennessee. Some of the higher mountain locations received more than 40 inches of snow for the four day period. Snowfall totals ranged up to 60 inches, measured at Newfound Gap in the Great Smoky Mountains National Park on the North Carolina - Tennessee border. This was a new single storm snowfall record for North Carolina.

The 24 NGM 500 mb forecast for 1200 UTC, 3 Apr 1987 (fig. 1), indicated a negatively tilted open trough over the Mississippi valley. Areas of cyclonic vorticity were forecast around the bottom of the trough, and also on the west side of the trough near the Minnesota/Wisconsin border, associated with the jet stream digging into the trough. The 24 hour NGM surface forecast indicated a surface low pressure area on a frontal zone

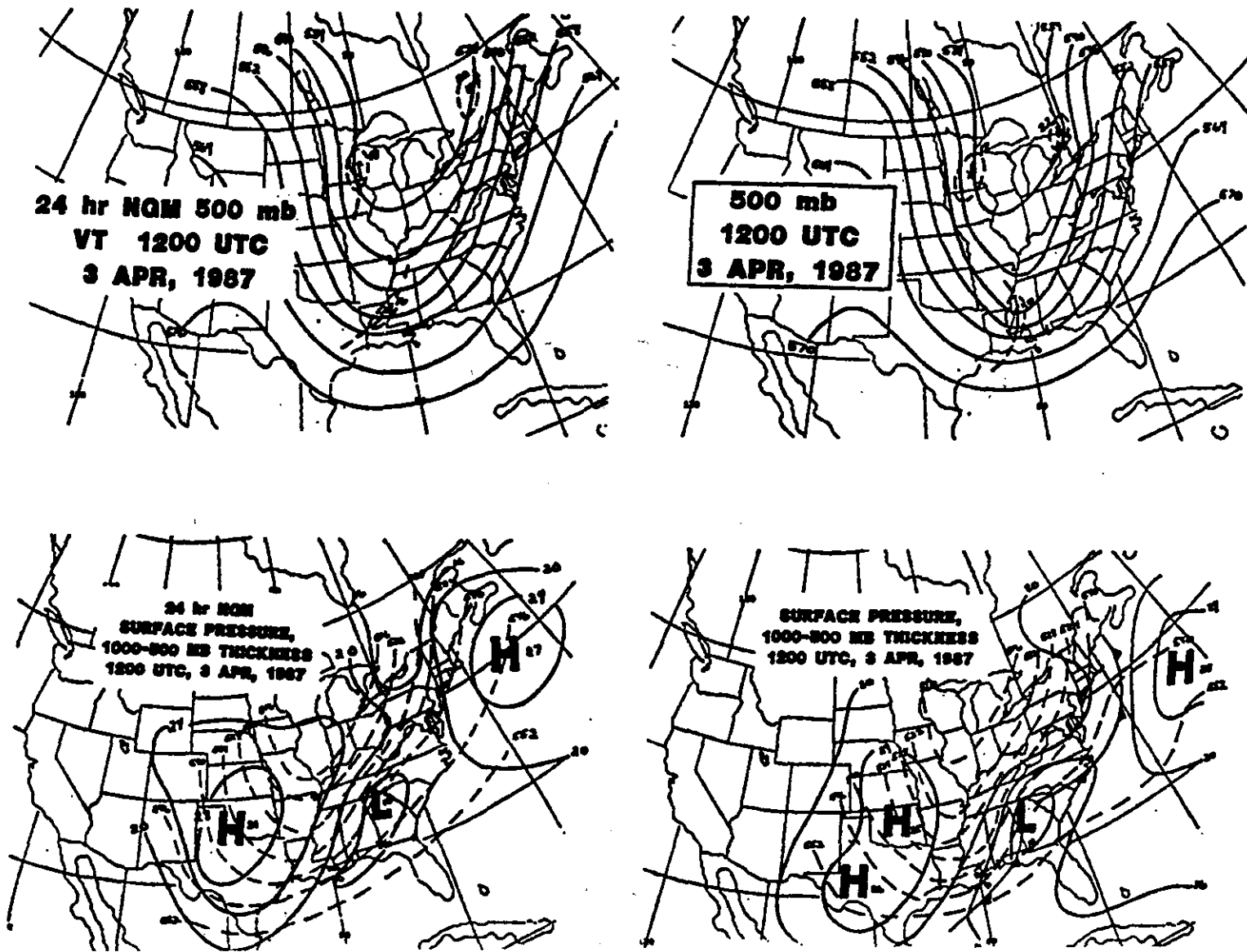


Fig. 1 NGM forecast and observed 500 mb height and vorticity, and surface pressure and 1000-500 mb thickness for 1200 UTC, 3 April 1987.

over northern Georgia.

These forecasts (fig. 1) verified quite well. The 1000-500 mb thickness values were cold enough to support snowfall over the area (generally accepted below 5430 m), so forecasting precipitation type was not a problem. The problem was how much.

The 24 hour NGM 500 mb forecast that was run 12 hours later for 0000 UTC, 4 Apr 1987 (fig. 2), indicated the open trough would continue to drift slowly eastward with cyclonic vorticity moving around the bottom of the trough. It had been snowing most of the day in the North Carolina mountains when this forecast was received. All indications were that the open trough would continue to move east.

Earlier model runs verified well so this scenario seemed reasonable. Snow was expected to taper off with only minor additional problems expected for the North Carolina mountains.

What verified 24 hours later was a different story! A cutoff low had formed at 500 mb over Kentucky and Tennessee (fig. 2). Cyclonic vorticity forecast to rotate around the system, and also on the back side of the trough associated with the digging jet max, was stronger than forecast. Once the 500 mb cutoff formed, the surface low deepened and moved into Virginia. Winds shifted from the southeast to the northwest with the passage of the low. Strong northwest winds on the back side of the low kept snow falling across many areas of the mountains all day on the 4th and 5th. The higher elevations received most of the snow in the later stages of the event.

One of the most important meteorological aspects leading up to the formation of the cutoff low with this event was the strong cyclonic vorticity related to the digging jet max on the back side of the trough. It would be difficult for a forecaster to determine the contribution of this factor to the formation of the cutoff low in real time, but it was one of the significant factors not handled particularly well by the numerical models.

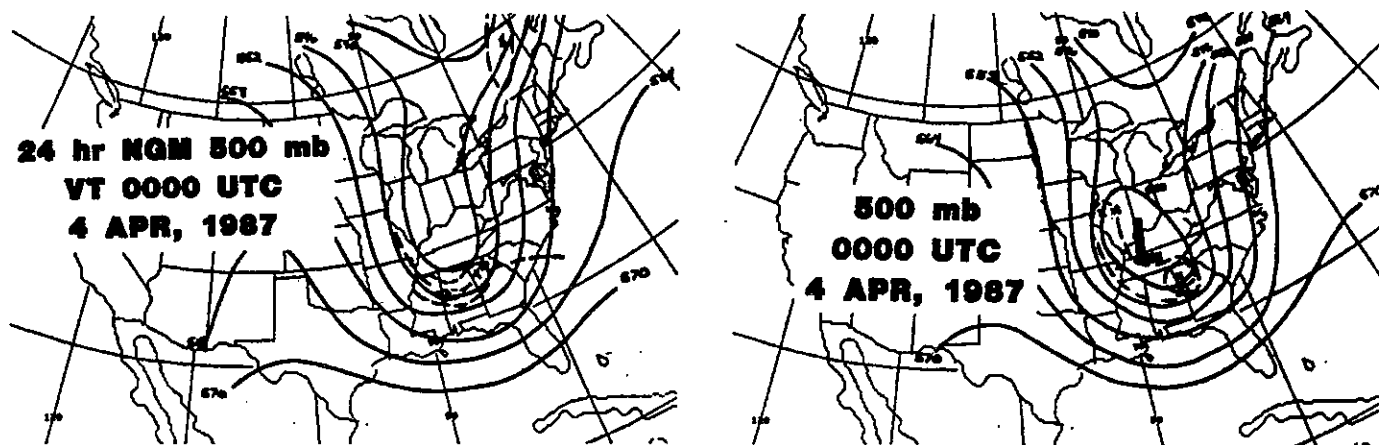


Fig. 2 NGM forecast and observed 500 mb height and vorticity, 0000 UTC, 4 April 1987.

Another forecast problem that is common with cutoff lows in the North Carolina mountains is strong winds when the cutoff low is east of the mountains. This cutoff low drifted east of the mountains on the 4th. Strong winds developed with blowing and drifting snow. Late evening of the 4th, the northwest winds became even stronger and reportedly toppled several trailer trucks on highway I-40 just east of Asheville.

III April 12, 1988

While this storm was not a record breaker in terms of snowfall, it posed some very difficult and unique forecast problems. Snowfall totals reached up to 18 inches on the higher peaks of western North Carolina with average snowfall totals in the North Carolina mountains between 4 and 8 inches. Cold air required for the snow in this case advected into the area from the south, a very rare occurrence for the North Carolina mountains.

The 24 hour NGM 500 mb forecast (fig. 3) for 1200 UTC, 12 Apr 1988, indicated the presence of a large 500 mb cutoff low over southern Alabama. This forecast verified with a deeper cutoff low a little further to east, over Georgia. This same trend was observed for the surface pressure field. The 24 hour NGM forecast indicated a surface low pressure area over Mississippi that actually verified a little further to the east.

The more important forecast problem for this case was in dealing with the forecast thermal field. The favored 1000-500 mb thickness threshold for snow in the North Carolina mountains is around 5430 m, as mentioned previously. The center of the cold air based on the 1000-500 mb thickness field was forecast by the NGM over southern Alabama (fig. 3). The observed center of the cold air at 1200 UTC, 12 Apr 1988, was further east, over Georgia. This was still south of North Carolina and forecast to move east. Yet snow began to fall in the North Carolina mountains around 0800 UTC and continued well into the afternoon. This took place despite the fact that almost all of the precipitation associated with this system prior to reaching the North Carolina mountains was in the form of rain, even in the center of the cold air.

A look at the 850-700 mb (fig. 4) helps explain what took place. An "X" marks the center of the 850-700 mb thickness cold air, first at 1200 UTC, 11 Apr 1988 (Missouri), then at 0000 UTC, 12 Apr 1988 (southwest Mississippi), and finally 1200 UTC, 12 Apr 1988 (north Georgia). The 850 mb level streamlines advect that cold air in Georgia directly into the North Carolina mountains from the south. The 1540 m thickness value for the 850-700 thickness field is used as the threshold value for snow in this column, so the 1520 m thickness air over Georgia certainly met that criteria. At lower levels, the 1000-850 mb thickness levels were generally too high (warm) for snow. This explains the lack of any previous history of snow with this system while it passed over lower terrain. The one exception occurred when snow was reported the morning of April 11, 1988 over the elevated terrain in the Ozarks of Missouri and Arkansas.

One of the most challenging questions that usually accompanies a cutoff low event is "how long will the thermal structure support snow?". Several mechanisms are usually at work with these systems that will affect the vertical temperature field, and most are difficult to judge in a rapidly

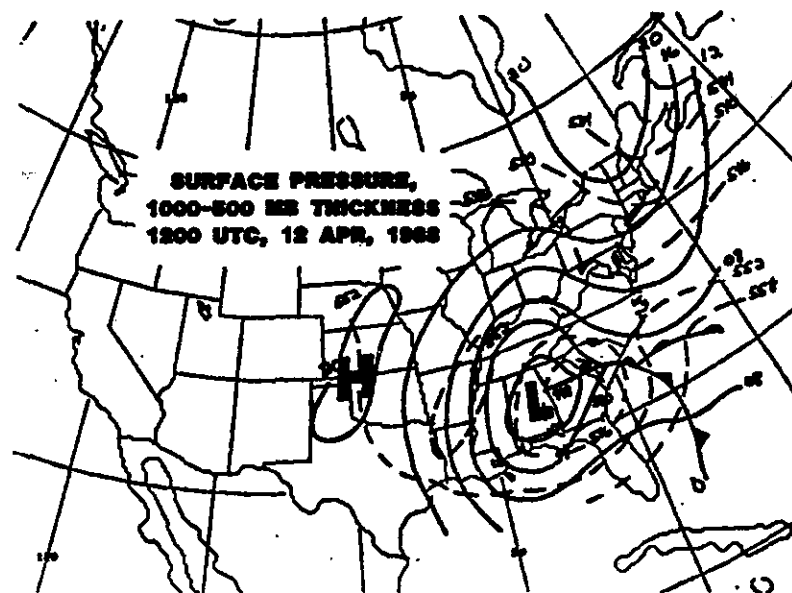
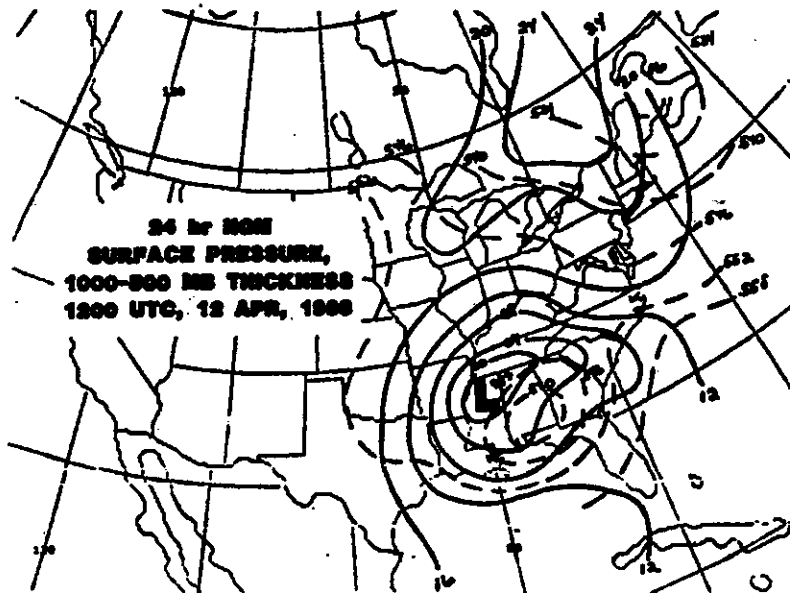
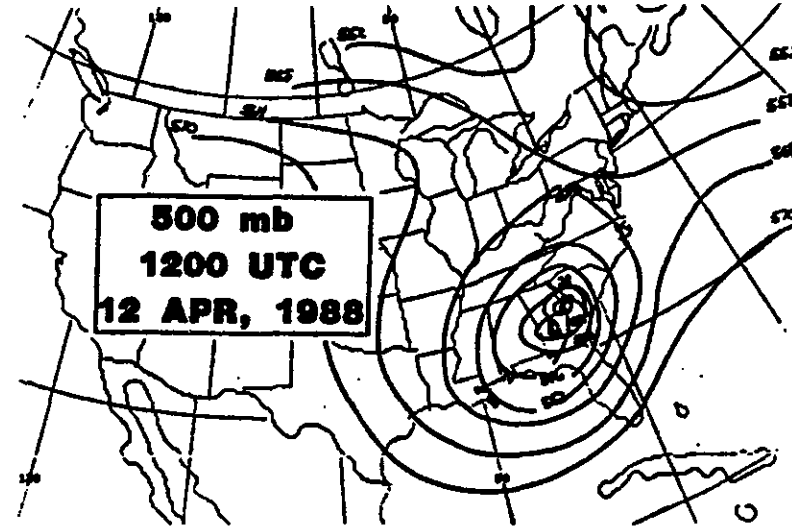
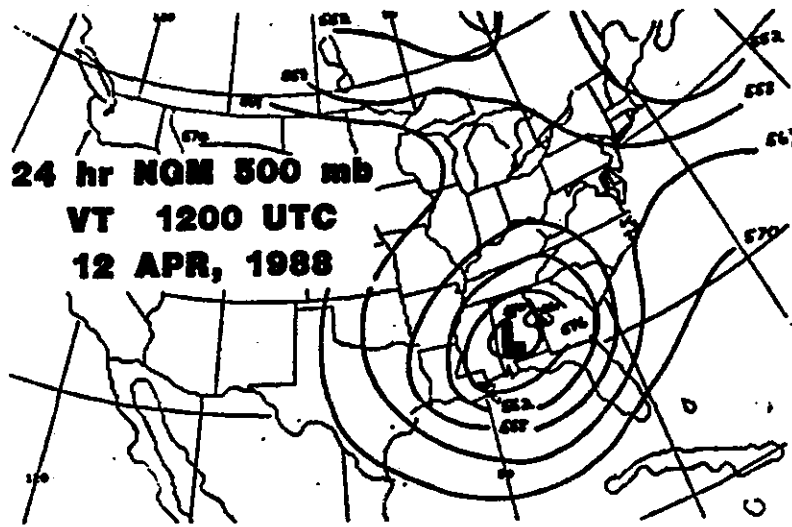


Fig. 3 NQM forecast and observed 500 mb height and vorticity, and surface pressure and 1000-500 mb thickness for 1200 UTC, 12 April 1988.

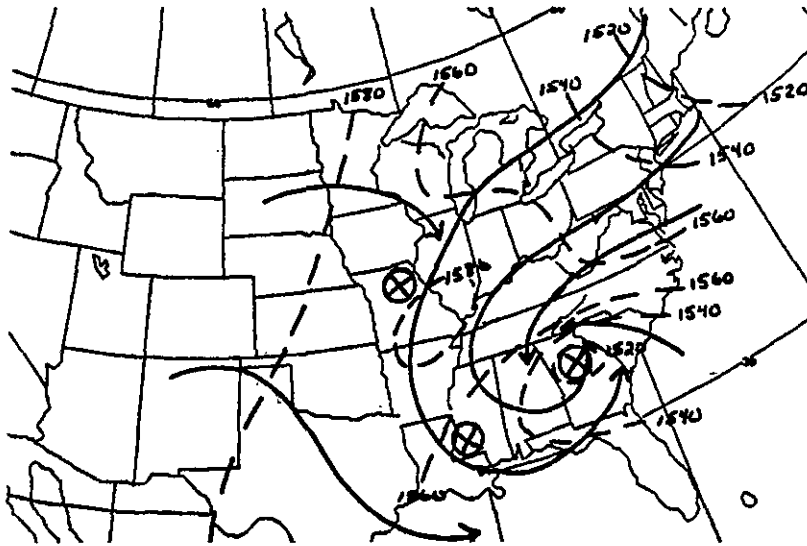


Fig. 4 850-700 mb thickness (dashed) and 850 mb streamlines (solid) 1200 UTC, 12 April 1988.

changing situation. In the 12 April 1988 case, the cold air advection from the south was then aided by evaporative cooling, cooling associated with orographic lifting, and cooling from dynamical lifting with the closed low. Cold air advection that was present from Virginia to Maine in the 850-700 mb column on 12 April 1988, may also have worked into the system during the later stages to prolong the snowfall.

One method used at WSFO RDU to account for the variety of mechanisms that affect the thermal structure, is a statistical approach based on the Greensboro sounding. The Greensboro sounding is usually representative of the air over North Carolina for a snowfall event. Regression equations have been developed to forecast the probability of frozen precipitation at a number of stations across the state based on this sounding. Unfortunately, this sounding was not representative of the air over North Carolina for this case. The frozen precipitation probability based on the Greensboro sounding for Asheville was quite low (fig. 5). However, if data from a sounding that was representative of the air over the area was used (Athens, Ga.), the forecast was quite good.

GREENSBORO SOUNDING
1200 UTC, 12 APR, 1988

GSO 1000-850 MB THICKNESS (METERS)....1333
GSO 850-700 MB THICKNESS (METERS)....1563
GSO 1000-700 MB THICKNESS (METERS)....2896

STATION	FROZEN PRECIPITATION PROBABILITY
AVL.....	12
HKY.....	0
GSO.....	0

ATHENS SOUNDING
1200 UTC, 12 APR, 1988

AHN 1000-850 MB THICKNESS (METERS)....1318
AHN 850-700 MB THICKNESS (METERS)....1519
AHN 1000-700 MB THICKNESS (METERS)....2837

STATION	FROZEN PRECIPITATION PROBABILITY
AVL.....	100
HKY.....	49
GSO.....	55

Fig. 5 Results of WSFO RDU's local guidance for predicting precipitation type, 1200 UTC, 12 April 1988 (Kermit Keeter, WSFO RDU, personal correspondence).

IV Conclusions

Every upper level cutoff low that develops in the late winter/early spring has its own individual characteristics, but there are also several common characteristics that can be applied to most of these systems for the North Carolina mountains.

The synoptic pattern at 500 mb usually is represented by a sharp, digging trough with a negative tilt, and a jet max on the backside. At the surface, there is a slow moving cold front with a low to the northwest of the North Carolina mountains along the cold front. As the 500 mb trough cuts off, the initial surface low fills, and a new surface low develops to the southeast of the old low. This system becomes vertically stacked, sits and spins, often for several days as in the 2-5 April 1987 case. Pockets of cold air capable of changing rain to snow in the mountains rotate around the system into the mountains from the north and west and even the south.

A snow advisory will probably be needed for the North Carolina mountains and a heavy snow warning will be possible. Strong winds will probably develop if the mountains are on the west side of the cutoff low. High wind warnings may be needed in this situation.

Significant weather is not only limited to the North Carolina mountains in these cases either. A pronounced dry slot may work into the systems, allowing clearing skies and rising temperatures east of the mountains. This results in a destabilizing atmosphere as colder temperatures aloft associated with the cutoff low move over the warmer air at the surface. Severe thunderstorms may then develop ahead of the cold front preceding the cutoff low.

At the North Carolina coast, gale warnings and possibly storm warnings may be needed if the low redevelops over the area south of Cape Hatteras and deepens.

There is one other major problem a forecaster usually has during these events. It is very difficult to find the time to properly analyze and then forecast all the implications that develop. Careful analysis and an understanding of the numerous forces at work and possible outcomes helps a great deal. It is also important to recognize the potential early so that adequate staffing can be made available.

V References

- Goodge, G.W. 1987: North Carolina - April 1987, Special Weather Summary. North Carolina CD Bulletin, April 1987, National Climatic Data Center, Asheville, North Carolina.
- Palmen, E. and C.W. Newton, 1969: Atmospheric Circulation Systems. Academic Press, 273-314.

GEORGIA WINTER STORM - JAN. 7, 1988

By

James Noffsinger and John Laing¹

DESCRIPTION OF EVENT:

A major winter storm occurred across a large part of the Southeast including North and Central Georgia on Thursday January 7, 1988. Accumulations of snow totaled 10 to 16 inches across the extreme northern counties of Georgia, and accumulations of mostly sleet totaled 2 to 4 inches in the north-central part of the state in a band across metropolitan Atlanta and Athens. (See Fig. 1). Farther south, in a broad band across the mid-state area from Columbus to Augusta, mostly sleet and freezing rain accumulated 1 to 3 inches on the average. A light glazing of freezing rain mixed with rain occurred across the south-central part of the state in a narrow band from Albany to Savannah. See Figs. 8 and 9 for the delineation of precipitation types.

This storm resulted in major disruptions of travel across the northern half of the state, and minor problems in the south-central area. About 36,000 power outages occurred in the state. Most occurred in the south-central part of the state where the freezing rain predominated, and in the extreme north where the heavier snowfalls occurred. Most businesses and nearly all of the schools closed down on the 7th and 8th, and most schools remained closed on Monday the 11th and Tuesday the 12th from the Atlanta and Athens areas north. Many school systems in the extreme northern counties, where the snow was more than a foot deep, remained closed through Friday the 15th due to snow-clogged streets and secondary roads.

The precipitation began as snow in the northwest corner of Georgia about 06Z on Jan. 7th and spread across the northern third of the state by 12Z. By 18Z on the 7th, the precipitation quickly encompassed the central part of the state as a mixture of sleet and freezing rain, and the southern third as a cold rain. The precipitation ended from the west between 00Z and 06Z on the 8th with the exception of some spotty freezing drizzle and light snow flurries.

SYNOPTIC SITUATION:

For several days prior to the event, the 500MB pattern was characterized by a deep low in southern Canada south of Hudson's Bay with a blocking ridge along the British Columbia coast. A strong northwesterly flow persisted from western Canada into the northern plains with a strong westerly flow across the Ohio Valley and Gulf Coast states around the base of the trough. The southerly branch of the westerlies was characterized by a strong zonal pattern from southern California across the northern Gulf.

¹National Weather Service Forecast Office; Atlanta, GA

A moderately strong short wave in the southerly branch moved on-shore into California at 00Z on Jan. 6th and continued east reaching West Texas by 00Z on the 7th. It then moved rapidly east across the Southeast between 00Z and 12Z on the 8th. (See Figs. 2 and 3).

At the surface, a cold arctic high across the plains states on the 4th and 5th established a pattern of cold air advection into the southeastern states. This high moved east into the Ohio Valley on the 6th, and was centered over Virginia on the 7th.

In response to the short wave in the southerly branch, a surface wave developed on the South Texas coast around 12Z on the 6th. (See Fig. 4). This weak low tracked east to the mouth of the Mississippi River by 12Z on the 7th, to the Florida Panhandle by 00Z on the 8th, and by 12Z on the 8th the primary surface low was on the North Carolina coast and moving northeast.

Very strong warm air advection developed aloft in conjunction with the surface cyclogenesis. The precipitation spread east just ahead of the strongest warm air advection and jet shown on the 850MB chart (Figs. 5, 6 and 7). In spite of the strong warm air advection aloft, the cold air held on stubbornly in the lower levels.

As the surface high moved east of the Appalachians, cold air damming developed down the eastern slopes of the mountains through the Carolinas and Georgia. The wedging nose of high pressure shown on Figs. 8 and 9 is evidence of the intensity of the cold air damming. Strong northeast winds with a cross-isobar flow developed in the lower 2,000 feet of the atmosphere, and the damming effect was intensified by the evaporational cooling as the overrunning precipitation began to fall into the cold dry surface air. As a result, surface temperatures held in the 20's across North Georgia and in the 30 to 35 degree range in the South throughout the day on the 7th.

The upper air soundings for Waycross and Athens at 12Z on the 7th are shown in Figs. 10 and 11. These soundings show the very strong temperature inversions in the lower levels, especially in the northern sections of Georgia. In addition, the sounding at Athens taken on the 8th at 00Z is shown as a dashed line to 850MB.

LOCAL FORECAST SOLUTION

Following the lead of the NMC extended forecast package, the possibility of frozen precipitation was first mentioned for Friday in the extended forecast issued at 445 AM on Feb. 4th. Although the actual event occurred one day earlier (on Thursday), this initial extended forecast alerted the public well in advance of the event.

The first zone forecast issuance to include the Wednesday night and Thursday time frame was the 445 PM issuance on Tuesday. This forecast correctly introduced sleet and snow for North and Central Georgia and mentioned the possibility of accumulations, although understated. This was followed by a winter storm watch issued at 445 AM Wednesday for North Georgia with a prediction of 4 inches in the extreme north and 1 to 3 inches in the Atlanta and Athens areas. The watch was extended south to include Central Georgia at 1110 AM, and the accumulations were increased to "4 inches or more" in the extreme North. The watch was upgraded to a warning at 430 AM Thursday. Special Weather Statements were issued frequently beginning early Wednesday morning.

In summary this winter storm event was predicted well in advance and comments from the Media and the Public were complimentary. The predictions of 1 inch in the mid-state area and 1 to 3 inches in the Atlanta and Athens areas proved to be very accurate. The snow did not change over to sleet in the extreme northern counties as expected, and thus the accumulations were understated in the early forecasts. Nevertheless, a prediction of "more than 4 inches" adequately alerted the public 18 hours in advance. The band of freezing rain was slightly further south than expected, and the advisory for the south-central part of the state was issued just at the onset.

FORECAST GUIDANCE

Extended guidance from NMC available the weekend before the storm gave strong indications that some type of winter weather would be in store for the Southeast later in the week. Both the extended forecasts Saturday and Sunday showed that maximum temperatures across Georgia Wednesday and Thursday would be 15 to 20 degrees below normal with nighttime lows well into the 20s. While precipitation chances were low on Wednesday, probabilities increased to 30 to 40 percent across the state on Thursday. For some reason the extended forecast guidance available on Monday delayed the onset of precipitation until Friday with smaller chances on Thursday.

Table A shows various forecast parameters derived from the LFM and NGM models beginning with the Tuesday morning run through the Wednesday evening run all valid Thursday 12Z (near the onset of precipitation in many areas). Table B shows similar forecasts for the LFM and NGM models only with valid time of Friday 00Z (about the ending time of precipitation in many areas). Forecasts for both Atlanta and Savannah are shown with the observed value of the various parameters. Atlanta and Savannah were chosen because each was near the border where the precipitation changed from rain to sleet (Savannah) or sleet to snow (Atlanta). Also more detailed FPC guidance was available for these two stations.

As can be seen from the tables both models were fairly consistent from run to run and were similar in their forecasts. Both models performed very well with neither model clearly superior.

From the LFM model, the FPC guidance for Atlanta and Savannah is shown in Table C for several runs preceding the storm. On the 00Z run the temperature in parentheses is an estimate of the Thursday morning minimum temperature derived from the 3 hourly values. For comparison the temperatures derived from the NGM/perfect prog technique are also shown.

It is interesting to review the Thursday 00Z guidance used in the forecast issued early Thursday morning. It was this guidance that would be critical in resolving the liquid/freezing/frozen precipitation areas within Georgia as well as snow amounts. The major (and as it turned out critical) shortcoming of this guidance was the overestimation of the surface dew points at nearly all points in Georgia. The observed dew points before the onset of precipitation, during the middle of the day, and late in the afternoon are shown as well as the ambient air temperature. It can be seen that this led to a serious underestimation of the cooling that took place as the precipitation began to fall into the very dry air. At several locations the precipitation began as rain but quickly changed to freezing rain, sleet, or a combination within an hour of onset. Thus rather than temperatures rising through the day with a changeover to liquid precipitation as indicated by guidance, temperatures fell and the precipitation remained a frozen mix as far south as an Albany to Savannah line.

The failure of the LFM model to correctly predict the dry air was due to the strength of the wedge along the east coast ahead of the developing storm system. This shallow pool of cold dry air is characteristically not handled very well by either model, especially the LFM. The strong northeasterly winds due to the cold air damming led to a reinforcement of the cool dry air over Georgia during the day Thursday. This in combination with the evaporative cooling which occurred with the onset of precipitation was responsible for the steady or slowly falling temperatures through the day rather than the warming as indicated by the FPC guidance. Therefore rather than the precipitation changing over to rain in the central and sleet in the north as indicated by MOS guidance, it continued as snow throughout the day in the north leading to an underestimation of snowfall amounts. The subjective guidance available from the Quantitative Precipitation Branch at NMC also placed the rain/snow line well north of Georgia.

It is interesting to note (See Figs. 8 and 9) that the surface temperatures across North Alabama were some 8 to 12 degrees F warmer than across North Georgia and Northwest South Carolina where the damming was in full force along the eastern slopes of Appalachians.

For example, the temperature at Savannah at the onset of precipitation around 9:30 AM was 32 degrees at Savannah with a dew point of 17 degrees. However the MOS guidance forecast an early morning dew point of 32 degrees. Guidance indicated a maximum temperature for Savannah of 48 degrees but at 1 PM Savannah was 32 degrees with a dew point of 22 degrees and intermittent freezing rain and freezing drizzle. Likewise at Atlanta the early morning dew point before the onset of precipitation was 9 degrees, considerably below the forecast of 19 degrees. Thus rather than warmer temperatures which would change the precipitation over to liquid in many areas, evaporative cooling allowed the precipitation to remain freezing or frozen throughout the day. Additional guidance for Columbus and Macon in Central Georgia also showed that the shortcoming was consistent throughout the state.

The sounding at Athens provides some insight into what happened during the day. As can be seen in Fig. 10 the sounding taken at 12Z Thursday shows the 850MB temperature was -7 C, about 7 degrees less than forecast by the models. However, this was near the base of a strong inversion and the temperature did rise to -1 C at 810MB. Below this level the dew point depression averaged about 9 C. The sounding at 00Z Friday shows dramatic warming at 850 MB (a temperature increase of 11 C in 12 hours) while the surface temperature was 5 C colder. The average dew point depression had decreased to less than 2 C. Therefore small scale effects due to the cold air damming that were not well resolved by either model served to prolong the winter type weather through the day despite the strong warm advection aloft.

WSFO Atlanta routinely analyzes the 1000-850 MB and 850-700 MB thickness charts from the AFOS plot routine which generates the plotted data locally. A careful analysis of these thickness values and applying "Younkin's Snow Index" has been very helpful in determining the boundaries between rain, freezing rain, and sleet/snow in previous winter storm events. Again this scheme proved to be very helpful on the January 7th storm.

Figs. 12, 13, and 14 show the "upper snow" line (850-700 MB thickness of 1555 meters), and the "lower snow" line (1000-850 MB thickness of 1310 meters). The area north of the "lower snow" line and south of the "upper snow" line usually defines the area of the freezing rain/sleet mixture. As seen on Figs. 12-14, this scheme worked out quite well and was generally accurate in defining the precipitation types. When the "upper snow" line lies along or to the south of the "lower snow" line, there will usually be a change over from rain to a wet snow with no intervening freezing rain or sleet.

Conclusion:

While available guidance did a good job in predicting the large scale features of this particular winter weather event, there were shortcomings in the details that were critical in determining the full impact of the storm. The shortcomings centered on the failure of the models to sufficiently account for the strong evaporational cooling in the lowest levels of the atmosphere which was caused by the cold air damming along the eastern slopes of the mountains. This in turn led to an erroneously fast warm-up by the models, and thus there was a much slower change-over from frozen precipitation to rain than indicated by the models. Subjective guidance from NMC generally followed the models. Forecasters at WSFO Atlanta recognized the potential for cold air damming early-on, and made significant adjustments in the guidance to more accurately assess the severity of the storm. Thus, the forecasts, watches, and warnings were very successful in alerting the public to the upcoming winter weather.

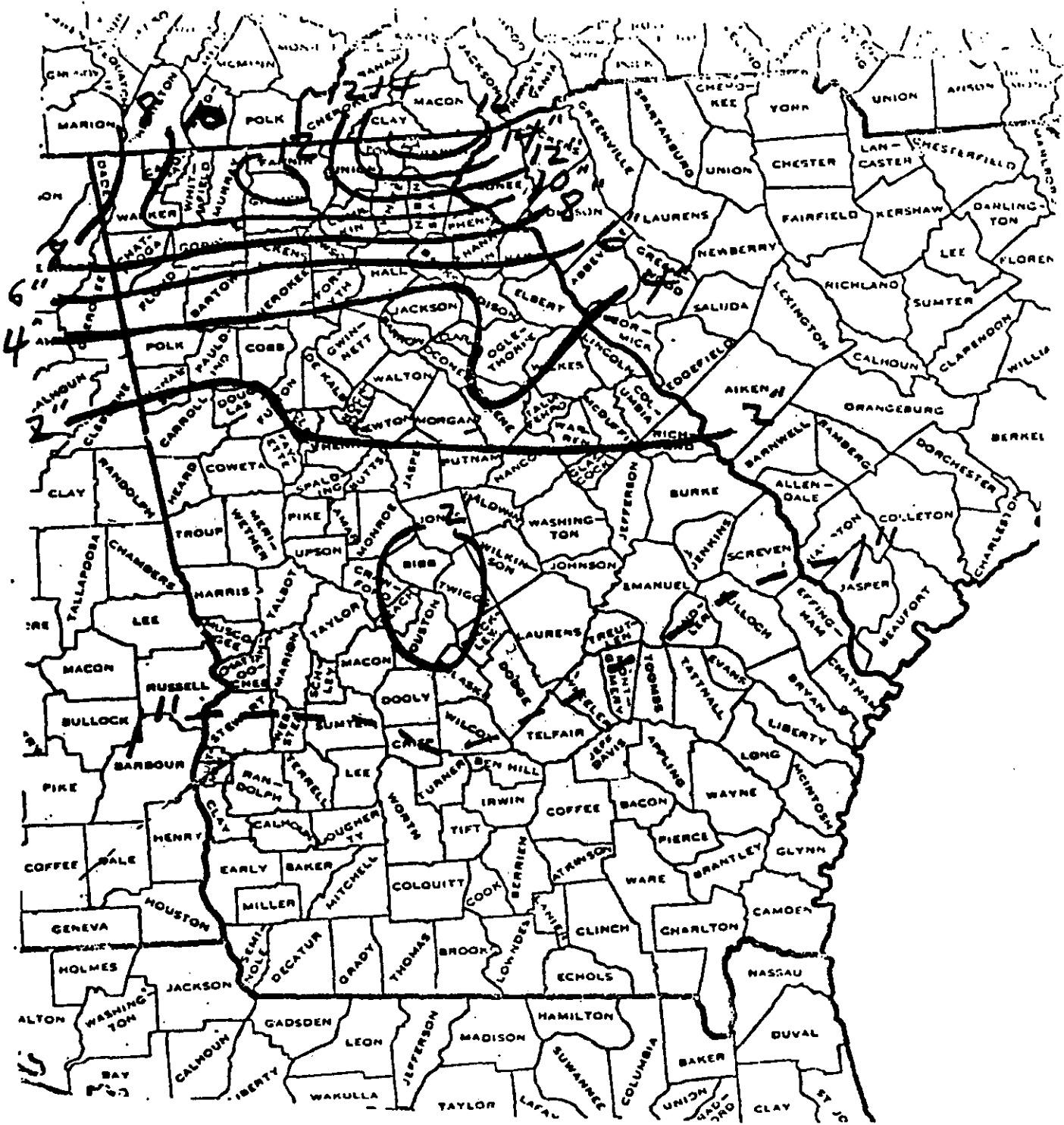


FIGURE 1. TOTAL ACCUMULATIONS OF SNOW/SLEET/FREEZING RAIN (INCHES) FOR JANUARY 7, 1988 STORM.

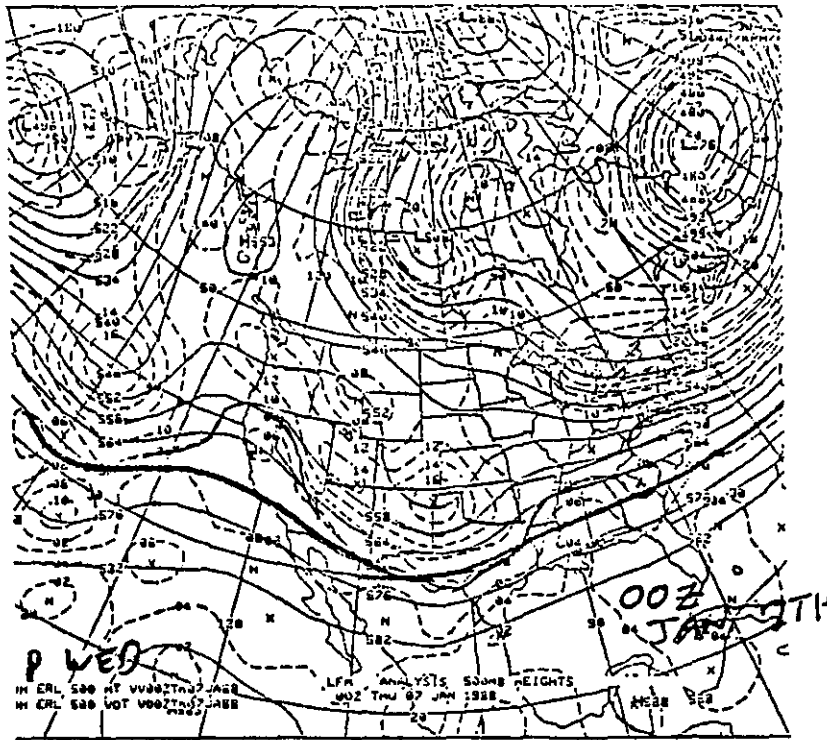


FIGURE 2. 500MB ANALYSIS AND VORTICITY PATTERN FOR 00Z, Jan. 7th, 1988.

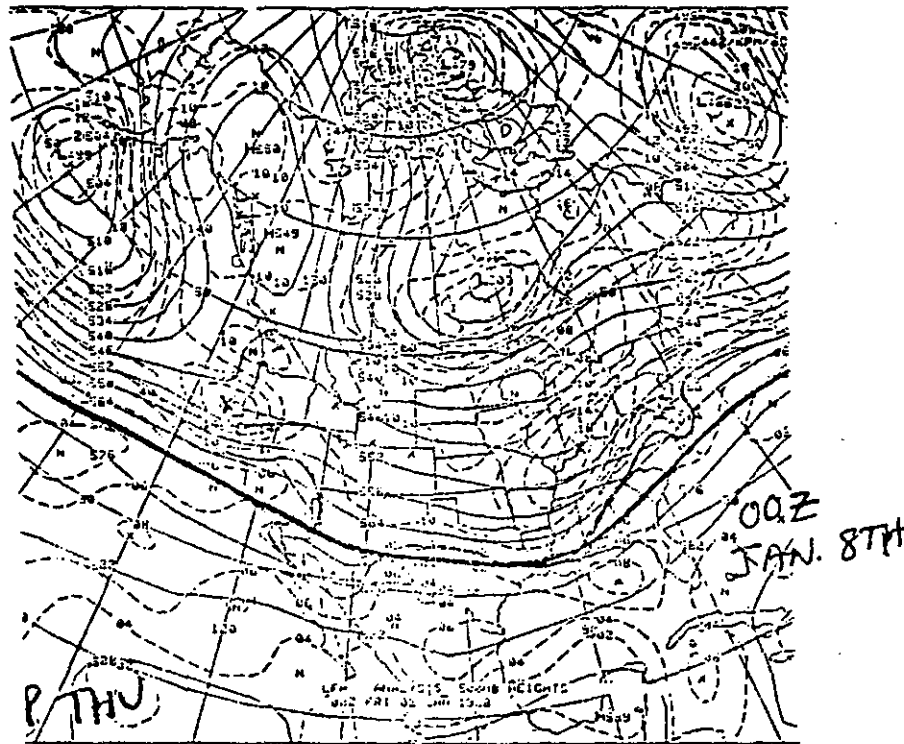


FIGURE 3. 500MB ANALYSIS AND VORTICITY PATTERN FOR 00Z, Jan. 8th, 1988.

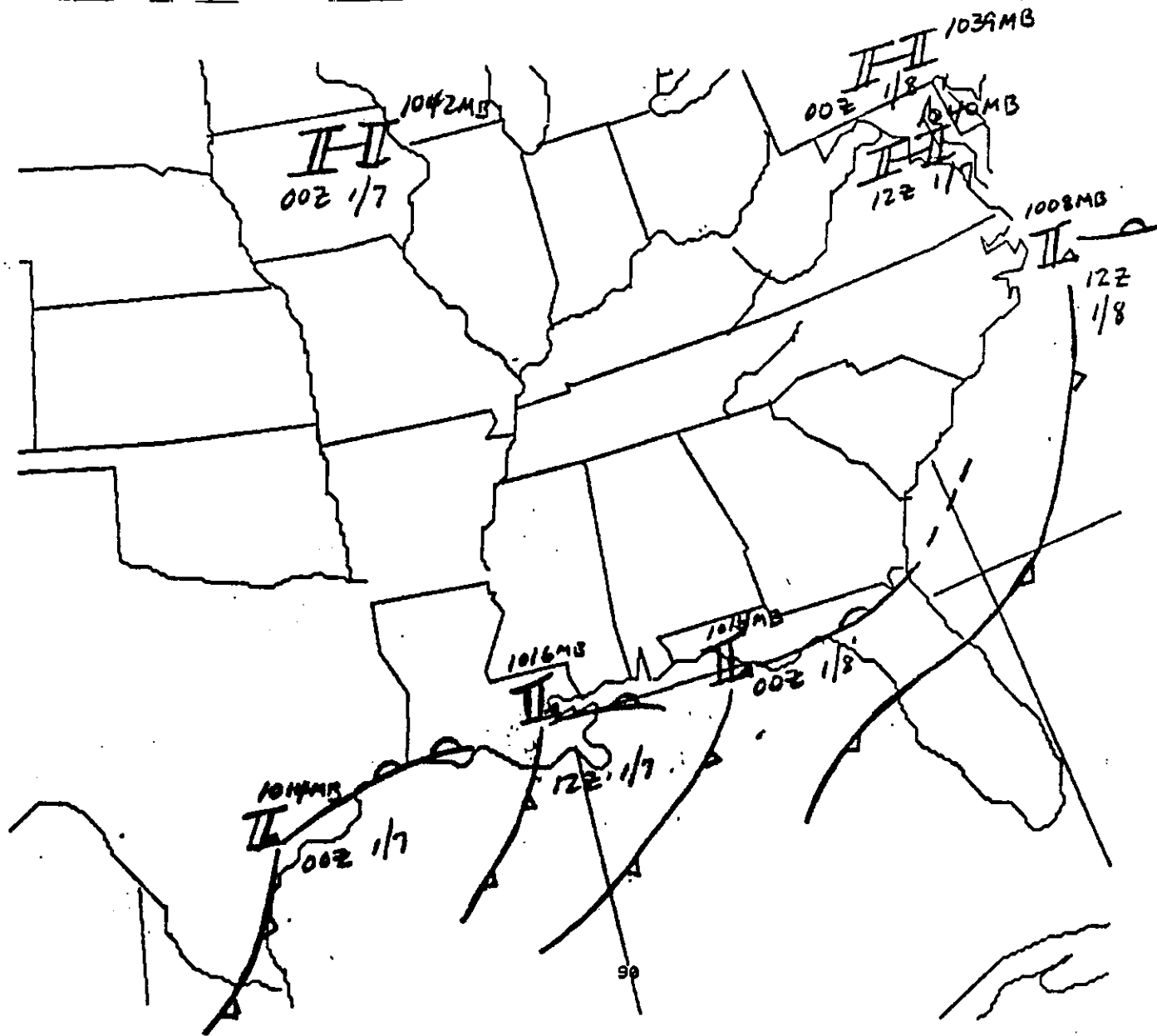


FIGURE 4. TRACK OF SURFACE LOW, HIGH, AND FRONTS FROM 00Z
 JAN. 7th THROUGH 12Z JAN. 8th.

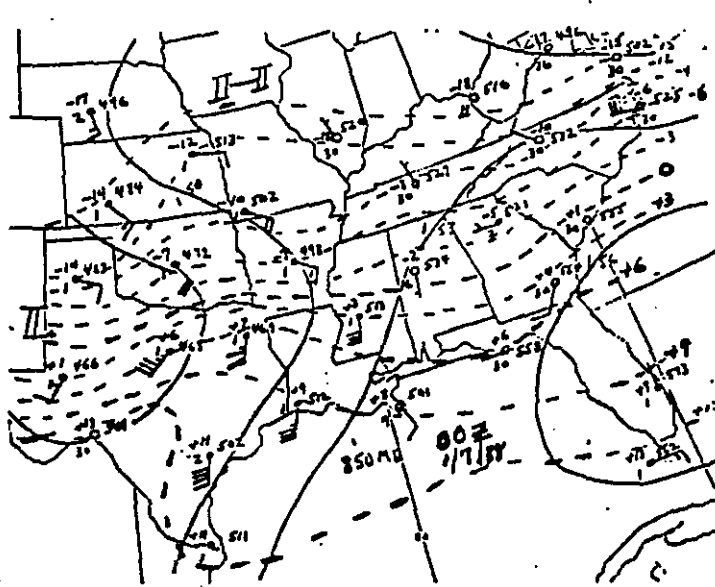


FIGURE 5

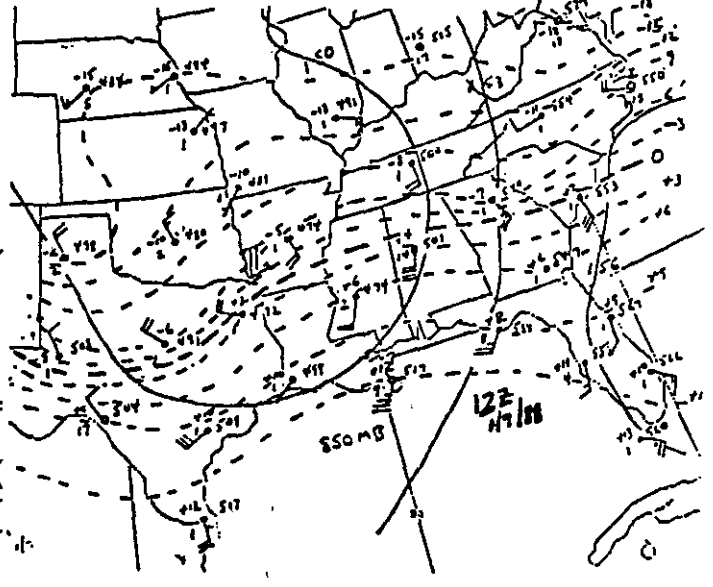


FIGURE 6

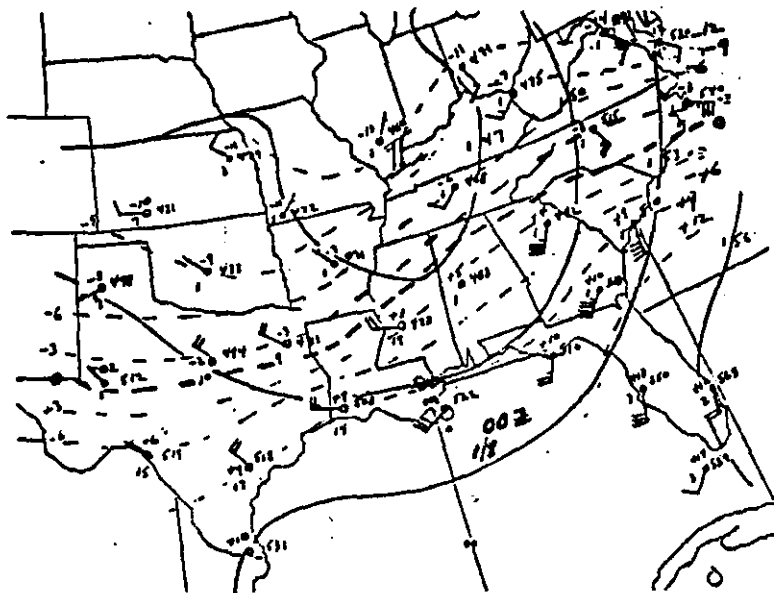


FIGURE 7

FIGS 5, 6, and 7.
 850MB ANALYSES FOR 00Z AND
 12Z JAN. 7th, AND 00Z JAN. 8th.
 ISOTHERMS AT 3 Degs. C intervals.

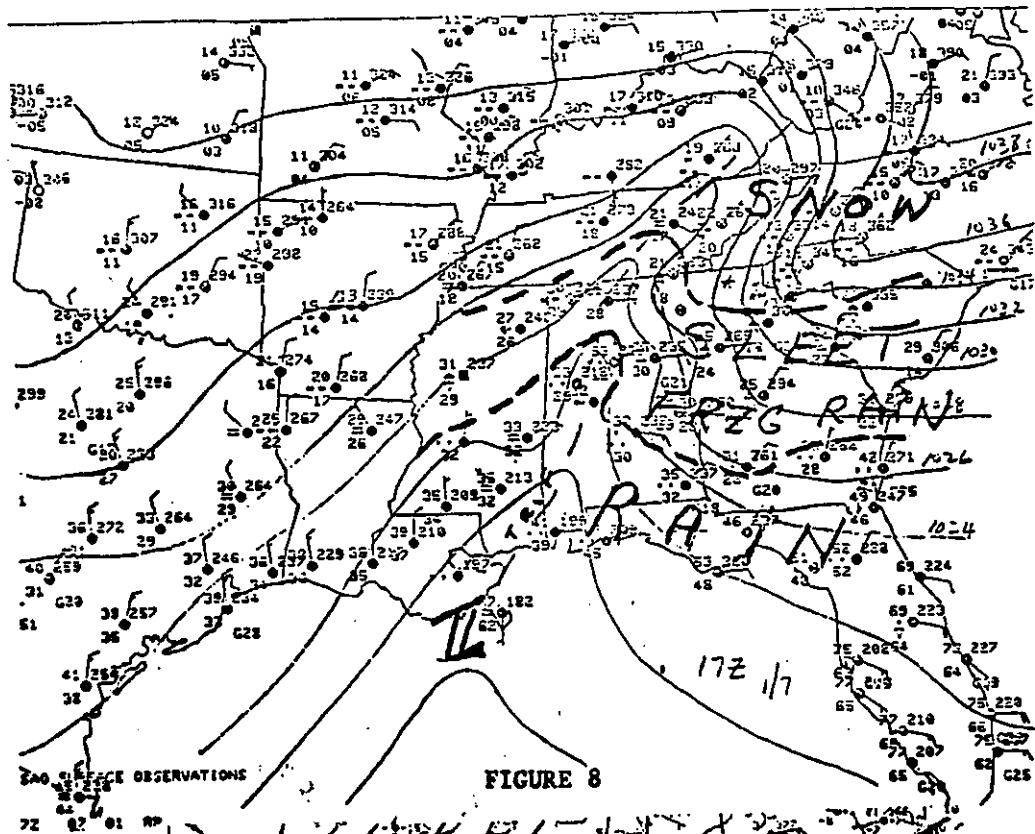


FIGURE 8

FIGS. 8 and 9.
 SURFACE ANALYSES FOR 17Z ON
 THE 7th and 00Z on the 8th
 DELINEATING RAIN, FREEZING
 RAIN, SLEET AND SNOW AREAS.
 NOTE ISOBARIC PATTERN
 SHOWING "NOSE" OF HIGHER
 PRESSURES THROUGH CAROLINAS
 AND GEORGIA TYPICAL WITH
 COLD AIR DAMMING.

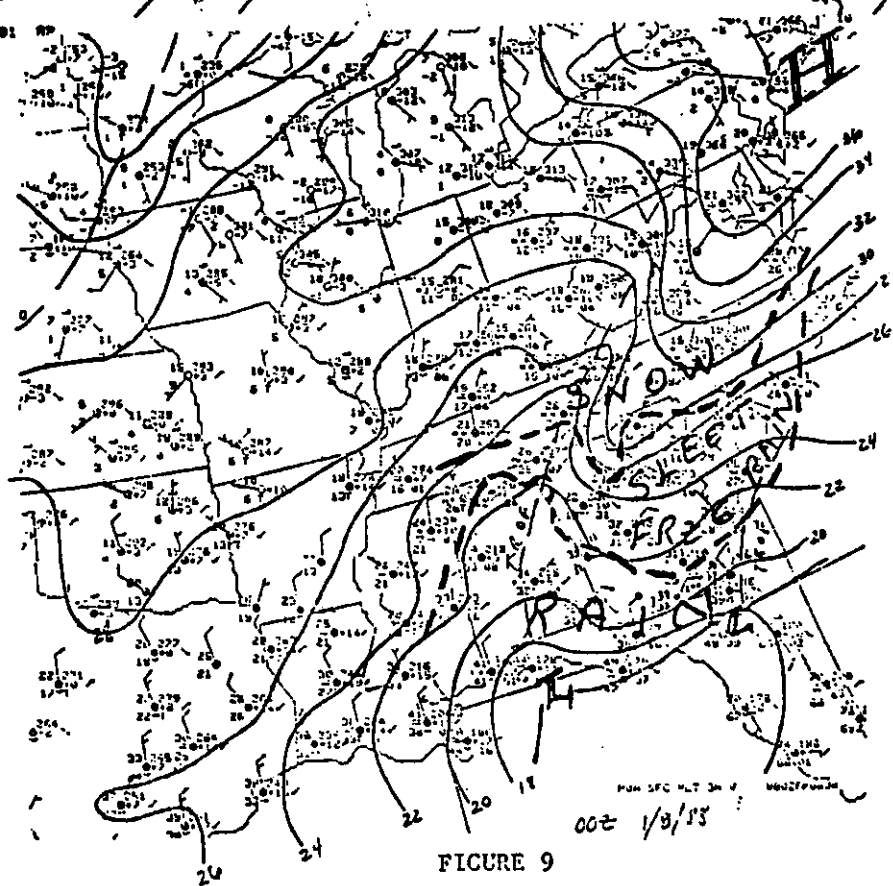
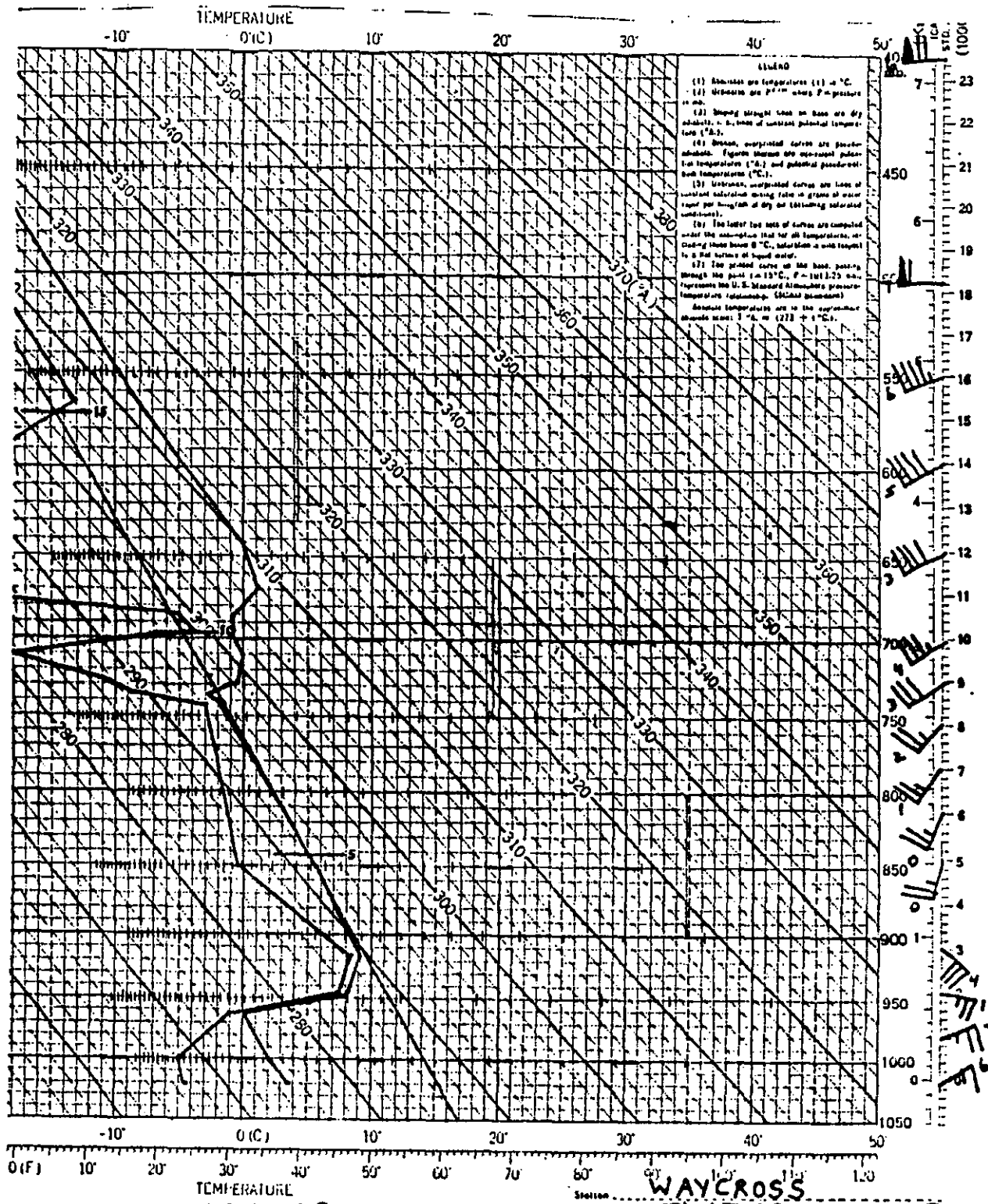


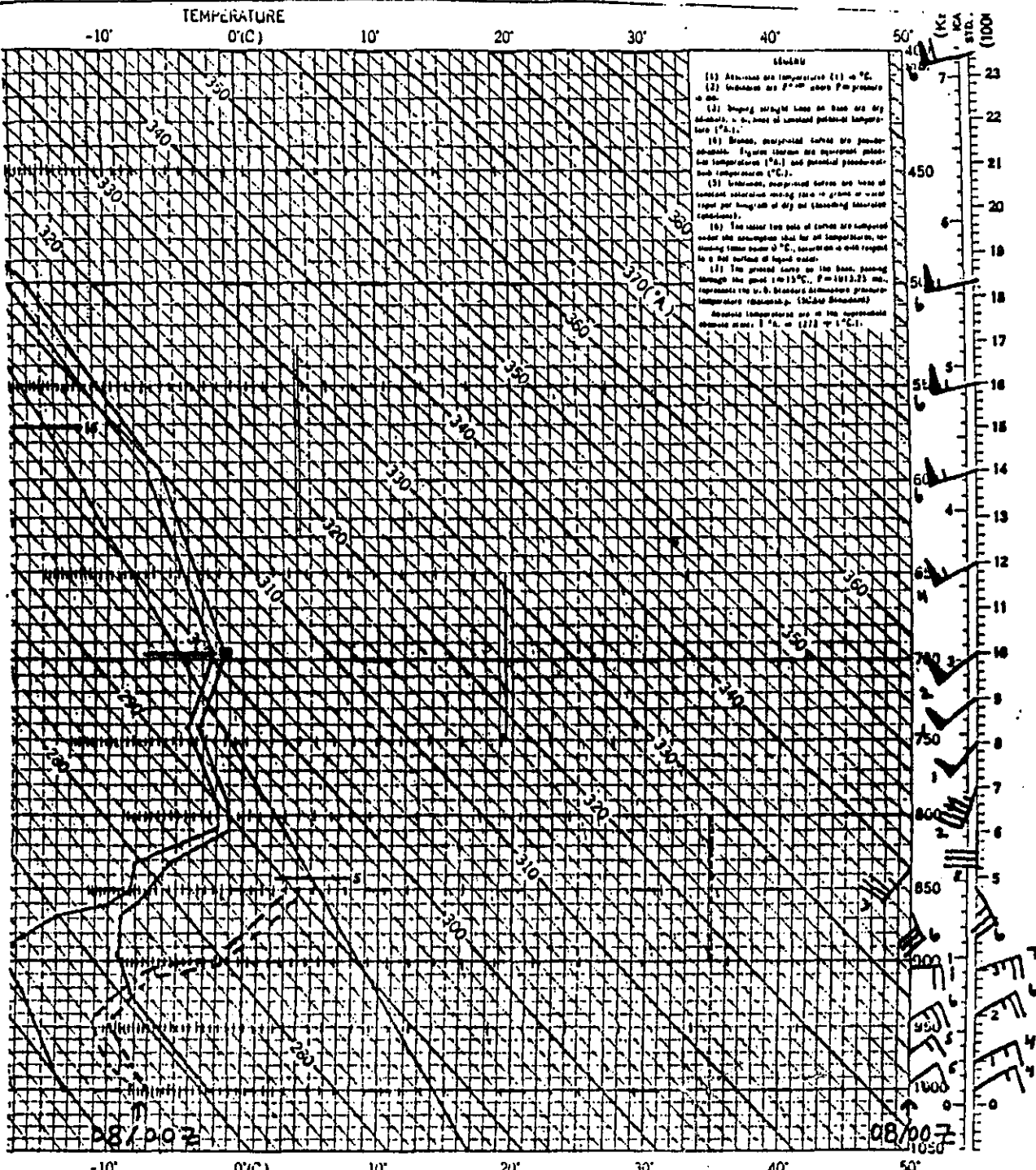
FIGURE 9



LEGEND

- (1) Humidity ratio temperatures (1) in °C.
- (2) Humidity ratio (1) in °F.
- (3) Sloping straight lines on base are dry-bulb lines, i.e., lines of constant potential temperature (°A.S.).
- (4) Dashed, overprinted curves are constant wet-bulb lines. Figure shows one constant potential temperature (18.2) and potential psychrometric temperature (18.2).
- (5) Vertical, overprinted curves are lines of constant saturated mixing ratio in grams of water vapor per kilogram of dry air (assuming saturated conditions).
- (6) The latter two sets of curves are computed under the assumption that for all temperatures, including those below 0°C, saturation vapor pressure is a half volume of liquid water.
- (7) The printed curve on the base, passing through the point 100°C, 0° = 100/2.5 mm. represents the U.S. Standard Atmosphere's pressure-temperature relationship. (SI units assumed).

Assume temperatures are in the appropriate absolute scale: 1 °A.S. = (273 + 1 °C).



(1) Absolute air temperature (t) in °C.
 (2) Wet-bulb air temperature (t_w) in °C.
 (3) Dew-point temperature (t_d) in °C.
 (4) Dry-bulb air temperature (t_d) in °C.
 (5) Saturation vapor pressure (e_s) in mm Hg.
 (6) Actual vapor pressure (e) in mm Hg.
 (7) Relative humidity (RH) in percent.
 (8) Mixing ratio (r) in grams of water vapor per gram of dry air.
 (9) Specific humidity (q) in grams of water vapor per kilogram of dry air.
 (10) Enthalpy (h) in kilocalories per kilogram of dry air.
 (11) Enthalpy of saturated vapor (h_g) in kilocalories per kilogram of dry air.
 (12) Enthalpy of saturated liquid (h_f) in kilocalories per kilogram of dry air.
 (13) Enthalpy of evaporation (h_{fg}) in kilocalories per kilogram of dry air.
 (14) Enthalpy of condensation (h_{cd}) in kilocalories per kilogram of dry air.
 (15) Enthalpy of fusion (h_{mf}) in kilocalories per kilogram of dry air.
 (16) Enthalpy of sublimation (h_{sg}) in kilocalories per kilogram of dry air.
 (17) Enthalpy of sublimation of ice (h_{si}) in kilocalories per kilogram of dry air.
 (18) Enthalpy of sublimation of water (h_{sw}) in kilocalories per kilogram of dry air.
 (19) Enthalpy of sublimation of snow (h_{sn}) in kilocalories per kilogram of dry air.
 (20) Enthalpy of sublimation of sleet (h_{sl}) in kilocalories per kilogram of dry air.
 (21) Enthalpy of sublimation of hail (h_{hl}) in kilocalories per kilogram of dry air.
 (22) Enthalpy of sublimation of rain (h_{rl}) in kilocalories per kilogram of dry air.
 (23) Enthalpy of sublimation of snowmelt (h_{sm}) in kilocalories per kilogram of dry air.
 (24) Enthalpy of sublimation of sleetmelt (h_{slm}) in kilocalories per kilogram of dry air.
 (25) Enthalpy of sublimation of hailmelt (h_{hlm}) in kilocalories per kilogram of dry air.
 (26) Enthalpy of sublimation of rainmelt (h_{rlm}) in kilocalories per kilogram of dry air.
 (27) Enthalpy of sublimation of snowmelt (h_{sm}) in kilocalories per kilogram of dry air.
 (28) Enthalpy of sublimation of sleetmelt (h_{slm}) in kilocalories per kilogram of dry air.
 (29) Enthalpy of sublimation of hailmelt (h_{hlm}) in kilocalories per kilogram of dry air.
 (30) Enthalpy of sublimation of rainmelt (h_{rlm}) in kilocalories per kilogram of dry air.

FIG. 11

Station **ATHENS**
 Date (G.C.T.) **JAN 7, 88** Hum (G.C.T.) **12Z (SOLID LINES)**
JAN. 8, 88 **00Z (DASHED LINES)**

TABLE A

FORECAST VALUES VALID THURSDAY 1200Z
ATLANTA

RUN	500MB H		1000-500 K		850MB T	
	LFM	NGM	-LFM	NGM	LFM	NGM
TUE/12Z	564	569	546	544	00 C	+1 C
WED/00Z	568	568	546	544	00 C	+1 C
WED/12Z	567	567	545	543	-1 C	+1 C
THU/00Z	568	567	545	545	-1 C	00 C
OBS	567		546		-7 C	

SAVANNAH

TUE/12Z	569	573	550	550	+2 C	+4 C
WED/00Z	573	573	549	547	+1 C	+5 C
WED/12Z	572	572	549	546	+2 C	+3 C
THU/00Z	572	571	549	551	+2 C	+2 C
OBS	574		552		+2 C	

TABLE B

FORECAST VALUES VALID FRIDAY 0000Z
ATLANTA

RUN	500MB H		1000-500 K		850MB T	
	LFM	NGM	LFM	NGM	LFM	NGM
WED/00Z	566	570	550	546	+3 C	+1 C
WED/12Z	564	568	550	546	+2 C	+2 C
THU/00Z	564	564	550	545	+3 C	+1 C
OBS	564		546		+4 C	

SAVANNAH

WED/00Z	572	575	554	552	+7 C	+3 C
WED/12Z	571	573	555	552	+7 C	+5 C
THU/00Z	571	571	558	552	+7 C	+9 C
OBS	573		557		+9 C	

TABLE C

FORECAST VALUES VALID THURSDAY 1200Z
ATLANTA

RUN	MIN TEMP		DEW POINT	POFT	PRECIP	PRECIP PROB	
	LFM/MOS	NGM/PP	LFM/MOS	LFM/MOS	TYPE	LFM/MOS	NGM/PP
TUE 12Z	24	MM	17	5627/1	ZR	40%	MM
WED 00Z	24	21	18	6422/1	ZR	10%	20%
WED 12Z	23	25	20	4242/1	ZR	40%	50%
THU 00Z	(26)	--	19	5637/1	ZR	--	--
OBSERVED	28		14		IP		

FORECAST VALUES VALID FRIDAY 0000Z
ATLANTA

RUN	MAX TEMP		DEW POINT	POFT	PRECIP	PRECIP PROB	
	LFM/MOS	NGM/PP	LFM/MOS	LFM/MOS	TYPE	LFM/MOS	NGM/PP
TUE 12Z	34	MM	--	--	--	70%	MM
WED 00Z	38	29	27	1010/3	R/MXD	80%	60%
WED 12Z	33	26	30	2014/3	R/MXD	90%	90%
THU 00Z	33	25	32	3407/1	ZR	100%	100%
OBSERVED	25 (21Z)		18		IP		
	22 (00Z)						

FORECAST VALUES VALID THURSDAY 1200Z
SAVANNAH

RUN	MIN TEMP		DEW POINT	POFT	PRECIP	PRECIP PROB	
	LFM/MOS	NGM/PP	LFM/MOS	LFM/MOS	TYPE	LFM/MOS	NGM/PP
TUE 12Z	28	MM	23	0807/3	R/MXD	20%	MM
WED 00Z	30	27	18	0707/3	R/MXD	10%	5%
WED 12Z	31	30	31	0703/3	R/MXD	20%	10%
THU 00Z	(35)	--	32	0102/3	R/MXD	--	--
OBSERVED	35		15		ZR/R (MOSTLY ZR)		

FORECAST VALUES VALID FRIDAY 0000Z
SAVANNAH

RUN	MAX TEMP		DEW POINT	POFT	PRECIP	PRECIP PROB	
	LFM/MOS	NGM/PP	LFM/MOS	LFM/MOS	TYPE	LFM/MOS	NGM/PP
TUE 12Z	45	MM	--	--	--	30%	MM
WED 00Z	43	36	41	0101/3	R/MXD	50%	10%
WED 12Z	44	38	41	0101/3	R/MXD	90%	60%
THU 00Z	48	40	43	0100/3	R/MXD	70%	90%
OBSERVED	30 (21Z)		28		ZR		
	31 (00Z)						

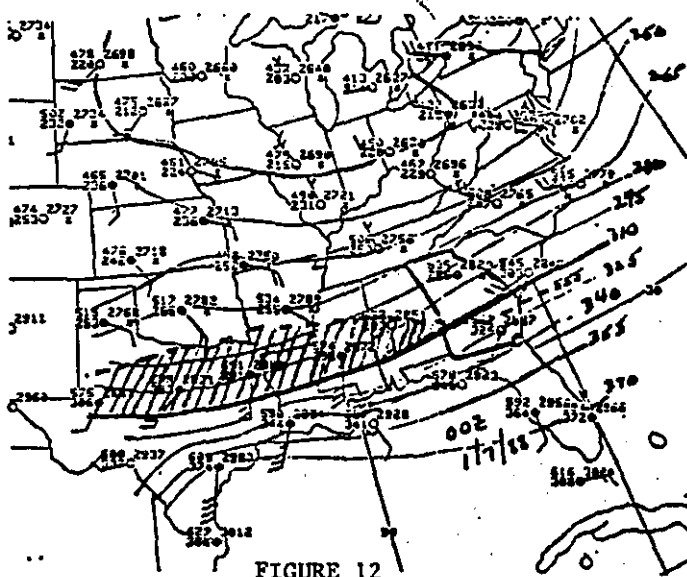


FIGURE 12

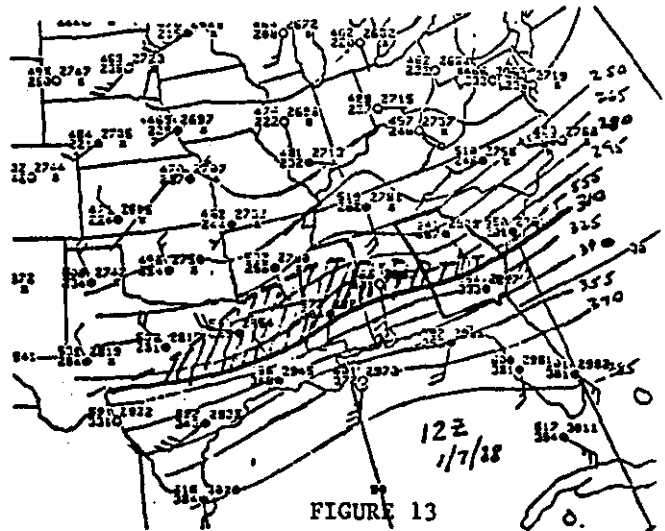


FIGURE 13

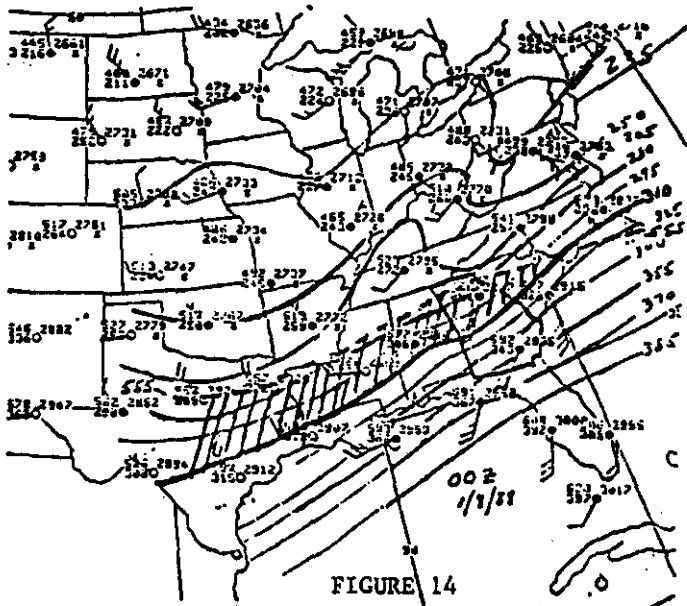


FIGURE 14

FIGS. 12, 13, and 14.
 1000-850MB Thickness Analyses
 in meters, and 1555 meter 850-700MB
 thickness line. (The first digit
 is omitted from chart, a one).
 Hatched area shows likely area
 of freezing rain/sleet located
 south of 1555m 850-700MB
 thickness contour, and north of 1310m
 1000-850MB thickness contour as
 suggested in "Younklin Snow Scheme."

RELATIONSHIP OF SNOW ACCUMULATION TO SOIL TEMPERATURE
IN SOUTH CAROLINA

Milton E. Brown
National Weather Service Forecast Office, Columbia, S.C.

ABSTRACT

On many occasions in the past 21 years, heat in the soil had a significant effect on winter weather in South Carolina. A heavy snow on roads was reduced to slush and a potential ice storm was prevented by the warm soil. There appears to be a good correlation between soil temperatures and the accumulation of snow or ice on the ground. An attempt has been made to stratify soil temperatures into three categories; (a) those which do not contribute to melting, (b) those which do contribute to melting, and (c) those in the intermediate range. This is considered a potential forecast tool for South Carolina. Caution should be taken in using it in other areas of the country without prior testing. Variations in soils and instrumentation may require some adjustments in the three categories.

1. Introduction

On February 26, 1982, measurable snow was expected to fall in Columbia, but since there had just been several days of mild weather, the forecaster felt the ground would be too warm for snow to accumulate. Realizing there were no temperature data available for the surface of the ground, he remembered having access to soil temperatures which are primarily used in agricultural weather forecasts in the spring. The soil temperature at the 4 inch depth at 7:00 a.m. that day was found to be 50°F which seemed to support the reasoning of the forecaster.

The local County Emergency Preparedness Director was briefed on the situation. He was told that significant snowfall would occur around midday and end during early afternoon. It was expected to melt on streets and roads and not be a serious problem for the late afternoon traffic. This turned out to be an accurate evaluation even though the air temperature remained at 31°F while the snow fell and for at least 6 hours after it ended.

2. Soil Temperatures

All references to soil temperatures from this point will be understood to be for the standard 4 inch depth. Maximum and minimum soil temperatures are available year-round on a daily basis from 15 locations in South Carolina (Fig. 1). Data from 4 of these sites are published in the monthly state climatological summaries by the National Climatic Data Center, Asheville, North Carolina.

Soil temperatures for a 5 day period prior to snow, sleet or freezing rain were examined. In nearly every case, the minimum soil temperature for the day before the occurrence of the precipitation was found to be as good or better than any other temperature or average as a predictor (Table 1). Minimum soil temperatures were primarily chosen because they do not fluctuate as much with sky cover as do maximum soil temperatures.

Minimum soil temperature for the day prior to precipitation is apparently a good predictor in South Carolina because winter storms usually last a day or less. Also, once the precipitation begins, it can take 12 to 24 hours for soil temperature to drop from one category to the next. Nevertheless, it would be beneficial to have soil temperature observations at least each six hours on the day of the event.

3. A Significant Heat Source

A weather event which occurred on Monday February 16, 1987, demonstrated just how significant a heat source the soil can be. A high pressure ridge was over much of the eastern seaboard east of the Appalachian Mountains, and a stationary front was along the Georgia-Florida border. A shortwave at 500 millibars moved eastward across the southeastern United States and caused a low to form at the surface off the Georgia coast. The low traveled northeast to near Cape Hatteras, North Carolina by 7:00 a.m. on February 17.

Rain began in Columbia at 12:40 a.m. and did not end until early evening. Total rainfall for the calendar day was 1.43 inches. The wind was brisk averaging northeast about 15 knots most of the day.

With an air temperature of 33°F at 9:52 a.m., a glaze began forming in trees about 50 feet and higher above the ground. Assuming the temperature where the glaze was occurring had to be 32°F or lower, the lapse rate would be approximately 20°F per 1000 feet for the shallow layer near the ground. A soil temperature of 50°F at 7:00 a.m. that morning indicated the soil was warm for that time of year and probably responsible for the super adiabatic lapse rate.

4. Soil Temperatures Not Associated With Melting

Snow, sleet or freezing rain occurred 26 times in Columbia from January 1968 - January 1988 with minimum soil temperatures of 42°F or below the day prior to precipitation. On 18 occasions the precipitation was not measurable or melted as it fell. Of the remaining 8 cases, snow or ice accumulated on the ground, and there was no apparent melting caused by heat from the ground.

5. Soil Temperature Range Associated With Melting

There were 17 cases found with snow, sleet or freezing rain and a minimum soil temperature of 48°F or higher the day preceding precipitation. On 10 occasions the precipitation was measurable. The ground was warm enough to cause melting in all except 2 cases which will be discussed in the conclusions.

In one case on March 24, 1983, in northwestern South Carolina, a nine inch snow was turned to slush on roads by warm soil. The air temperature was 34-35°F most of the day, but there was no sunshine to help the melting process. The minimum soil temperature was 48°F the day before. Although the slush slowed traffic a bit, it was never a serious problem for motorists. Five inches of snow remained on the ground over dormant grass at 7:00 a.m. the next day, but it had all melted by the morning of March 26.

6. Intermediate Range Of Soil Temperatures

The intermediate range has been tentatively defined as minimum soil temperatures of 43°F to 47°F, but most of the temperatures in the 22 cases in the study were closer to the middle of the range. There were 10 cases with measurable snow and/or ice on the ground and 12 cases with no accumulation.

In this category the temperature of the air became the most important factor in determining whether snow and ice would accumulate on the ground. Snow and sleet accumulated with an air temperature of 33°F or less, and rain formed a glaze on the ground at temperatures below freezing.

A good example occurred on March 25, 1971, when up to 10 inches of snow fell in northwestern South Carolina, stranding hundreds of motorists. The minimum soil temperature on the date prior to the precipitation was 46°F. Once the precipitation began the air temperature dropped into the lower 30's.

7. Ice Storm Just Across State Border In North Carolina

On January 3, 1988, there was a weather event which illustrates the effect of soil temperatures on winter weather. The plot of minimum soil temperatures for the Carolinas for January 2 (Fig. 2) would indicate that the soil was warm enough to melt ice which fell on the ground in all of South Carolina except for the northwest tip. But a large part of North Carolina was in the intermediate category and accumulation would occur if the air temperature dropped below 32°F.

Although a glaze formed on power lines and trees in northern South Carolina, the only ice on roads was within two to three miles of the North Carolina border in the north-central part of the state.

In North Carolina there was an ice storm which paralyzed the piedmont delaying or canceling commercial airline flights in and out of major airports, canceling some school days and causing numerous auto accidents. The mountain tops were above the shallow cold air and escaped the ice.

8. Conclusions

If the minimum soil temperature at the 4 inch depth is 42°F or colder in South Carolina on the day prior to the occurrence of snow, sleet or freezing rain, there is a very good chance that whatever falls to the surface of the ground will accumulate.

Soil temperatures in the intermediate range of 43 to 47°F do not appear to be a factor in determining whether snow or ice will accumulate. In this range the temperature of the air is the most important predictor. Air temperatures below freezing will cause the precipitation to accumulate, but when the air is above 35°F, there will usually be melting after snow or sleet reaches the ground.

The following examples show that the heat in the soil can be overcome if the volume of precipitation is heavy and the air temperature is cold enough. Both cases were rather unusual. The first occurred on January 7 and 8, 1973. The minimum soil temperature was 54°F on January 6. Measurable rain began between 6:00 p.m. and 7:00 p.m. on the 7th. The air temperature dropped to 30°F by midnight, and a glaze began forming. Cold air advection continued through January 8, and the temperature fell to 26°F. The freezing rain ended around 10:30 a.m. on the 8th, and very light snow was reported until late afternoon. Rainfall for the two days was 1.94 inches. The ice storm turned out to be one of the worst in years resulting in \$8 million worth of damage to the forests in the midlands.

The other case was about a month later on February 9 and 10, 1973. The minimum soil temperature on the 8th was 53°F which is quite warm, but a major winter storm moving northeastward well off the South Carolina dumped a 100 year record snowfall of 15 inches (water equivalent of 1.79 inches) on Columbia. The snow began during early afternoon but did not begin sticking to roads until the air temperature dropped to 30°F around 7:00 p.m.. There were four inches of snow on the ground at midnight, and an additional 11 inches fell on February 10. The soil temperature had dropped to 48°F by midnight on February 9 and to 45°F by 7:00 p.m. on the 10th.

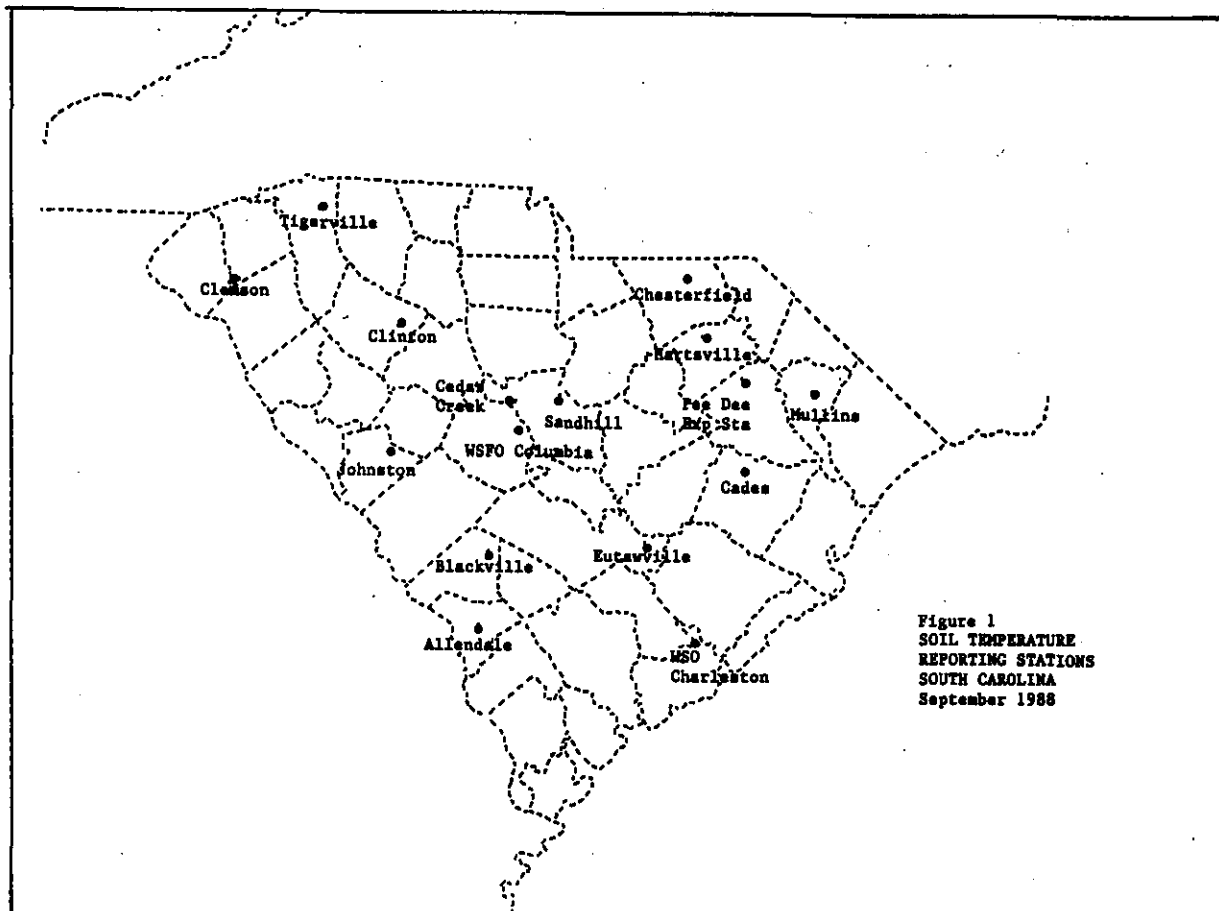


Figure 1
SOIL TEMPERATURE
REPORTING STATIONS
SOUTH CAROLINA
September 1988

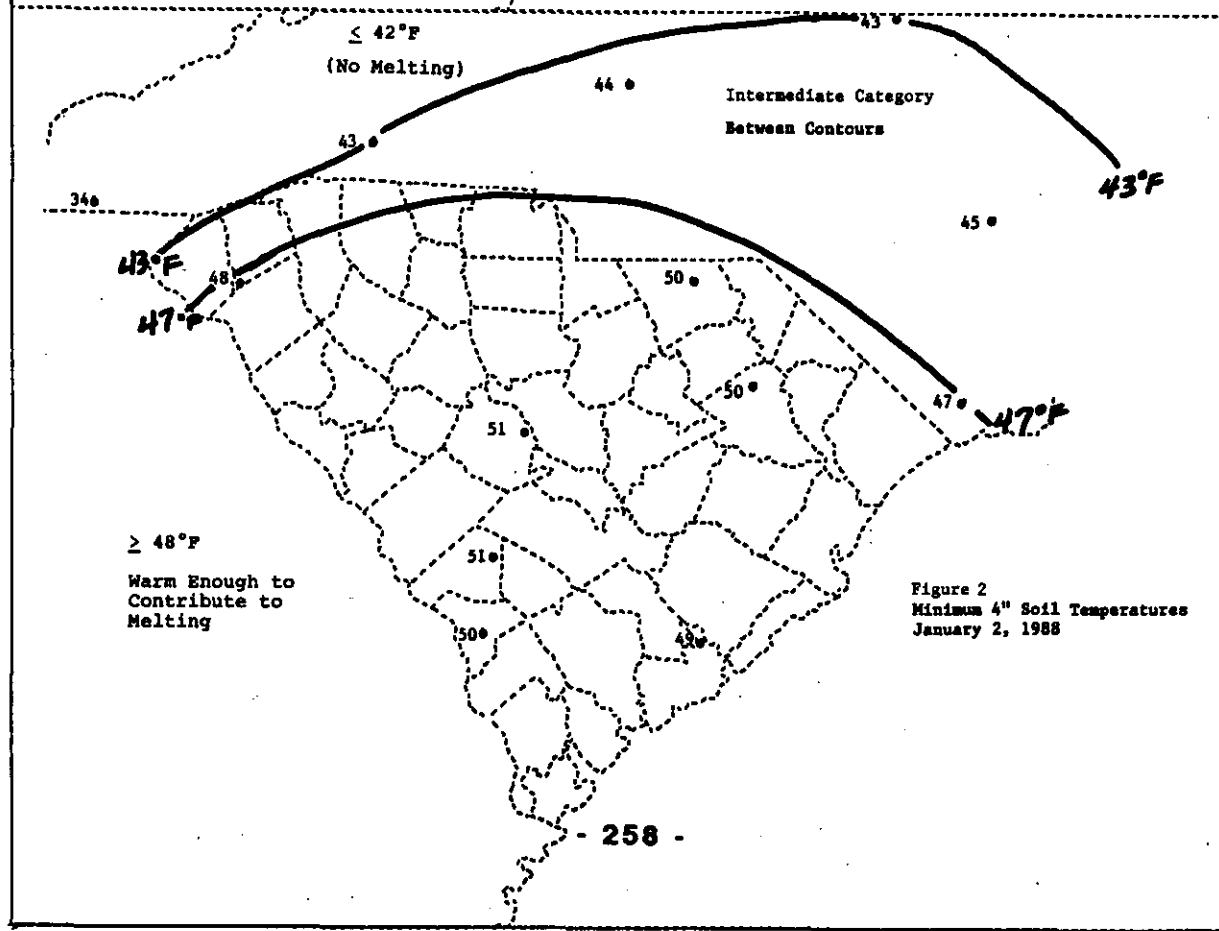


Figure 2
Minimum 4" Soil Temperatures
January 2, 1988

TABLE 1. Local Climatological Data for Columbia, S.C.
for February 1982.

Date	Air Temperature MAX/MIN	Soil Temperature MAX/MIN	Precipitation (Water Equiva- lent in inches)
21	72/48	60/51	0
22	59/32	56/50	0
23	73/29	58/48	0
24	81/52	60/52	0
25	59/42	57/53	0
26	43/31	53/43	0.64
27	37/32	44/43	0.39

SOME SYNOPTIC AND MESOSCALE INTERACTIONS IN A LAKE EFFECT SNOWSTORM

Thomas A. Niziol NWS Office, Buffalo, N.Y.

Abstract

On January 04-05 1988 a very localized, heavy snowfall event occurred to the lee of Lake Ontario, across the Tug Hill region of New York State. A narrow single band of lake effect snow deposited a maximum of 175 cm (70 inches) of snowfall over that area during a 2-day period. Synoptic scale weather features pre-conditioned the lower atmosphere for snowband development. Mesoscale features associated with Lake Ontario interacted with the synoptic scale weather pattern to produce the narrow band of heavy snowfall. This paper will present a short review of some of the more important synoptic and mesoscale characteristics associated with single banded storms on Lake Ontario, and relate these to the lake effect storm of January 04-05 1988.

1. Introduction

The term Lake Effect Snow refers to the mesoscale snow storms that occur as a result of cold air passing across the warmer waters of the Great Lakes during the late Fall and Winter months. Hill(1971) described the synoptic scale pattern responsible for heavy Lake Effect Snows to the lee of Lake Erie. In general, these conditions are representative for Lake Ontario as well. They include:

- (a). strong flow of arctic air across the lakes after a surface low pressure center has moved into eastern Canada.
- (b). southwestward extension of the parent Low in the form of a trough over the Great Lakes.
- (c). trough aloft over the eastern U.S. and Canada that frequently stagnates or broadens to the west.

2. Single banded storms on Lake Ontario

Usually a few times each winter season, single banded mesoscale

snowstorms occur to the lee of Lake Ontario that produce exceptional snowfalls. These storms exhibit similar synoptic and mesoscale features that can be forecast to some extent, over a relatively short (6-24h) timeframe.

Single band snows occur when the winds are directed roughly down the long axis of the lake. The bands are truly mesoscale in nature with lengths averaging up to 200km and widths about 20km. In a snow study on Lake Erie, McVehil and Peace (1971) further classified single band storms into two separate categories, overlake, and shoreline bands. They had similar characteristics, except, as their names imply, for their location over the lake. Overlake bands were aligned parallel to the average wind direction in the lower atmosphere, considered to be about the 850 mb level. Shoreline bands however, formed with steering winds oriented from just north of the long axis of the lake. They stated "that the shoreline band and its attendant surface convergence



Fig 1. Visible satellite imagery depicting snowbands to the lee of the Great Lakes at 1801 UTC, 05 January 1988. (imagery courtesy of NESDIS)

zone remain quasi-stationary along the shore of the lake, despite a "slight" crosswind component in the winds aloft". They suggested that the stagnation of the surface convergence zone and snowband offshore, was a result of a land-sea breeze circulation caused by a strong temperature contrast. This was considered a primary factor for snowband orientation. The similar elliptical shape of Lake Ontario to Lake Erie should also allow for this type of snowband formation.

Peace and Sykes (1966) also were able to observe the very strong mesoscale convergence zone associated with a single banded storms on Lake Ontario. The vertical motion field that developed under the snowband as a result of the strong surface convergence zone, literally created a self-sustaining environment for the snowband, until some synoptic scale feature could displace it.

Synoptic scale forcing, in the form of cyclonic vorticity advection below 500 mb, can moisten and destabilize a column of air for some vertical extent in the lake effect snow environment (Jiusto and Paine 1971). This promotes convective development of lake clouds that are otherwise capped by a low level arctic

inversion. Snowfall rates are greatly increased, as a result of the deeper convective layer, and lightning and thunder are not uncommon.

A relatively flat, or broad east-west trough across the Great Lakes assures an extended period of westerly winds over the long axis of Lake Ontario. The snowband therefore, remains relatively stationary over one locale, for an extended period of time, and produces extreme, localized snowfall amounts.

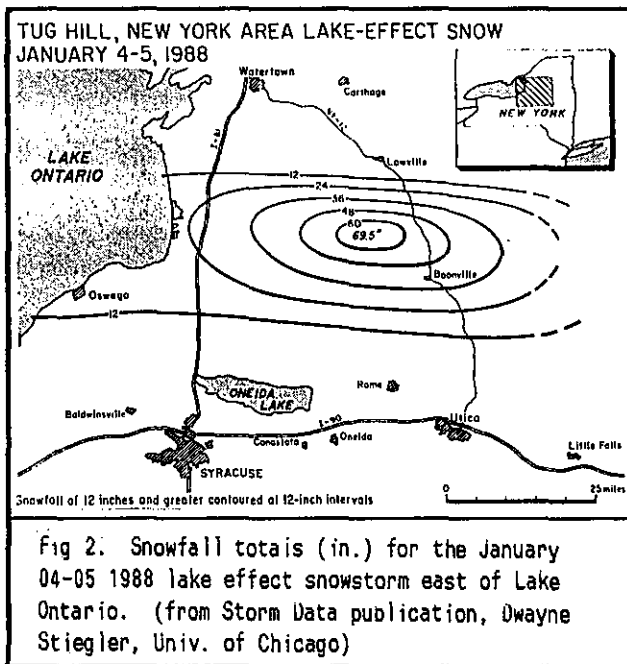
The abrupt rise in elevation to the lee of Lake Ontario (about 500m from the lakeshore to the top of the Tug Hill plateau some 30 miles to the east), further enhances snowfall rates. Muller (1960) noted a substantial increase in annual snowfall, directly attributable to the rise in elevation to the lee of Lake Ontario.

All of these factors contributed in varying degrees to the lake effect storm of January 04-05 1988, and will be discussed on the following pages.

3. The Lake Effect Storm of January 04-05 1988

During the first week of January 1988, an arctic outbreak occurred across the Great Lakes Region, and produced very heavy mesoscale snowstorms to the lee of the Great Lakes. This event was spectacular to the east of Lake Ontario, where a very narrow band of snow deposited nearly 175 cm (70 in) of snowfall during a 2-day period (Fig 1).

Some important factors contributed to the extreme snowfall amounts. These included a combination of very strong cold air advection over the relatively warm lake, wind direction at 850 mb that was nearly parallel to the long axis of Lake Ontario, and synoptic scale forcing that contributed to convective enhancement of the snowband. The highly localized snowfall maximum was a result of a nearly constant wind direction over the lake, for about a 36 hour period, which confined the snowband over one, select location.



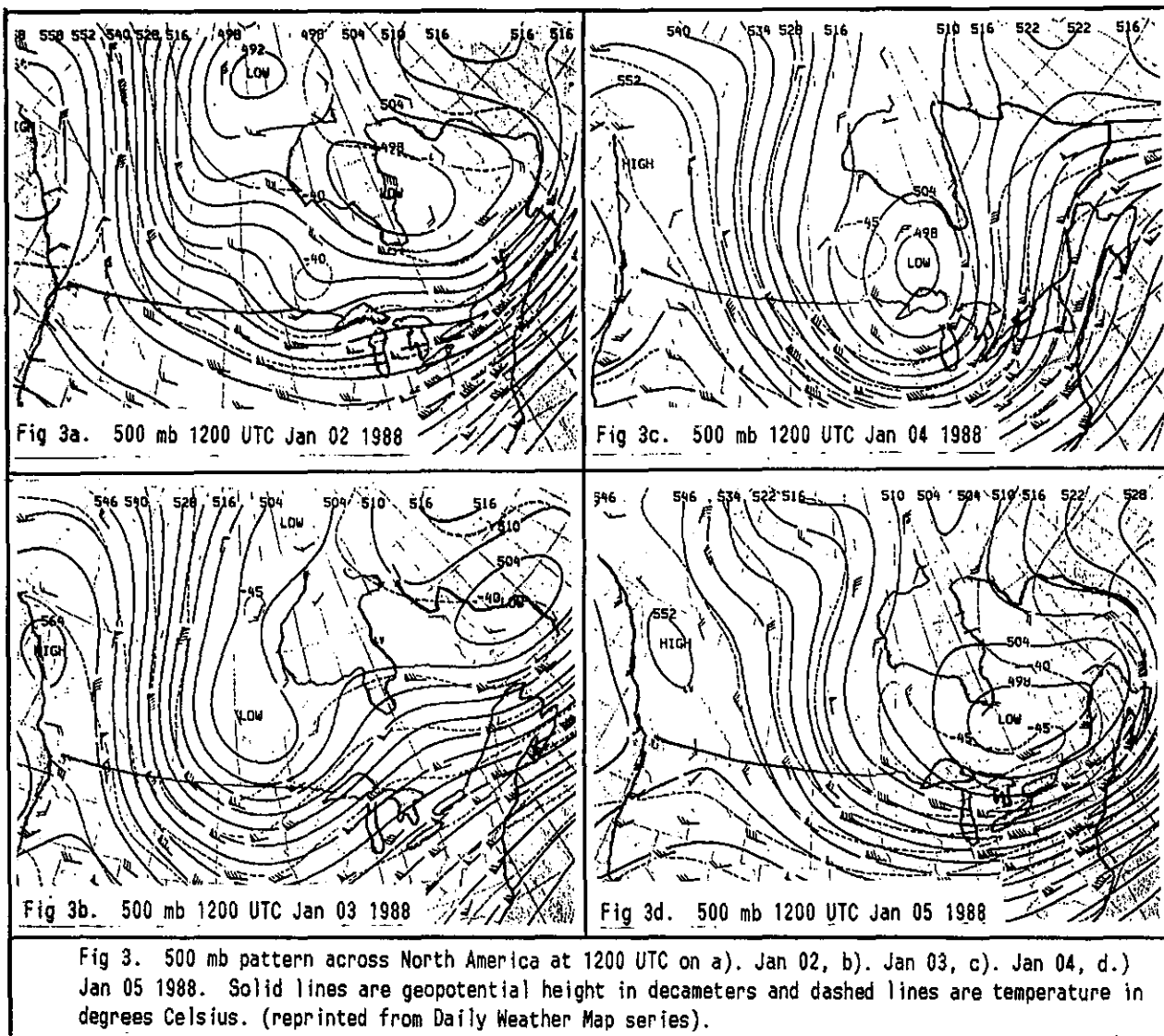
The mesoscale nature of the storm is readily apparent from the map of the snowfall totals east of Lake

Ontario (Fig 2). The maximum snowfall occurred at Highmarket, where 175 cm (69.5 in) accumulated over a 2 day period. Only 15 miles to the north, storm totals were 15 cm (6 in) or less, and the same was true about 25 miles to the south (storm totals dropped off a bit slower to the south due to the southward migration of the snowband before it dissipated). According to Gerald Morczk, the cooperative observer at Highmarket, this was one of the heaviest snows in his location that he could remember. That was a strong statement for a spot that averages over 225 inches of snow annually!

The snow to water ratio computed for the Highmarket area was about 20:1. That is not uncommon for Lake Effect storms that often occur in an "arctic" airmass. Hill(1971) stated that snow to water ratios as high as 50:1 have been reported from these events.

4. Synoptic scale weather pattern responsible for the Highmarket snowstorm.

During the first week of January 1988, a 500 mb pattern developed over North America that allowed for a significant arctic outbreak across the Great Lakes Region (Fig 3a). A meridional 500 mb ridge was over the west coast of North America, and there was a deep polar vortex over Hudson Bay. On Jan 3rd, a Low north of the arctic circle, began to move due south toward the upper Great Lakes, and carved out a new trough that eventually deepened into a closed Low just south of James Bay Canada (Figs 3b,3c). This position is a preferred one for the single band storms that occur to the east of Lakes Erie and Ontario, due to the combination of strong cyclonic vorticity advection over a

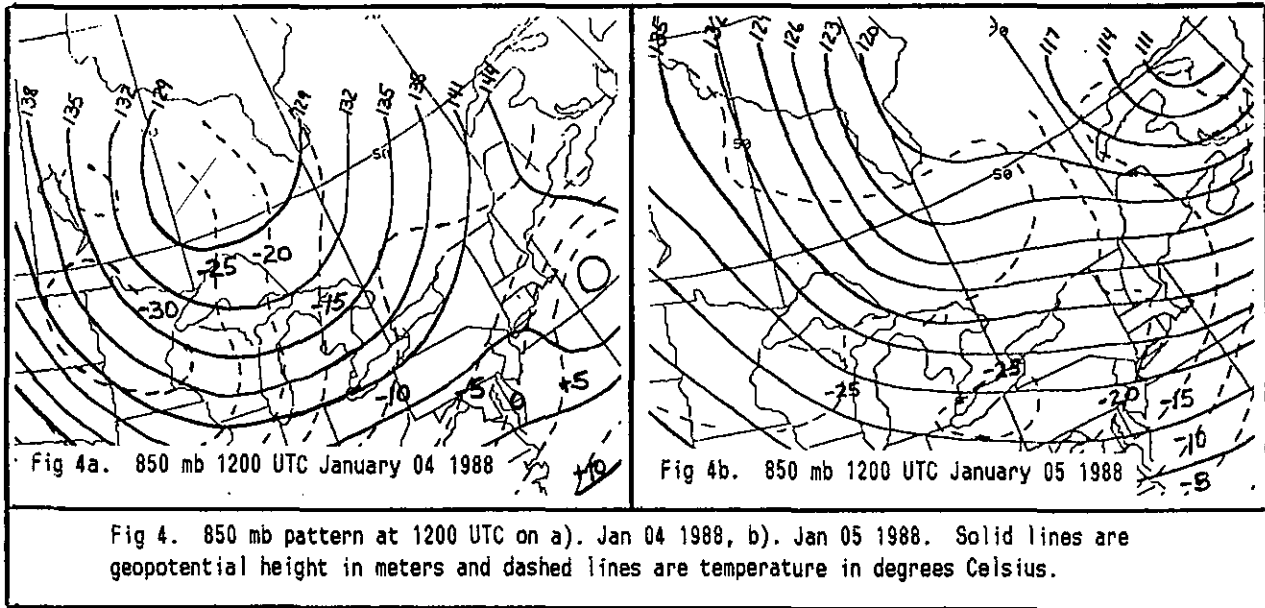


pre-existing deep layer of cold air.

The location of the Low center at the 850 mb level and the surface was similar to that at 500 mb, the feature was nearly vertically stacked. Vertical stacking of the Low below 500 mb is a preferred pattern for this type of storm. There is little change in wind direction with height in the mesoscale environment of the elliptically shaped lake, especially in the first 3000m of the atmosphere. This aids the development of a narrow, single band of snow. By 1200 UTC on the 4th, the

850 mb Low was also over James Bay, and strong cold air advection was occurring in its wake across the western Great Lakes. (Fig 4a).

Snowband formation began around 2100 UTC on the 4th, soon after the surface cold front crossed the region. Based on interpolation of the 850mb temperature field, this was also about the time that the temperature difference between the Lake (+3C) and the 850 mb layer (~ -10C) reached 13C. Holroyd (1972) noted that the 13C temperature difference



is considered a benchmark for the initiation of "pure" lake effect snow formation.

Based on the 850 mb wind direction at Buffalo for 1200 UTC on the 5th, and some subjective interpolation on the part of the author, the orientation of the Lake Ontario snowband was over the long axis of Lake Ontario, while the 850 mb winds were about 10 to 15 degrees north of the long axis of the lake. Although there was insufficient data to verify this observation, it seems likely that the band was exhibiting the same shoreline type of characteristic that McVehil et al. observed on Lake Erie storms.

The snowband extended parallel with, and just north of the south shoreline, remaining stationary during the entire night of the 4th. There was little synoptic scale cloudiness over the Great Lakes, so the lake effect clouds were quite easy to detect with infrared satellite imagery from GOES (Geostationary Operational Environmental Satellite) imagery (Fig 5). Forecasters at Buffalo consider

satellite imagery to be the single most important operational tool for observation and short term forecasting of lake effect snow to the east of Lake Ontario. This is true mainly because network radars are located too far from this area to detect the low level precipitation echoes associated with Lake effect snows. The usefulness of infrared satellite imagery is often limited during the winter over the Great Lakes, due to small differences in the temperature of the low cloud

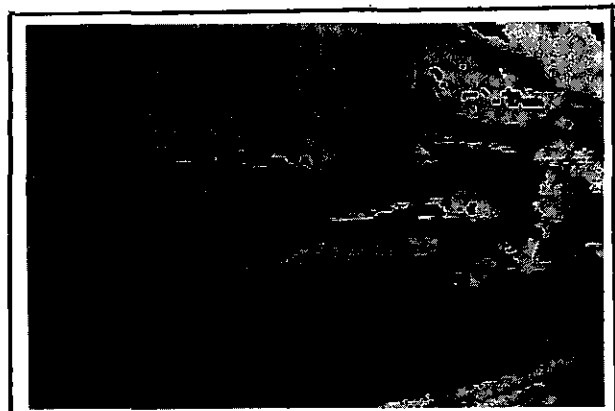


Fig 5. One-mile IR satellite imagery for 0301 UTC, January 05 1988. Note cold top enhancement associated with convective activity at the east end of Lake Ontario.

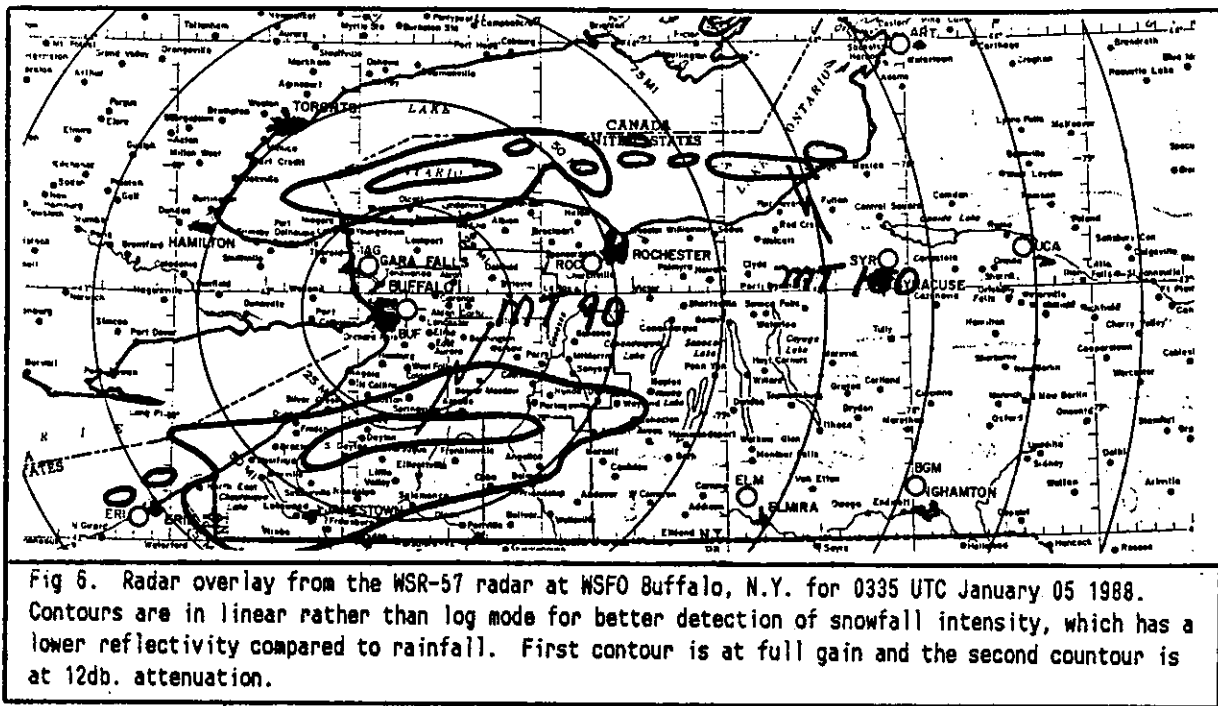


Fig 6. Radar overlay from the WSR-57 radar at WSFO Buffalo, N.Y. for 0335 UTC January 05 1988. Contours are in linear rather than log mode for better detection of snowfall intensity, which has a lower reflectivity compared to rainfall. First contour is at full gain and the second countour is at 12db. attenuation.

tops, and cold surface temps. However, the relatively warm water of the lake, provided good contrast to the cold cloud tops, allowing for easy detection of the snowband to the east of the lake at that time of night.

As with many lake effect storms of this category, the Highmarket snowburst was also convectively active. There were numerous reports of lightning and thunder over the eastern end of the Lake on the evening of the 4th. Infrared satellite imagery indicated cloud top enhancement at the eastern end of the lake, and precipitation echoes were detected by the Buffalo radar as far east as Oswego, with maximum tops as high as 3000 m. (Fig 6). Most often, precipitation tops associated with lake effect snows are in the range of 1500 to 2000m (Hill 1971). However, as mentioned earlier, single banded storms that are accompanied by strong synoptic scale forcing, may not be limited by the "capping" inversion that is present with most lake effect snowbands. There are no upper air stations located in close proximity to the east end of Lake Ontario, so

the upper air data from Buffalo, located at the eastern end of Lake Erie, was analyzed for the existence of an inversion. The atmospheric sounding at Buffalo for 0000 UTC January 05 (Fig. 7), was taken just before the reports of lightning and thunder at the east end of Lake Ontario. At this time, a relatively deep unstable layer existed from the surface through about 650 mb, or nearly 3.5 km above the surface. It

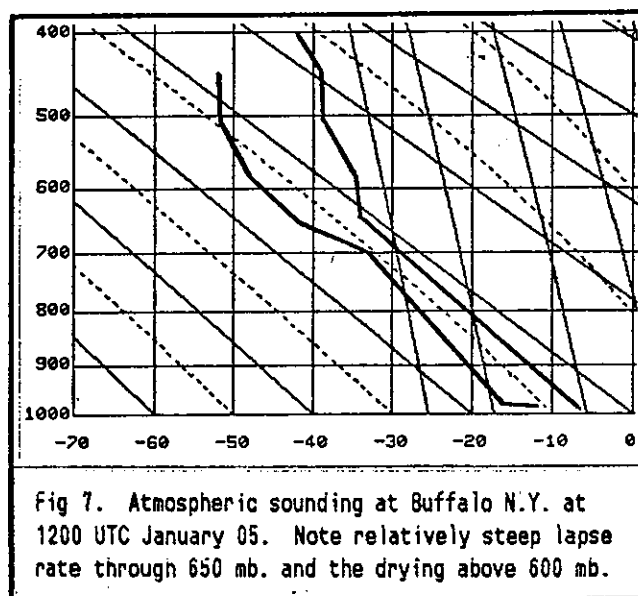


Fig 7. Atmospheric sounding at Buffalo N.Y. at 1200 UTC January 05. Note relatively steep lapse rate through 650 mb. and the drying above 600 mb.

was also at this time that the cooperative observer at the Highmarket station reported snowfall rates as high as 4 inches per hour.

The snowband remained nearly stationary for a most of the daylight hours on the 5th, due to very little change in the prevailing wind during that time. The cold core at 850 mb crossed the lake that day (Fig 4b). The interpolated temperature at 850 mb over the lake was about -25C, while the temperature of the surface of the lake was about +3C. In addition to the extreme thermal instability over the lake, strong cyclonic curvature continued across the lake, as shown on the 1200 UTC 500 mb analysis (Fig 3c).

Surface analyses across the Great Lakes at 1800 UTC, 05 January indicated a trough across the Great Lakes, and wind reports hinted at the existence of surface convergence zones associated with snowbands on Lake Erie, Ontario, and Huron (Fig 8).

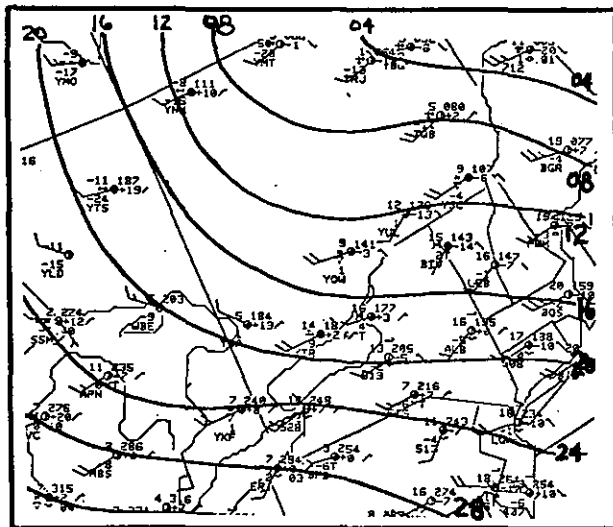


Fig 8. Contours of Sea level pressure for 1800 UTC January 05, 1988. Solid lines are pressure in millibars, labeled in the tens and units digits.

Additional surface wind reports were available during the 5th, from a series of wind towers operated by a

consortium of power companies in New York State (Caiazza). A mesoscale plot of the tower winds and other wind reports around Lake Ontario for 1800 UTC January 05, indicate very clearly the strong mesoscale surface convergence zone associated with the lake effect snowband (Fig 9).

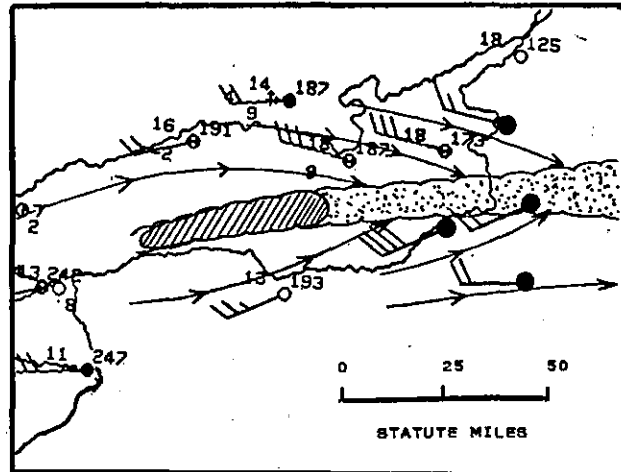


Fig 9. Streamlines show mesoscale convergence zone associated with the snowband at 1800 UTC January 05, 1988. Stippled area locates snowband based on satellite imagery. Hatched area is the precipitation echo from WSR-57 Buffalo radar.

Conditions directly under the snowband east of Lake Ontario were very treacherous throughout January 05. The north-south thoroughfares that connect downstate New York with the "North Country" were closed that day, including Interstate 81, the main artery. Highmarket reported nearly 120 cm (4 ft) of snow for the day. Boonville totalled almost 60 cm (2 ft) of snow and Pulaski picked up 40 cm (16 in).

Finally, late on the evening of the 5th, the axis of the 500 mb trough crossed the lake, and the snowband began to move south in response to a change in wind direction. However, upon close inspection of the IR satellite imagery from 0330 UTC Jan 06, the snowband seemed to maintain its west-east orientation over the lake, while inland, the band shifted to a

northwest-southeast orientation (Fig 10). It seems possible that the intense mesoscale convergence zone over the lake played an important role maintaining the orientation of the band over the lake, while inland the band reacted immediately to the synoptic scale windshift. The entire band eventually broke up into less intense multiple bands southeast of the lake, on the afternoon of 06 January.



Fig 10. One-mile IR satellite imagery for 0330 UTC January 06, 1988. Note the bending of the snowband down the Mohawk Valley of New York, southeast of Lake Ontario, while over the lake, the band maintains a west-east orientation.

4. Summary of forecasts for the Eastern Lake Ontario Counties

The NWS office in Buffalo runs a computer program on AFOS called the L.E.G. (Lake Effect Guidance) product, which compiles select forecast parameters from large scale models (Niziol 1987). Based on the L.E.G. run for this storm, the forecast office issued a "Special Weather Statement" for potential snow squall activity off Lake Ontario about 24 hours before the event began. (It should be pointed out that lake effect snows are commonplace in this part of the state, and weather statements were in effect previous to this event for a lake effect storm on

January 02 that produced 20 inches of snow!)

"Snow Squall Warnings" were issued for the counties east of Lake Ontario about 12 hours before the event began. For the Buffalo WSFO area of responsibility, the term "Snow Squall Warning" is issued when lake effect snow bands will cause intense snowfall (greater than 6 inches in a 12 hour period) over limited areas. Near zero visibilities and rough travel are to be expected in the squalls.

Another "Special Weather Statement" updated the warnings as the event was beginning on the afternoon of the 4th, calling for another "foot or more snow" overnight, with areas to the east of Lake Ontario being singled out as being "hard hit by evening".

There were some problems with forecasting total snowfall amount, and when the snowband would actually move southward. The NGM and LFM both tried to shift the winds a bit earlier than they actually shifted, and it was felt that the band might begin to move southward earlier than it did. In addition, standard forecast procedure is to predict snowband location and orientation parallel to the 850 mb wind forecast. Because this event took on the configuration of a shoreline band, the snowband set up a bit north of the standard forecast location. However, forecasters try not to be too limiting on areal location, and in this case, the public forecasts and statements actually worked quite well.

The forecasts did not come near the 69.5 inch total that occurred in Highmarket, for a reason. Lake effect snow forecasts are issued from WSFO Buffalo to indicate the potential for heavy snowfalls, without causing undue panic to the

public. Snowfall forecasts are categorized in general amounts over a discreet period. A typical forecast may read, "6 inches or more" or "a foot or more" snow during a 12 hour period. By categorizing amounts, and leaving the upper end of snow accumulation open, school districts, highway departments, public officials, etc. can institute their snow emergency plans. We alert the public to significant snowfall without causing undue panic. "Special Weather Statements" and radar summaries are issued as a "Nowcast" to update snowband location and movement.

It must be pointed out that personal communication can be very important in these mesoscale events. Early on the morning of the 4th, the day the snowstorm developed, the public forecaster at WSFO Buffalo called the Lewis county sheriff department, and briefed the staff that "heavy lake effect snows could occur over parts of their county for the next couple of days, and as much as 3 feet to 4 feet of snow is not unlikely for some areas."

4. SUMMARY

The Highmarket snowburst of January 4th and 5th 1988, produced one of the greatest snowfall's for a particular Lake Effect Snowstorm in recent years. Snowfall rates in excess of 4 inches per hour at times were attributed to a combination of factors, strong cold air advection over the Lake, strong cyclonic vorticity, and "steering winds" directed nearly over the longest fetch of the lake. A secondary effect was most likely the orographic influence of the Tug Hill plateau to the east of the lake. Local wind reports indicated the presence of a strong mesoscale convergence zone directly under the snowband, which no

doubt greatly increased vertical motion, and consequently, snowfall rates within the band.

The extreme snowfall total for the storm over such a localized area, was attributable to wind direction in the lower atmosphere that remained nearly constant for a 36 hour period.

Synoptic pattern recognition is the first factor the forecaster must take into account to anticipate such a snow event. A broad 500 mb trough over eastern Canada, with a prolonged source of arctic air is a necessity. In some of the most intense lake effect storms that have been studied during the past few years by the staff at WSFO Buffalo, a select synoptic scale pattern seems to dominate. Once the 500 mb trough is in place over eastern Canada, a strong arctic short wave moves down the backside of the trough and digs around the base, sometimes carving out a new closed Low, that crosses just south of James Bay. The accompanying cyclonic vorticity advection destabilizes the lower atmosphere, allowing for relatively deep convection to occur over the eastern Great Lakes. The 500 mb Low is usually vertically stacked through the lower atmosphere. If the Low is slow moving, or the trough is broad, the "steering winds" will remain nearly constant for an extended period of time. This in turn produces a stationary band, which can produce extreme amounts of snow in a very localized area.

It is a fact of a forecaster's life that the location of a lake effect storm, and total snowfall, are impossible to predict with total accuracy. However, recognizing synoptic scale characteristics that accompany this type of storm is the first step in identifying their potential. Following the mesoscale features of the snowband in the short term (6 hours or less), with tools

like satellite and radar, can significantly aid in the prediction of future movement and intensity. Each case study that is documented and analyzed will no doubt add to the local knowledge at the forecast office, as has already been the case for the WSFO at Buffalo.

The author wishes to express his appreciation to Roger Caiazza, for his information on wind tower data. Also thanks to Brian Murphy of the Ontario Weather Centre and Frank Kieltyka of WSFO Cleveland for data, comments, and discussion on this storm event. Special thanks to Dwayne Stiegler from the University of Chicago for "Storm Data" figures, and Michael Mogil of NESDIS for satellite imagery.

References:

- Caiazza, R. 1988: Niagara Mohawk Power Corporation, Syracuse, N.Y. personal communication.
- Hill, J.D., 1971: Snow squalls in the lee of Lake Erie and Ontario. NOAA Tech. Memo. NWS ER-43.
- Holroyd, E.W., III, 1971: Lake effect cloud bands as seen from weather satellites. J. Atmos. Sci., 28, 1165-1170.
- Jiusto, J.E., Paine, D.A., Kaplan, M.L. 1970: Great Lakes snowstorms Part 2. Synoptic and Climatological aspects. ESSA Grant E22-13-60 (G) ASRC, SUNY Albany.
- McVehil, G.E., and Peace, R.L. Jr., 1966: Project Lake Effect. A study of lake effect snowstorms. Final contract report., CWB 1231, 52 pp. available from CALSPAN, Buffalo, N.Y.
- Muller, R.A. 1966: Snowbelts of the Great Lakes. Weatherwise. 19,

249-55.

Niziol, T.A. 1987: Operational forecasting of lake effect snow in western and central New York. Weather and Forecasting. Vol 1, No. 4.

AN OVERVIEW OF FORECAST SCHEMES USED BY WSFO CLEVELAND, OHIO TO
FORECAST LAKE EFFECT SNOW

Frank Kieltyka
WSFO, Cleveland, Ohio

During the last decade several methods for forecasting lake effect snow over Northeast Ohio have been tested by forecasters at WSFO Cleveland with limited success. These include the Rothenberg Trajectory Envelopes, the Collier Index and the Dockus Lake Effect Scheme.

The purpose of this paper is not intended to show which scheme is better, but to indicate some of the methods that have been used at WSFO Cleveland over the years.

The Rothenberg Trajectory Envelopes:

The Rothenberg Trajectory Envelopes (figure 1) developed by an employee at Cleveland in the 60s shows probabilities of lake effect snow reaching at least four hundredths of an inch of water equivalent in a 6 hour period for varying wind directions at Cleveland and Erie, Pennsylvania. Rothenberg used 6 hour periods to coincide with the 6 hour surface trajectory forecast. Rothenberg eliminated all cases where fronts or troughs were involved, so the envelopes were restricted to lake effect snows.

Results from studies done in the mid 70s indicated the envelopes were helpful in pinpointing the direction that would give lake effect snow.

The Collier Index:

The Collier Index (figure 2) provides a 12 hour snowfall forecast and was developed for Buffalo in the 60's. The index was modified slightly for use in Cleveland. The index used the difference between the lake temperature and the 850 mb temperature and the difference between the lake temperature and the 700 mb temperature to provide a 12 hour snowfall forecast. The snowfall forecast is a maximum amount and verification statistics show the index was worthy of further consideration.

The Dockus Lake Effect Scheme:

The Dockus Lake Effect Scheme for Lake Erie was developed by Dale Dockus formerly of the Weather Channel and now a meteorologist with Federal Express in Memphis. The method was computerized by Mark Fenbers an intern at WSO Columbus, Ohio.

The scheme considers 3 types of lake snows.

- 1) Lake Effect: NVA, fetch 100 miles or more and 850 mb temperatures -10C or colder.
- 2) Lake Enhanced: PVA, fetch 40 miles to 99 miles and 850 MB temperatures -4C to -9C.

3) Combination: PVA, fetch 100 miles or more and 850 mb temperature -10C or colder.

The scheme is computerized for use on the IBM and generates two separate outputs solely based upon the NGM and LFM FOUS/trajectory guidance. The output is in the form of 6 hour snowfall totals through 48 hours (figures 3A and 3B). The Dockus program requires wind direction and speed, vertical velocities, and 850 mb temperatures.

All this data can be obtained from the NGM FRHT64. The 850 mb temperature is determined by averaging T3 and T5 and the vertical velocities are also averaged.

For the LFM output the wind direction, wind speed and vertical velocities are easily obtainable from the FOUS FRH64. For ease of automation the LFM 850 mb temperatures are obtained by using the 24 hour trajectory forecast and time weighted NGM 850 MB temperatures. While the results are deemed satisfactory, if preferred, the 850 MB temperatures can be obtained from the graphics and input manually.

With the Dockus scheme some of the major forecast busts occur when the flow is anticyclonic. The scheme tests for this by comparing the wind direction at Cleveland versus Dayton and Pittsburgh depending on whether the trajectory is from Lake Huron or Lake Erie respectively.

Fifteen tables are used to take into account the many variations of Northeast Ohio Lake Effect (figure 4). Three tables are for enhanced lake effect cases, four of the tables take into account combination lake effect and eight of the tables are for pure lake effect cases.

Three maps are used to show the three distinct sources of lake-effect snow. A Lake Erie Fetch Map (figure 5), A Lake Huron Fetch Map (figure 6) and a Map for Lake Enhanced cases (figure 7). The maps are divided into various regions depending on topography and the boundary layer wind direction. Maximum upslope areas are denoted by X, while the lower elevations adjacent to the lake or elevations considered to be downslope are identified by O.

Because of programming problems early in the 1987-88 lake effect season the Dockus Scheme was not verified. However, some subjective observations of the scheme showed the LFM seemed to perform better than the NGM, the reliability decreased significantly after 30 hours and overforecasting was a major problem. In many cases the storm totals were good, while the 6 hour totals were poor.

In the latter part of the 1987-88 winter season significant differences were noted between the NGM snowfall QPF and LFM QPF, i.e., the NGM forecasted less than a foot of snow over a 48 hour period while over 3 feet was forecast by the LFM. Actual storm totals were a foot or less.

An Example:

All 3 schemes were tested on a January 5-6, 1988 lake effect snowstorm that dumped 6 to 18 inches of snow over Northeast Ohio from 1/5/00Z-1/7/00Z. The output from both the LFM and NGM for this storm is contained in figures 3A and 3B.

Using the boundary layer wind forecast for Cleveland instead of the trajectory forecast, the Rothenberg trajectory envelope for Cleveland indicated a 50-66% probability of .04 or more of water equivalent in each 6 hour period for much of the duration of the storm. Only a trace of water equivalent was reported at Cleveland.

The Collier Index was tested using the observed data and the results were good in regards to forecasting the highest amounts. For the 48 hour period from 1/5/00Z to 1/7/00Z 15 or more inches of snow was forecasted by the index.

The Dockus Scheme results were best using the LFM data, even though it over-forecasted the snow in most areas. The following are forecast and observed snowfall in inches for the 48 hour period 1/5/00Z-1/7/00Z.

AREA	LFM	NGM	OBSERVED
EO0	1	0	<1
EX0	2	0	2-6
EO1	13	5	2-6
EX1	22	13	12-18
EO2	13	1	6-12
EX2	25	6	12-18
EO3	13	5	10-17

Conclusion:

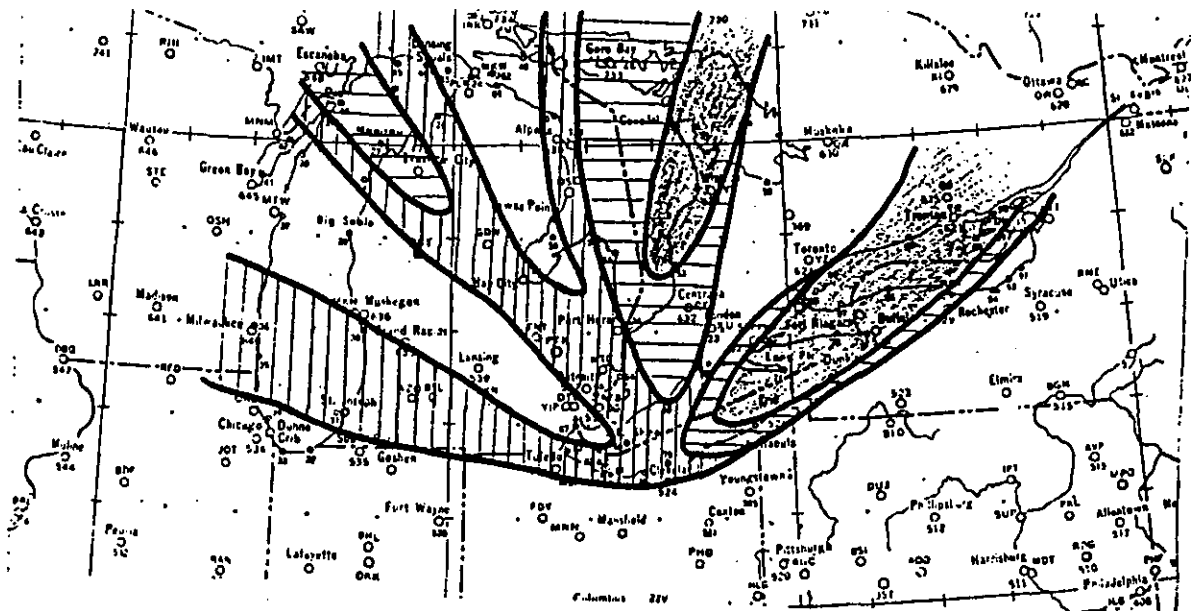
The Dockus scheme is a modernized version of the Rothenberg Trajectory Envelopes and the Collier Index. The computer allows the scheme to be complex, however, the output (lake effect snow forecasts) can only be as good as the input used to derive the forecasts. To this end, as our forecast models improve so will Lake effect snowfall forecasts.

References:

Dockus, D. 1985: Lake-Effect Snow Forecasting in the Computer Age, National Weather Digest., Vol 10 pp 5-19.

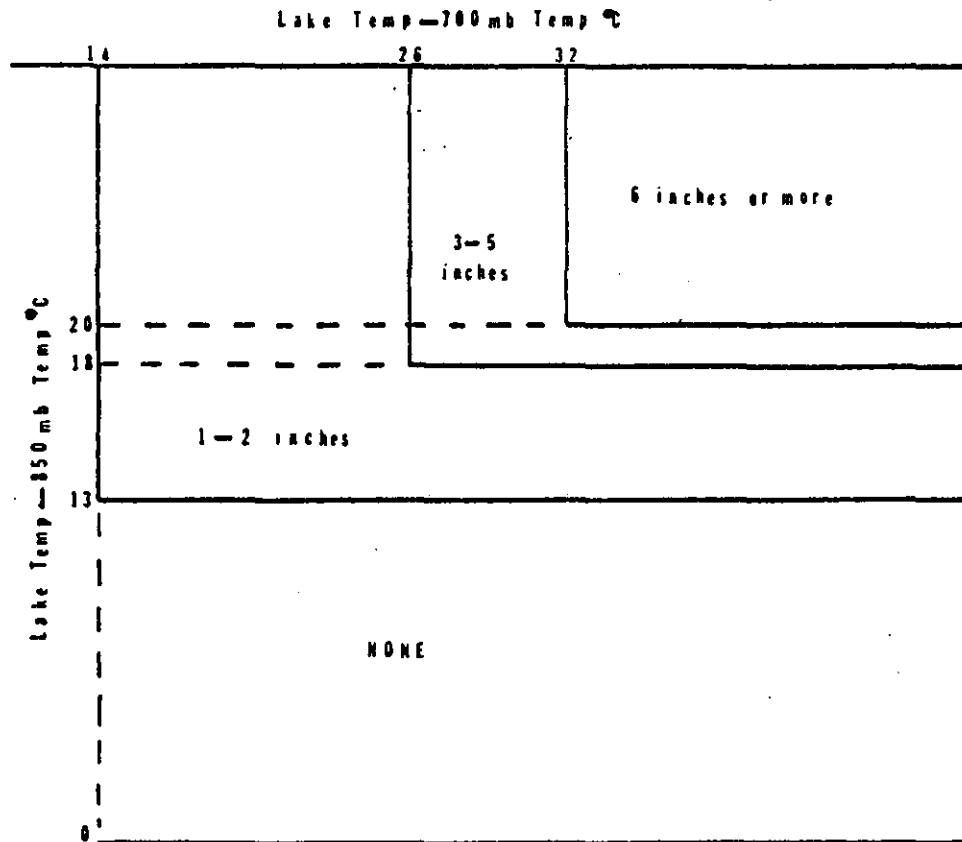
Dockus, D. and Fenbers, Mark J. 1987: A Computerization of Lake Effect Snowfall in Northeast Ohio, Personal Communication.

Webb, George H. 1977: Using the Collier Index and Rothenberg's Trajectory Envelopes to Forecast Snow in Cleveland and the Northeast Ohio Snowbelt., October 1977, Personal Communication.



Air trajectory envelopes for Cleveland showing probabilities of snow shower activity reaching (.04"/hr liquid equivalent).
 Vertical hatching indicates 25-49% probability.
 Horizontal hatching indicates 50-66% probability.
 Stippling indicates 67% or greater probability.

FIGURE 1 ROTHENBERG TRAJECTORY ENVELOPE FOR CLEVELAND.



Lake effect snowfall amounts per 12 hours developed for Buffalo. Lower amounts subjectively for sharp anticyclonic flow with light winds.

FIGURE 2 THE COLLIER INDEX.

First time period... (0-6 hr fcst) Valid for period beginning 00Z Jan 5.
 Since no initial LFM VV value is available, an assigned neutral value
 of +.01 is used in its place for this period only. Use cautiously.

Table 6. Winds 30 and 27.

E00	EX0	E01	EX1	E02	EX2	E03
1"	2"	2"	4"	2"	4"	2"

Add 0.00 inches (water-equivalent) precip from the synoptic system.

Second time period... (6-12 hr fcst) Valid for period beginning 06Z Jan 5.

Table 3. Winds 27 and 27.

E00	EX0	E01	EX1	E02	EX2	E03
-	-	-	1"	3"	5"	3"

Add 0.00 inches (water-equivalent) precip from the synoptic system.

Third time period... (12-18 hr fcst) Valid for period beginning 12Z Jan 5.

Table 3. Winds 27 and 28.

E00	EX0	E01	EX1	E02	EX2	E03
-	-	2"	3"	2"	4"	2"

Add 0.00 inches (water-equivalent) precip from the synoptic system.

Fourth time period... (18-24 hr fcst) Valid for period beginning 18Z Jan 5.

Table 3. Winds 28 and 27.

E00	EX0	E01	EX1	E02	EX2	E03
-	-	2"	3"	2"	4"	2"

Add 0.00 inches (water-equivalent) precip from the synoptic system.

Fifth time period... (24-30 hr fcst) Valid for period beginning 00Z Jan 6.

Table 3. Winds 27 and 28.

E00	EX0	E01	EX1	E02	EX2	E03
-	-	2"	3"	2"	4"	2"

Add 0.00 inches (water-equivalent) precip from the synoptic system.

Sixth time period... (30-36 hr fcst) Valid for period beginning 06Z Jan 6.

Table 3. Winds 28 and 28.

E00	EX0	E01	EX1	E02	EX2	E03
-	-	2"	3"	1"	2"	1"

Add 0.00 inches (water-equivalent) precip from the synoptic system.

Seventh time period... (36-42 hr fcst) Valid for period beginning 12Z Jan 6.

Table 3. Winds 28 and 28.

E00	EX0	E01	EX1	E02	EX2	E03
-	-	2"	3"	1"	2"	1"

Add 0.00 inches (water-equivalent) precip from the synoptic system.

Eighth time period... (42-48 hr fcst) Valid for period beginning 18Z Jan 6.

Table 13. Winds 28 and 28.

E00	EX0	E01	EX1	E02	EX2	E03
-	-	1"	2"	-	-	-

Add 0.00 inches (water-equivalent) precip from the synoptic system.

FIGURE 3A THE DOCKUS SCHEME OUTPUT USING THE LFM.

DDT: NGM

First time period...(0-6 hr fcst) Valid for period beginning 00Z Jan 5.
Table 13. Winds 28 and 28.

E00	EX0	E01	EX1	E02	EX2	E03
-	-	1"	2"	-	-	-

Add 0.00 inches (water-equivalent) precip from the synoptic system.

Second time period...(6-12 hr fcst) Valid for period beginning 06Z Jan 5.
Table 3. Winds 28 and 28.

E00	EX0	E01	EX1	E02	EX2	E03
-	-	2"	3"	1"	2"	1"

Add 0.00 inches (water-equivalent) precip from the synoptic system.

Third time period...(12-18 hr fcst) Valid for period beginning 12Z Jan 5.
Table 13. Winds 28 and 26.

E00	EX0	E01	EX1	E02	EX2	E03
-	-	-	1"	-	1"	1"

Add 0.00 inches (water-equivalent) precip from the synoptic system.

Fourth time period...(18-24 hr fcst) Valid for period beginning 18Z Jan 5.
Table 13. Winds 26 and 28.

E00	EX0	E01	EX1	E02	EX2	E03
-	-	-	1"	-	1"	1"

Add 0.00 inches (water-equivalent) precip from the synoptic system.

Fifth time period...(24-30 hr fcst) Valid for period beginning 00Z Jan 6.
Table 13. Winds 28 and 28.

E00	EX0	E01	EX1	E02	EX2	E03
-	-	1"	2"	-	-	-

Add 0.00 inches (water-equivalent) precip from the synoptic system.

Sixth time period...(30-36 hr fcst) Valid for period beginning 06Z Jan 6.
Table 13. Winds 28 and 28.

E00	EX0	E01	EX1	E02	EX2	E03
-	-	1"	2"	-	-	-

Add 0.00 inches (water-equivalent) precip from the synoptic system.

Seventh time period...(36-42 hr fcst) Valid for period beginning 12Z Jan 6.
Table 13. Winds 28 and 26.

E00	EX0	E01	EX1	E02	EX2	E03
-	-	-	1"	-	1"	1"

Add 0.00 inches (water-equivalent) precip from the synoptic system.

Eighth time period...(42-48 hr fcst) Valid for period beginning 18Z Jan 6.
Table 13. Winds 26 and 28.

E00	EX0	E01	EX1	E02	EX2	E03
-	-	-	1"	-	1"	1"

Add 0.00 inches (water-equivalent) precip from the synoptic system.

FIGURE 3B THE DOCKUS SCHEME OUTPUT USING THE NGM.

SNOWFALL (INCHES) FOR GEOGRAPHIC LOCATIONS (SEE FIGURE 6)

WIND DIRECTIONS	HO0	HO1	HX1	HO2	HX2	HO3	HX3	HO4	HX4	HO5	HO6
30,33	2"	2"	4"	2"	4"	2"	4"	3"	4"	3"	3"
30,34	2"	2"	4"	2"	4"	2"	4"	3"	4"	3"	3"
31,33	2"	2"	4"	2"	4"	2"	4"	3"	4"	3"	3"
31,34	2"	2"	4"	2"	4"	2"	4"	3"	4"	3"	3"
30,31	2"	2"	4"	2"	4"	2"	4"	2"	4"	4"	5"
30,32	2"	2"	4"	2"	4"	2"	4"	2"	4"	4"	5"
31,31	2"	2"	4"	2"	4"	2"	4"	2"	4"	4"	5"
31,32	2"	2"	4"	2"	4"	2"	4"	2"	4"	4"	5"
31,35	2"	2"	4"	2"	4"	3"	5"	3"	5"	3"	3"
32,35	2"	2"	4"	2"	4"	3"	5"	3"	5"	3"	3"
32,32	2"	2"	4"	2"	4"	2"	4"	3"	5"	3"	3"
32,33	2"	2"	4"	2"	4"	2"	4"	3"	6"	5"	5"
32,34	2"	2"	4"	2"	4"	3"	5"	3"	6"	5"	4"
32,36	2"	2"	4"	3"	5"	3"	5"	3"	5"	3"	2"
33,33	2"	2"	4"	2"	4"	3"	5"	5"	9"	5"	4"
33,34	2"	2"	4"	3"	5"	4"	8"	5"	9"	5"	3"
33,35	2"	2"	4"	3"	5"	4"	7"	4"	7"	4"	3"
33,36	2"	3"	5"	3"	5"	3"	6"	3"	5"	3"	2"
33,01	2"	2"	4"	3"	5"	3"	5"	3"	5"	3"	2"
34,34	2"	2"	3"	3"	5"	6"	9"	6"	9"	3"	2"
34,35	2"	2"	3"	4"	8"	6"	9"	5"	8"	3"	2"
34,36	2"	3"	5"	4"	7"	4"	7"	3"	6"	2"	2"
34,01	3"	3"	5"	3"	6"	3"	5"	3"	5"	2"	2"
34,02	3"	3"	5"	3"	5"	3"	5"	3"	5"	2"	2"
35,35	2"	3"	5"	6"	9"	6"	9"	3"	5"	2"	2"
35,36	3"	4"	7"	6"	9"	4"	7"	2"	4"	2"	2"
35,01	3"	4"	6"	4"	7"	3"	5"	2"	4"	2"	2"
35,02	3"	3"	6"	3"	5"	3"	5"	2"	4"	2"	2"
36,36	3"	6"	8"	6"	8"	3"	5"	2"	4"	2"	2"
36,01	4"	5"	8"	4"	7"	2"	4"	2"	4"	2"	2"
36,02	4"	4"	6"	3"	5"	2"	4"	2"	4"	2"	2"
36,03	3"	3"	5"	2"	4"	2"	4"	2"	4"	2"	2"
36,04	3"	3"	5"	2"	4"	2"	4"	2"	4"	2"	2"
01,01	6"	4"	6"	2"	4"	2"	4"	2"	4"	2"	2"
01,02	5"	3"	5"	2"	4"	2"	4"	2"	4"	2"	2"
01,03	3"	2"	4"	2"	4"	2"	4"	2"	4"	2"	2"
01,04	3"	2"	4"	2"	4"	2"	4"	2"	4"	2"	2"
02,02	4"	2"	4"	2"	4"	2"	4"	2"	4"	2"	2"

FIGURE 4 SNOWFALL AMOUNTS (COMBINATION CASES AFTER DOCKUS) FOR VARYING WIND DIRECTIONS AND GEOGRAPHIC AREAS.

LAKE ERIE FETCH MAP

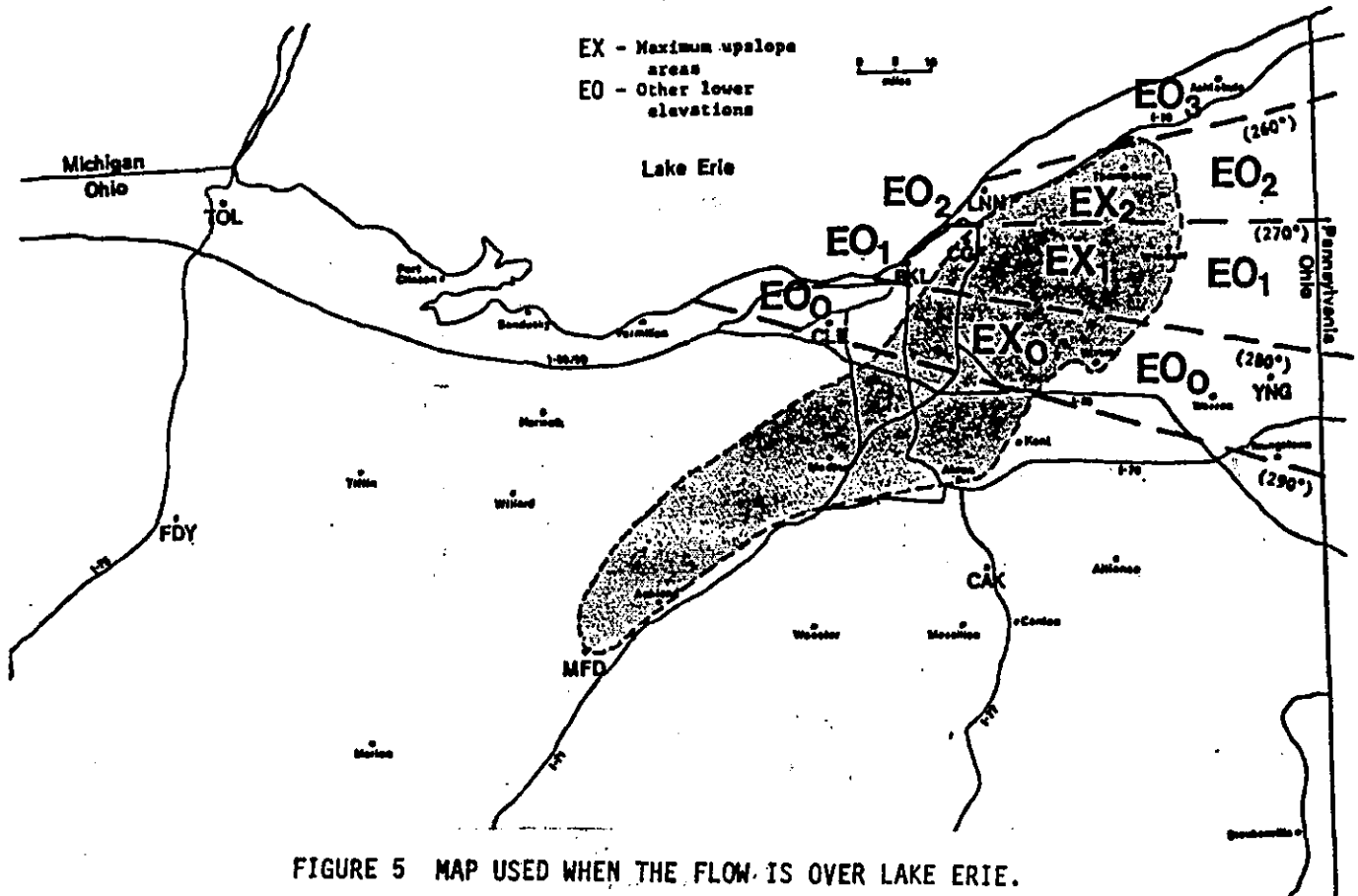


FIGURE 5 MAP USED WHEN THE FLOW IS OVER LAKE ERIE.

LAKE HURON FETCH MAP

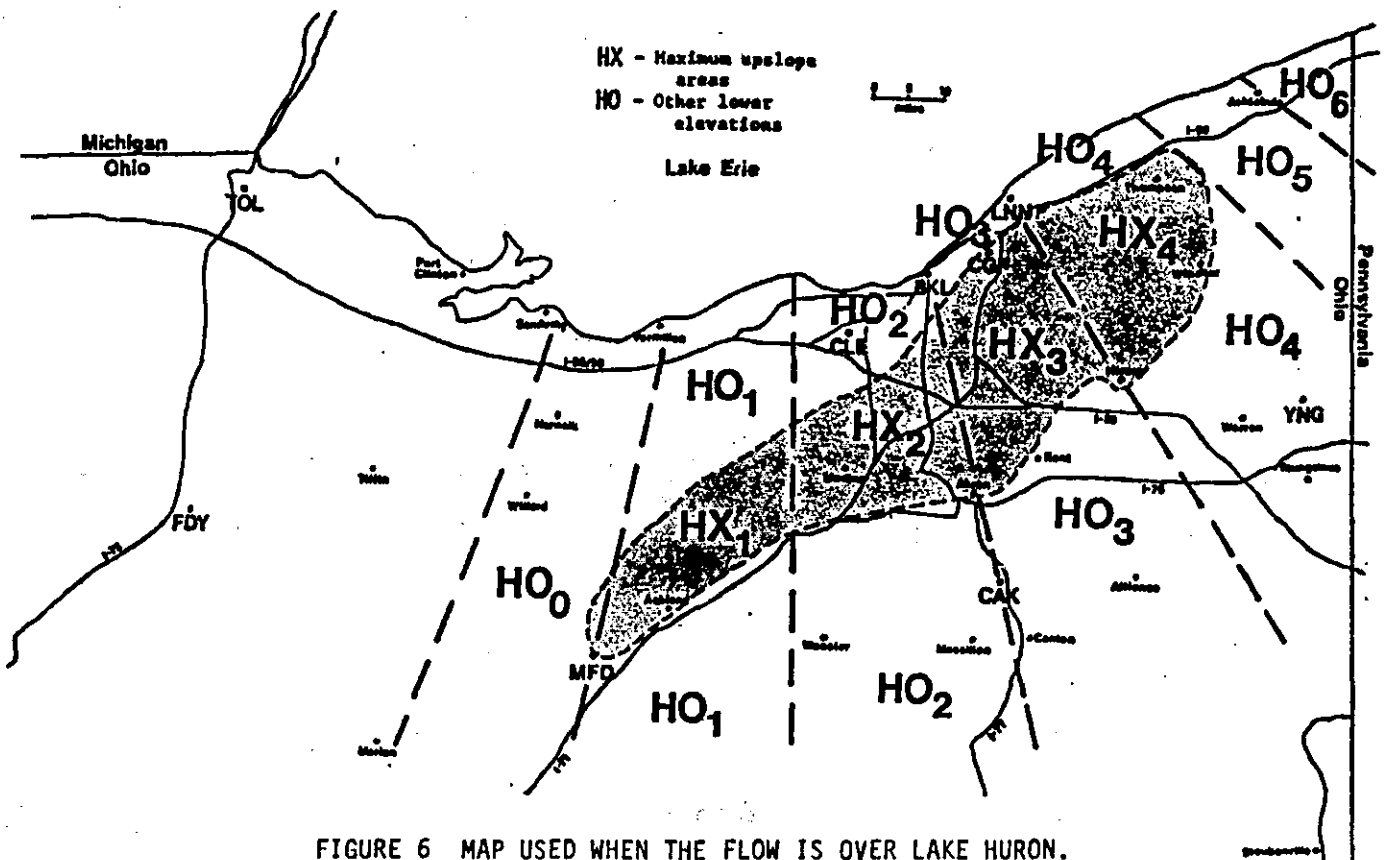


FIGURE 6 MAP USED WHEN THE FLOW IS OVER LAKE HURON.

LAKE-ENHANCED MAP

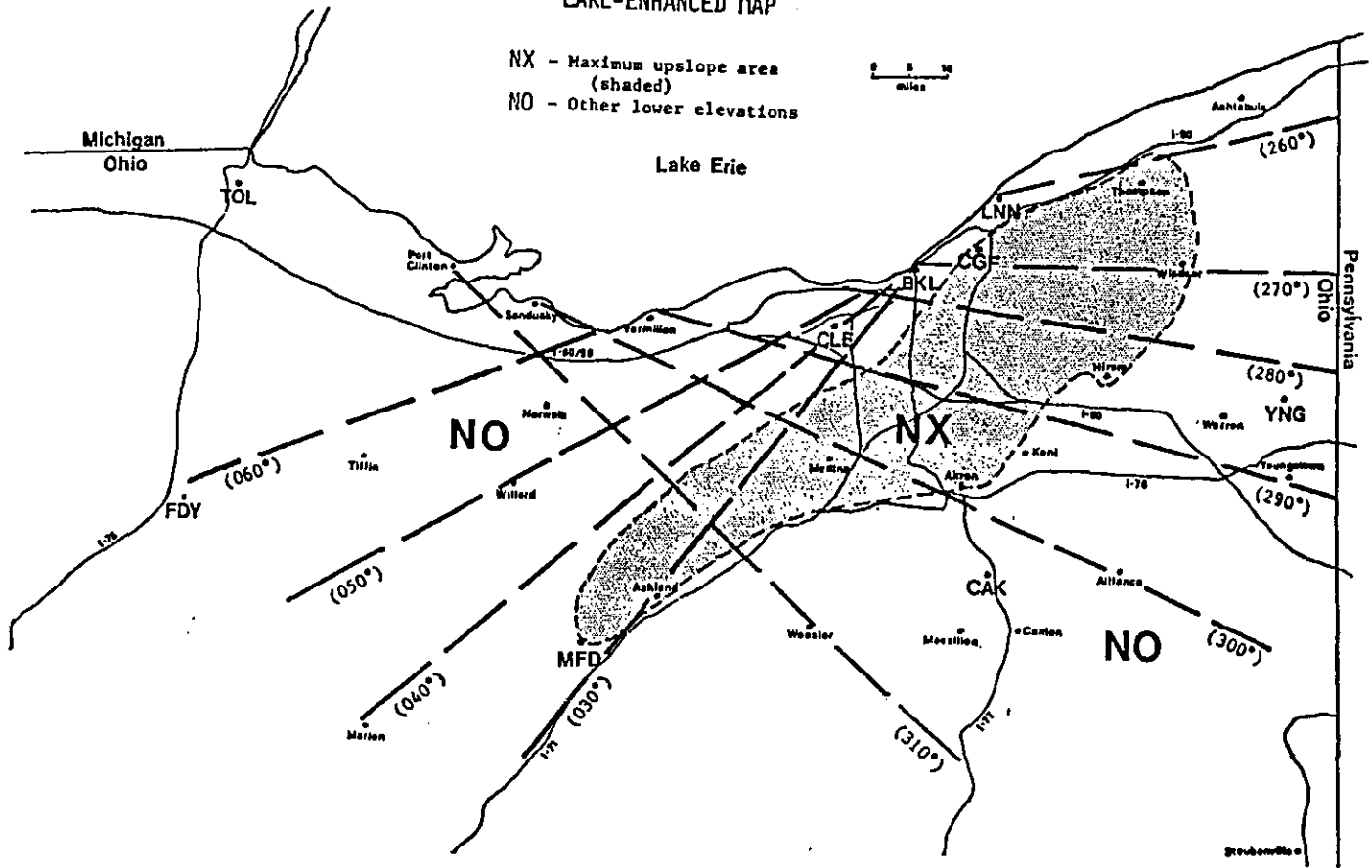


FIGURE 7 MAP USED FOR LAKE-ENHANCED CASES.

SNOW FORECASTING: COMMENTS ON A FEW LOOSE ENDS

Edward C. Johnston
National Weather Service Forecast Office
Milwaukee, Wisconsin

INTRODUCTION

Accurate prediction of heavy snow band location continues to be one of the greatest challenges faced by the operational forecaster. There are numerous published guidelines used to aid in positioning these bands in mature storm situations. But there is much to consider before applying these "rules"...and many less mature systems to deal with that are also capable of producing heavy snowfall. This paper concentrates mainly on the latter type of system. It attempts to organize a few ideas and comment on one of the more important positioning guidelines that could use some clarification.

DISCUSSION

The forecaster must make a series of important determinations in the course of a developing winter storm situation. A sample thought process which might be followed is suggested in Figure 1 in the form of a "decision tree".

The first consideration is the type of snow producing event one is dealing with. Simply stated...strong upward vertical motion associated with significant snowfalls is mainly generated either by warm air advection (isentropic lift), or vorticity advection (increasing with height)...or both.

In an ideal situation, they would appear to work together in the manner suggested in Figure 2. Southwest flow ahead of an upper level trough becomes strongest over a tight thermal baroclinic zone, due to the additive effect of the thermal wind. This in turn intensifies the cyclonic shear zone just to the left of the "jet", where one or more vorticity maxima may form and move up along the shear zone.

Meanwhile downstream...a strengthening lower level jet is beginning to "overrun" the baroclinic zone. This strong vertical motion leads to precipitation being deposited just north of the thermal ribbon...which then coincides with the band of maximum vorticity advection along the shear zone. This combination would produce the heaviest snows.

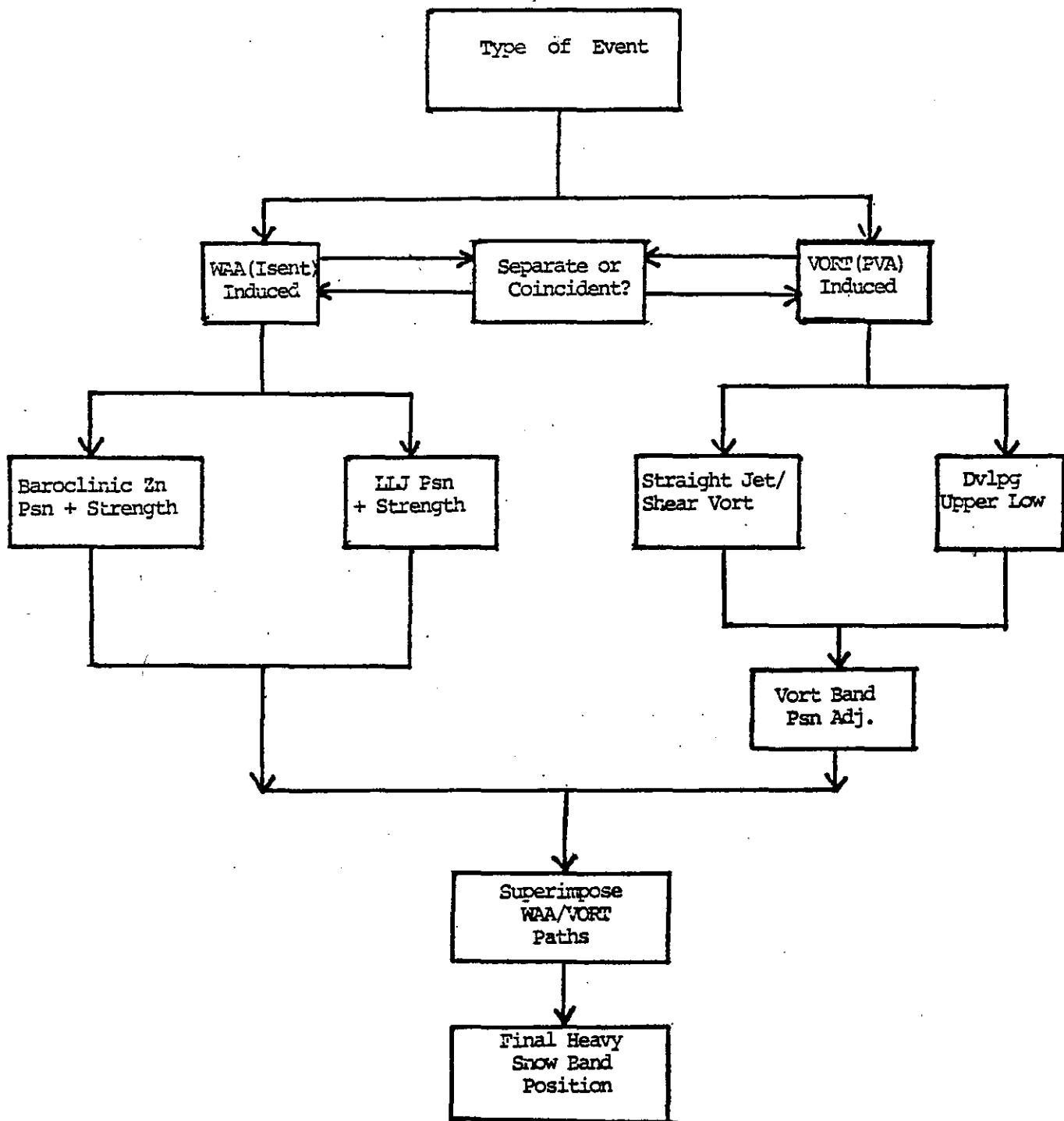


Figure 1: Winter Storm thought process "Decision Tree"

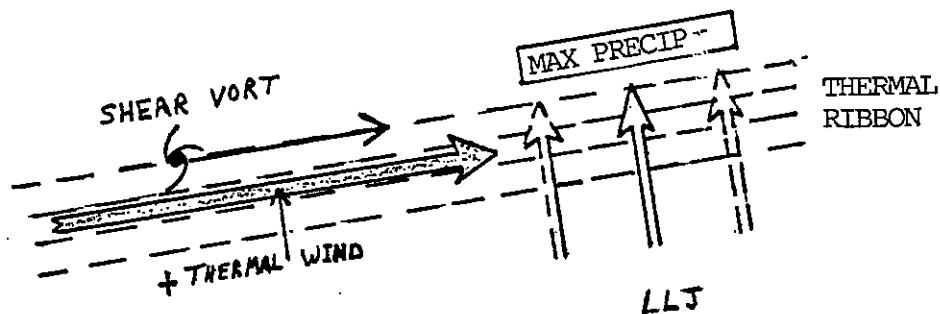


Figure 2: Shear Vorticity and Warm Air Advection

But these processes often work separately. The warm advection snow area is often well ahead of the vorticity induced band...and not directly downstream. In any event, each must be evaluated individually, then combined to come up with the final forecast locations...as shown in the table. The remainder of this discussion deals mainly with the right side of the table. Experience suggests that correct adjustments here provide one of the most reliable indicators of eventual heaviest snow band position.

Note that vorticity induced snows are grouped into two categories for developing storms. Straight jet/strong cyclonic shear zone vorticity systems are of the type described in Figure 2...where a jet streak races out ahead of the main upper trough. Figure 3 shows an example of this type of system. Warm air advection and shear vorticity advection are working together along much of the "enhanced band" southern edge (Beckman, 1987) to produce heavy snow. The vorticity center is moving toward Iowa from southwest Kansas. Note that its path is only 1 degree (60 nautical miles) from the enhanced band southern edge.

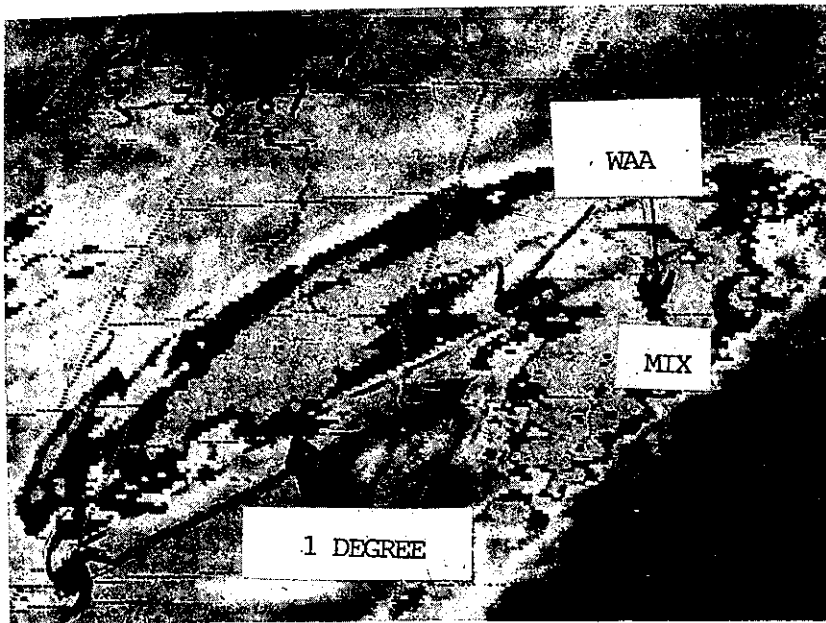


Figure 3: Satellite Image from 2200Z 3-28-87

One of the established guidelines (Goree-Younkin, 1966) for positioning snow bands states that the heaviest snow will fall 2.5 degrees north of the vorticity center track. we can see in Figure 3 that this is apparently not always true. More will be said about this shortly.

Figure 4 shows the progression of the system downstream. Vorticity advection and warm advection were still combining to produce heavy snow along the enhanced band southern edge...still about 1 degree north of the vorticity center track.



Figure 4: 1500Z 3-29-88

An example of a developing upper level low type of snow band is shown in Figures 5 through 10.

In figure 5...the system was still an open trough. The vorticity center was moving eastward along the Minnesota-Iowa border. at the time, heavy snow was falling at Rochester, Minnesota (RST) under the southern edge of the enhanced clouds, again about 1 degree left of the vorticity center path. Rochester received over 13 inches from this storm. Based on the previous examples, the tendency would have been to extrapolate the heavy snow band downstream into southern Wisconsin.

The NGM 500 mb projection for 12Z the next day is shown in Figure 6. The vorticity center near the Wisconsin-Illinois border continues tracking eastward. But the model prints out an upper low in southern Wisconsin. This will prove to be a key to the future evolution of this system.

Going back to the satellite picture at 0200Z (figure 7), it was already becoming apparent that a closed cyclonic circulation aloft was forming along the Minnesota-Iowa border. The "dry slot" was beginning to wrap around the developing low. In doing so, the dry air pushes the enhanced band northward, further away from the track of the circulation center. (Note that in the straight jet system, the dry slot punches downstream - but does not wrap around the vorticity center..due to the lack of a closed circulation).

In figure 8, the dry slot has curled into the northwest quadrant of the circulation. Note that the slot has pushed the southern edge of the enhanced band a full 2.5 degrees north of the circulation center. This is now in agreement with the Goree-Younkin vorticity center track vs. snow band relationship mentioned earlier.

Figure 9 shows the upper low/circulation center continuing eastward into Lower Michigan. Figure 10 shows the resultant snow band the next day. Note again that the band position varies from 1 degree north of the vorticity center track in Minnesota (shown earlier) to 2.5 degrees north of the upper low/circulation center track in northern Wisconsin.

It is very important that this adjustment be made if a snow system develops from an open trough or shear zone into an upper low. If it remains in a shear zone configuration...as is frequently the case when a jet streak comes out ahead of the main trough...the snow band will likely be closer to 1 degree north of the vorticity center/shear zone path.

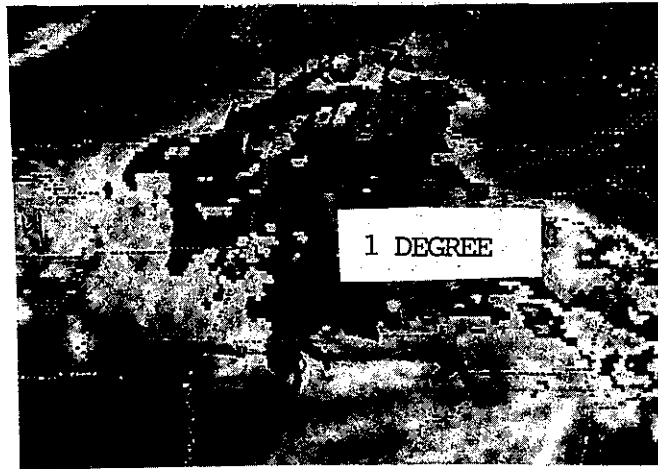


Figure 5: 2100Z 4-26-88

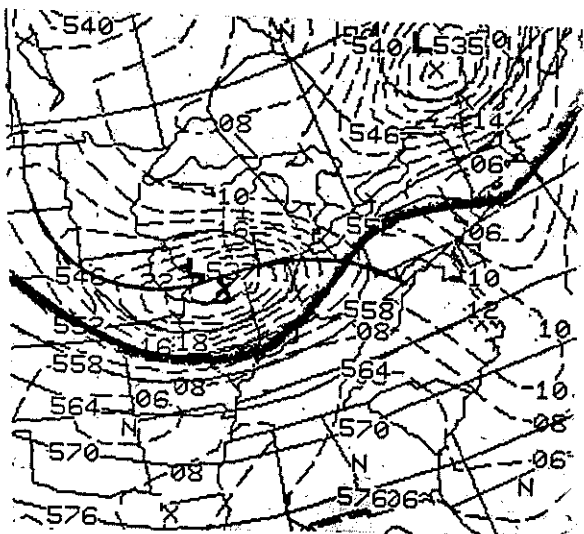


Figure 6; NGM 500 mb VT 1200Z
4-27-88

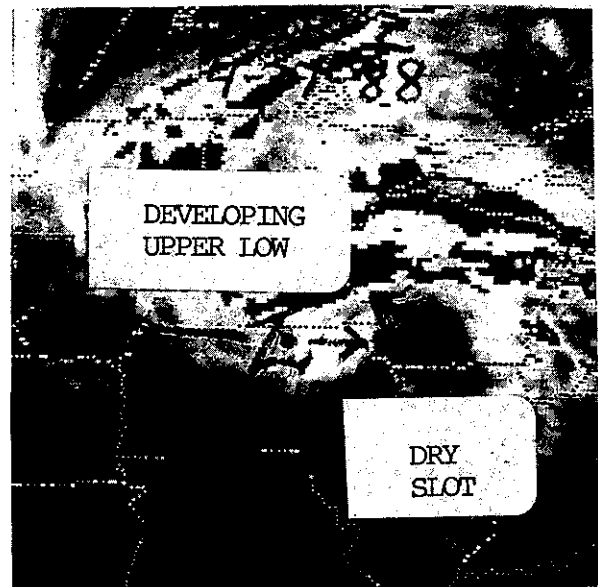


Figure 7: 0200Z 4-27-88



Figure 8: 1200Z 4-27-88

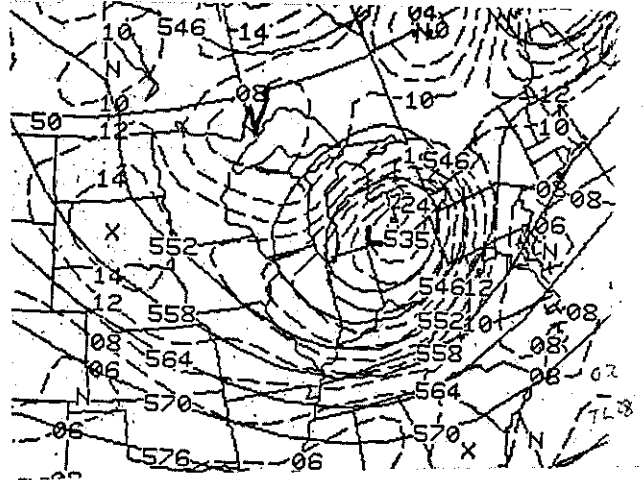


Figure 9: NGM 500 mb VT 00Z 4-28-88

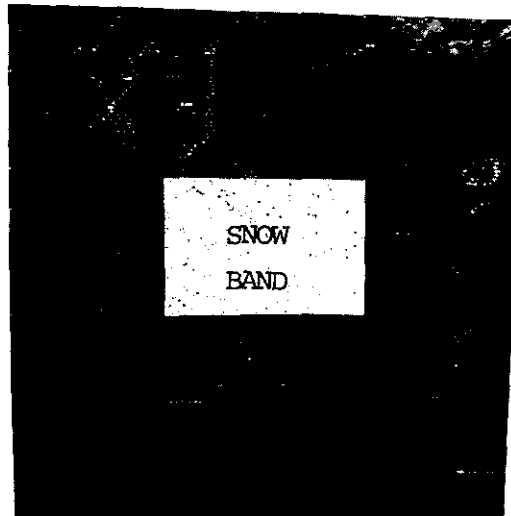


Figure 10: 1430Z 4-28-88

CONCLUSIONS

The forecaster in an impending winter storm event is faced with the situation of "so much to consider in so little time". He or she needs reliable and simplified solutions to a complex problem.

This paper attempts to make a little progress toward that goal. It also suggests that by recognizing the upper air processes in a heavy snow system...one will be focusing on one of the most dependable parameters - since the lower level scenario responds to developments aloft.

The examples presented attempt to clarify an important relationship between the path of the vorticity/circulation center of a snow system and that of the resultant heavy snow band. Making the proper adjustments here...as shown in the discussion presented...will hopefully lead to more consistently reliable results when putting the complete package together.

ACKNOWLEDGEMENTS

Thanks to Timothy Oster for his review and suggestions and to Todd Morris for his ideas on some of the content. Both are forecasters at WSFO Milwaukee.

REFERENCES

- Beckman, S.K.: Use of Enhanced IR/Visible Satellite Imagery to Determine Heavy Snow Areas. Monthly Weather Review, Vol. 115, No. 9, September, 1987, 2060-2087.
- Goree, P.A., and Younkin, R.J.: Synoptic Climatology of Heavy Snowfall over the Central United States. Monthly Weather Review, Vol. 94, No. 11, November, 1966. pp 663-668.

ERICA Plans for Winter Storms Field Study

Ron Hadlock, Battelle Ocean Sciences
Carl W. Kreitzberg, Drexel University

The Experiment on Rapidly Intensifying Cyclones over the Atlantic field study will be conducted between 1 December 1988 and 28 February 1989. The oceanic area that is approximately bounded by the Gulf Stream and North America, from coastal Carolina to just east of Newfoundland, will be the region for special observations obtained by recently-developed measurement systems including high-resolution and safe Loran-C dropwindsondes, CLASS rawinsondes, an array of drifting data buoys, and multiple airborne Doppler radars. The special observations will be acquired within a framework of all conventional operational data available for the eastern United States and Canada including that from the national weather services' land sites (plus supplemental rawinsonde observations), ocean platforms, U. S. Air Force WC-130 National Winter Storms Operational Plan reconnaissance flights, and civilian and military weather satellites. Satellite imagery and soundings will be available in real-time and archived through facilities of NOAA and the military.

The research program, which was initiated by and is funded by the Office of Naval Research, has been joined by many partners in research, including a dozen universities and about two dozen governmental organizations from the United States and Canada. Together, the participants will obtain the special and conventional data and assure its timely availability to researchers, including critically important data from aircraft: two NOAA/OAO WP-3Ds, the NCAR Electra and Sabreliner, and NRL and operational Navy P-3s. Research aircraft operations will be based at the Naval Air Station, Brunswick, Maine, and coordinated by Carl Kreitzberg, utilizing facilities provided by the U. S. Navy.

The field study will be directed by Ron Hadlock from NOAA's World Weather Building (WWB), Camp Springs, Maryland. At the WWB, ERICA forecasters and storm nowcasters, coordinated by Gregory Forbes, The Pennsylvania State University, will work closely with NOAA National Meteorological Center and National Environmental Satellite Data and Information Service personnel in facilities provided by those organizations. An ERICA Forecast Center at the Atmospheric Environment Service's Maritimes Weather Centre, Bedford, Nova Scotia, will participate in the forecasting/nowcasting decision-making processes. Additionally, special ERICA data will be acquired at operational and research sites in Atlantic Canada. Communications among all of these locations, and with aircraft in flight, are crucially important; the pre-ERICA field test - aircraft measurements on a rapidly-intensifying storm during January 1988 - showed that electronic mail, telephone, and telephone facsimile links for information and data transfer are effective.

The goals of the field study are to better understand the physical processes occurring in the atmosphere during the rapid intensification of winter storms at sea; to identify characteristics of the storms that can be used to predict their behavior; and to determine which of the physical processes need to be incorporated into numerical prediction models to better forecast the storms.

ERICA plans have proceeded from several planning workshops and are documented in the ERICA Overview (March 1987), Field Implementation Plan (November 1987), and Field Operations Plan (July 1988 and update - November 1988), along with storm climatological studies and journal articles in press, e.g., the November 1988 issue of the Bulletin of the American Meteorological Society.

ERICA -- EXPERIMENT ON
RAPIDLY INTENSIFYING CYCLONES OVER THE ATLANTIC

Gregory S. Forbes
The Pennsylvania State University

ERICA: FIELD PROGRAM PLANS

Special data sets will be collected over the western North Atlantic during winter 1988-89 in intense winter storms that intensify rapidly during periods of about a day or less. In many cases the bulk of the lowering of the central pressure in the deepening cyclone occurs in one or more 6-hour periods, or "explosive phases", in which the central pressure falls at least 10 mb/6h. The objective of the data collection is to enable post-field-phase determination of the processes that drive these explosive phases, as contrasted with processes at work during more normal deepening rates.

Data will be collected on about 8 storms, of which it is intended that 4-6 will be of the rapid deepening type and 2-4 will be "normal". The intensive observing period, or IOP, will normally be about 36h and include observations before, during, and after the "explosive" phase. Because the scientific objectives are all concentrated on the explosive phase of the cyclogenesis, IOP duration and total number of days of data collection are expected to be more controlled than in GALE, in which many different weather scenarios required data collection. While GALE almost turned into one 60-day IOP, data will be collected in ERICA on no more than about 16 days spread over three months, due to limited objectives, limited resources, and limited numbers of explosive storms expected. This will allow for more analysis and real-time learning than proved possible during GALE. There could very well be a lull of two weeks in duration when the long-wave pattern is adverse, especially around the time of the January thaw.

Two NOAA P-3 aircraft, each equipped with a tail Doppler radar, will be used to deploy ERICA dropwindsondes, collect Doppler radar data, and perform other in situ measurements. The NCAR Sabreliner and NCAR Electra aircraft will be made available for high-level and low-level special missions, respectively, during much of the 3-month field experiment. A Naval Research Laboratory P-3 will be available for deploying drifting buoys and dropwindsondes during a portion of the field experiment. The Air Force is very excited to participate in ERICA through the NOAA Winter Storms Operations Plan (NWSOP), and will be using aircraft equipped to provide wind (plus normal thermodynamic) data most,

if not all, of the time. There will be 6-hourly and 3-hourly NWS special rawinsonde launches in the U.S. and Canada, 7 CLASS sites, and a special surface mesonet on coastal Nova Scotia. The Penn State UHF wind profiler will be deployed at Otis Air Force base throughout ERICA.

The ERICA Operations Plan describes the details of the experiment. In a nutshell, the data collection strategy is to obtain meso-alpha-scale data (100 km or coarser resolution) at 6-hourly intervals and finer-scale data for limited intervals and regions during the period from about 18 hours prior to the start of rapid deepening until after the rapid deepening has ceased. The meso-alpha-scale data set will be collected by land-based rawinsondes, NWSOP dropwind-sondes, and specially designed P-3 missions which enable two P-3 aircraft to collect data simultaneously for about an hour at "synoptic" times. The finer-scale data will be collected from the Sabreliner and Electra, from the P-3 Doppler radars, and via 2-hour special observing sessions between periods of P-3 dropwindsonde releases.

The ERICA Forecast Office activities will begin on 27 November 1988, in order to be prepared for data collection on 1 December. The two basic functions of the Forecast Office will be (1) to issue medium-range (1-4 day) outlooks and forecasts of the likelihood of rapid cyclone deepening (nominally 10 mb per 6h) over the western Atlantic in order to activate and deactivate data collection facilities and (2) to issue nowcasts at frequent intervals to brief and update mission scientists participating in the airborne data collection.

Since conventional data over the ocean are sparse in space and time, nowcasting activities, which will require accurate knowledge of the position and movement of the surface low and upper-air forcing, will normally need to be done at a location where the special (i.e., real-time ERICA) data are available. Since NMC and Satellite Applications Lab facilities are available in the World Weather Building (WWB) in Camp Springs, MD, it was decided to locate the ERICA Forecast Office there.

The 1987-88 experiment demonstrated that the outlook/forecast preparation can be done quite effectively from a diversity of sites using conventional data and guidance products and disseminated via electronic mail. Thus, it is likely that some of the outlooks/forecasts can be prepared from remote sites, requiring fewer personnel at the ERICA Forecast Office. This is desirable, as space at WWB is limited. It will be necessary to operate the ERICA Forecast Office using a "skeleton crew" of forecasters at WWB on a daily basis, plus outlook/forecasters at remote sites and with teams of nowcasters ready to mobilize to WWB for periods of a few days whenever an ERICA storm is forecast. Remote participation, and most dissemination of forecasts and nowcasts, will be via electronic mail (OMNET).

ERICA: MISSION ACCOMPLISHED

Since the Workshop summary was not finalized until after ERICA data collection was concluded, the following preliminary summary was added. Overall, ERICA was extremely successful. Although the winter was not very snowy along the East Coast, and despite much of the winter being characterized by a 500 mb ridge off the Southeast Coast, 4 legitimate rapidly deepening cyclones and 3 marginal-rate deepening cyclones occurred within the ERICA domain. The strongest of these cyclones reached a central pressure of 938 mb south of 40N, and is believed to be one of the deepest extratropical cyclones ever occurring that far south over the western Atlantic. ERICA was successful not only because 4 rapidly deepening cyclones were measured, but also because most of the lesser storms had intriguing mesoscale structures. Unlike some field projects in which only a portion of the data collected is later used extensively in research, most of the ERICA cases seem to merit considerable study in the years to come.

A preliminary summary of the intensive observation periods (IOPs) and limited observation periods (LOPs) follows.

Cases of Rapid Deepeners (> 10 mb/6h) -- 4

IOP 2	-- 18mb/6h	13-14 December 1988
IOP 4	-- 20mb/6h	3-4 January 1989
IOP 5	-- 20mb/6h	18-19 January 1989
LOP 5A	-- 15mb/6h	20-21 January 1989

Cases of Marginal Rapid Deepeners (8 - 10 mb/6h) -- 3

IOP 1	-- 8mb/6h	9-10 December 1988
IOP 3	-- 9mb/6h	17-18 December 1988
IOP 8	-- 9mb/6h	24-25 February 1989

Comparison Cases (weak to normal deepening rates) -- 3

LOP 6P		27 January 1989
LOP 6		8 February 1989
IOP 7		12-13 February 1989